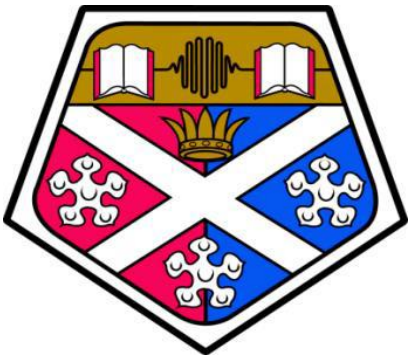

University of Strathclyde
Strathclyde Institute of Pharmacy and Biomedical Sciences

Investigating the protein-protein interactions of SCO3607 and SCO3608 and their role in cell morphology in *Streptomyces coelicolor*.

Charles Fredrik Webb

Thesis presented in fulfilment of the requirements for the degree of Doctor of Philosophy

2017

Declaration

This thesis is the result of the author's original research. It has been composed by the author and has not been previously submitted for examination which has led to the award of a degree.

Signed:

Date:

Abstract

Flotillin is a protein intrinsic to cell viability in humans, where it plays a role in cell morphology and structure. In *Bacillus subtilis*, it is involved in sporulation. NfeD always accompanies flotillins in prokaryotes, normally as an adjacent gene, though it is not present in eukaryotes. *SCO3607* and *SCO3608*, encoding flotillin and NfeD, respectively, are present in *Streptomyces coelicolor*. No previous studies have examined the role of these two proteins in *S. coelicolor*.

Preliminary bioinformatics revealed NfeD-encoding genes in actinobacteria, which was tentatively suggested as a new group of NfeD proteins; NfeD1b-5. Tn*5062* transposon insertions in *SCO3607* and deletions of both genes, separately and together, displayed no macroscopic phenotype; whilefluorescence microscopy revealed phenotypes related to cell polarity. *SCO3607* mutants displayed shorter tip to branch and cross-wall to cross-wall distances, while *SCO3608* mutants displayeda milder phenotype. A double knockout mutant displayed shorter intra cross-wall distances and enlarged spores. Bacterial two hybrid experiments were also performed, revealing SCO3607-SCO3607 interactions, though N-terminal fusions of the *cya*-domains to *SCO3607* abolished the interaction, suggesting the N-terminus is essential for the interaction.

Acknowledgements

I am beyond thankful to the many people without whose help this would be impossible. First and foremost, my supervisor, Dr. Paul Herron, for the patience shown and the guidance offered throughout the process. Thank you for not giving up on me; I will always appreciate the hours we spent talking about possible experiments and improvements!

A big thank you to everyone in the lab, especially John, Lewis, Craig, Richard, Alison, Leena, Sara, Kirsty, and Emilio! From protocols to morale support, you were amazing. Loads of thanks to SIPBS football team and everyone associated – especially Tam, Mark, and Scott. Further thanks to everyone else associated with my time at Strathclyde that made it such a great time! Fernanda, Kristian, Nils, Casper, Aksel, Anna, and James, you are all fantastic!

Last, but not least, I want to thank my family, without whose support this would not have been possible.

Thank you all for the amazing years!

Table of contents

List of figures

List of tables

List of abbreviations

bld	Bald
CAP	Cytidinediphosphate-diacylglycerol-alcohol phosphatidyltransferase
CDP-DAG	Cytidinediphosphate-diacylglycerol
CL	Cardiolipin
CM	Cytoplasmic membrane
CRISPR	Short palindromic repeats
DLCL	Dilysocardiolipin
d_N	Nonsynonymous
DRM	Detergent Resistant Membrane
d_S	Synonymous
FTs	Filamentous temperature sensitive
GFP	Green fluorescent protein
GPI	Glycosylphosphatidylinositol
Gro-P	Phosphodiester-linked poly(glycerophosphate)
Kin	Kinase
KinA-D	Autophosphorylating histidine kinases
LCL	Lysocardiolipin
l_d	Disordered phase domains
Lgt	Lipoprotein diacylglycerol transferase
Lnt	N-acyl transferase
l_o	Ordered phase domains
Lol	Lipoprotein localisation
LPG	Lysylphosphatidylglycerol
Lsp	Lipoprotein signal peptidase
LTA	Lipo-TAs
NAG	N-acetylglucosamine
NAM	N-acetylmuramic acid
NAO	10-*N*-nonyl acridine orange
OB	Oligosaccharide/oligonucleotide-binding
PA	Phosphatidic acid
PAML	Phylogenetic Analysis by Maximum Likelihood
PBP	Penicillin-binding protein
PCR	Polymerase chain reaction
PE	Phosphatidylethanolamine
PG	Phosphatidylglycerol
PI	Phosphatidylinositol
PI	Propidium iodide
PIM	Phosphatidylinositol mannoside

PMF	Proton motive force
PrP	Prion protein
SFM	Soya flour mannitol media
SLP-2	Stomatin-like protein 2
SLP-3	Stomatin-like protein
SPaseI	Signal peptidase I
SRD	Sterol-rich plasma membrane domains
SRP	Signal recognition particle
TA	Teichoic acids
TIPOC	Tip-organising complex
TSST-1	Toxic shock syndrome toxin-1
WGA	Wheat germ agglutinin
whi	White
WTA	Wall-TA

1. Introduction

1.1. Structure of the cell surface

1.1.1. Eukaryotic membrane structure and lipid rafts

Cell membranes feature in all cells, where they determine the boundary of the cell and its constituents. A cell membrane is a lipid bilayer consisting of lipids and proteins, where the nonpolar hydrocarbon lipid tails face inwards, while the polar hydrophilic heads face outwards. Essentially, these membranes regulate what enters and what leaves the cell. There are three major classes of lipids in the membrane; phospholipids, glycolipids, and sterols. Phospholipids are the most abundant class, including phosphoglycerides, of which the most common are phosphatidylcholine, phosphatidylethanolamine (PE), phosphatidylserine, phosphatidylinositol, and sphingolipids, of which sphingomyelin is the most common Glycolipids are formed by the addition of carbohydrate groups to lipids, which can be split into cerebrosides and gangliosides. The main sterol is cholesterol, which can be up to 50% of total membrane lipid in humans. Plant membranes contain less cholesterol than humans, but more phytosterols (Becker *et al.*, 2006).

The cell membrane was originally proposed to be a homogenous liquid mosaic of protein and lipid diffusing throughout the cell (Singer & Nicolson, 1972). This view was challenged, and during the 70's and 80's this was gradually shown to be incorrect, and the concept of lipid domains – membrane regions of non-homogenous lipid and protein content - was finally formalised in 1982 (Karnovsky *et al.*, 1982). The concept was that there were two liquid phases, ordered and disordered, that contained different sets of lipids and proteins. So while the lipid membrane is fluid, there are islands of less fluid lipids within the membrane. The ordered phase (l_o) domains were proposed to consist of densely packed sterol-dependent lipids, whereas the disordered phase (l_d) domains consist of loosely packed lipids (Ipsen *et al.*, 1987, Veatch & Keller, 2005). Conversely, proteins with an affinity for l_o localise to the regions of l_o, proteins with medium affinity for l_o will be more uniformly distributed, while proteins with low affinity are repelled from these regions. Thus the biochemical properties of the lipids can compartmentalise protein distribution (Simons & Toomre, 2000).

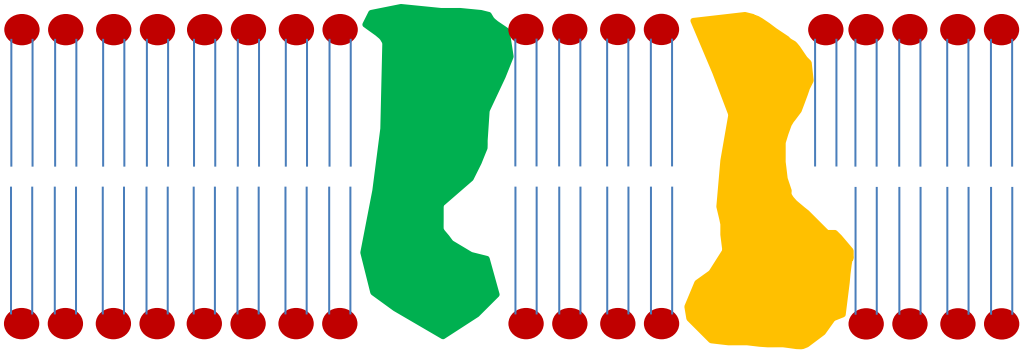

Fig1-1. The lipid bilayer. The hydrophilic lipid heads are in red, the hydrophobic lipid tails are in blue. Integral membrane proteins are in green and yellow (Becker *et al.*, 2006).

This dense packing of the lipids in l_o also prevents detergent incorporation into the membrane, which lent further support to the lipid microdomain hypothesis when glycosylphosphatidylinositol (GPI)-anchored proteins in mammals were isolated with the DRM (Detergent Resistant Membrane). These lipid microdomains, termed lipid rafts, were hypothesised to contain heterogeneously distributed proteins and lipids, specifically sterols, sphingolipids, and GPI-anchored proteins (Brown & Rose, 1992, Hakomori, 2003, Hakomori, 2008). In short, the DRM, which is not to be confused with the lipid raft, can be isolated by the addition of Triton X-100 to the cells at 4°C, then separating the cellular components by centrifugation (Brown, 1994). However, such methods are controversial and not without problems. Depending on the detergent used, different proteins are isolated, highlighting requirements for negative controls, and the possibility of different subsets of lipid domains (Arni *et al.*, 1998, Ostermeyer *et al.*, 1999). Additionally, lipids act in a temperature-dependent manner, and, as such, at lower temperatures lipids domains form larger domains, thus potentially artificially creating these lipid domains. Further compounding the validity of the methods is evidence that lower temperatures are required for isolation of the DRM. However, model membranes show that phase separation can occur at 37°C, further questioning the validity of the methods. Regardless, this should be seen as questioning the method for extracting lipid rafts rather than a critique of the hypothesis of the lipid domain, This emphasises the DRM should not be equated with lipid rafts, but rather an attempt at isolating lipid rafts (McGuinn & Mahoney, 2014).

Lipid rafts, as defined by the 2006 Keystone Symposium of Lipid Rafts and Cell function, are "… are small (10–200 nm), heterogenous, highly dynamic, sterol- and sphingolipid-enriched domains that compartmentalize cellular processes. Small rafts can sometimes be stabilized to

form larger platforms through protein–protein and protein–lipid interactions (Pike, 2006).” Thus, lipid rafts differ in lipid content from the rest of the membrane, which again differ depending on the kind of cell or membrane in question (Becker *et al.*, 2006). Specifically, lipid rafts in eukaryotes typically have 50% sphingolipids, and due to cholesterol preferentially interacting with sphingolipids, they contain 3 to 5-fold the amount of cholesterol found in the bilayer, which is offset by lower amounts of phosphatidylcholine (Pike, 2009, Simons & Ikonen, 1997, Anchisi *et al.*, 2012). These main lipids of the lipid raft in the outer exoplasmic leaflet are mirrored by phospholipids and cholesterol on the inner cytoplasmic leaflet. These rafts are more ordered than other regions of the membrane due to the saturation of the hydrocarbon chains of the sphingolipids and phospholipids compared to that of the rest of the membrane (Brown & London, 1998). It is partially due to their size that they have been so elusive; indeed, each lipid raft consists of only around 3000 sphingolipids spread over 50nm (Pralle *et al.*, 2000).

The proteins associated with lipid rafts can be divided into three groups; proteins found mostly in rafts, proteins in the liquid-disordered phase, and the proteins moving in and out of the lipid rafts. The previously mentioned GPI-anchored proteins are proteins found mostly in rafts, and include G-protein Gα subunits, endothelial nitric oxide synthase, and Src tyrosine kinases (Jeong & McMahon, 2002). Many of these proteins required cholesterol for localisation; indeed, depletion of cholesterol renders lipid rafts non-functional, and altered cholesterol metabolism has a profound effect in eukaryotes (Simons & Toomre, 2000).

Mainly involved in signal transduction and lipid tracking, lipid rafts are also used by many pathogens and toxins, such as HIV and cholera toxin, as a way of entering and exiting the cell (Sezgin *et al.*, 2017). Additionally, a subset of lipid rafts called caveolae are required to convert the cellular prion protein PrP(C) to the pathogenic isoform PrP(Sc), a step intrinsic to the development of Creutzfeldt-Jakob disease in humans and scrapie in sheep (Hooper, 2011, Schengrund, 2010). Other diseases associated with lipids rafts include, but are not limited to, Alzheimer’s disease, Huntington’s disease and Parkinson’s disease (Watt *et al.*, 2014, Korade & Kenworthy, 2008, Fabelo *et al.*, 2011)

Lipid rafts have been implicated in ApoE-mediated cholesterol delivery to neurons and oligodendrocytes, and are thought to be involved in axon growth, synaptic maintenance, axon regeneration and growth post nerve injury, and myelination (Vance *et al.*, 2000, Posse De Chaves *et al.*, 2000, Simons & Lyons, 2013). ApoE is a protein made by glial cells involved in

cholesterol homeostasis; inheriting the E4 isoform greatly increases the risk of Alzheimer's disease, while other forms have a protective effect (Rebeck *et al.*, 2002, Vance, 2012, Zlokovic, 2013). Similarly, Huntington's disease is also associated with changes to cholesterol metabolism, specifically those caused by polyglutamine expansion in the N-terminal part of the huntingtin protein, which causes the protein to affect sterol regulatory element-binding proteins, and leads to altered cholesterol levels (Block *et al.*, 2010, Karasinska & Hayden, 2011, Valenza & Cattaneo, 2011). Altered cholesterol levels are also found in patients with Parkinson's disease, though no causative effect has been shown (Vance, 2012). Other proteins that correlate with Parkinson's disease and interact with lipid rafts are parkin, PINK1, α-Synuclein, and DJ-1 (Kim *et al.*, 2013, Fallon *et al.*, 2002, Silvestri *et al.*, 2005, Martinez *et al.*, 2007). In essence, it appears altered cholesterol metabolism has an effect on many neurodegenerative diseases.

Yeast membranes differ from mammalian membranes, especially with regards to lipid rafts, as they contain neither sphingomyelin nor cholesterol. Instead yeast produce inositol phosphosphingolipids, which is hypothesised to be orthologous to sphingomyelin, and ergosterols, which are even stronger lipid raft formers than sterols (Xu *et al.*, 2001, Matmati & Hannun, 2008). Furthermore, lipid domain formation in yeast model membranes is dependent on interactions between inositol phosphosphingolipid and ergosterol (Klose *et al.*, 2010). Another point where yeast lipid rafts differ is the sphingolipid of yeast is odd in that not only is it very long at 26 carbon atoms, but when it is synthesised it is coupled to Pma1p in the endoplasmic reticulum, a lipid raft marker proton pump protein (Schneiter *et al.*, 2004, Schneiter *et al.*, 1999). The synthesis of the lipid rafts themselves is also different in fungi when compared to mammals, as the fungal lipid raft is formed in the endoplasmic reticulum as opposed to Golgi apparatus (Brown & Rose, 1992, Bagnat *et al.*, 2000).

Glycosphingolipids, sphingolipids with an attached carbohydrate, were originally characterised as structural components of eukaryotic membranes related to membrane fluidity and stability, but were later discovered to be a major component of the lipid raft in eukaryotes (Feinstein *et al.*, 1975, Tinker *et al.*, 1976, Aaronson & Martin, 1983, Campanella, 1992, Hakomori, 2008, Hakomori, 2003, Bagnat *et al.*, 2000, Wachtler & Balasubramanian, 2006). Glycosphingolipids in yeast are present in cell wall, cell membrane, and extracellular spaces, where they are involved in cell-to-cell interactions, polarisation, cell signalling and protein sorting (Rodrigues *et al.*, 2000, Nimrichter *et al.*, 2005, Hakomori, 2003, Rodrigues *et al.*, 2008, Bagnat *et al.*,

2000). Polarisation is intrinsic for the morphological change from yeast to hyphal growth in *Candida albicans*, which is again required for virulence (Whiteway & Bachewich, 2007, Mitchell, 1998). Polarisation, and thus lipid rafts, are also required for the same morphological switch in *Aspergillus nidulans* and *Fusarium graminearum* (Nimrichter & Rodrigues, 2011). Lipid rafts are involved in the virulence of *Cryptococcus neoformans*, as proteins involved in virulence were isolated from its lipid rafts, which are thought to organise these proteins at the cell surface (Siafakas *et al.*, 2006). Furthermore, vesicles were found to contain sterols, glycosphingolipids, and protein involved in virulence which was found in lipid rafts of *C. neoformans*, suggests that lipid rafts are present in vesicles, where they are hypothesised to stabilise (Rodrigues *et al.*, 2007). Edelfosine, a lysophosphatidylcholine analogue, is an antitumour drug that targets the cell membrane, but which also causes acidification of the intracellular compartment of yeast and causes disruptions to the cell membrane organisation. It is thought to affect the cells by disrupting lipid rafts, as the organisation of lipid raft markers was also disrupted (Czyz *et al.*, 2013). This all suggests that targeting lipid rafts is a potential mode of action for novel anti-fungal drugs. Other roles for lipid rafts in yeasts have been identified in *Saccharomyces cerevisaea* where it was also involved in mating, and in cytokinesis in *Schizosaccharomyces pombe* (Proszynski *et al.*, 2006, Rajagopalan *et al.*, 2003).

Plant membranes, lipid rafts, and DRMs differ in a few ways from their mammalian and fungal counterparts. Plant sphingolipids have a ceramide backbone and up to eight different long chain bases of esterified fatty acid, which are enriched in the DRM, with a polar head containing up to 13 sugar moieties. The major plant sphingolipid is glycosylinositolphosphoceramide (GIPC) and glucosylceramides (Pata *et al.*, 2010). DRMs in plants have so far been isolated from the plasma membrane and the Golgi apparatus, and in the former the DRMs account for between 5 and 10% of the plasma membrane proteins. Sterols make up about 20% of plant plasma membranes, but this doubles in DRMs, in addition to elevated levels of conjugated sterols, such as sterylglucosides and acylated sterylglucosides (Borner *et al.*, 2005, Furt *et al.*, 2007, Laloi *et al.*, 2007, Mongrand *et al.*, 2004, Lefebvre *et al.*, 2007). Phytosterols mainly differ from cholesterol by having an extra alkyl group at the C24 position. Two of the most common plasma membrane phytosterols are sitosterol and stigmasterolcontain an additional ethyl group, and stigmasterol has an additional double bound at the C22 position (Schaller, 2004). Polyphosphoinositides, which are involved in signalling, are also enriched in plant DRMs, while the major structural glycerophospholipid is barely present in the DRM (Furt *et al.*, 2010).

The animal and fungal DRM differ when compared with the plant DRM, as mammalian and fungal lipid domains can be isolated as low-density fractions, while all investigated plant lipid domains separate as high-density fractions (Brown & Rose, 1992, Mongrand *et al.*, 2004, Kierszniowska *et al.*, 2009, Borner *et al.*, 2005, Lefebvre *et al.*, 2007, Morel *et al.*, 2006, Furt *et al.*, 2010, Stanislas *et al.*, 2009, Carmona-Salazar *et al.*, 2011). An exception to the binary are human neutrophils, which are capable of containing both high and low-density lipid domains, where the former also contained cytoskeletal proteins (Nebl *et al.*, 2002). Plant DRMs also differ from the two others by sometimes displaying a mixed population of vesicular and non-vesicular bilayer membranes. This is thought to be due to the high rigidity due to the L_o phase, though it is possible this is an artefact from the Triton X-100 treatment used to extract the DRM (Carmona-Salazar *et al.*, 2011, Mongrand *et al.*, 2004). While mammalian and fungal DRMs are enriched in ergosterol and cholesterol, higher plant DRMs are enriched with a variety of sterols. As an example of this variety, 61 phytosterols and pentacyclic triterpenes were discovered in maize seedlings (Guo *et al.*, 1995).

1.1.2. Prokaryotic membranes and lipid microdomains

Bacteria, like eukaryotes, have a cell membrane, though some have an additional outer membrane. The bacterial cell membrane is very rich in proteins, and up to 70% of the membrane consists of proteins. The chromosome is anchored to the cell membrane, where DNA, cell wall polymers, and membrane lipids are synthesised (Champoux *et al.*, 2004).

The general purpose of eukaryotic lipid rafts and bacterial microdomains are the same; compartmentalisation and organisation of cellular processes. However, the manner in which this is achieved, while superficially similar, has some key differences. Eukaryotic lipid rafts mainly contain sphingolipids and cholesterol, of which the latter is only known to occur in a few bacteria, namely Borrelia burgdorferi, Helicobacter pylori, Mycoplasma spp, Ehrlichia chaffeensis, and Anaplasma phagocytophilum (Simons & Ikonen, 1997, Bramkamp & Lopez, 2015). However, as sterols are not found in other bacteria, and sphingolipids are not common either, and were only found in 2007, though they likely originated in bacteria (Bourquin *et al.*, 2010, Geiger *et al.*, 2010, Hannich *et al.*, 2011, Yard *et al.*, 2007). Thus bacterial lipid microdomains must be constituted by other lipids than those in eukaryotes. Bacterial microdomains have been hypothesised to contain polyisoprenoid lipids and cyclic polyisoprenoid lipids (also called hopanoids), in addition to cardiolipin (CL), which only occurs in energy transducing bacterial membranes, such as the mitochondria and cytoplasmic bacterial membrane (Lopez & Kolter, 2010, Donovan & Bramkamp, 2009, de Andrade Rosa *et al.*, 2006). It is worth noting the mitochondrial membrane is a bacterial membrane due to evolving from several bacterial families,

notably the Rickettsiaceae, Anaplasmataceae, and Rhodospirillaceae families (Abhishek *et al.*, 2011, Choi *et al.*, 2005)

1.1.2.1. Cardiolipin

That many lipids and proteins are heterogeneously distributed suggests that there must be a degree of self-organisation inherent to the cell which to base the localisation patterns on (Huang *et al.*, 2006). Examples of self-organisation include CL in the presence of Ca^{2+} and unsaturated PE (Cullis & de Kruijff, 1978, Rand & Sengupta, 1972). CL gets its name from where it was originally found – beef heart (Pangborn, 1942). It is present in the bacterial cytoplasmic membrane and mitochondria, which is bacterial in origin, and even though CL is not present in most Archaea, where bisphosphatidylglycerol is thought to perform an analogous function, halophilic archaea contain CL (Andersson *et al.*, 1998, Corcelli, 2009, Angelini *et al.*, 2012). It is also worth noting that eukaryotes without mitochondria, such as *Giardia lambli* and *Trichomonas vaginalis*, do not synthesise CL, suggesting a, evolutionary bacterial origin for the CL (Guschina *et al.*, 2009, Rosa Ide *et al.*, 2008).

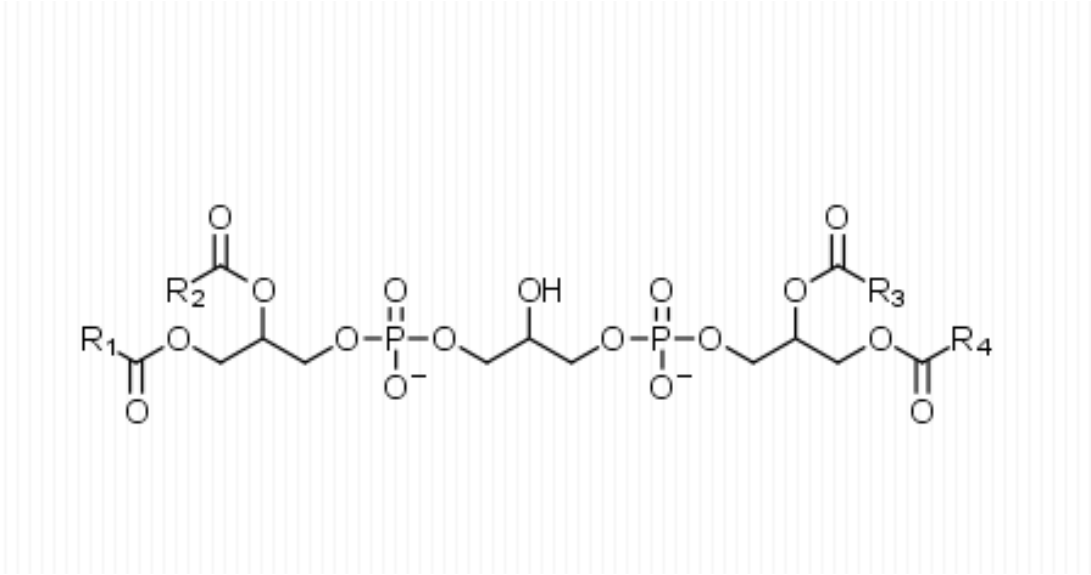

Fig1-2 The structure of CL. The R groups denote alkyl groups. Drawn using Chemdoodle (Todsen, 2014).

Structurally, CL is a dimeric anionic phospholipid consisting of a glycerol backbone linking two phosphatidyl groups which can carry two negative charges due to its four alkyl groups (see Fig1-2). CL is a high-curvature lipid due to the small cross-sectional area of the head group compared to the hydrophobic domain, and introduces negative curvature to membranes. Due to its dimeric structure CL can be utilised as a flexible linker, filling cavities on protein surfaces

and stabilising interactions between the subunits of oligomeric proteins and larger, multi-protein structures (Mileykovskaya *et al.*, 2005, Hunte, 2005). CL can form non-bilayer structures, such as hexagonal structures, under certain physiological conditions and can thus participate in the formation of dynamic protein-lipid membrane structures of high curvature, e.g. mitochondrial membrane cristae, membrane fusion and bacterial division sites (Mileykovskaya & Dowhan, 2005). Several techniques have allowed for breakthroughs in protein and CL detection; CL is easily detectable using the dye 10-*N*-nonyl acridine orange (NAO), though this somewhat controversial as often membrane depolarisation stops NAO-CL binding (Garcia Fernandez *et al.*, 2004)An equilibrium-based mechanism based on microphase separation has been proposed to explain polar and septal localisation of CL in rod-shaped bacteria. The model suggests that it is more energetically favourable for CL aggregates to localise to regions of higher negative curvature and thus localise as a larger group to the poles and septa, introducing more curvature due to their structure. There is an optimal size for these lipid microdomains, as too much curvature will make it energetically unfavourable, thus limiting the size of the domain. Thus, the short range attractive interactions between individual CL molecules affect the long range interactions as well (Huang *et al.*, 2006, Mukhopadhyay *et al.*, 2008).

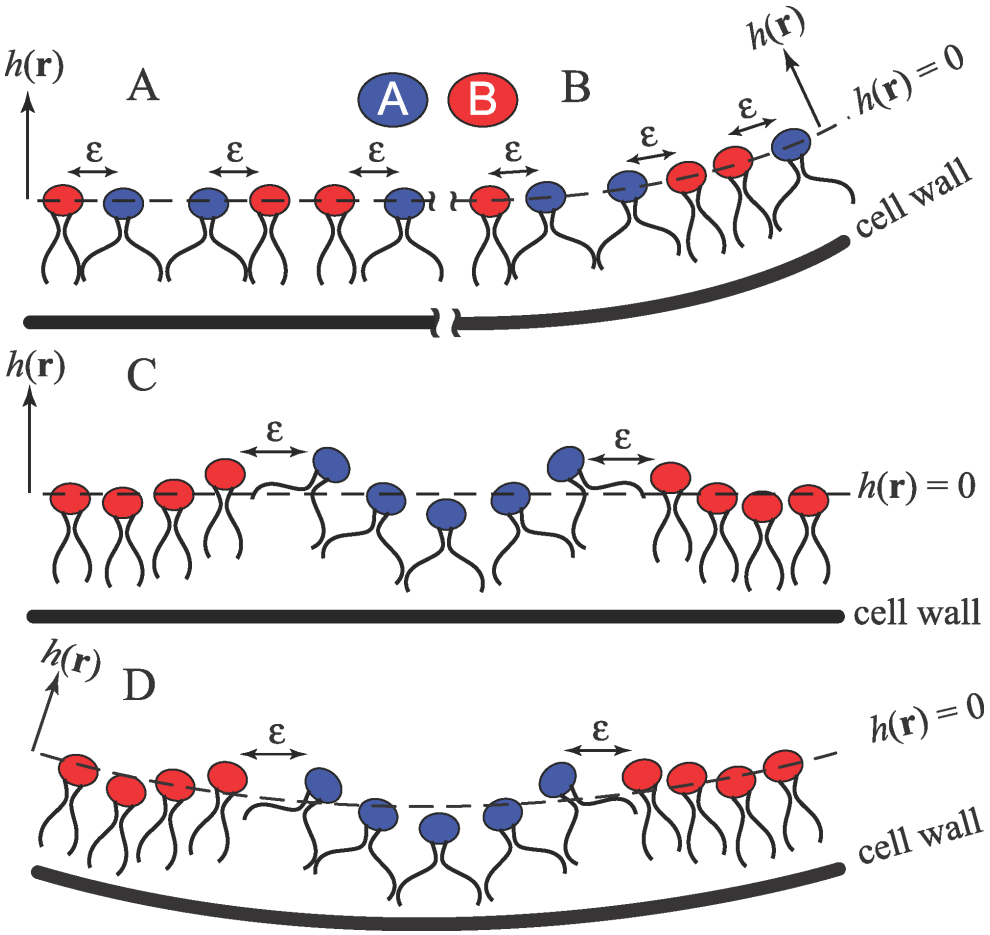

Fig1-3. CL is in blue, phospholipids in red. The membrane of A) has a high energy state ε due to the homogenous mixture of lipids. The cell wall in B) results in a lower membrane energy level due to the higher curvature. The clustering of favourable lipids results in a lower total energy level in C). The membrane in D) has the lowest energy level, as it has both cell wall and clustering of lipids.CL is restricted to energy-transducing membranes bacterial membranes, such as the bacterial cytoplasmic membrane and the inner mitochondrial membrane (de Andrade Rosa *et al.*, 2006). This is likely due to the ability CL to act as a proton sink, making it intrinsic to mitochondrial enzymes and pathways like the oxidative phosphorylation complexes (Haines & Dencher, 2002, Schlame, 2008). CL plays a major role in inner leaflet of the mitochondrial membrane in addition to being implicated in cancer, Barth syndrome, and diabetes amongst many other diseases (Kiebish *et al.*, 2008, Han *et al.*, 2007, Schlame *et al.*, 2002). It is also involved in the apoptopic pathways, where Cytochrome P450 oxidises CL (Schug & Gottlieb, 2009).

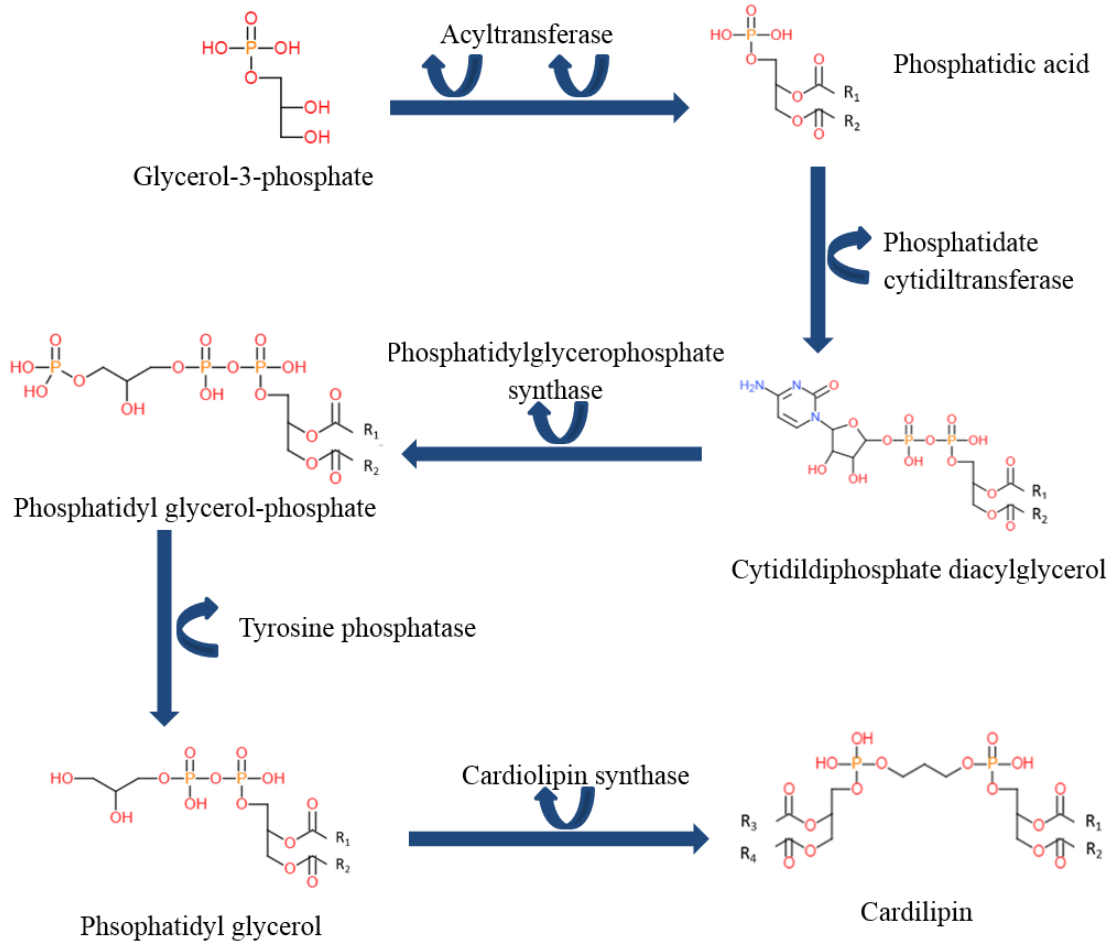

Fig1-4. Eukaryotic and prokaryotic CL pathway. A) is a diagram of CL synthesis of the eukaryotic type, whereas B) is the prokaryotic type of CL synthesis (Schlame, 2008).

CL is synthesised, as illustrated in Fig1-4, through one of two distinctively different enzymes, which are cytidinediphosphate-diacylglycerol-alcohol phosphatidyltransferase (CAP) and phospholipase D, which are dubbed the eukaryotic-type and prokaryotic-type, respectively (Schlame, 2008). These are broad groups, and some bacteria use the typically eukaryotic enzyme, such as the alpha proteobacteria and the actinobacteria, while some eukaryotes synthesise CL through the prokaryotic type enzyme, such as *Trypanosoma brucei*, which has an essential bacterial-type CL synthase (Serricchio & Butikofer, 2012, Sandoval-Calderon *et al.*, 2009, Luevano-Martinez, 2015). It is likely the eukaryotic CAP arose from a chimeric event involving archaeal and alpha proteobacterial CAPs, as they are more closely related to them than the actinobacterial CAPs. This is consistent with the theory of mitochondria being of alpha proteobacterial origin (Luevano-Martinez, 2015, Tian *et al.*, 2012).

In detail, the eukaryotic CL synthesis is an irreversible pathway, where glycerol-3-phosphate is acylated twice, synthesising phosphatidic acid, which is converted into cytidinediphosphate-diacylglycerol (CDP-DAG). CDP-DAG is further converted into phosphatidylglycerophosphate, which is then dephosphorylated into phosphatidylglycerol (PG) before another CDP-DAG molecule is added to the PG, creating CL (Tan *et al.*, 2012). CDP-DAG is also a precursor for other phospholipids, including phosphatidylglycerol, phosphatidylinositol, and phosphoinositides (Athenstaedt & Daum, 1999). Interestingly, the breakdown of CL in eukaryotes is facilitated by a phospholipase D that shares some similarity with the bacterial CL synthesising phospholipase D (Choi *et al.*, 2006).

Prokaryotic CL synthesis is much simpler than the eukaryotic type; a molecule of PG transfers one of its phosphatidyl moieties to another PG, performed by diphosphatidylglycerol synthase, and then has a glycerol group removed by phospholipase D. However, as opposed to the eukaryotic pathway, phospholipase D can also function in reverse (De Siervo & Salton, 1971, Hirschberg & Kennedy, 1972). An example of a bacteria with a bacterial-type CL synthase is *Chlamydophila pneumoniae* (Mancini & Ciervo, 2015). However, as previously mentioned, actinobacteria can synthesise CL irreversibly, typical of the eukaryotic pathway, and the eukaryotic CL synthase is descended from the alpha proteobacterial CL synthase (Sandoval-Calderon *et al.*, 2009, Tian *et al.*, 2012).

CL in bacteria localises to cell poles and septal region (Kawai *et al.*, 2004, Mileykovskaya & Dowhan, 2000, Barak *et al.*, 2008, Maloney *et al.*, 2011). *B. subtilis* synthesises CL from PG, and a double knockout mutant of the genes that encode the biosynthetic proteins is not viable; however, cells depleted of PgsA survive for a few hours due to PA and CDP-DAG being able to temporarily substitute for them (Barak *et al.*, 2008). *E. coli* is viable without CL and PG, but is temperature-sensitive (Kikuchi *et al.*, 2000). *Staphylococcus aureus* requires CL under conditions of high salinity, but is otherwise viable. It also has two CL synthases (Tsai *et al.*, 2011). Changes to CL distribution, specifically from septa to membrane, increases daptomycin resistance in *S. aureus*, *Enterococcus* species, and *Salmonella typhimurium* (Dalebroux *et al.*, 2014, Tran *et al.*, 2013). CL also stops daptomycin translocation in liposomes, which is likely how it functions *in vivo* (Zhang *et al.*, 2014). CL is also a virulence factor for *Moraxella catarrhalis*, where deletion of CL greatly hampers the bacterial adhesion to epithelial cells (Buskirk & Lafontaine, 2014). Furthermore, deletion of the CL synthase in *Pseudomonas putida* resulted in increased antibiotic sensitivity, likely due to faulty efflux pumps (Bernal *et*

al., 2007). CL also likely plays a role in DNA replication, through its interaction with the DNA replicator DnaA, and cell division, through its effect on the remodelling of the membrane. This is coherent with its previously mentioned roles (Mileykovskaya & Dowhan, 2005). These discoveries suggest prokaryotic-type CL synthases are potential targets for a multi-drug antibiotic resistance therapy. Daptomycin resistance in *Enterococcus faecalis* is mediated by a redistribution of CL from the septum, facilitated by a mutation in *liaFSR*, a three-component regulatory system involved in cell envelope homeostasis. Full resistance to daptomycin is achieved with mutations to its CL synthase and a glycerophosphoryl diester phosphodiesterase (Tran *et al.*, 2013).

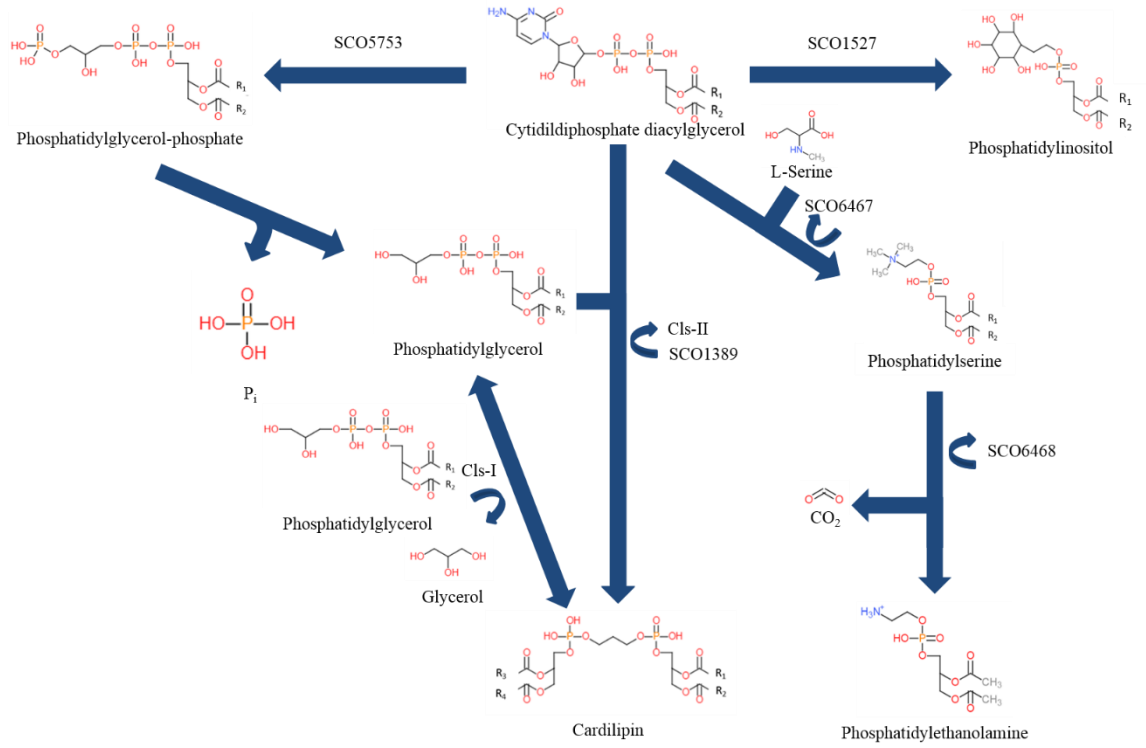

Fig1-5. *S. coelicolor* phospholipid synthesis pathway. A diagram showing the different known phospholipid synthesis pathways in *S. coelicolor* (Sandoval-Calderon *et al.*, 2009).

CL synthesis in filamentous actinobacteria, such as *S. coelicolor,* is different in several ways. Its distribution is different; it does not localise to specific regions, but rather is enriched in regions with no chromosomes, hyphal tips, and branch points (Jyothikumar *et al.*, 2012). It contains both prokaryotic and eukaryotic-type CL synthases, of which its eukaryotic-type synthesises CL irreversibly (Sandoval-Calderon *et al.*, 2009, Arabolaza *et al.*, 2010). Even though *S. coelicolor* contains several putative and confirmed CL synthases, at least one of

these, ClsA, a eukaryotic type CL synthase, is essential for growth. Furthermore, overexpression of ClsA caused morphological defects (Jyothikumar *et al.*, 2012).

1.1.2.2. Hopanoids

Hopanoids are another source of lipids that potentially localise to the bacterial lipid microdomains. Hopanoids are pentacyclic triterpenes (also called hopanes), a subgroup of the triterpenoids. Triterpenoids are a large class of natural compounds built from six C5-isoprenoids units that also includes sterols (Mahato & Sen, 1997, Mahato *et al.*, 1992). Hopanoids get their poetic name from the *Hopea* trees due to the presence of other pentacyclic triterpenes in the resin of the tree, where they were first isolated from in 1955 (Siedenburg & Jendrossek, 2011, Mills & Werner, 1955).

Hopanoids are synthesised from squalenes by squalene-hopene cyclases in one of the most complex single-step biochemical reaction known; the altering of 13 covalent bonds to form 5 cycles and establishment of nine stereo centres. In a very similar reaction, eukaryotes utilise the closely related 2,3-oxidosqualene cyclases to form a variety of sterols, also a triterpenoid, from squalene, where four cycles are formed from the alteration of 14 covalent bonds, and seven stereo centres are formed (Yoder & Johnston, 2005). However, there is evidence that some horizontal gene transfer has taken place, as some eukaryotes have the primarily prokaryotic squalene-hopene cyclases and vice versa (Frickey & Kannenberg, 2009). Interestingly, because the synthesis does not require oxygen, it is possible hopanoids predate oxygen on Earth, and this is especially interesting as cyanobacteria can produce them (Hartner *et al.*, 2005). Due to their resilient skeleton, they are physically conserved in nature and are the most abundant compounds in nature and are present in all soils and sediments (Saito & Suzuki, 2007).

Hopanoids occur in a varying estimate of bacteria, from 10-50%, but are absent in Archaea, and neither is it present in *E. coli* (Frickey & Kannenberg, 2009, Sahm *et al.*, 1993, Siedenburg & Jendrossek, 2011). It has been suggested that due to their prevalence and biochemical properities hopanoids may be the main lipid homologue in some prokaryotic lipid microdomains, similar to the role of the structurally similar cholesterol, which being a sterol is also formed from squalene, in eukaryotic lipid rafts (Lopez & Kolter, 2010, Crane & Tamm, 2004). Due to this, hopanoids are considered the bacterial functional cholesterol homologue (Saenz *et al.*, 2015).

The biochemically simplest of hopanoids, diplopterol, from which many of the others are modified from, had *in vitro* the ability to form l_o microdomains in giant unilamellar vesicles. This effect is similar to cholesterol, and diplopterol also modulated the order of lipid A, a lipopolysaccharide endotoxin unique to Gram-negative bacteria (Saenz *et al.*, 2012). Hopanoids in *Rhodopseudomonas palustris* are dispensable for growth, but are involved in membrane integrity and pH homeostasis (possible due to affecting lipid A), and when methylated at the C2 position hopanoids increase cell membrane rigidity which protects against stress, similar to cholesterol (Wu *et al.*, 2015, Welander *et al.*, 2009, Crane & Tamm, 2004). Furthermore, when no hopanoids are synthesised, CL production increases several fold (Neubauer *et al.*, 2015). The other pentacyclic triterpenes betulinic acid, oleanolic acid, and ursolic acid interact with CL to modulate membrane fluidity in model membranes (Broniatowski *et al.*, 2014). This is similar to the properties of cholesterol. There is further evidence for lateral cell membrane protein and lipid heterogeneity in the hopanoid producing species *Gloeobacter violaceus* (Rexroth *et al.*, 2011). Furthermore, squalene, a precursor in hopanoid synthesis, localised in a single spot in the cell membrane of *S. aureus*, which suggests it may spontaneously localise to more energetically favourable patterns, similar to CL. Interestingly, when the squalene-hopene cyclase YisP of *B. subtilis* was inhibited, several proteins failed to localise to the membrane (Lopez & Kolter, 2010). Additionally, when treated with nystatin, an anti-fungal compound that binds the sterol ergosterol, biofilm formation was induced in *B. subtilis* and cation leakage occurred. As bacteria do not synthesise ergosterol, it potentially binds hopanoids or similar squalene-derived products (Lopez *et al.*, 2009). In a mutant *Methylobacterium extorquens* strain lacking the hopanoid synthesis cluster the multidrug efflux system ceased to function, but was restored upon addition of cholesterol or diplopterol (Hopanoids as functional analogues of cholesterol in bacterial membranes.). This is similar to what has been observed for the antimicrobial resistance of *Burkholderia multivorans*, where a transposon insertion in the hopanoid synthesis cluster increased membrane permeability and prevented removal of antimicrobials (Malott *et al.*, 2012).

Hopanoids are also present in streptomycetes. In *Streptomyces scabies*, hopanoids are not required for growth, and upregulation occurs during hyphal growth (Seipke & Loria, 2009). In *S. coelicolor*, hopanoids have also been suggested to alleviate osmotic stress during aerial hyphal growth by minimising outward diffusion of water and protecting the hyphae against desiccation by tightening the space between lipids (Poralla *et al.*, 2000).

There are many factors suggesting hopanoids are an important part of the lipid microdomain; its distribution mimics the distribution of CL, they are structurally and functionally homologous to cholesterol, are required for membrane integrity, mutant phenotypes are similar to CL-deficient phenotypes and have less antimicrobial resistance, and are involved in protein localisation (Lopez & Kolter, 2010, Lopez *et al.*, 2009, Tran *et al.*, 2013, Malott *et al.*, 2012). And while hopanoid synthesising genes are missing from many bacterial genomes and are dispensable for growth in the bacteria they are present in, hopanoids are still an intriguing piece of the puzzle based on *in vitro* biochemical properties and *in vivo* cell membrane functions.

That hopanoids and CL are not required for viability in bacteria, with a CL synthase in at least *S. coelicolor* being an exception, can be interpreted to mean there are other unknown, major factors in bacterial lipid microdomains, and that lipid microdomains are not as vital as in eukaryotes (Jyothikumar *et al.*, 2012, Arora *et al.*, 2004). There are several avenues available with regards to the relationship between CL, hopanoids, and bacterial microdomains: measuring hopanoids synthesis in a CL synthase knockout, as per what has been done vice versa in *Rhodopseudomonas palustris*, elucidating whether CL overexpression can alleviate the phenotypes associated with hopanoid depletion, and following up with whether hopanoid and a double CL synthase and squalene-hopene cyclase knockout mutant strain is lethal (Neubauer *et al.*, 2015).

1.1.3. Cell wall

The cell membrane is protected by the cell wall, a peptidoglycan structure that surrounds and protects the cell. Bacteria can be divided into two main groups based on their cell walls' retention ofthe Gram stain, which is named after the inventor Hans Christian Gram. The testdifferentiates between these two types of bacteria; the Gram-positive and the Gram-negative. Gram-positive bacteria contain a single membrane and thick cell wall consisting of 50% peptidoglycan, also called murein, which causes the cell to retain the Gram stain (Koch, 2000). Gram-negative bacteria are characterised by two membranes and a thin peptidoglycan layer, which results in failure to retain the stain. The peptidoglycan consists of linked monomers of N-acetylglucosamine (NAG) and N-acetylmuramic acid (NAM), with the linking of the monomers facilitated glycosidic bonds. These long glycan chains are then cross-linked by tetrapeptides on the NAMs (Madigan *et al.*, 2012).

The role of the cell wall is to support the cytoplasmic membrane from internal osmotic pressure, ensure correct cell shape, and adhesion to surfaces and other bacteria. However, the cell wall

does not keep antibiotics out, and the Gram-negative outer membrane contributes to the greater antibiotic resistance in Gram-negative bacteria through preventing uptake of antibiotics. However, there are some examples of the cell wall evolving to keep antibiotics out (Munita & Arias, 2016). Additionally, due to important roles of the cell wall and only being present in Archaea, algae, and bacteria, it makes for an excellent target for antibiotics, whether directly or indirectly. Notably, the β-lactams exploit this by binding the penicillin-binding proteins (PBPs), which are proteins involved in the last steps of peptidoglycan synthesis. However, resistance to β-lactams is increasingly common, both through β-lactamases that hydrolyse the β-lactam ring, and PBPs changing to be unaffected by β-lactams (Skalweit, 2015). The latter is the mode of resistance in methicillin-resistant *Staphylococcus aureus* (Lambert, 2002).

Also present in the Gram-positive cell wall are proteins, teichoic acids (TAs), and some bacteria produce polysaccharide capsules as well (Lambert, 2002). Not all Gram-positive organisms have TAs, but most have some anionic analogue (Sutcliffe & Shaw, 1991, Reusch, 1984). TAs can be split into wall-TAs (WTAs) and lipo-TAs (LTAs), where WTAs are covalently linked to the cell wall, whilst the LTAs are tethered to the membrane by a glycolipid anchor, generally a disaccharide linked to a diacylglycerol, and the repeating unit chain extends into the cell wall (Fischer, 1988). The specific mechanisms and roles of TAs are largely unknown, however, 30-60% of the cell wall in Gram-positive bacteria that can produce LTAs consists of LTAs (Neuhaus & Baddiley, 2003, Streshinskaya *et al.*, 2007). While WTAs are dispensable in some bacteria, such as *S. aureus*, they are essential in others such as *B. subtilis* (D'Elia *et al.*, 2006, Weigel *et al.*, 2003, Schertzer & Brown, 2003).

Structurally, WTAs consist of two parts: a polymer chain consisting of phosphodiester-linked poly(glycerophosphate) (Gro-P) repeats bound to a disaccharide linker which covalently binds the chain to the rest of the cell wall. The linker consists of an N-acetylmannosamine attached to a NAG-1-phosphate with 1-2 glycerol-3-phosphates attached to the C4 oxygen of NAG. The most common of the Gro-P repeats are a ribitol-5-phosphate or glycerol-3-phosphate, though many other monomers exist, such as arabitol-phosphate in the case of *Agromyces cerinus* or erythritol-phosphate in *Glycomyces tenuis* (Potekhina *et al.*, 1993, Shashkov *et al.*, 1995, Neuhaus & Baddiley, 2003). Protonated D-alanyl residues are covalently linked to these Gro-P chains, granting the TAs their anionic charge (Neuhaus & Baddiley, 2003). This D-alanylation also increases the virulence of Gram-positive bacteria and increase their resistance to cationic antimicrobial peptides, as well as *B. subtilis* cells being prone to lysis in the presence

of glycine if they were defective in D-alanine synthesis (Peschel *et al.*, 1999, Abachin *et al.*, 2002, Collins *et al.*, 2002, Kovacs *et al.*, 2006, Heaton *et al.*, 1988). The chains themselves vary in length, repeating unit, anchor, and D-glucosylation, which depend on factors as diverse as organism and strain, media and phosphate availability, temperature, and life cycle (Leopold & Fischer, 1992, Pollack *et al.*, 1992, Boylen & Ensign, 1968, Grant, 1979, Baddiley *et al.*, 1961, Baddiley *et al.*, 1962, Sanderson *et al.*, 1962, Dehus *et al.*, 2011, Botella *et al.*, 2014).

LTAs also consist of phosphodiester-linked repeats, most commonly ribitol-5-phosphate or glycerol-3-phosphate, similar to WTAs, but rather than being covalently bound to the cell wall, LTAs are linked to the cytoplasmic membrane (Neuhaus & Baddiley, 2003). LTAs are much more common in low GC-content bacteria (55 mol%>), and in high GC-content bacteria LTAs are normally replaced by lipoglycans (Sutcliffe & Shaw, 1991). LTAs can be further divided into five different types: I – V (Schneewind & Missiakas, 2014). Type I LTAs are the most common and are comprised of glycerol-3-phosphates. They vary in length, sidechain substituent, and the glycolipid anchor that tethers them to the membrane. Type I LTAs are also further subdivided based on their sidechain substituent, α-GlcNAc or α-Gal, into group A or B, respectively (Schneewind & Missiakas, 2014). Type II LTAs have a galactose-galactose-Gro-P repeating unit, while type III LTAs have a galactose-Gro-P repeating unit (Neuhaus & Baddiley, 2003, Fischer, 1994). Type IV are the WTAs and LTAs of *Streptococcus pneumoniae*, which are has choline sidegroups (Fischer, 1997, Bergmann & Hammerschmidt, 2006).

Type V LTAs include lipid-anchored polysaccharides, such as lipoglycans, Gro-P lipoglucogalactofuranan from *Bifidobacteira bifidum*, and succinyl lipomannan from *Micrococcus luteus*, and are very common among acid-fast bacteria that often lack conventional LTAs (Fischer, 1987, Fischer, 1991, Berg *et al.*, 2007). Though the definition of an LTA states the requirement for phosphodiester-linked repeating units, these are included regardless (Schneewind & Missiakas, 2014). Actinomycetes generally synthesise lipoglycans rather than "true" LTAs, though some Tenericutes and Actinobacteria, which are mostly high G + C, synthesise both lipoglycans of the type V LTAs in addition to type I LTAs, while most Firmicutes, which are mostly low G + C, synthesise only one type of LTAs (Rahman *et al.*, 2009c, Rahman *et al.*, 2009b, Schneewind & Missiakas, 2014, Rahman *et al.*, 2009a).

While the exact functions of LTAs remain elusive, it is documented that LtaS (lipotechoic acid synthase) is required for *S. aureus* growth under normal laboratory conditions; tryptic soy broth

at 37ºC (Grundling & Schneewind, 2007). It is speculated LTAs play a role in membrane stability, and *B. subtilis* strains defective in D-alanine production, an intrinsic part of most TAs, would readily lyse in the presence of glycine (Jorasch *et al.*, 1998, Heaton *et al.*, 1988). More information was yielded when it was discovered how glycolipid synthesis affects the LTAs; alterations to a glycosyltransferase resulted in aberrant cell shapes and enlarged cell sizes in *Staphylococcus aureus* due to changes to the glycolipid anchor of the LTA, and in *Streptococcus* lead to a drop in mortality from 90% to 20% in mice and four-fold drop in invasiveness (Kiriukhin *et al.*, 2001, Doran *et al.*, 2005). In *S. pneumonia*, proteins involved in defence against the immune system and normal cellular functions use the exposed cholines of its unique type V LTAs as anchors, and other examples are proteins involved in cellular adhesion, such as PspC, and autolysins, such as LytA, LytB, and LytC, involved with the cell wall modulation (Bergmann & Hammerschmidt, 2006, Gamez & Hammerschmidt, 2012). Due to all these effects, LTAs are a potential target for new vaccines (Chapot-Chartier & Kulakauskas, 2014).

Actinomycetes generally synthesise lipoglycans rather LTAs, though LTAs are present in *S. albidoflavus*, *S. hygroscopicus*, and *S. coelicolor*, and the first mention of LTAs in a Streptomycete occurs in a Russian paper from 1983 (Rahman *et al.*, 2009a). The deletion of two TagF (teichoic acid glycerol) homologues, a protein involved in LTA synthesis pathways, in *S. coelicolor* affected sporulation (Kleinschnitz *et al.*, 2011b).

1.2. Proteins associated with the membrane

1.2.1. Protein export

Bacteria have a highly organised subcellular distribution of membrane lipids and cell wall constituents, but also of proteins. This cellular heterogeneity serves to compartmentalise cellular processes and organise the cell. This compartmentalisation is intrinsic for correct protein function, e.g. cytosolic proteins remain in the cytosol, membrane proteins localise to the membrane etc. A majority of proteins are secreted by the Sec system (the general **sec**retory pathway; type II), which also folds precursor proteins, a minority of fully-folded proteins are secreted by the Tat system (the **t**win **a**rginine **t**ranslocase pathway), and a subset of small, mature proteins are exported to the inner membrane by the YidC insertase (Dalbey *et al.*, 2011). There are also the ABC transporters (type I), flagellar secretion (type III), and conjugative secretion (type IV). However, roughly 20% of bacterial proteins are predicated to be targeted for secretion by the Sec system, making it the most common secretion system (Song *et al.*, 2009).

Proteins are targeted to the Sec pathway by a 20-30 residue N-terminal sequence (Natale *et al.*, 2008). It consists of an N-terminal basic region, a hydrophobic patch, and a three-residue motif for signal peptidase I (SPaseI) cleavage, which is normally expressed as AxA in prokaryotes, where alanine is the most common residue (von Heijne, 1990, Paetzel *et al.*, 2002). Secretory proteins are targeted to the Sec pathway by either the co-translational or the post-translational mechanism. In the post-translational pathway the protein to be exported is targeted by the chaperon SecB, which binds to the unfolded protein and directs it to the SecYEG translocase via SecA, consisting of SecY, SecE, and SecG, which is in turn powered by the SecB-activated ATPase SecA, and finally SecD and SecF promote the release of the now fully-folded protein (Driessen, 2001, Randall & Hardy, 1995, Hartl *et al.*, 1990, Hanada *et al.*, 1994, Douville *et al.*, 1995, Gierasch, 1989). Additionally, proton motive force (PMF) is also used to translocate the protein through an unknown mechanism in addition to ATP (Schiebel *et al.*, 1991). The co-translational pathway is more common for integral membrane proteins, where the signal recognition particle (SRP) binds the signal peptide of the nascent secretory protein as it is being synthesised, creating an SRP-ribosome-protein chain and targets it to the Sec translocase via interactions with the membrane receptor FtsY (Natale *et al.*, 2008, Luirink & Sinning, 2004). However, folding of newly synthesised proteins is aided by up to three other highly conserved chaperones: Trigger factor, DnaK/DnaJ/GrpE, and GroEL/GroES (Deuerling *et al.*, 1999,

Agashe *et al.*, 2004, Kerner *et al.*, 2005). These are common to all proteins, including integral membrane proteins and other secreted proteins.

The Tat system works differently from the Sec system, with the biggest difference being the source of energy powering the translocation, as the Sec system exports and folds precursor proteins in an ATP-dependent manner, whilst Tat exports fully formed proteins using proton motive force (Palmer & Berks, 2012, Yahr & Wickner, 2001). Proteins are targeted to the N-terminal-binding site of TatBC by an N-terminal peptide, [(S/T)RRxFLK], the twin-arginine motif (Berks, 1996, Gerard & Cline, 2006, Alami *et al.*, 2003, Kreutzenbeck *et al.*, 2007). TatB serves to stabilise TatC, which is believed to act as the motor (De Keersmaeker *et al.*, 2007, Bruser *et al.*, 2003). Furthermore, TatB is dispensable for growth and is missing from many genomes (Blaudeck *et al.*, 2005). If PMF is available, the translocator TatA is recruited at this stage. Exactly how TatA functions is unknown, but it is postulated it forms a stable aqueous pore in the membrane, as a proton efflux is observed during Tat-dependent translocation in thylakoid membranes (Alder & Theg, 2003). Naturally, it would require sealing immediately after translocation, and PspA, a protein that aids in dealing with membrane stress and alterations to PMF (DeLisa *et al.*, 2004).

In *S. lividans* both TatB and TatC are dispensable for growth, but TatA is not, though this is not due to redundancy, as TatB and TatC have different functions (De Keersmaeker *et al.*, 2005a). The Tat system of *S. lividans* differs from that of *E. coli*, as the Tat proteins have been found localised in the cytoplasm in the former, but not in the latter (De Keersmaeker *et al.*, 2005b).

S. coelicolor exports a total of roughly 800 proteins, of which 190 are predicted to be exported by the Tat pathway. Of these 190 proteins, spanning a wide variety of proteins, 25 are confirmed to be translocated by the Tat pathway (Widdick *et al.*, 2006). One example of a Tat pathway translocated protein is chitosanase, an enzyme that breaks down the antimicrobial chitosan (Ghinet *et al.*, 2010). Cytochrome bc_1, a part of the aerobic respiration chain, activity is abolished in the absence of an active Tat pathway (Hopkins *et al.*, 2014). The lethality of a *chpE* null mutant was also suppressed by inactivation of the Tat pathway (Di Berardo *et al.*, 2008). Several other industrially important *S. coelicolor* enzymes are also exported by the Tat pathway, though in other bacteria (van Bloois *et al.*, 2009, Scheele *et al.*, 2013).

1.2.1.1. Lipoproteins

A type of protein that requires the Sec or Tat machinery for correct localisation are the lipoproteins, a class of membrane-associated proteins involved in signal transduction and nutrient uptake, and make up 1-3% of the protein encoding genes of a given bacteria (Berks *et al.*, 2000)(Sutcliffe *et al.*, 2012). They all share a conserved type II signal peptide sequence, called a lipobox sequence motif, characterised by a modified cysteine residue, which is required for proper protein modification. The lipobox is traditionally expressed as a "L-3 – (A/S/T)-2 – (G/A)-1 – C+1, where the latter cysteine residue is the aforementioned modified cysteine (Thompson *et al.*, 2010). Once the lipoprotein has been translocated across the membrane, the lipoprotein diacylglycerol transferase (Lgt) adds a thioether-linked sulphydryl group to the cysteine residue of the lipobox. Lipoprotein signal peptidase (Lsp) then cleaves the signal peptide, leaving the cysteine with the sulphydryl group at the N-terminal of the protein, which is now attached to the outer face of the cytoplasmic membrane (Hutchings *et al.*, 2009). While this is where the reaction stops in most Gram-positive bacteria, in Gram-negative bacteria and a few high G + C content Gram-positive bacteria, the lipoprotein may have a further fatty acid attached to the modified cysteine residue by N-acyl transferase (Lnt), then transported to the outer membrane by the lipoprotein localisation (Lol) pathway (Narita *et al.*, 2004, Tokuda, 2009). Gram-positive bacteria known to encode N-acyl transferases are *S. aureus* and mycobacteria (Rezwan *et al.*, 2007, Tschumi *et al.*, 2009, Kurokawa *et al.*, 2009).

1.2.2. Protein localisation

However, it is not always clear why a protein localises to a specific area of the cell, while in other cases it is, such as the polar localisation of ProP in *E. coli* being dependent on CL (Mileykovskaya, 2007). Exactly what causes the protein to localise to a certain region f the cell can be a lipid, DNA, other proteins, etc. Many proteins are localised heterogeneously due to protein-protein interactions such as MinCD and RacA in *B. subtilis (Wu & Errington, 2003, Barak et al., 1998).* In their case they require DivIVA for their polar localisation. DivIVA is an example of a prokaryotic protein organising in a non-homogenous manner in relation to lipids (Ben-Yehuda *et al.*, 2003).

A model for protein localisation has been suggested, a "diffusion-and-capture" model, where a protein travels round the cell until it reaches its designated site, such as has been suggested for DivIVA in *S. coelicolor* (Rudner & Losick, 2010). Often in this case it will be said proteins are "targeted" to e.g. the poles, which is misleading, as they reach it by passive diffusion. The

correct use of targeted in relation to bacteria would be used to describe the active mechanism in which plasmid segregation occurs. Plasmid segregation occurs by protein polymerisation and depolymerisation pushing, and in some cases pulling, the newly synthesised plasmid molecules to either side of the cell. In summary, a protein is not targeted if it reaches its localisation through passive diffusion (Rudner & Losick, 2010, Ebersbach & Gerdes, 2005).

1.2.3. Protein structure and how it relates to function

Proteins interact with each other not just for localisation, but also for function. Proteins usually assemble into complexes with other proteins or the same protein, forming hetero-oligomers or homo-oligomers, respectively. These can range in size from ribosomes of 2.5 mega daltons to the much smaller histone octamers, where the monomers range from 11400 to 15400 daltons (Bashan *et al.*, 2003, Luger, 2003).

The assembly of these multi-protein complexes are carried out by non-covalent interactions dependent on quaternary structure of the proteins (Jones & Thornton, 1996). Other types of protein-protein interactions include stable and transient interactions subject to covalent, electron pairing and disulphide bonds, and non-covalent bonds, such as van der Waal's forces, ionic interactions, hydrophobic bonds, and hydrogen bonds (Westermarck *et al.*, 2013). Most proteins are not covalently bound, but a few exceptions such as ubiquitin, exist (Kaiser *et al.*, 2011).

The CM is selectively permeable due to a variety of channels, e.g. ion channels (Katz & Miledi, 1973). It is thus natural to presume that certain protein structures are more suited for membranes than others, e.g. the β -barrel of the outer membrane of Gram-negative bacteria, chloroplasts and mitochondria (Schulz, 2002, Wimley, 2003). Generally, a β-sheet is more likely to be a part of the protein-lipid interface due to the higher structural regularity. Membrane proteins are classified as either integral or peripheral, based on how easily they dissociate from the membrane, with peripheral membrane proteins generally released by quite mild conditions, due to their weaker binding, which is generally by electrostatic interactions or hydrogen bonds between the protein and lipid components, though the interaction can be between a peripheral membrane protein and an integral membrane protein as well (Findlay, 1987). For integral membrane proteins, the residues localised inside the CM are also generally hydrophobic, making it relatively easy to predict with hydropathy plots (Lodish, 1988). The regions immediately flanking the transmembrane regions are usually positive, which is probably to confer selectivity for negatively charged phospholipids (Watts, 1993).

There are other structures important for lipid binding, such as tertiary structure and structural motifs. The different types of binding can be divided into four binding types; non-specific hydrophobic association, covalently bound lipid anchors, specific protein-lipid binding and protein-lipid electrostatic interactions. Binding through non-specific hydrophobic association includes amphiphilic α-helices, exposed non-polar loops, post-translationally acylated or lipidated amino acid residues, or acyl chains of specifically bound regulatory lipids. An example of a non-specific hydrophobic interaction is the amphiphilic helix of the PBP-5 of *E. coli*, and an example of a putative amphiphilic helix in *S. coelicolor* is DivIVA (O'Daniel *et al.*, 2010, Yang *et al.*, 2002). An example of a protein that is membrane anchored through a covalently bound lipid anchor are the GPI-anchored proteins, which is associated with lipid rafts, though no example of a prokaryotic GPI-anchored protein is evident in the literature (Levental *et al.*, 2010).

Quite a few proteins require anionic phospholipids, such as CL, for correct function. In *B. subtilis*, the aforementioned sporulation protein FisB remodels the membrane during sporulation through interacting with CL, and MurG, associated with the peptidoglycan machinery, binds anionic phospholipids, preferably CL (Doan *et al.*, 2009, van den Brink-van der Laan *et al.*, 2003). Furthermore, DnaA, the initiator of DNA replication, co-localises with and is activated by CL (Sekimizu & Kornberg, 1988, Maloney *et al.*, 2011). CL is also required for properly function efflux pumps in *Pseudomas putida* (Bernal *et al.*, 2007).

1.2.4. Proteins associated with the mammalian lipid raft

Further proteins that require a specific subset of lipids, the lipid raft, are flotillins. These proteins are highly conserved membrane-associated proteins, first identified as reggie-1 and reggie-2 in goldfish and rats as plasma membrane associated proteins upregulated during axon regeneration (Malaga-Trillo *et al.*, 2002, Schulte *et al.*, 1997, Lang *et al.*, 1998). At the same time, reggie-1 and reggie-2 were identified independently in mice and fruit flies as flotillin-2 and flotillin-1, respectively (Bickel *et al.*, 1997, Galbiati *et al.*, 1998). Humans have two flotillins, flotillin-1 and flotillin-2 (Bickel *et al.*, 1997).

Depending on the type of cell, lipid rafts also contain additional proteins, specifically caveolin, which are present in the previously mentioned specialised lipid rafts called caveolae, which are flask-shaped regions with roles in membrane integrity, vesicular trafficking and signal transduction, present in glial, epithelial, endothelial, muscle and adipose cells. Flotillins have a tripartite structure in common; an N-terminal membrane domain, a central SPFH (Stomatin,

Prohibitin, Flotillin and HflK/C) domain, and a variable heptad repeat-rich sequences predicted to form inter and/or intermolecular coiled-coil structures known as the flotillin domain (Dempwolff *et al.*, 2012). Bacterial stomatin-containing proteins, such as flotillin, form various oligomers; dimers, trimers, tetramers and multimers, even though it lacks the normal coiled-coils required for oligomerisation (Kuwahara *et al.*, 2009). Stomatins were originally described as integral membrane proteins in red blood cell, and loss of stomatin results in red blood cells leaking Na+ and K+ (Hiebl-Dirschmied *et al.*, 1991, Delaunay *et al.*, 1999). Stomatin-like protein 2 (SLP-2) localises to CL-rich domains in the mitochondria, and upregulation of SLP-2 increases the amount of CL and induces biogenesis, while in upregulation of SLP-2 in T-lymphocytes was found to inhibit apoptosis, increase ATP-storage, where it is likely to recruit prohibitins to CL-rich microdomains in mitochondria (Christie *et al.*, 2011). Prokaryotic stomatin-like proteins arose first from a common ancestor. Paraslipins likely arose through a duplication process, and there is strong support for a paraslipin of *Rickettsia*-like proteobacterium, the progenitor of the mitochondria, being the origin of the eukaryotic stomatin (Fitzpatrick *et al.*, 2006, Green & Young, 2008).

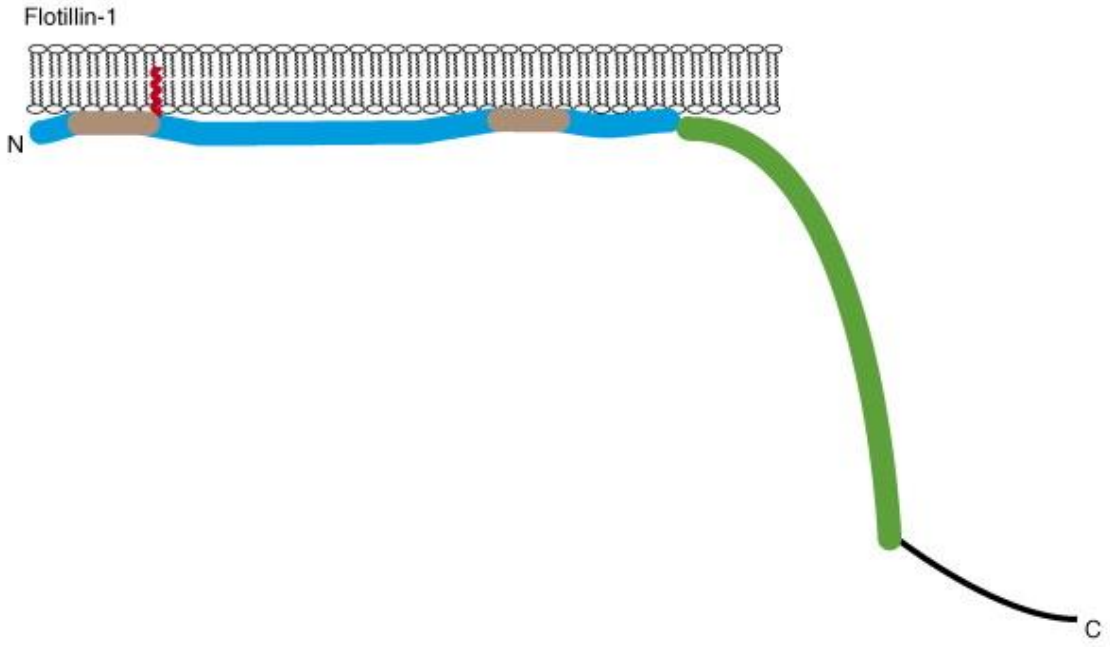

Fig1-6. The domain structure of flotillin-1 of *Homo sapiens sapiens*. The grey membrane-associated hydrophobic sections intersect the blue SPFH domain, with the green C-terminal tail being the flotillin domain, with the red palmitate reside also enhancing membrane association. The image has been copied (Browman *et al.*, 2007).

Flotillins are termed raft markers as they are found in all tissues due to ubiquitous expression, as opposed to the caveolins (Tavernarakis *et al.*, 1999). These cholesterol-binding proteins are the three caveolins; caveolin-1, caveolin-2 and caveolin-3. The caveolin-1 and caveolin-2 encoding genes are located next to each other on the same chromosome and form a hetero-oligomeric complex. Caveolin-3, which is located on a different chromosome, has been shown to interact with caveolin-2. Additionally, caveolin-2 levels are higher in lungs, and caveolin-3 has been implicated in muscular diseases (Gazzerro *et al.*, 2010, Zhu *et al.*, 2010).

Flotillins interact with many proteins in eukaryotes; Src kinases, actin, N-methyl-D-aspartate receptors and each other (Langhorst *et al.*, 2007, Babuke *et al.*, 2009, Swanwick *et al.*, 2009). Flotillins also interact with vinexins, CAP/ponsin and ArgBP2 in eukaryotes and is required for the localisation of cadherin to cell-cell junctions. These proteins are all associated with the actin cytoskeleton, which flotillin also interacts with, an interaction which is dependent on its SPFH domain (Stuermer *et al.*, 2001, Guillaume *et al.*, 2013, Rivera-Milla *et al.*, 2006, Stuermer *et al.*, 2004, Baumann *et al.*, 2000, Kokubo *et al.*, 2003, Kioka *et al.*, 2002, Kimura *et al.*, 2001, Langhorst *et al.*, 2007). Flotillin are also associated with Parkinson's and Alzheimer's disease, specifically abnormal upregulation of the protein, though no direct link has been shown (Jacobowitz & Kallarakal, 2004, Kokubo *et al.*, 2000, Girardot *et al.*, 2003). Flotillin also plays a role in collagen uptake (Lee *et al.*, 2014).

In *Aspergillus nidulans* GFP-tagged flotillin formed foci along the plasma membrane, but not around the hyphal tips, and deletion caused slower growth, irregular shaped hyphae and impaired formation of sterol-rich plasma membrane domains (SRD), and it was suggested flotillin was involved in cellular compartmentalisation. A stomatin null mutant caused irregular hyphae and increased hyphal branching in young hyphae, but did not affect SRDs (Takeshita *et al.*, 2012).

1.2.5. Proteins associated with the bacterial lipid raft

Many bacterial proteins contain SPFH domains, a protein domain family associated with lipid raft proteins in eukaryotes, and this protein family is broadly split into twelve different subfamilies. Of the two of interest to this work, due to the immediate presence of *nfeD*, are SPFH1a and –b, notating stomatins, SPFH2a, -b, and –c, notating flotillins. (Hinderhofer *et al.*, 2009). SCO3607, from *S. coelicolor*, has 33.1% amino acid identity with the human flotillin-1, consistent with what has been shown for *B. subtilis*. Furthermore, bacterial flotillins

are very common and are present in a wide variety of genomes, suggesting a conserved role (Donovan & Bramkamp, 2009).

The first bacterial flotillin was discovered in 1999, and was first isolated from the DRM of the *B. halodurans*, in addition to being upregulated following alkaline stress conditions (Zhang *et al.*, 2005, Tavernarakis *et al.*, 1999). *B. subtilis* encodes two flotillins, FloA (previously YqfA) and FloT (previously YuaG). FloA shares very little sequence similarity with other flotillins, and it is counted as an SPFH protein based on its genetic association with an *nfeD*. The *yuaFGI* operon of *B. subtilis* is induced strongly by σ^w, which is induced by alkaline conditions, similar to what was observed in *B. halodurans*, though that stationary phase induction was independent of σ^w in the stationary phase in a strain lacking *sigW* (Huang *et al.*, 1999, Wiegert *et al.*, 2001). FloT disruption in *B. subtilis* led to delayed sporulation and decreased sporulation efficiency, and likely involved in early stage of sporulation onset. This was due to a delay in transcription of *spoIIAB*, which phosphorylates Spo0A, leading to sporulation (Donovan & Bramkamp, 2009). Additionally, the deletion of the *B. subtilis* flotillins (*floA* and *flo*T) greatly impairs biofilm formation (Yepes *et al.*, 2012). FloA and FloT deletions impact biofilm formation through its interactions with FtsH, an ATP-dependent metalloprotease required for biofilm formation. The expression of the two flotillins is important for FtsH functionality, in addition to flotillin null mutants resulting in reduced levels of FtsH. The flotillins also co-localised with FtsH at the septum during exponential growth. In an FtsH null mutant the sporulation frequency is greatly reduced due to an increased amount of Spo0M, which is *in vitro* a substrate for protease FtsH (Thi Nguyen & Schumann, 2012). Spo0M is a sporulation control protein, which overexpression leads to impaired sporulation, but also impaired sporulation when depleted or absent. *spo0M* deletion also results in lower expression of *spo0A*, which encodes a downstream protein also involved in sporulation. Spo0A, encoded by *spo0*A, is a phosphatase and a master regulator which affects the transcription of 121 genes (Han *et al.*, 1998). Thus FtsH indirectly regulates phosphorylation of many downstream proteins involved in sporulation (Le & Schumann, 2009, Perego, 1998, Ohlsen *et al.*, 1994, Molle *et al.*, 2003). Depending on the amount of Spo0A~P, cells sporulate or differentiate into matrix-producing cells required for biofilm formation, which requires FtsH (Yepes *et al.*, 2012). Upregulation of the two flotillins in *B. subtilis* also caused problems with signal transductions, shape, and cell differentiation, likely through the increased stabilisation of FtsH (Mielich-Suss *et al.*, 2013). As a FloT null mutant resultes in decreased sporulation efficiency in *B. subtilis*, it is likely it interacts with as

of yet unknown proteins involved in phosphorylating Spo0A, but the exact mechanisms are unclear due to the multiple levels of control (Donovan & Bramkamp, 2009). In *E. coli*, overproduction of a flotillin orthologue compensates for a missing membrane-associated protease (Chiba *et al.*, 2006).

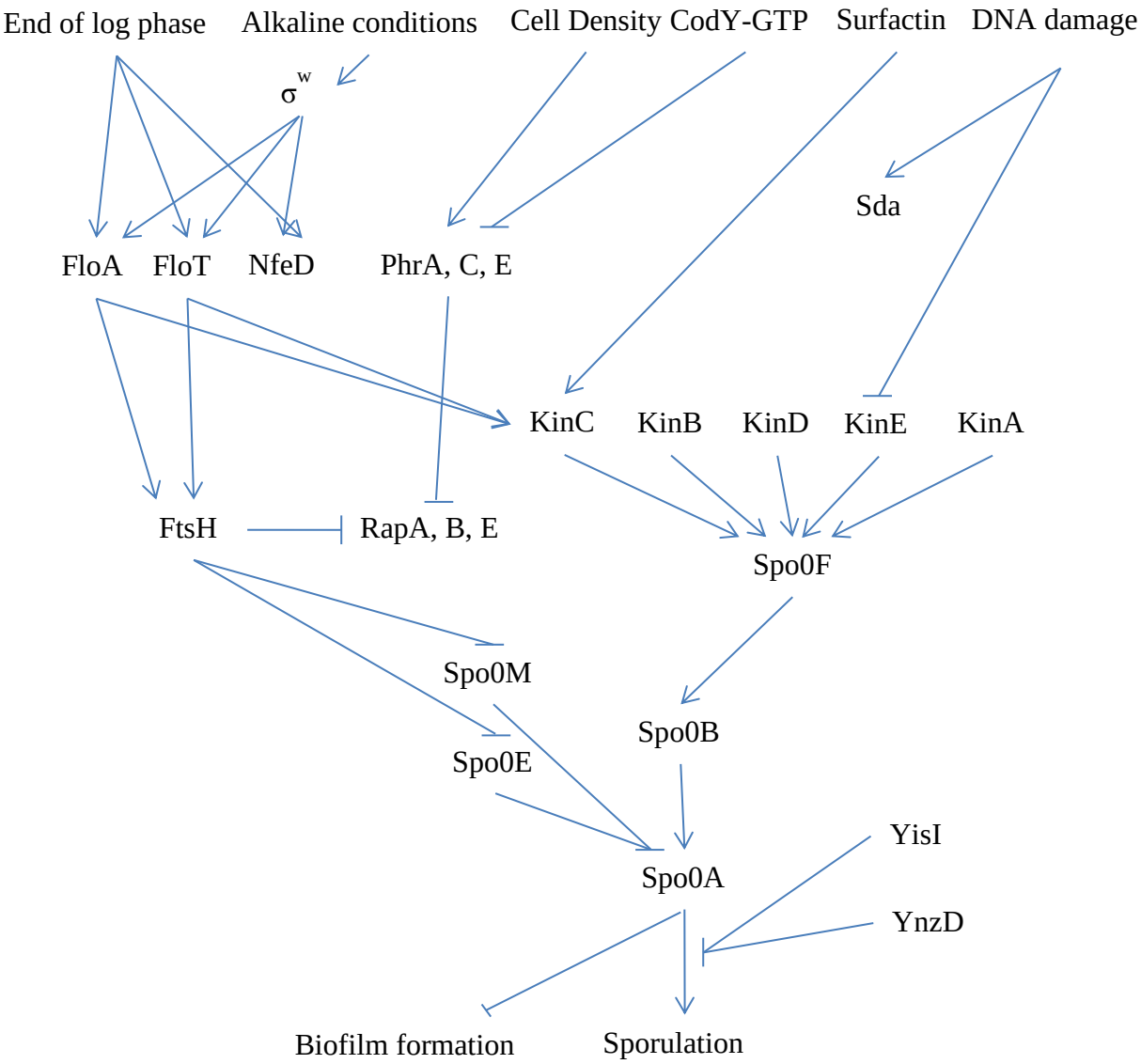

Fig1-7. Simplified *B. subtilis* phosphorelay with NfeD and flotillin added. Adapted from Piggot & Hilbert, 2004, with NfeD and flotillin added from Lopez & Kolter 2010, and Donovan & Bramkamp, 2009.

Several other proteins with known roles in secretion and signalling were also discovered in the DRM isolated from *B. subtilis* and *B. halodurans*. These heterogeneously distributed proteins are also likely lipid raft proteins (Lopez & Kolter, 2010, Donovan & Bramkamp, 2009).

FloT potentially forms a homo-oligomer forming foci in the septal and polar regions, overlapping with CL. However, it is not likely that CL is a target for FloT, as during sporulation the CL and PG localised to the prespore membrane, while the FloT localised to the mother cell membrane. This does not necessarily disprove that CL is a target; if they hypothetically interact, an unknown factor could make the two dissociate. GFP-tagging showed that only a few foci were visible during the early exponential phase, but an increased amount of foci was observed during stationary phase (Donovan & Bramkamp, 2009). Another possible localisation target for flotillin in bacteria is hopanoids. When YisP, a squalene synthase in a pathway that produces a C30 hopanoid, was inhibited by zaragozic acid the heterogeneous membrane distribution of the flotillin-yfp ceased, suggesting the C30 hopanoid is required for correct membrane localisation of flotillin. It is thus likely that cytoplasmic flotillin is degraded. A protein that also was not detected in the membrane following interference in hopanoid pathways, was KinC (Lopez & Kolter, 2010). KinC is a kinase homologous to KinA and KinB that phosphorylates Spo0A, required for sporulation, and is involved in quorum sensing and matrix production (LeDeaux & Grossman, 1995, Lopez *et al.*, 2009). This further implicates the role of the bacterial lipid raft in a variety of cellular functions. Similarly, a flotillin homologue and a KinC homologue were co-isolated with the DRM in *S. aureus* and found to localise in a heterogeneous manner. In the same experiment, YqiK, a protein very similar to flotillin-1 in *E. coli*, was also found to localise to the membrane in a non-homogeneous manner (Lopez & Kolter, 2010).

1.2.6. Nodulation formation efficiency D

NfeD proteins have a conspicuous relationship with SPFH-domain containing genes; genes containing SPFH-domains are usually found adjacent to an *nfeD* (Hinderhofer *et al.*, 2009). NfeD is not found in eukaryotes, yet is present in both Archaea and bacteria. NfeD proteins are categorised as either long (~400 amino acids) or short (~145 amino acids), which can be further divided into three groups: NfeD1a, NfeD1b and truncated NfeD1b. *nfeD1b* is further organised into 4 groups, where *nfeD1b-1* is bacterial and is found upstream of eoslipin, *nfeD1b-2* is found in Archaea and bacteria and is found upstream of *yqeZ*, *nfeD1b-3* is similar to *nfed1b-2* but is upstream of eoslipin, whereas *nfed1b-4* is the main archaeal group and is found downstream of eoslipin (Green *et al.*, 2004). However, due to the presence of *nfeD* immediately downstream of the *floT* of *S. coelicolor*, it is worthwhile exploring at least an indirect relationship between the two.

However, the nomenclature can be extremely confusing; two groups have separately suggested systems for annotating the different *nfeD*s associated with different SPFH proteins. The first to published suggested the system mentioned in the section on flotillins, with SPFH1 being in the same operon as NfeD1, SPFH2 with NfeD2 and so forth, while another suggested an entirely separate method for annotating NfeD, by doing it as the aforementioned NfeD1a, NfeD1b, and truncated NfeD1b (Hinderhofer *et al.*, 2009). For this section, the latter is used.

In total, 76% of NfeD homologues are associated with a slipin gene, and over 85% of *nfeD1b* and *nfeD1a* either have an adjacent eoslipin, paraslipin, *yqfA* or flotillin. The NfeD of *B. subtilis*, YuaF, has not been assigned to any of these groups, as bioinformatics have not yielded enough evidence to assign it to any group as of yet (Green *et al.*, 2009). Sequence analysis show the long variant contains an N-terminal serine protease domain with sequence similarity with the ClpP protease of *E. coli*, a multi-spanning membrane domain and a soluble C-terminal NfeD domain (Yokoyama *et al.*, 2006, Yokoyama & Matsui, 2005). It has been suggested that this protease domain either arose through a deletion whereby a *clpP* protease domain was fused to an *nfeD*, or that *nfeD* originally contained one, but was lost later by some genes (Hinderhofer *et al.*, 2009, Green *et al.*, 2009). The truncated version has an N-terminal hydrophobic region, a soluble five-stranded β-barrel domain homologous to the C-terminal domain of the long variant NfeD, which is thought to form a novel oligosaccharide/oligonucleotide-binding (OB) fold, but it is missing conserved residues normally required for OB, suggesting a protein-protein interactions (Walker *et al.*, 2008, Kuwahara *et al.*, 2008, Green *et al.*, 2009, Yokoyama & Matsui, 2005). The YuaF/NfeD protein of *B. subtilis* colocalises with FloT, but YqeZ, which is encoded directly upstream of *floA*, acts independently of FloA (Dempwolff *et al.*, 2012). A study in *Pyrococcus horikoshii* showed that an NfeD protein was a serine protease that cleaved a flotillin found in the same operon in the C-terminal hydrophobic region, and it was hypothesised that this opened an ion channel (Yokoyama & Matsui, 2005). The σ^{w}-controlled *yqeZyqfAB* operon, which includes an *nfeD*, but no SPFH-encoding gene, grants resistance to the SPβ prophage-encoded bacteriocin sublancin (Butcher & Helmann, 2006). It is worth noting that the NfeD proteins referenced here are genetically unrelated to the original NfeD protein due to automated gene annotation incorrectly annotating sequences as NfeD proteins. The original NfeD protein shows similarity to an ornithine cyclodeaminase, as opposed to the β-barrel and protease domain containing proteins investigated in this study (Garcia-Rodriguez & Toro, 2000, Soto *et al.*, 1994).

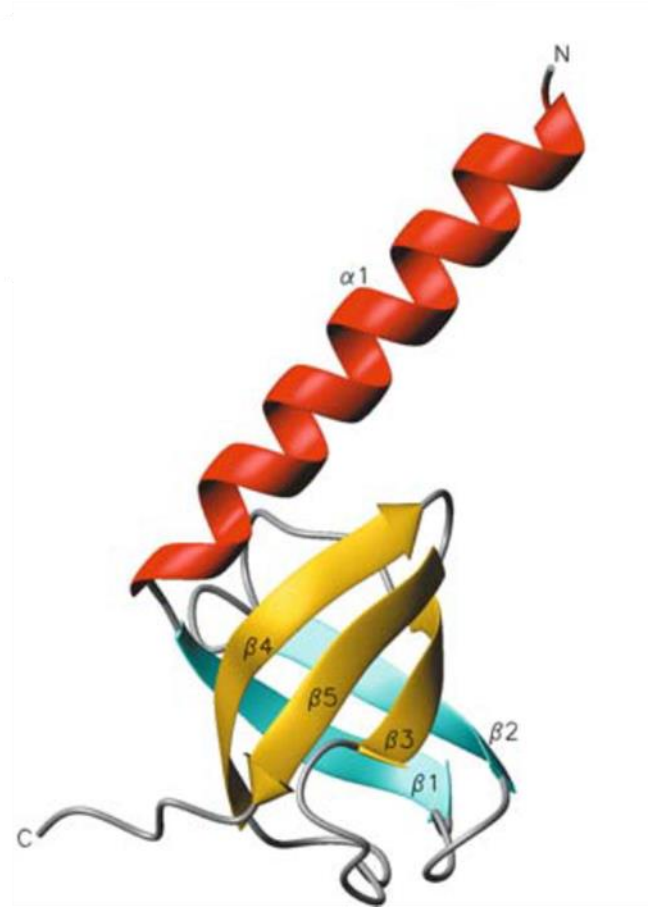

Fig1-8. The sYuaF structure contains an OB-fold. The residues visible are the 97-174 of full-length YuaF from *B. subtilis*. The five β-sheet barrel is the OB-fold, which was previously identified using NMR. The image has been copied (Walker *et al.*, 2008).

While there is no literature available on *SCO3607* and *SCO3608*, the flotillin and NfeD homologues of *S. coelicolor*, respectively, the amino acid structure of the flotillin is remarkably similar to that of both the flotillin of *B. subtilis* and humans. The amino acid structure of *SCO3608* is also very similar to its counterpart in *B. subtilis*, albeit less than the flotillin, and there are no *nfeD*s present in eukaryotes.

1.2.7. Bacterial phospholipids

The main bacterial lipids are PE, PG, and CL. Additionally, many other different phospholipids are synthesised; sphingolipids, sterols, PG derivatives, PG, and the previously mentioned hopanoids (Aktas & Narberhaus, 2015). Bacterial lipids vary greatly depending on the species, stimulus, stress, and part of the life cycle. These differences set them firmly apart from many eukaryotes, however, some differences are less obvious than others; difference in lipid raft phospholipids, and the lack of, with a few exceptions, cholesterol and sphingolipids, but the

presence of hopanoids and CL, with the mitochondrial membrane being considered a bacterial membrane (Pike, 2009, Simons & Ikonen, 1997, Anchisi *et al.*, 2012, Bramkamp & Lopez, 2015). There are also great differences in phospholipid content and not just present phospholipids; of the cell membrane phospholipids in *E. coli* roughly 70% are phosphatidylethanolamine (PE), 20% phosphatidylglycerol (PG), and 5% CL (Raetz & Dowhan, 1990). There is also lipid A, a phospholipid unique to, and synthesised by most, Gram-negative bacteria classed as an endotoxin (Raetz & Whitfield, 2002). On the other hand, in *B. subtilis* PE comprises only 20%, PG, 40%, and CL 25%; the remaining 15% is the zwitterionic lipid lysyl-phosphatidylglycerol (Mileykovskaya & Dowhan, 2005). Changes also occur to phospholipid content during the different life cycle stages; in *S. aureus* phospholipid content changes from the exponential to the stationary phase, CL, PE, and phosphatidylglucose (PGL) increase, respectively from 5-30%, 0.3-7%, and 0.7-1%, while lysylphosphatidylglycerol (LPG) remained constant at around 14% and PG dropped from 76-38% (Short & White, 1971).

1.3. Bacterial biology

1.3.1.1. Cell division in model organisms

Most bacteria grow by binary fission; each cell divides in two. In the case of *E. coli*, the model Gram-negative bacteria, the cell elongates to approximately twice its normal length, doubles its cellular constituents such as DNA and plasmids, and forms a septum in the middle. The septum is the physical barrier formed by the inwards growth of the cell membrane(s) and cell wall. This eventually event causes the cell two split in two. In. *B. subtilis*, the model Gram-positive bacteria, the split occurs without the cell wall as part of the septum (Madigan *et al.*, 2012). In general, most bacteria share the first few stages of cell division, but diverge during the later stages (Errington *et al.*, 2003). Additionally, while E. coli proteins are recruited in a linear process, *B. subtilis* proteins are recruited in a co-dependent manner (Daniel & Errington, 2000).

In this process there are 10-15 proteins that are conserved throughout eubacteria; FtsZ, FtsI, FtsW, FtsA, FtsK, FtsN, FtsL/DivIC, FtsQ/DivIB, ZipA, RodA, MinC, MinD (Natale *et al.*, 2013). It is still not entirely clear what signals the cell to divide, but the two main factors are that of nucleoid occlusion and the Min system. Just prior to cell division initiation there are DNA-free regions of the cell; the two poles and the midcell position. The theory of nucleoid occlusion is based on the divisome, the cell division enzymes and proteins, sense the lack of DNA at the centre of the cell, through unknown mechanisms, whereupon sensing the lack of DNA at the midcell form a Z-ring, which plays a central role in causing the cell contraction. FtsZ is the bacterial tubulin homologue and polymerises to form the Z-ring in a GTP-dependent manner (Lowe & Amos, 1998, Nogales *et al.*, 1998, Scheffers *et al.*, 2002, Diaz *et al.*, 2001). Fts stands for filamentous temperature sensitive, which is due to when these proteins are deleted, the cells become filamentous and temperature sensitive (Errington *et al.*, 2003). Evidence so far shows that as Z-ring can form where there are low concentrations of DNA, suggesting that it is not a binary presence/no presence mechanism, but rather the concentration of DNA that is facilitator (Regamey *et al.*, 2000).

The membrane-associated FtsA and the membrane-bound ZipA anchors the Z-ring to the membrane, though the Z-ring can still form in the absence of either protein, but not both (Pichoff & Lutkenhaus, 2002, Pichoff & Lutkenhaus, 2005, Hale & de Boer, 1997). The same FtsZ residue interacts with both ZipA and FtsA, so these factors suggests FtsA and ZipA have at least partially overlapping roles (Erickson, 2001). *E. coli* containing FtsA mutants with

decreased self-interaction compensated to a large degree for ZipA deletions, suggesting the role of ZipA is actually to antagonise FtsA (Pichoff *et al.*, 2012, Szwedziak *et al.*, 2012).

B. subtilis does not have ZipA; however, it has EzrA. EzrA is conserved in other Gram-positives. EzrA acts as a direct inhibitor of Z-ring polymerisation, and null mutants have additional Z-ring formation and the poles and septa (Levin *et al.*, 1999, Haeusser *et al.*, 2004). EzrA does however also play a secondary role, as loss of function mutation in EzrA and GpsB, which is involved in cell elongation through translocation of PBP-1, severely affects viability (Claessen *et al.*, 2008). Viability is also severely affected by loss of function mutations with SepF and ZapA, both which stabilise FtsZ protofilaments (Hamoen *et al.*, 2006, Gueiros-Filho & Losick, 2002). Finally, EzrA also acts in concert with FtsL in contraction of Z-ring (Kawai & Ogasawara, 2006).

FtsA is thought to promote Z-ring formation through ATP-hydrolysis, recruits further divisome enzyme, and drives cell contraction (Errington *et al.*, 2003). FtsA:FtsZ ratios are important; in *E. coli* the optimal ratio is 1:100, whereas it is 1:5 in *B. subtilis* (Dai & Lutkenhaus, 1992, Dewar *et al.*, 1992). ZipA also localises to the Z-ring, in an FtsZ-dependent, FtsA-independent manner. Increased levels of FtsN can also compensate for ZipA deletions, probably by binding directly with FtsA (Busiek *et al.*, 2012).

The Min system in *E. coli*, consisting of MinC, MinD, and MinE, is better understood. The Min protein name is derived from the mini cells formed by bacteria missing these proteins due to Z-rings forming at the poles (de Boer *et al.*, 1989). MinC, a dimer, is the actual inhibitor of Z-ring formation (Bi & Lutkenhaus, 1993). MinC dimerises is bound by the ATPase activator MinD at the C-terminal, while the depolymerisation of FtsZ occurs at the N-terminal (Hu & Lutkenhaus, 2000, de Boer *et al.*, 1991). MinCD inhibits Z-ring formation at the cell poles by oscillating back and forth every 20 seconds (Raskin & de Boer, 1999b, Raskin & de Boer, 1999a, Hu & Lutkenhaus, 1999). This is driven by MinE, which is localised more centrally than MinCD, but when it moves towards the pole containing MinCD the two proteins move quickly to the opposite pole (Fu *et al.*, 2001, Hale *et al.*, 2001). MinE dimerises at the C-terminal, but its N-terminal interacts MinCD, probably hydrolysing the ATP of the ATP-bound MinD, forcing it from the membrane and into the cytoplasm, whereupon it migrates to the other MinE-free pole (King *et al.*, 1999, Zhang *et al.*, 1998, Zhao *et al.*, 1995, Hu *et al.*, 2002). MinCD statistically spends more time at the cell poles, making the midcell position the favourable position for cell division (Madigan *et al.*, 2012).

However, different bacteria have different approaches to the Min system. *B. subtilis* contains both MinC and MinD, but no MinE. Instead, MinC and MinD stably localise to the poles through the interaction of MinD with DivIVA (Levin *et al.*, 1992, Cha & Stewart, 1997, Karoui & Errington, 2001, Marston *et al.*, 1998). It is worth bearing in mind DivIVA localises to the cell poles due to the negative curvature in these regions (Ramamurthi & Losick, 2009).

Another factor in Z-ring formation is RodA. RodA is an essential protein that translocates Lipid II, a peptidoglycan precursor, across the membrane (Mohammadi *et al.*, 2011, Mohammadi *et al.*, 2007). Cells without RodA do not form a complete septum, leading to a spherical cell shape (Addinall & Lutkenhaus, 1996, Henriques *et al.*, 1998).

FtsK is the next enzyme to be recruited to the divisome, and is recruited before initiation of constriction, but does not become active until later in the cell division process (Lowe *et al.*, 2008, Wang *et al.*, 2005). FtsK is a DNA translocase that assembles as a hexamer, which C-terminal is a DNA translocase domain and N-terminal is required for recruitment of other divisome proteins (Draper *et al.*, 1998, Yu *et al.*, 1998, Di Lallo *et al.*, 2003, Geissler & Margolin, 2005, Dubarry *et al.*, 2010, Massey *et al.*, 2006). Its role is to separate daughter and mother chromosomes, which is done by bringing the *dif* terminus region to the septum where the XerCD recombinase performs decatenation and dimer resolution (Massey *et al.*, 2006, Sherratt *et al.*, 2010). It specifically recruits FtsQ, ZapC, and TolQ (Dubarry *et al.*, 2010, Hale *et al.*, 2011, Gerding *et al.*, 2007).

FtsQ is a 276 residue membrane protein, which periplasmic α-domain contains a POTRA domain, which are domains involved in protein-protein interactions. Its β-domain is also associated with protein-protein interactions (D'Ulisse *et al.*, 2007). Two-hybrid experiments showed FtsQ interacted with up to ten different proteins in the cell divisome, but immunoprecipitation showed it primarily interacts with two of them, FtsB and FtsL (Buddelmeijer & Beckwith, 2004). FtsQ is also considered an attractive target for antibiotics due to its protein-protein interactions with other divisome proteins, its highly conserved nature, lack of eukaryotic homologues that would be affected, and the FtsQBL complex being present in almost all bacteria (den Blaauwen *et al.*, 2014, van den Ent *et al.*, 2008, Grenga *et al.*, 2010, Gonzalez *et al.*, 2010). This complex initiates septal peptidoglycan synthesis and are associated with Z-ring regulation, the latter of which also requires FtsN and FtsA (Tsang & Bernhardt, 2015, Bottomley *et al.*, 2014, Liu *et al.*, 2015). The FtsB of *B. subtilis* is DivIC, and DivIB is its FtsQ homologue (Masson *et al.*, 2009).

Though exact role of FtsL remains elusive, it contains a coiled-coil motif and a leucine zipper motif, both of which are involved in protein-protein interactions (Villanelo *et al.*, 2011). Combined with its poorly conserved structure and that mutagenesis does not seem to be affect it too much, it is likely it is the structure of the protein rather than the residues themselves that are required for function (Sievers & Errington, 2000)

FtsW, the next protein to be recruited to the divisomes, is thought to have a role in lipid 2 translocation, and *ftsW* and its homologues are found close to a class B PBP, such as *ftsI* (Ishino *et al.*, 1989, den Blaauwen *et al.*, 2014). The two types of PBPs, class A and class B, are different in that slass A are bigger and have both transglycosylase and transpeptidase activity, while class B only have transpeptidase activity (Goffin & Ghuysen, 1998). SpoVE is the *B. subtilis* homologue of FtsW based on position on the genome, but its role is in sporulation. (Henriques *et al.*, 1992). However, *ylaO* is thought to be a functional homologue (Errington *et al.*, 2003). FtsW and FtsI have a perfect presence-absence correlation, illustrating their linked functions. Though no direct link between FtsZ and FtsW is evident in *E. coli*, FtsZ-FtsW interactions take place in *M. tuberculosis*, mediated by a C-terminal extension absent in most bacteria (Datta *et al.*, 2002).

FtsI, also known as PBP-3, interacts directly with MrcB, also known as PBP1b, through its N-terminal to catalyse peptide cross-bridging between peptidoglycan glycan chains (Bertsche *et al.*, 2006). Furthermore, it also interacts with the aforementioned FtsW and FtsN, which also interacts with PBP1b and is thought to play a role in modulating its activity (Muller *et al.*, 2007). FtsN is another essential protein required for the recruitment of two non-essential components, AmiC and the Tol-Pal complex (Gerding *et al.*, 2007, Bernhardt & de Boer, 2003).

13.1.2. Sporulation

A few bacteria are capable of undergoing sporulation in response to nutrient depletion or other stress factors, producing endospores. They are much smaller than normal cell, tougher, dehydrated, and metabolically quiescent, making them difficult to kill, as most antibiotics target dividing cells. Upon favourable conditions they become active, undergo germination and outgrowth, making the endospore metabolically active again (Champoux *et al.*, 2004).

B. subtilis has several strategies for survival, such as motility, forming biofilms, taking up DNA, and undergoing sporulation (Vlamakis *et al.*, 2013, Burton *et al.*, 2007, Rao *et al.*, 2008).

When nutrients become lacking or other factors cause *B. subtilis* to undergo sporulation, five autophosphorylating histidine kinases (KinA-D) phosphorylate Spo0F, which phosphorylates Spo0B, which phosphorylates the master regulator Spo0A, now the active Spo0A~P, initiating Stage 0 (Hamon & Lazazzera, 2001, Burbulys *et al.*, 1991). The specific ligands that cause this cascade of events remain elusive, but pyruvate has been identified as a potential candidate (Wu *et al.*, 2013). Spo0A~P then begins to regulate 121 genes to begin sporulation (Molle *et al.*, 2003). Counteracting phosphorylation of Spo0A are the Rap phosphatases (RapA, RapB, RapE and RapH) and Spo0E phosphatases (Mueller & Sonenshein, 1992). Low levels of Spo0A~P will only start biofilm formation as a survival response, whereas higher levels with start sporulation. This is facilitated by its effect on SinI, the inhibitor of the biofilm repressor SinR. At low levels of Spo0A~P it will bind to *sinI* regulatory regions with a high affinity for it, promoting expression, thus inhibiting SinR. However, at higher concentrations, Spo0A~P will also bind the regulatory regions of low affinity, which hinders expression (Fujita & Losick, 2005, Chai *et al.*, 2010).

Once sporulation begins, the cell will now contain two copies of the chromosome. However, these will be entwined with each other and stretching from pole to pole, forming the axial filament, the beginning of Stage 1 (Ryter *et al.*, 1966). It bears reason the exact number of chromosomes is tightly regulated, which is done by three separate proteins. Spo0A~P binds to regions near the *dif* site, the origin of replication, inhibiting additional chromosome replication (Boonstra *et al.*, 2013). Spo0A~P also plays an indirect role in activating transcription of *sirA*, which product inhibits DnaA binding to *dif*, preventing further chromosomal replication (Rahn-Lee *et al.*, 2011). Sda binds to KinA, one of the histidine kinases that starts aforementioned phosphorelay resulting in Spo0A~P, and inhibits sporulation if there is DNA damage or replication effects, thus preventing the cell from initiating sporulation during DNA replication (Cunningham & Burkholder, 2009, Veening *et al.*, 2009). Furthermore, the RacA protein, which localises to the cell poles in a DivIVA-dependent manner, anchors the chromosomes by binding GC-rich inverted repeats at the *dif* site to the cell poles, ensuring each pole receives one chromosome (Ben-Yehuda *et al.*, 2003, Ramamurthi & Losick, 2009).

Up until this point, things have been quite similar to normal cell division; the first obvious difference between cell division and sporulation is the septum forming at one of the cell poles rather than at the midcell position (Levin & Losick, 1996). This stage is the asymmetric septation stage, and the change in the Z-ring position is dependent on increased FtsZ and

SpoIIE levels, a polar septum protein which plays an elusive role in causing polar localisation of FtsZ (Carniol *et al.*, 2005). SpoIIE also dephosphorylates SpoIIAA, which binds SpoIIAB, an inactivator of σ^F, which synthesis has already occurred due to the master regulator Spo0A~P (Duncan *et al.*, 1995). Though SpoIIE is synthesised in both compartments, σ^F is only activated in the forespore, possibly due to the localisation of SpoIIE and decreased levels of SpoIIAB in the forespore (Guberman *et al.*, 2008, Dworkin & Losick, 2001). This asymmetric gene expression is due to only about a third of the chromosome being present in the forespore at this stage, which is thought to be one of the mechanisms through with spatial gene regulation and compartmentalisation occurs (Wu & Errington, 1998, Frandsen *et al.*, 1999).

Spo0A~P also causes expression of σ^E, a sigma factor leading to the expression of genes involved in de novo fatty acid synthesis (Pedrido *et al.*, 2013). Though σ^E is synthesised as an inactive precursor, it is present in both compartments (Fujita & Losick, 2002). To activate σ^E, σ^F leads to expression of SpoIIR in the forespore, which is secreted to the intermembrane compartment, where it activates SpoIIGA, an aspartic protease, through an acylation event (Diez *et al.*, 2012). SpoIIGA then processes σ^E to its active form, beginning the next stage of sporulation, engulfment (Imamura *et al.*, 2008).

During the engulfment step, the mother cell engulfs the forespore. To allow this process to happen, the peptidoglycan must be remodelled, which is carried out by SpoIID, SpoIIM and SpoIID (Abanes-De Mello *et al.*, 2002). While most of the peptidoglycan is degraded, a small amount is still left, and is required for membrane movement during engulfment and thus probably serves as scaffolding role, similar to actin in phagocytosis (Meyer *et al.*, 2010, Tocheva *et al.*, 2013). The engulfment mechanism is a ratchet-like mechanism, where the membrane engulfs the pre-spore compartment through random movements in a SpoIIQ and SpoIIIAH dependent manner, which prevent movement backwards (Broder & Pogliano, 2006, Blaylock *et al.*, 2004, Doan *et al.*, 2005). Membrane fission is then facilitated by FisB, a CL-associated protein (Doan *et al.*, 2013). At this point, the metabolism of the forespore begins to drop considerably, whereupon the mother cell translocates small molecules that continue the expression of genes required for sporulation (Doan *et al.*, 2009, Camp & Losick, 2009). At this point, σ^G, also known as SpoIIIG, is expressed under control of the forespore-specific σF and activated by SpoIIIAA-SpoIIIAH, though chromosome translocation is also thought to play a role, regulating further downstream pre-spore genes, such as the protease SpoIVB and CtpB (Regan *et al.*, 2012). The two serine proteases then cleave SpoIVFA and BofA, two proteins

that form a complex with the metalloprotease SpoIVFB to inhibit it. Active SpoIVFA then converts pro-σ^K into active σ^K (Campo & Rudner, 2007, Resnekov & Losick, 1998, Lu *et al.*, 1995).

The forespore is now completely engulfed, and the coat and cortex assembly stage is inititated. The coat, which is the outermost layer, consists of seventy proteins spread across four layers, the basement layer, inner layer, outer layer, and crust, each of which is dependent on proper assembly of the previous layer, while the cortex consists of specialised peptidoglycan, consisting of an inner layer similar to the vegetative cell wall, while the outer cortex differs in transpeptidation frequency and that it contains muramic lactam (McKenney *et al.*, 2013, Henriques & Moran, 2007, McKenney *et al.*, 2010, Roels *et al.*, 1992, Tipper & Linnett, 1976, Warth & Strominger, 1972, Popham & Setlow, 1993). Its lower transpeptidation is thought to allow the spore to contract and expand in response to otherwise harmful stimuli, such as pH and heat, without germinating, alternatively to allow the spore to rehydrate during germination (Ou & Marquis, 1970, Lewis *et al.*, 1960, Gould & Dring, 1975, Popham *et al.*, 1999).

The coat and cortex assembly stage begins with SpoVM, a very small protein of 26 residues synthesised in the mother cell, localising to the forespore surface through positive curvature (Levin *et al.*, 1993, Ramamurthi *et al.*, 2009). SpoIVA then localises to SpoVM, and begins to form the basement layer of the coat, acting as a scaffolding protein, driving the assembly by ATP hydrolysis (Ramamurthi *et al.*, 2006, Roels *et al.*, 1992, Ramamurthi & Losick, 2008, Castaing *et al.*, 2013). Required for the correct assembly of the inner coat, outer coat, and crust are SafA, CotE, and CotZ and CotY, respectively (Tan & Ramamurthi, 2014). The mother cell synthesises the coat proteins, however some are dependent of signals such as SpoIIQ, SpoVM, and SpoIVA from the forespore for correct coat assembly, but deletion of the two latter abolishes cortex assembly, suggesting they are co-coordinated (McKenney & Eichenberger, 2012, Tan & Ramamurthi, 2014). Though the exact mechanisms of the linked coordination remains elusive, a small mother cell protein named CmpA is involved in cortex assembly through inhibiting cortex peptidoglycan assembly, which effect is overcome by SpoVM and SpoIVA through proteolytic activity (Ebmeier *et al.*, 2012).

The ways in which the cortex differs from the normal cell wall is due to different PBPs, and CwlD and PdaA, which convert muramic acid into muramic lactam, which is required for germination and is required for the cortex-lytic enzymes SleB and CwlJ (Popham *et al.*, 1999,

Gilmore *et al.*, 2004, Popham *et al.*, 1996, Ishikawa *et al.*, 1998). The σK-regulated Mur proteins, MurAA, MurB, MurC, and MurF, are proteins that modify peptidoglycan precursors.

Mutations in two proteins with potential Lipid II flippase activity, SpoVB and SpoVE, the homologue of the aforementioned FtsW, which has flippase activity in vitro, result in peptidoglycan precursor build up in the mother cell and stops cortex assembly. This is due to once the precursors are modified, they are anchored to the outer forespore membrane through Lipid I and Lipid II, with the complex then being flipped into the intermembrane space, where they are subject to further modification by PBBs before forming the cortex (Fay & Dworkin, 2009, Vasudevan *et al.*, 2007, Ruiz, 2008, Ikeda *et al.*, 1989, Mohammadi *et al.*, 2011).

1.3.2. Introduction to *Streptomyces*

There are over 500 different *Streptomyces* identified, making Streptomycetaea the largest family of the actinobacteria. They are Gram-positive, aerobic, sporulating, filamentous, primarily soil dwelling bacteria that grow by as branching hyphae. Its life cycle is essentially split in three stages; sporulation upon favourable conditions, followed by vegetative hyphal growth and scavenging for nutrients. When the nutrients becoming limiting the vegetative hyphae are cannibalised for aerial hyphal growth and begin producing spores. Each of the spore-containing aerial hyphae will contain roughly 50 spores. They are industrially important, with half of Streptomycetes producing antibiotic compounds, 500 different ones in total. This is due to the extensive secondary metabolism of Streptomycetes. However, some streptomycetes produce anti-fungals, anti-parasitic compounds, anti-cancer compounds, respectively nystatin by *S. noursei*, avermectin by *S. avermitilis*, and migrastatin by *S. platensis* (Champoux *et al.*, 2004, Nakae *et al.*, 2000).

Streptomycetes are generally not pathogens, but a few, such as *S. somaliensis* and *S. sudanensis* can cause actinomycetoma (Quintana *et al.*, 2008, el Hassan *et al.*, 2001). Actinomycetoma usually occurs in the cervicofacial area, while other infections, such as thoracic and abdominal infections are rare, can follow traumatic damage. These lesions can generally be treated, but can be difficult to the antibiotic resistance inherent in Streptomycetes (Champoux *et al.*, 2004, Hamid, 2011). Streptomycetes can also be plant pathogens, were they can cause potato scabs. The two types of scabs are common scab and netted scab. The common scab is normally caused by *S. scabei*, but other Streptomycetes can also cause it (Bouchek-Mechiche *et al.*, 2006). These infective species produce a phytotoxin called thaxtomycin located on a pathogenicity island (Bukhalid *et al.*, 1998, Loria *et al.*, 2008, Kers *et al.*, 2005). *S. reticuliscabiei* was found to be

the main cause of the netted scab, but did not contain the thaxtomycin pathogenicity island (Bouchek-Mechiche *et al.*, 2000).

1.3.3. Life cycle of *S. coelicolor*

Streptomycete life cycle is quite different from both *E. coli* and *B. subtilis*. When a streptomycete spore germinates, it forms one to two germ tubes which develop as branching vegetative hyphae. As the spore germinates, it forms hydrophilic vegetative mycelia, which aids in adhering the mycelia the environment (Claessen *et al.*, 2006). Peptidoglycan is incorporated at the hyphal tip, as opposed to *E. coli* and *B. subtilis* incorporating it along the lateral walls in an MreB-dependent manner (Schwedock *et al.*, 1997, de Pedro *et al.*, 2003, Flardh & Buttner, 2009). The mycelium secretes hydrolytic enzymes, many of which are exported with the twin arginine transport system, to break down the insoluble nutrients, such as chitin and cellulose, allowing for absorption of the nutrients (Fukamizo & Brzezinski, 1997). Once nutrients become limiting, the vegetative mycelium is broken down to provide fuel for the aerial hyphae. The aerial hyphae are long, non-septated apical compartments containing at least 50 chromosomes known as the sporogenic cell. It is during this phase that most of the secondary metabolism takes place (Chater *et al.*, 2010).

During its vegetative growth and sporulation *S. coelicolor* utilises many proteins homologous to cell division proteins of *Escherichia coli*, e.g. FtsZ, FtsI and FtsK (Flardh, 2003b, Flardh & Buttner, 2009). Additionally, a protein similar to FtsK, called TraB, is essential for plasmid conjugation in *S. coelicolor* (Thoma *et al.*, 2015). Interestingly, FtsA, ZipA, ZapA, ZapB, EzrA and SpoIIE are all absent in streptomycetes. These proteins are involved in Z-ring assembly or membrane anchoring of Z-ring in *E. coli* and *B. subtilis*, though FtsW and FtsI are possible candidates for Z-ring stabilisation and anchoring in *S. coelicolor* (Datta *et al.*, 2002, Datta *et al.*, 2006). It is thought that the newly incorporated components at the apex are far softer than the ones incorporated earlier, causing turgor pressure to stretch the tip, thus contributing to the cell elongation (Goriely & Tabor, 2003, Miguelez *et al.*, 1992).

The initiation of the aerial hyphae is regulated by the *bld* (for bald, due to the null mutants' inability to form aerial hyphae) cascade, which results in the transcription of surface active proteins, which coats the aerial hyphae in a hydrophobic sheath, allowing for aerial growth by breaking surface tension. Colonies with *bld* mutations are unable to form aerial hyphae, and thus appear to have a bald phenotype, and furthermore, as they cannot sporulate, cannot synthesise antibiotics. The *bld* proteins and enzymes have a wide array of different functions,

as it is not a term for a family of related proteins but rather a phenotype, though many *bld* genes encode regulatory proteins. E. g. *bldA* encodes a tRNA required for the translation of the rare leucine codon TTA, which is present in ~2% of *S. coelicolor genes*, while *bldN* encodes an extracytoplasmic sigma-factor (Leskiw *et al.*, 1991, Bibb *et al.*, 2000, den Hengst *et al.*, 2010). *bldD*, a transcriptional regulator involved in supressing morphological differentiation by supressing transcription of genes required for morphological development. This repression is mediated by c-di-GMP, which forms a tetramer, which causes BldD to dimerise and repress sporulation genes (Tschowri *et al.*, 2014). BldD putatively regulates 167 genes, and of these at least two sigma factors, σ^{BldN} σ^{WhiG}, and 42 (25%) genes encode regulatory proteins (den Hengst *et al.*, 2010).

However, all but two of the *bld* mutants (*bldM* and *bldN*) fail to form SapB, a surface active peptide (Claessen *et al.*, 2006). SapB is a lantibiotic-like peptide encoded in the *ram* (rapid aerial mycelium formation) cluster as *ramS*, which also comprises *ramA* and *ramB*. Molecular modelling supports the hypothesis that SapB coats the hyphal surface. The C-terminus of the *ramC* protein is very similar to lantibiotic modifying enzymes, such as CinM and MrsM, and is thought to modify, at least in part, the *ramS* product to make SapB, though it is not known whether this occurs before or during export (Kodani *et al.*, 2004). *ramA* and *ramB* encode components for an ABC transporter, and RamR, a response regulator, activates the *ramCSAB* operon by binding to its promoter region (Ma & Kendall, 1994, Keijser *et al.*, 2002, O'Connor *et al.*, 2002). Interestingly, when a *bld* mutant is grown in close proximity to a different *bld* mutant or wild-type *S. coelicolor* strain, wild-type phenotype is restored. This is called extracellular complementation (Claessen *et al.*, 2006). Similarly, applying SapB to *bld* mutants also restores the wild-type phenotype (Willey *et al.*, 1991, Willey *et al.*, 1993).

When aerial hyphae escape the aqueous environment, they acquire the rodlet layer. This is a thin, fibrous sheet consisting of paired rods of 8-12 nm in width and 450 nm in length. They are superficially similar in function to the fungal SC3 hydrophobins, and *S. coelicolor* and *S. tendae* complemented with SC3 hydrophobins restores the wild-type phenotype, even if they have no sequence similarity (Wosten, 2001). The is an excellent example of convergent evolution of unrelated organisms exploiting the same niche Furthermore, the fungal hydrophobins can be extracted from SDS-treated cell walls with trifluoracetic acid, and when applied to the cell wall of *S. coelicolor*, this results in the isolation of two homologous proteins, RdlA and RdlB, which is the constituents of the sheet described above. *rdl* mutant strains

lacking a rodlet layer exibit a phenotype where they are covered in fine fibrils with a diameter of 4-6 nm. These fibrils are amyloids, insoluble fibrous protein aggregates, of five proteins, ChpD-H. They are about 55 amino acids long, though there are three other larger chaplins; ChpA-C. The larger ones are about four times as larger, with two domains similar to mature forms of ChpD-H with a C-terminal sorting signal that anchors them peptidoglycan wall (de Jong *et al.*, 2009). Chaplins are secreted by the Sec system to the cell wall where they form amyloid fibrils of paired rodlets in a process that is hypothesised to be dependent on the rodlins. All chaplins provide the cell wall with rigidity and suface hydrophobicity, and ChpE and ChpH perform an additional function, similar to that of SapB, by lowering the surface tension of the medium in submerged cultures (de Jong *et al.*, 2009).

White (*whi*) mutants are capable of forming aerial hyphae, but are unable to sporulate. Their distinctive colour is due to the grey polyketide pigment associated with mature spores being absent in mutants with defects in sporulation pathways. *whi* mutants are linked with *bld* mutations, as some are regulated by *bld* genes, such as BldD, which represses the promoter of *whiG* (den Hengst *et al.*, 2010). *whi* genes can be divided into two groups, early and late, depending on when they are produced. Aerial growth lessens BldD-mediated repression of an early *whi* gene encoding σ^{WhiG}, which signals the onset of sporulation. σ^{WhiG} transcribes *whiH* and *whiI*, which regulate both themselves and each other and are thought to lose their autorepressive abilities in response to lack of growth. *whiA* and *whiB*, two σ^{WhiG}-independent genes, are constantly expressed at low levels, but in response to aerial growth they are strongly upregulated. The function of WhiA is unknown, and WhiB is likely to be a DNA-binding protein. The last early *whi* gene is *whiJ*. Surprisingly, when whiJ The late *whi* genes are *whiD*, which is similar to *whiD, whiE*, which is an enzyme for polyketide synthesis, *whiF*, which is an allele of *whiG*, and three of unknown function, *whiL*, *whiM* and *whiO* (Chater, 2001).

Additionally, the small integral membrane protein CrgA is thought to be involved in the coordination of the switch, maybe by inhibition of cell division (Del Sol *et al.*, 2003, Del Sol *et al.*, 2006). It is during sporulation that many of the secondary metabolites are produced, in response to nutrient depletion, as the secondary metabolites include antibiotics which would reduce competition for the remaining nutrients.

S. coelicolor contains three *mreB* genes, *mreB, mbl* and *SCO6166,* and of these three proteins MreB and Mbl are the most closely related and have a very similar function. SCO6166 is much smaller than MreB and Mbl, of 28.7kDa compared to 36.5 and 37.5kDA, respectively, and

lacks two subdomains of actin-like proteins, IB and IIB. SCO6166 is also transcribed along with a protein homologous to the DnaK-suppressor DksA of *E. coli*. Additionally, SCO6166 is not present in all Streptomycetes, suggesting a non-essential function (Heichlinger *et al.*, 2011a, Jones *et al.*, 2001).

All the proteins show different expression levels during vegetative growth and sporulation; SCO6166 showed high levels of expression during vegetative growth but dwindles rapidly towards sporulation; MreB was expressed at an intermediate level during the vegetative state before dwindling as the cells reach sporulation, whereas Mbl level of expression increased the closer to sporulation the culture was. Mbl and MreB both direct synthesis of the stress-resistant spore wall, with *Δmbl* spores almost as resistant as wild type, but *Δmreb* strains were highly sensitive to lysozyme and vancomycin (Heichlinger *et al.*, 2011a).

S. coelicolor's RodZ homologue, a multidomain protein that localises in a helical manner which in it interacts with MreB in other rod-shaped bacteria, was also interacts with MreB, but not Mbl or SCO6166 (van den Ent *et al.*, 2010, Heichlinger *et al.*, 2011a). MreB and Mbl also colocalise, and Mbl requires MreB for correct localisation.

As mentioned above, MreB in *S. coelicolor* has little effect on hyphal tip extension and rod-shape of *S. coelicolor*, but seems to be involved in sporulation (Flardh & Buttner, 2009). Another protein seems to perform this role in *S. coelicolor*; DivIVA is conserved throughout the Gram-positive bacteria, but has different roles and varying degrees of importance depending on the bacterium. Indeed, most rod-shaped relatives of *S. coelicolor* lack *mreB* genes and assemble their cell walls at the cell poles as opposed to the more common MreB-directed lateral cell wall assembly (Hempel *et al.*, 2008). Deletion and two-hybrid experiments in *Streptococcus pneumonia* showed that deletion caused severe cell division defects, and consistently the two-hybrid experiments suggest DivIVA interacted with cell division proteins. However, DivIVA is required for polar growth in the actinomycetes *Corynebacterium glutamicum* and *M. tuberculosis*, though DivIVA from *M. tuberculosis* and *S. coelicolor* was able to restore polarity in *C. glutamicum* (Lenarcic *et al.*, 2009, Letek *et al.*, 2008). Furthermore, DivIVA is directs hyphal branching by creating foci, marking the site for future branching hyphae. A small number of foci do not develop into hyphae, suggesting it may be a dynamic process (Hempel *et al.*, 2008).

In all the aforementioned bacteria DivIVA-GFP localises to the polar regions and septa, i. e. areas of negative curvature, and it is likely that DivIVA serves as a target for localising proteins to the polar and septal regions (Lenarcic *et al.*, 2009). DivIVA in *B. subtilis* is a 164-amino acid protein and is predicted to be comprised mainly of α-helices and coiled coil, forms dimeric dimer through coiled-coil interactions with the N- and C-terminals linked by a flexible linker at the 57-65 residues, with the F17 and R18 residues part of crossed-loop essential for membrane binding. The F17 and R18 residues are not entirely conserved throughout the Gram-positive bacteria, though the basic properties, hydrophobic and basic, respectively, are conserved (Oliva *et al.*, 2010).

DivIVA in *S. coelicolor,* SCO2077, has a role similar to that of DivIVA in the other actinomycetes, where it is an essential protein and has an important role in tip growth, branching and as a polar determinant. There are a few differences between *B. subtilis* DivIVA and *S. coelicolor* DivIVA; the latter being considerably larger, and the F17 residue substituted for a valine, which is consistent with regards to the hydrophobicity of the residue. The N-terminal is highly conserved in relation to *B. subtilis*, though the rest of the protein is less conserved, maybe due to the C-terminal being responsible for protein recruitment or that less conservation is required for its α-helix structure. Its localisation is the same as other DivIVAs; DivIVA-EGFP fusions localised to areas of negative curvature, but it also localises to the lateral cell walls, where branching occured at small foci of DivIVA (Hempel *et al.*, 2008). It has also been implicated in the localisation of cellulose-like protein to the hyphal tip, consistent with its suggested role in cell division protein localisation (Xu *et al.*, 2008). Overexpression of DivIVA results in aberrantly shaped branches due to DivIVA localising to the lateral walls (Hempel *et al.*, 2008). It is essential for the viability of *S. coelicolor*, and partial depletions led to phenotypes similar to fungal mutants with defects in tip growth or nuclear migration genes, which had not been observed in *S. coelicolor* previously (Flardh, 2003a).

S. coelicolor also contains a protein similar to the *B. subtilis* DivIVA; SCO2669 is similar to DivIVA and contains a predicted forkhead domain. This suggests it anchors DNA to the membrane, if it also binds to the membrane. SCO2669 is also conserved throughout streptomycetes, suggesting an essential function. However, based on sequence similarity, it does not look like it is a membrane protein, regardless of low e values when compared to DivIVA.

Proteins such as DivIVA are localised to areas of high curvature, which is likely due to the CL in these regions (Flardh, 2003a). In eukaryotes, proteins of the BAR domain superfamily are also involved in membrane structure and also contain coiled-coil motifs, in addition to structurally resembling DivIVA (Peter *et al.*, 2004, Shimada *et al.*, 2007, Oliva *et al.*, 2010). BAR domains are also thought to induce and stabilise membrane curvature, moulding membranes to suit cellular processes (Ayton *et al.*, 2007). BAR domains insert like a wedge into the membrane that pushes polar headgroups apart (Farsad *et al.*, 2001, Gallop *et al.*, 2006).

1.3.4. Streptomycete phospholipids

Actinomycetes have extensive fatty acid synthesis pathways, which do not only supply fatty acids for lipid synthesis, but also for triacylglycerides (Olukoshi & Packter, 1994). Though no phospholipid profile is available for *S. coelicolor* in the literature, there is one for the closely related *Streptomyces hygroscopicus*: 27% CL, 46% PE, 5% lysocardiolipin (LCL), 4% dilysocardiolipin (DLCL), 12% phosphatidylinositol mannoside (PIM, and phosphatidic 12% acid (PA) (Hoischen *et al.*, 1997). *S. coelicolor* does synthesise CL, LCL, DLCL, phosphatidylinositol (PI), PE, and PIM. Of these, CL is around 30% of the total phospholipid content of *S. coelicolor*, while in *E. coli* this number is around 5%, yet in *Streptomyces pristinaespiralis* up to 65% (Falcioni *et al.*, 2006). Phosphatidylinositol is absent in *E. coli*, but present in *S. coelicolor* (Raetz & Dowhan, 1990, Borodina *et al.*, 2005).

1.4 Research aims

In order to determine the role of membrane organisation in the establishment of morphological complexity in *Streptomyces*, we investigated the role of SCO3607 and SCO3608, the FloT and NfeD homologues on the morphological development of the model organism *S. coelicolor*. As FloT, at least, is associated with lipids rafts in eukaryotes, a role of these proteins in morphological development might suggest that membrane organisationmight play a role in streptomycete branching development. As the two proteins are found next to each other and are likely to be in the same operon, and additional evolutionary evidence suggests at least an indirect interaction between the two proteins, further bioinformatic information and experiments are required to expand on their evolutionary relationship. With this in mind, elucidating their role in the complex life cycle of *S. coelicolor* through disruption and deletion experiments is the next logical step, similar to what has been done in *B. subtilis*. This allowed a more complete picture of the role of flotillin in *B. subtilis*, and will also give a much more complete picture in ascertaining the phenotypic and microscopic effects the lack of these

proteins will have in *S. coelicolor*. Whether their roles will be similar is uncertain due to the differences in life cycle, but their molecular mechanisms are likely to be the same due to their highly conserved nature.

Furthermore, data on how flotillin potentially interacts with NfeD or other flotillin proteins can yield information about the molecular mechanisms of protein-protein interactions in flotillins in humans and other species due to their highly conserved nature. To this end, bacterial two hybrid experiments represent a simple, yet elegant, route to take. This will potentially not only show whether FloT binds NfeD, but also whether FloT binds FloT or NfeD binds NfeD, and also potentially which region the binding takes places. In short, the aims are to

1) Explore the evolutionary relationship between SCO3607 and SCO3608 and their respective evolutionary origins. Phylogenetic trees will potentially yield information on the evolution of SCO3607 and SCO3608, both within *Streptomyces* and in a wider context. Multiple sequence alignment and evolutionary pressure tests may reveal conserved residues involved in the function of the relevant protein.

2) Conduct mutagenesis assays to test whether the genes are essential for viability. If the genes are essential, knock-down mutants may be attempted. If they are not essential, testing for mutant phenotypes on a variety of agars is the next step.

3) Perform microscopic analysis of the mutants to potentially show additional phenotypes. As it is hypothesised to be involved in cell polarity, special care will be paid to branching and cross-wall assembly, in addition to spore sizes.

4) Test for protein-protein interactions between the two proteins using bacterial two-hybrid assays. The information gleaned from the multiple sequence alignment and bioinformatics will help explore the potential mechanisms involved.

2. Materials and methods

2.1. Growth conditions for bacterial strains and preservation

2.1.1. Plasmids, cosmids, and bacterial strains

Table 2-1A. Table listing the bacterial strains with their genotypes. Antibiotic resistances are listed as amp^r to ampicillin, am^r to apramycin, chlr^r to chloramphenicol, hyg^r to hygromycin, kanr^r to kanamycin, and str^r to streptomycin.

Bacterium genus	**Characteristics**	**Source**
E. coli JM109	Cloning host	(Yanisch-Perron *et al.*, 1985)
E. coli ET12567	*Methylation-deficient strain,* chlr^r	(MacNeil *et al.*, 1992)
E. coli DH5α	Cloning host	(Taylor *et al.*, 1993)
E. coli BW25113	*ΔaraBAD, ΔhsdR*	(Datsenko & Wanner, 2000)
E. coli BTH101	*cya*-deficient strain, str^r	(Karimova *et al.*, 1998)
S. coelicolor BAD106	Control strain, kan^r, am^r	Rajaghopal & Herron, unpublished
S. coelicolor BAD107	Control strain, kan^r	Rajaghopal & Herron, unpublished
S. coelicolor M145	Wild-type	(Gramajo *et al.*, 1993)
S. coelicolor CFW3607A	Tn*5062* insertion at the 3983859 position on the reverse strand, am^r	This study
S. coelicolor CFW3607B	Tn*5062* insertion at the 3983859 position on the reverse strand, am^r	This study
S. coelicolor CFW3607C	Tn*5062* insertion at the 3983859 position on the reverse strand, am^r	This study
S. coelicolor CFW3607D	Tn*5062* insertion at the 3983859 position on the reverse strand, am^r	This study

Table 2-1B. Table listing the bacterial strains with their genotypes.

S. coelicolor CFW3607E	Tn*5062* insertion at the 3983859 position on the reverse strand, am^r	This study
S. coelicolor CFW3607F	Tn*5062* insertion at the 3983859 position on the reverse strand, am^r	This study
S. coelicolor CFW3607G	Tn*5062* insertion at the 3983859 position on the reverse strand, am^r	This study
S. coelicolor CFW3607H	Tn*5062* insertion at the 3983859 position on the reverse strand, am^r	This study
S. coelicolor CFW3607I	Tn*5062* insertion at the 3983859 position on the reverse strand, am^r	This study
S. coelicolor CFW3607J	StH66.1.H03 inserted at the 3983859 position on the reverse strand, am^r, kan^r	This study
S. coelicolor CFW3607K	Tn*5062* insertion at the 3984837 position, am^r	This study
S. coelicolor CFW3607L	Tn*5062* insertion at the 3984837 position, am^r	This study
S. coelicolor CFW3607M	Tn*5062* insertion at the 3984837 position, am^r	This study
S. coelicolor CFW3607Δ	M145 Δ*SCO3607*, am^r, amp^r	This study
S. coelicolor CFW3608Δ	M145 Δ*SCO3608*, am^r, amp^r	This study
S. coelicolor CFW3607/8Δ	M145 Δ*SCO3607* Δ*SCO3608*, am^r, amp^r	This study

Table 2-2A. Table describing the various plasmids and cosmids used in this study.

Plasmid/Cosmid name	**Characteristics**	**Source**
StH66	Cosmid containing *SCO3607* and *SCO3608*, amp^r, kan^r	(Redenbach *et al.*, 1996)
StH66.1.A02	*SCO3607*::Tn*5062*, am^r, amp^r, kan^r	This study
StH66.1.H03	*SCO3607*::Tn*5062*, am^r, amp^r, kan^r	This study
StH66.1.C09	*SCO3609*::Tn*5062*, am^r, amp^r, kan^r	This study
StH66.1.D07	*SCO3606*::Tn*5062*, am^r, amp^r, kan^r	This study
pIJ773	am^r, amp^r, *FRT/FLP*, *oriT*	(Gust *et al.*, 2003)
pIJ790	$chlr^r$, λ RED	(Gust *et al.*, 2003)
StH66C3	*SCO3607* deletion cosmid, am^r, amp^r	This study
StH66C4	*SCO3608* deletion cosmid, am^r, amp^r	This study
StH66C5	*SCO607* and *SCO3608* deletion cosmid, am^r, amp^r	This study
pUZ8002	Non-transmissible *oriT* mobilizing plasmid, kan^r	(Paget *et al.*, 1999)
pMS82	Integrative vector for *Streptomyces*; *oriT*RK2 *int attP*ΦBT1; hyg^r	(Gregory *et al.*, 2003)
pUC19	amp^r	(Yanisch-Perron *et al.*, 1985)
pBGS19	kan^r	(Spratt *et al.*, 1986)
pUT18	*cya-T18* , amp^r	(Karimova *et al.*, 1998)

Table 2-2B. Table describing the various plasmids and cosmids used in this study.

Plasmid/Cosmid name	**Characteristics**	**Source**
pUT18C	*cya-T18* , amp^r	(Karimova *et al.*, 1998)
pUT18C-zip	*GCN4-cya* containing positive control plasmid, amp^r	(Karimova *et al.*, 1998)
pKT25	*cya-T25*, kan^r	(Karimova *et al.*, 1998)
pKNT25	*cya-T25*, kan^r	(Karimova *et al.*, 1998)
pKNT25-zip	*GCN4-cya* containing positive control plasmid, kan^r	(Karimova *et al.*, 1998)
pCFW102	*SCO3607* and *SCO3608* in pUC19, amp^r	This study
pCFW103	*SCO3607* and *SCO3608* in pBGS19, kan^r	This study
pCFW103	*SCO3607* and *SCO3608* in pBGS19, kan^r	This study
pCFW104	*SCO3607* and *SCO3608* in pMS82, hyg^r	This study
pCFW106	*SCO3607* in pUC19, amp^r	This study
pCFW108	*SCO3608* in pUC19, amp^r	This study
pCFW109	*SCO3607* in pUT18, amp^r	This study
pCFW111	*SCO3607* in pUT18c, amp^r	This study
pCFW112	*SCO3608* in pUT18, amp^r	This study
pCFW113	*SCO3607* in pKT25, kan^r	This study
pCFW114	*SCO3608* in pKT25, kan^r	This study
pCFW115	*SCO3607* in pKNT25, kan^r	This study

2.1.2. Antibiotics, chemicals, and media

All media bar SFM was autoclaved at 121°C and 15 psi for 15 minutes. SFM was autoclaved for 30 minutes. Concentrations given as a percent are w/v. Reagents added after autoclaving were filtered through a 0.22µm filter. All media was made up according to Kieser or Sambrook unless otherwise stated (Kieser *et al.*, 2000, Sambrook *et al.*, 1989).

Table 2-3A. Table describing the media used. All agar was adjusted to pH 7.0 with NaOH if necessary. Agar and yeast extract were from Oxoid, tryptone and NaCl from Fisher Scientific, glucose from BDG and mannitol was from Fisher BioReagents. When required, antibiotics were added to the media after autoclaving (see Table 2-4 for concentrations).

Media	**Reagents**
2xYT (Kieser *et al.*, 2000)	16g tryptone 10g yeast extract 5g NaCl dH_2O up to 1L
Luria-Bertani (Sambrook *et al.*, 1989)	10g tryptone 5g yeast extract 5g NaCl 10g agar (plates only) dH_2O up to 1L

Table 2-3B. Table describing the media used.

Media	**Reagents**
Minimal media (MM) (Hopwood, 1967)	0.5 L-asparagine 0.5g K_2HPO_4 0.2 $MgSO_4 \bullet 7H_2O$ 10g agar dH_2O up to 1L 10g glucose added after autoclaving
M9 minimal salts media	33.9g Na_2HPO_4 15g KH_2PO_4 5g NH_4CL 2.5g NaCl 10g agar dH_2O up to 1L 10g glucose added after autoclaving

Table 2-3C. Table describing the media used.

Media	**Reagents**
R5 media (Okanishi *et al.*, 1974)	10.12g glucose 5g yeast extract 5.73g TES buffer 0.1g casaminoacids 2mL trace element solution (see below) 10.12g $MgCl_2 \cdot 6H_20$ 103g sucrose 0.25g K_2SO_4 The following were added after autoclaving: 10mL (0.5%) KH2PO4 4mL (5M) $CaCl \cdot 2H_20$ 15mL (20%) L-proline 1.4mL (1M) NaOH
SFM (MS agar) (Doull & Vining, 1989)	20g soya flour 20g mannitol 20g agar Tap water up to 1L.

Table 2-3E.

Media	**Reagents**
S. O. B. (Hanahan, 1983)	20 tryptone 5g yeast extract 0.548g NaCl 0.186g KCl dH_2O up to 1L $MgCl_2$ added after autoclaving to make a final 10mM solution
S. O. C. (Sambrook *et al.*, 1989)	As S. O. B., but with 3.603g sucrose
Trace Element Solution	40mg $ZnCl_2$ 200mg $FeCl•H_2O$ 10mg $CuCl_2•H_2O$ $MnCl_2•4H_2O$ $Na_2B_4O_7•10H_2O$ $(NH_4)6MO_7O_{24}•4H_2O$ Up to 100mL

Table 2-3E.

Media	**Reagents**
Yeast extract-malt extract medium (YEME) (Kieser *et al.*, 2000)	3g yeast extract 5g peptone 3g malt extract 10g glucose 340g sucrose dH2O up to 1L $MgCl_2 \cdot H_2O$ added after autoclaving to make a final 2mM solution

Table 2-4. Table describing antibiotic usage dependent on bacteria. All antibiotics except chloramphenicol were dissolved in sterile dH_2O, which was dissolved in 96% ethanol.

Antibiotic	**Concentration (*E. coli*)**	**Concentration (*S. coelicolor*)**	**Manufacturer**
Ampicillin	50 μg/mL	N/A	Sigma
Apramycin	100 μg/mL	25 μg/mL	Sigma
Chloramphenicol	10 μg/mL	N/A	Sigma
Kanamycin	50 μg/mL	25 μg/mL	Sigma
Hygromycin	100 μg/mL	100 μg/mL	Sigma

2.1.3. *E. coli* growth conditions

E. coli cultures were grown at 37ºC for 16 hours unless otherwise noted. If grown in liquid cultures, the cultures would be grown at 225rpm sealed with sponge to keep the culture sterile.

2.1.4. *S. coelicolor* growth conditions.

S. coelicolor plate cultures were grown at 30ºC until grey-coloured spores were observed. Liquid cultures were grown until sufficient biomass was observed, or until the liquid cultured entered stationary phase. This was determined by the initiation of the red pigment antibiotic undecylprodigiosin. This usually took two to three days. As with *E. coli*, if a culture was grown in liquid it was grown at 225rpm, but at 30ºC.

2.*1.5.* *S. coelicolor* glycerol stocks

S. coelicolor was streaked out for single colonies on SFM and a single colony was used to make a lawn of bacteria on a fresh plate of SFM. 10mL of sterile 10% glycerol in dH_2O was added to the plate and a sterile cotton bud was used to gently suspend the spores in the 1mL 10% glycerol. The suspension was then transferred to 1.5mL Eppendorf tubes and stored at -20ºC.

2.1.6. *E. coli* glycerol stocks

E. coli was grown overnight with antibiotic selection in 5mL of LB broth at 37ºC at 225rpm. 670µL of the overnight culture was transferred to a sterile Eppendorf tube and 330µL sterile 80% glycerol in dH_2O was then added to the Eppendorf tube. The stock was then stored at -80ºC.

2.1.7. PCR primers

Table 2-5. List of PCR primers used in this work. EZR1 and EZL2 were from a different study (Herron *et al.*, 2004).

Name	Sequence (5' to 3')
SCO3607DELF	TGTTCTCTTCTCTCTGTGTGATTCGGGGGCGTTGTCATGATTCCGGGGATCCGTCGACC
SCO3607DELR	CACGGGCTCTCCCGGCAACCGGTCGACGCGGGGGCGTCATGTGGCTGGAGCTGCTTC
SCO3608DELF	CGAAGCTCAGCGACGGGCGGGAGGGGGACGGCACGCATGATTCCGGGGATCCGTCGACC
SCO3608DELR	ACGAGTGAAGGCAGGGAAGGCAGGAAGGCGCGGACCTCATGTAGGCTGGAGCTGCTTC
SCO3607AF	ATATCTAGAGATGAGTCCTGTCGTCATCG
SCO3607AR	ATAGGTACCCGGTCCGTGATCTCCACCTT
SCO3608AF	ATATCTAGAGATGGCCTGGTTTCTCGG
SCO3608AR	ATAGGTACCCGTCAGCGGTCGACCGGGC
A02F2	GCCTTCCAGATCCAGGACATCAC
A02R2	ATGGTGGTGTGCGGCGACGAC
H03F	GGTCGTGGAGAGCGCGCTCATCTCCCGC
H03R	GCGCGCCGCCGGTATCGCCGCGGCCCA
EZR1	ATGCGCTCCATCAAGAAGAG
EZL2	TCCAGCTCGACCAGGATG

2.1.8. Intergeneric conjugation of *E. coli* with *S. coelicolor*

Transformed *E. coli* ET12567/pUZ8002 was used to inoculate 10mL of LB broth containing kanamycin and chloramphenicol and the appropriate antibiotic for the cosmid and grown overnight. 0.4mL of the culture was then used to inoculate 40mL of LB with the same antibiotic selection and grown to an O. $D._{600}$ of 0.4-0.6. The cells were then washed twice with 25mL of fresh LB to remove antibiotics that might inhibit *Streptomyces* growth. The cells were then resuspended in 1mL of LB. 100µL of *S. coelicolor* spore suspension were added to 500µL of 2xYT and heat-shocked at 50^{o}C for 10 minutes and allowed to cool. 500µL of *E. coli* cells were added to the *S. coelicolor* spores, mixed and pelleted by centrifugation. Most of the supernatant was poured off and the pellet resuspended in the residual liquid (roughly 200µL). From this a 1/1, 1/10 and 1/100 dilution were made and plated out on SFM + 10mM $MgCl_2$ and incubated at 30^{o}C for 16 hours (Kieser *et al.*, 2000).

The plates were then overlaid with 1mL water containing 0.5mg nalidixic acid and the appropriate antibiotic for the resistance cassette being conjugated and incubation was continued at 30^{o}C for another two to three days. Potential exconjugants were selected and plated onto two separate SFM plates, one with apramycin selection and another with apramycin and kanamycin selection. 50 colonies were plated onto each plate in a hex grid and numbered (Kieser *et al.*, 2000). From these two plates double crossovers could be selected based on kanamycin sensitivity and apramycin resistance. The double crossovers were then verified by PCR using the primers in table 2-5.

2.2. Bioinformatics

Protein sequences were retrieved for all experiments by using the Basic Local Alignment Research Tool (BLAST) on the NCBI website, with the accession numbers for SCO3607 and SCO3608 being NP_627802 and NP_627803 (Coordinators, 2017, Altschul *et al.*, 1990). The proteins were selected for the multiple sequence alignment on the basis of articles published about the protein and they were then retrieved from the NCBI website as above. These were then imported in CLC Viewer 7, which was used to perform the multiple sequence alignment.

To construct the phylogenetic trees, the protein query sequence used to retreieve the sequences from NCBI were SCO3607, both human flotillins, and the *Arabidopsis thaliana* sequences. This multiple query method was used to avoid getting false negative results, as there is quite some difference between the flotillin sequence of *Arabidopsis thaliana* and the other flotillins. To find NfeDs, YuaF, YqfA, and SCO3608 were used, as no *nfeD* is present in non-prokaryote genomes as well as guaranteeing both truncated and full-length NfeDs in the BLAST searches. Once all the sequences were compiled, CLC Viewer 7 was used to create a multiple sequence alignment, which was in turn used to construct the phylogenetic trees.

To find sequences for the synteny figure (see Fig3-6), http://strepdb.streptomyces.org.uk was used to find the *SCO3607* and *SCO3608* homologues in other streptomycetes (Fernandez-Martinez *et al.*, 2011).

To calculate the d_N/d_S ratios for evolutionary rogramme can be found here: http://abacus.gene.ucl.ac.uk/software/paml.html pressure for *SCO3607* and *SCO3608*, Phylogenetic Analysis by Maximum Likelihood (PAML) was performed in Yn00, with genetic sequences retrieved from NCBI as above (Coordinators, 2017, Yang, 2007, Yang & Bielawski, 2000).

With protein sequences retrieved from NCBI for SCO3607 and SCO3608 using the accession numbers above, InterPro was used for domain prediction (Hunter *et al.*, 2012).

2.3. Molecular Microbiology methods

2.3.1. Buffers and reagents

Table 2-6. Buffers and reagents used in isolation of plasmid and cosmid DNA from *E. coli*.

Solution	**Reagents**
Solution I	50mM glucose, 25mM Tris-Cl (pH 8), 10mM EDTA, 100µg/mL RNAse A (pH 8).
Solution II	0.2 M NaOH, 1% SDS.
Solution III	60mL 5 M potassium acetate, 11.5mL glacial acetic acid, 28.5mL H2O, results in a final 3M potassium and 5M acetate solution. This was measured pH 5.5.
Lysozyme buffer	0.3M sucrose (10.3%), 25mM Tris, 25mM EDTA, pH 8
Lysozyme	50mg/mL in dH_2O
Proteinase K	50mg/mL in dH_2O.
Phenol: Chloroform	A 1:1 mix of phenol and chloroform.
RNAase A	10mg/mL in 10mM Tris, 15mM NaCl, pH 7.5. Heated to 100^{o}C for 15 minutes.
TAE buffer	

2.3.2. Isolation of plasmid and cosmid DNA from *E. coli*

Cosmid and plasmid DNA was prepared according to (Birnboim & Doly, 1979) or using a Bioline MiniPrep Kit. The former method was used to identify potential clones while the latter was used to isolate DNA for cloning and subcloning.

The relevant cosmid- or plasmid-containing *E. coli* culture was streaked out for single colonies on LB agar containing appropriate antibiotic selection and grown overnight at 37ºC. The single colonies were used to inoculate 25mL Universal tubes containing 5mL LB broth and appropriate antibiotic selection. The culture was grown overnight at 37ºC. 5mL in total of the overnight culture was transferred to a 1.5mL Eppendorf tube and pelleted by centrifugation at 13,000rpm for a minute and the supernatant fraction poured off. This was repeated and 100µL of Solution I (see Table 2-6) was added and mixed by vigorous vortexing until the pellet was fully resuspended. 200µL of freshly prepared ice cold Solution II was added and the contents were mixed by inverting the Eppendorf tube 5 times. 150µL of Solution III was added and mixed by inversion for 10 seconds. The Eppendorf tube was then stored on ice for 5 minutes.

The contents were then pelleted by centrifugation at 13,000rpm for 5 minutes and the supernatant was transferred to a fresh Eppendorf tube containing 400mL of chloroform: phenol. The contents were then mixed by vortexing and then pelleted by centrifugation at 13,000rpm for 5 minutes. The top layer was then transferred to a fresh Eppendorf tube and DNA was precipitated with 600µL of 100% v/v ethanol, mixed by inversion and set to stand at 2 minutes. It was then pelleted by centrifugation at 13,000rpm and the supernatant removed. The remaining 100% v/v ethanol was evaporated by leaving the Eppendorf tube open on the lab bench, and the DNA was then resuspended in 30mL of dH_20. This was then stored at -20ºC.

2.3.3. *S. coelicolor* genomic DNA extraction

50mL YEME media was inoculated with 500µL of *S. coelicolor* spore suspension and grown overnight. 50mg of mycelium was pelleted by centrifugation and resuspended in 500µL lysozyme buffer. 25µL lysozyme and 3µL RNAase A was then added and left to incubate at 37ºC for 30-60 minutes with occasional vortexing and mixing. 10µL 10% SDS was added and the mixture was incubated at 55ºC for 15 minutes. It was then incubated at 37ºC for 30 minutes. 5µL proteinase K was then added and the mixture was incubated at 55ºC for 15 minutes before 200µL 250mM KCl was added and vortexed. 500µL phenol-chloroform was added to remove the protein and the mixture was vortexed for 1 minute before it was centrifuged for 5 minutes at 13,000rpm.

The aqueous layer was then transferred to a new tube with a cut pipette tip, leaving behind as much white interface as possible. The phenol-chloroform step was repeated at least once. This step was repeated twice with 500µL chloroform to remove the phenol which can interfere with downstream applications. The aqueous phase was transferred to a new Eppendorf tube with

3M NaAc (pH 5.2) and dH_2O to make a final concentration of 0.3M NaAc. 54 volumes of isopropanol were added. This was then mixed by inversion until the DNA formed a white lump. The DNA was then transferred to a fresh Eppendorf tube and washed with 70% EtOH by centrifuging it for 5 minutes at 13,000rpm. The supernatant was then removed and the DNA was resuspended in dH_2O (Kieser *et al.*, 2000).

2.3.4. DNA digestion with restriction enzymes.

DNA, either plasmid, cosmid, or nucleoidal in dH_2O was digested with restriction enzymes according to the details of the manufacturer. A standard 20µL DNA digestion was conducted, in order, as follows:

15.5µL of dH_2O containing 1µg DNA

2µL of appropriate 10x buffer

2µl of 1µg/µl acetylated BSA

This was made up in a 0.6mL Eppendorf tube on ice and mixed by pipetting. 0.5µL of 10u/µL restriction enzyme was then added to take the restriction enzyme mixture up to 20µL. The Eppendorf tube was then transferred to a 37^{o}C water bath and incubated for 2-4 hours. For higher DNA concentrations, the digestion mixtures were left overnight in the 37^{o}C water bath.

For double digestions, 0.5µL of dH_2O was replaced with another 0.5µL of restriction enzyme. Acetylated BSA was diluted from manufacturer's stock and stored at -4 ^{o}C to minimise thawing and refreezing. The restriction enzymes utilised were from Promega.

2.3.5. Agarose gel electrophoresis

Agarose was added to TAE buffer to make a 1% w/v mixture and microwaved until the agarose was dissolved. This was left to cool at room temperature until steam was no longer visible. Ethidium bromide was then added to make a solution of 0.5µg/mL ethidium bromide. All equipment was handled using gloves. The liquid was then poured into the casting tray and the comb added to form the wells. Either plastic walls or autoclave tape was used to prevent the liquid from spilling out the sides. This was then left to stand until the gel had solidified. The size of the wells was dependent on the size of the sample to be run.

Once the gel had solidified, the comb and tape or plastic walls were removed and the gel, still on the casting tray, was put into the tank. It was then filled up with TAE buffer so the gel was covered. This was the running buffer. Dye was added to the DNA samples to be run at a ratio

of 1:10 of dye: DNA. The samples were loaded into the wells. DNA was loaded at the negatively charged end of the tank, allowing the DNA to migrate to the positively charged pole at the other end of the tank. Gel electrophoresis was conducted until the bands had migrated $3/4^{th}$ of the agarose gel, at 50 or 100 volts for 1-2 hours.

Alternatively, gel electrophoresis was conducted without ethidium bromide being added to the gel before the it had set. This was performed at 40 volts and when the DNA had migrated across three quarters of the gel, ethidium bromide was added to the running buffer to make an 0.5µg/mL concentration. All waste was then disposed of accordingly and all equipment which had been in touch with ethidium bromide rinsed thoroughly with water. Gloves were used to handle all the equipment.

2.3.6. DNA extraction from agarose gels.

The PCR and gel electrophoresis DNA was cleaned and extracted in accordance with the manufacturer's instructions, with some minor changes. The NucleoSpin® Extract II (Macherey-Nagel) kit was used. The band containing the DNA to be purified was cut out of the gel. The slice could weigh up to 100ng and was dissolved in 200µL buffer NT. This was then incubated in a water bath for 10 minutes at 50^{o}C with brief vortexing every 2-3 minutes. The mixture was then transferred to a column in a 2mL collecting tube and centrifuged at 13,000rpm for 1 minute. The DNA, now bound to the column, was kept and the flowthrough discarded. 600µL buffer NT3 was added to the column and was then washed by centrifugation at 13,000rpm for 1 minute. It was then centrifuged again at 13,000rpm for 2 minutes to remove residual buffer NT3. Buffer NT3 contains ethanol and this could potentially interfere with downstream applications. The DNA was eluted by transferring the column to a 1.5mL Eppendorf tube and adding 20µL sterile dH_2O to the column before centrifuging it at 13,000rpm for 1 minute.

2.3.7. Polymerase chain reaction

2.3.7.1. PCR primer design

Polymerase chain reaction (PCR) primers were designed by using Clone Manager 3.0 by SciEd Software to analyse the sequence and relevant restriction sites were added to either side. PCR primer length was restricted to less than 25 nucleotides, unless otherwise noted. Primer3 software was used to analyse the primers to check for issues related to the primers, such as self-

annealing primers, similar denaturation temperatures, and hairpin loops (Rozen & Skaletsky, 2000).

2.3.7.2. PCR reaction

OneTaq DNA polymerase from NEB was used for all standard PCR reactions. OneTaq PCR reactions were set up as follows: 5µL 10x OneTaq Reaction Buffer, 1µL 10mM dNTP mixture, 2µL 0.4µM primer mixture in dH_2O, 1µL 1-10ng template in dH_2O, 1µL MyTaq DNA polymerase, and dH_2O up to 50µL. MyTaq from Bioline was used to find out the different annealing temperatures and confirm the presence of genes. MyTaq PCR reactions were set up as follows: 10µL 5x MyTaq Reaction Buffer, 1µL 0.4µM primer mixture, 1µL 1-10ng template, 1µL MyTaq DNA polymerase, dH_2O up to 50µL. Bovine serum albumin (Bioline) was added to make a final solution of 20mg/mL if the PCR yield was poor.

The PCR cycle was done as described in Table 2-7.

Table 2-7. Table detailing standard PCR programme.

Step	Temperature	Time	Number of cycles
Initial denaturation	94°C	30 seconds	1
Denaturation	94°C	30 seconds	30
Annealing	45-68°C (up to 72°C for MyTaq	1 minute	30
Extension	68°C for OneTaq and 72°C for MyTaq	1 minute per kb	30
Final extension	68°C for OneTaq and 72°C for MyTaq	5 minutes	1
Hold	4°C		

2.3.8. DNA ligation

When inserting a stretch of DNA (insert) into a plasmid or cosmid (vector), a ligation experiment was conducted. The insert to be ligated into the vector originated from either a PCR experiment (cloning) or already existed in a separate plasmid or cosmid (subcloning). PCR was

typically used when restriction enzyme sites had to be added to the ends of the insert, thus the PCR was conducted as described (See Chapter 2.3.7.) to create these sites and amplify the insert. The insert was then isolated from an agarose gel (See Chapter 2.3.6.). This was then restriction enzyme digested with the appropriate restriction enzymes (See Chapter 2.3.4.) If the insert was already available in an existing plasmid or cosmid or originated from an earlier cloning experiment, this was isolated from *E. coli* (see Chapter 2.3.2.), but was otherwise subject to the same procedures.

Once the insert and vector were both digested, the appropriate concentrations for the ligation reaction mixture were calculated according to the following equation:

Insert ng = (Ng of vector x kb size of insert)/(kb size of vector) x molar ratio of insert/vector

The amount of vector was typically 100ng and the molar ratio from 3-10, and dH2O was added to make the ligation reaction 8.5 µL. 1µL of 10x ligase buffer (Promega) was then added before 0.5µL T4 DNA (Promega) ligase was added. This was left at 4 ^{o}C overnight. The ligated plasmid was then transformed into *E. coli* DH5α (See Chapter 2.3.10-11).

Concentrations were measured using a NanoDrop 2000c (Thermo Scientific).

2.3.9. Preparation and transformation of electro-competent *E. coli*

All equipment was chilled on ice or in a freezer prior to production of electro-competent cells. *E. coli* DH5α was streaked out for single colonies from -80^{o}C glycerol stocks on M9 minimal salts agar and incubated overnight at 37^{o}C. Single colonies were used to inoculate 5mL LB broth cultures and incubated overnight at 225rpm at 37^{o}C.

50mL LB broth containing 1mL 1M $MgSO_4$ in a 250mL Erlenmeyer with relevant antibiotics was inoculated with 0.5mL from the overnight cultures and grown to between 0.3 and 0.45 $O.D_{600}$. The cultures were then chilled on ice for 30 minutes, transferred to 50mL Falcon tubes and pelleted by centrifugation at 4^{o}C for 10 minutes at 2500rpm. The supernatant was poured off and 25 mL of 10% glycerol was added. They were left on ice for 90 minutes and were very gently resuspended. The cells were washed another two times with 10% glycerol. The cells were then resuspended in the remaining 10% glycerol. 50µL aliquots were stored at -80^{o}C.

5µL plasmid or cosmid DNA was added to a 50µL electro-competent cell aliquot and the mixture was electroporated in an electroporation cuvette. 1mL of ice cold LB was immediately added, and transferred to a 10mL Universal tube. This was then grown without antibiotics for

1 hour at 225rpm and 37ºC (an extra half hour was added for cosmid transformation and/or ET12567/pUZ8002). 250µL of the culture was spread onto LB agar containing the appropriate antibiotics and grown overnight.

2.3.10. Preparation and transformation of chemically competent *E. coli*

E. coli was streaked out for single colonies and used to inoculate a culture as per electro-competent *E. coli*. The 50mL culture was then pelleted by centrifugation for 10 minutes at 4100rpm and resuspended in 12.5mL of ice cold 100mM $MgCl_2$.The cultures was pelleted by centrifugation again for 10 minutes at 4100rpm and the pellet was resuspended in ice cold $CaCl_2$. 22mL of $CaCl_2$ was then added and kept on ice for at least 20 minutes. It was again pelleted by centrifugation for 10 minutes at 4100rpm and resuspended in 100mM $CaCl_2$ in 20% glycerol w/v and dispensed in 100µL aliquots.

Chemically competent cells were thawed on ice, moved to a 15mL Falcon tube, and the relevant cosmid, plasmid, or ligation mixture was added and left on ice for a minimum of 30 minutes. They were then heat-shocked at 42ºC for 45-50 seconds, stored on ice for 10 minutes before 900µL of ice-cold SOC was added. The culture was then incubated at 37ºC degrees for 1 hour. If it was a cosmid being transformed or ET12567/pUZ8002 was used, an extra hour was added to the incubation period. The transformations were then plated out on LB with appropriate antibiotic selection, with 250µL transformation culture per plate, and left incubated overnight at 37ºC degrees. If ET12567/pUZ8002 was used it could take longer for colonies to become visible.

2.3.11. PCR targeted mutagenesis in *S. coelicolor*

The PCR targeting system protocol is used to insert PCR products into cosmids which are used downstream to alter stretches of the chromosome of *S. coelicolor* through genetic recombination, such as redirect knockouts and GFP-tagging. Long PCR primers (39 nucleotides) were used amplify the sequence, and then used to transform *E. coli* cells containing the cosmid with the relevant gene after the induction of the *E. coli* λ RED gene. Due to *E. coli* normally degrading linear DNA through the RecBCD exonucleases, a strain containing λ RED is used, as it improves the recombination rate of linear DNA. A genetic cross-over event takes place, and the new cosmid, now containing the desired changes, is extracted and purified. This is then used to transform the methylation-deficient *E. coli* strain ET12567 to circumvent the methyl-specific restriction system of *S. coelicolor*. The cosmid is

then conjugated into *S. coelicolor*, where another cross-over event takes place, resulting in the desired change.

Long PCR primers were designed for this and Expand high fidelity PCR system (Roche) was used for the PCR.

Table 2-8. PCR reaction composition for PCR targeted mutagenesis.

Reagent	Amount
Primers (100pmoles/µL)	0.5µL each
Template DNA (100ng/µL)	0.5µL
Buffer (10x)	5µL
dNTPs (10mM)	1µL each
DMSO	2.5µL
DNA polymerase	1µL
dH_2O	36µL
Total volume	50µL

Table 2-9. PCR cycle conditions for PCR directed mutagenesis.

Step	Temperature	Time	Number of cycles
Initial denaturation	94^{o}C	2 minutes	1
Denaturation	94 ^{o}C	45 seconds	10
Annealing	50^{o}C	45 seconds	10
Extension	72 ^{o}C	90 seconds	10
Denaturation	94 ^{o}C	45 seconds	15
Annealing	50^{o}C	45 seconds	15
Extension	72 ^{o}C	90 seconds	15
Final extension	72 ^{o}C	5 minutes	1
Hold	4 ^{o}C		

The PCR product was gel purified as detailed above.

E. coli BW25113/pIJ790 was grown overnight at 30^{o}C in 10mL LB with chloramphenicol. Electrocompetent cells were made from the overnight culture, with the following adjustments: they were grown at 30^{o}C in SOB containing 20mM $MgSO_4$. The cosmid to be subject to genetic recombination was then used to transform the cells.

New electro-competent cells were made from the newly transformed cells, containing the cosmid, with the following alterations from the previous protocol: They were grown at 30^{o}C and in S. O. B. containing 10mM L-arabinose and grown to an O. $D._{600}$ of 0.5-0.6. They were then electroporated with the purified PCR product.

Antibiotics were used to screen the transformants for recombinants, and then the recombinants were isolated and used to transform chemically competent *E. coli* JM109 for storage. The cosmid was then conjugated into *S. coelicolor* M145 using the protocol described earlier, and double crossovers were screened for. Double crossovers were then verified by PCR (Gust *et al.*, 2003).

2.4. Bacterial two hybrid experiments

Bacterial two hybrid experiments were performed using two plasmids containing genes translationally fused to one of two CyaA domains, T-18 and T-25, derived from pUC18, pUC18C, pKNT25, or pKT25. The two former plasmids contain the T-18 domain, while the two latter contain the T-25 domain. Positive controls were performed with pKNT-zip and pUC18C-zip (Karimova *et al.*, 1998).

Each combination strain was created by transforming chemically competent *E. coli* BTH101 with two plasmids with complementary CyaA domain fusions, selecting with kanamycin and ampicillin (See Chapter 2.3.10). The strain was then plated out on an LB agar plate containing kanamycin and ampicillin selection, 0.1mM IPTG, and 20 µg/mL X-GAL and incubated at 37˚C for 24 hours. They were then transferred to a fridge for 48 hours, which further developed the colours. If the two proteins interacted, the two CyaA domains, T-18 and T-25, would associate and cAMP would be produced. cAMP then associates with CAP, which activates the *lac* operon, which ferments X-GAL, which turns the colonies blue, confirming the interaction of the two CyaA domains (Karimova *et al.*, 1998).

2.5. Microscopy methods

2.5.1. Preparation of samples for microscopy

A Schwedock stain was used to visualise peptidoglycan and DNA (Schwedock *et al.*, 1997). Fluorescein wheat germ agglutinin (WGA) and propidium iodide (PI) stain peptidoglycan and DNA, respectively. Eight microscope slips were sterilised by dipping in ethanol and flaming and set at a 45^{o} angle in SFM. An *S. coelicolor* spore suspension diluted 1/10 in dH_2O was used to inoculate the sterile microscope slips in SFM and incubated at 30^{o}C.

Measurements were performed in IPLab on the images taken at the three different time points.

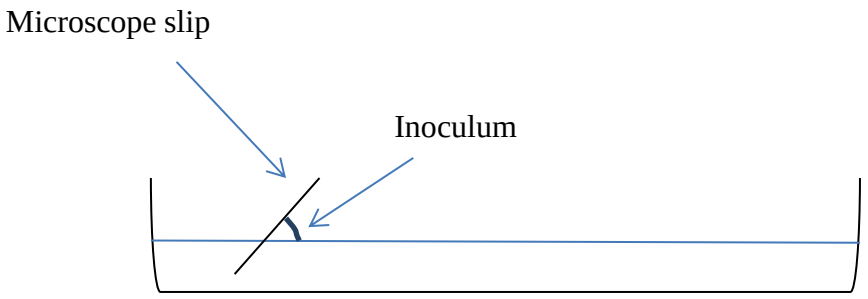

Fig 2-1. Schematic describing microscope slip preparation for Schwedock staining.

A sample was taken at three times points; after 24, 48, and 72 hours. Each slip subject to the same stain. Cells were fixed using 500µL fixative (see Table 2-10) at incubated for 15 minutes, then washed twice with PBS and allowed to air dry. The slip was then rehydrated in PBS for 5 minutes before being incubated with 2mg/mL lysozyme in GTE for 1 minute and being washed with PBS. The slip was then incubated with 2% BSA in PBS for minutes before stain was added and was then left to incubate for 1-3 hours in the dark. The slip was then washed 8 times with 10µg/mL propidium iodide in PBS in the dark. 10µL of SlowFace® Gold Antifade reagent (Life Technologies) was then added and the slides were mounted on microscope slides using clear nail varnish.

Table 2-10. Composition of reagents required for Schwedock staining.

Solution name	Reagents
PBS	8g NaCl 0.2g KCl 1.44 Na2HPO4 KH2PO4 dH2O up to 800mL pH to 7.4 with HCl and then add dH_2O up to 1L
GTE	50mM glucose 20mM tris, pH 8 20mM EDTA
Stain	2µg/mL fluorescein-WGA 10µg/mL propidium iodide
Fixative	0.0045% glutaraldehyde 2.8% formaldehyde In PBS

2.5.2. Fluorescence Microscopy

Microscopy was performed using a Nikon TE2000S inverted microscope at 100x magnification. A Hamamatsu Orca-285 Firewire Digital CCD camera was used to take the photos, and image processing was done using IPlabs 3.7 image processing software (BD Biosciences Bioimaging, Rockville, Maryland, USA). FITC, TRITC and Brightfield filters were used for imaging.

2.5.3. Image analysis

Images were analysed using ImageJ, IPLab, and Microsoft Excel. IPLab was used to analyse and measure the distances for the various experiments detailed in Chapter 5. These results were

then exported to Excel, which was used for statistical analysis of the results. ImageJ was used as an image editing programme for the images in Chapter 5. The data was then expressed as a histogram. The distribution of each measurement was organised into increments of 5µm to create a set of concise and manageable data. Tip to cross-wall and tip to branch were expressed up to 70µm, while cross-wall to cross-wall and branch to branch expressed up to 40µm. This was due to the much shorter distance between the two latter measurements. Standard error was calculated for each bar within the histogram separately. Standard error was expressed as: $\sqrt{\frac{\frac{y}{n}\times\left(1-\frac{y}{n}\right)}{n}}$

where y= % of the total distribution within the specific range and *n* is the total number of samples. Standard error was chosen instead of standard deviation, as ascertaining the accuracy of the sample representing a population was deigned the most appropriate. Tests of significance were performed using p-tests in MiniTab17, found using the Whitney-Mann test, due to the non-parametric nature of the data.

3. Bioinformatics

3.1.1. Introduction

Genes encoding NfeD and SPFH proteins, sometimes referred to as slipins, are rarely found without the other adjacent in prokaryotes, though exceptions such as *yqeZ/nfeD* of *B. subtilis* exist. Over 85% of *nfeD* homologues are immediately adjacent to a gene encoding one of the following SPFH proteins eoslipin, paraslipin, or flotillin, with one paper erroneously reporting all known genes encoding stomatins being immediately adjacent to *nfed*, as examples to the contrary exist in at least actinobacteria (Green *et al.*, 2009, Dempwolff *et al.*, 2012, Green *et al.*, 2004). *nfeDs* are not found outside prokaryotes, making this association exclusive to prokaryotes (Green *et al.*, 2004). Attempts to organise the SPFH domain proteins began in 1999, when the SPFH domain was first conceptualised to describe the shared domain of stomatins, prohibitins, flotillins, and HflC/K, though this domain superfamily has later been criticised for its lack of sequence alignment and the position the domain assumes in the various proteins (Tavernarakis *et al.*, 1999, Rivera-Milla *et al.*, 2006). The SPFH proteins were then later split into 12 groups, with the four first groups being the ones of interest; stomatins belong to group SPFH1, flotillins to group 2, HflC/K to group 3, and prohibitins to group 4 (Hinderhofer *et al.*, 2009).

In *S. coelicolor*, the protein most similar to the human flotillins is SCO3607, though there are several other proteins that are similar. SCO3532, SCO5397 (Scy), SCO3286, SCO6053, and SCO4254 all show similarity with flotillin, though this due to being members of the wider SPFH family or containing similar domains. SCO3608 is the only protein present in *S. coelicolor* similar to YuaF of *B. subtilis*. All of this taken together means SCO3607 and SCO3608 are the best candidates for flotillin-like and NfeD homologues in *S. coelicolor*.

Nomenclature for *nfeD* is slightly trickier than that of flotillin, as the originally characterised NfeD is unrelated to the NfeDs discussed here. NfeD was originally the name given to a 320-residue ornithine cycloamidase involved in **n**odulation **f**ormation **e**fficiency due to its role in nodulation (Soto *et al.*, 1994). Later, genes were incorrectly labelled *nfeD* due to a software error, and though attempts were made to rectify this, *nfeD* became the name for a new type of gene. The *nfeD*s discussed here do not encode the originally annotated ornithine cycloamidases, but rather a full-length protein of 460 amino acids, or a truncated protein of roughly 145 amino acids. The full-length NfeDs contain an N-terminal serine protease domain,

similar to ClpP protease domains, and a C-terminal soluble 5-strand β-barrel, the NfeD domain (Yokoyama & Matsui, 2005, Yokoyama *et al.*, 2006). The truncated version differs by not encoding the N-terminal serine protease domain.

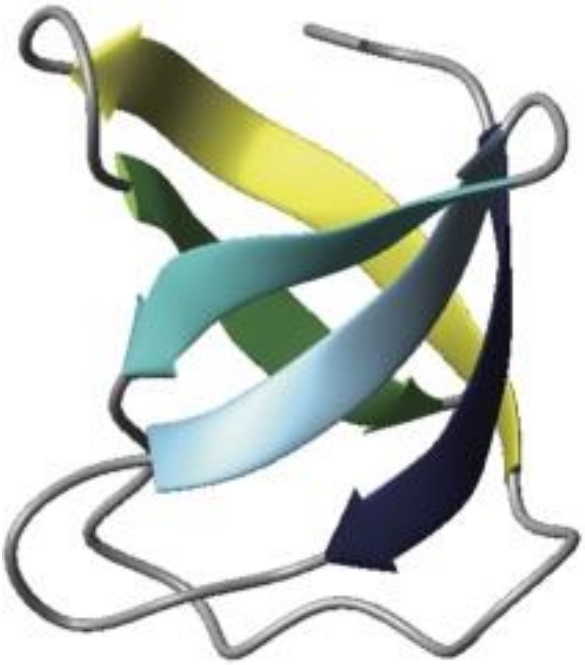

Fig3-1. The C-terminal domain of PH0471, an NfeD present in *P. hyrokoshii*. The 5 β-sheets are, in order, navy, sky blue, cyan, yellow, and green. The image is reproduced (Kuwahara *et al.*, 2008)

There are two systems of nomenclature for NfeDs. The first is based on which SPFH it is associated with, resulting in stomatin-associated NfeDs being designated as NfeD1, and the flotillin-associated as NfeDd2 (Hinderhofer *et al.*, 2009). However, this system of nomenclature is very wide, so a different system of nomenclature has been suggested for *nfeD*-like genes as a whole, as *nfeD* is not always found adjacent to an SPFH-encoding gene, such as *yqeZ* (Dempwolff *et al.*, 2012). This system of nomenclature bases itself more on genetic similarity than genetic association with other proteins, though this is problematic due to horizontal gene transfer that has taken place, which makes a fully comprehensible system difficult to achieve (Green *et al.*, 2009). In the latter system of nomenclature, which only deals with NfeD, the NfeD family consists of three groups; NfeD1a, NfeD1b, and truncated NfeD1b. NfeD1b consists of roughly 460 residues, organised into an N-terminal Clp-protease domain, a central membrane-spanning domain, and C-terminal soluble domain consisting of β-sheets

which assembles into an oligosachaccaride binding-fold (OB-fold). Normally, OB-folds interact with nucleic acid, however, the OB-fold of the NfeDs lack ionic residues required for oligosaccharide binding (Kuwahara *et al.*, 2008, Theobald *et al.*, 2003).

The C-terminal domain is what forms the main body of the NfeD1a, which are around 160 residues long. They are highly divergent, and though they more closely resemble the structure of NfeD1b, they are more closely related to NfeD1b. NfeD1a has four separate subgroups, all of which arose independently from a common ancestor (Green *et al.*, 2009).

3.1.1.2. Aims and goals

In elucidating the role of flotillins and NfeD proteins in the life cycle of *S. coelicolor*, bioinformatic investigation of the candidate genes and their product will provide a solid foundation for future experiments. Clarifying their evolutionary relationship will also provide a clearer basis to which create hypotheses concerning their roles.

The goal of this Chapter is

1) To ascertain the domains present in the two proteins to find potential domains or motifs involved in different types of interactions, such as OB-fold potentially involved in protein-protein or protein-DNA interactions and protein cleavage (as in *P. hyrokoshii*) (Yokoyama *et al.*, 2006, Kuwahara *et al.*, 2008). Identifying how closely related SCO3607 is to human flotillin also impacts the possibility of the protein being used as a model for research into human flotillin. This will allow for better hypotheses on potential interactions based on other experiments.
2) To explore which residues or base pairs are highly conserved throughout the streptomycetes and a wider range of organisms, to identify genetic and protein regions of greater importance to cellular function.
3) To examine the evolutionary relationship between flotillins and NfeD proteins through the use of phylogenetic trees. This, together with 2), can help elucidate where the genes fit in the different families, such as the NfeD1A, Nfed1B, and the four independently truncated NfeD1B groups (Green *et al.*, 2009).
4) To investigate the evolutionary pressure on each gene to calculate the *in silico* importance of the conservation of the gene.

3.2. Multiple sequence alignment and domain prediction

3.2.1. Multiple sequence alignment.

3.2.1.1 Flotillin

A multiple sequence alignment of SCO3607 and other relevant proteins was conducted. While there are other proteins similar to flotillin in *S. coelicolor*, SCO3607 is the most similar protein. SCO3542 is the protein that is a distant second most similar protein, based on its coiled-coil region. However, it is three times as large as flotillin. Other proteins include Scy due to its coiled-coil region being somewhat similar to HflC, a member of the SPFH superfamily, but similar to SCO3542, it is three times as large and only slightly similar to flotillin. These were picked based on how well each is characterised and give a wide spread of evolationarily related organisms.

Flotillins from humans and the *Bacillus* genus were picked, in addition to the flotillin homologue of *S. lividans*. These were picked to potentially identify conserved residues or regions that may be involved in protein function rather than map their evolutionary relationship, which is investigated using phylogenetic trees. Several studies of the flotillin, and NfeD, of *B. subtilis* have been conducted, and one has been conducted for *B. halodurans*, improving the usefulness of comparisons with the *S. coelicolor* proteins (Schneider *et al.*, 2015, Mielich-Suss *et al.*, 2013, Bach & Bramkamp, 2013, Yepes *et al.*, 2012, Dempwolff *et al.*, 2012, Zhang *et al.*, 2005). As they are already somewhat characterised, the level of similarity could hint at shared functionality and conserved regions important to them. The two human flotillins were picked as they are currently subject to rigorous research and much is known about them, so lessons learned from them may be applicable to the flotillin of *S. coelicolor* (Zhao *et al.*, 2011). Depending on their degree of similarity, research on flotillins in *S. coelicolor* may shed light on the more difficult to research human flotillins. *S. lividans* was also picked, as genetic drift between these two very similar organisms would illuminate potentially non-essential residues. Proteins were used rather than genes; this is due to the problems with introns and exons associated with comparing eukaryotic and prokaryotic genes. Proteins are also conserved at a functional level, as silent mutations do not affect protein function. Though RNA structure can affect transcription, such as stem-loops in for example bacilli, this is generally not an issue with prokaryotes (Deiorio-Haggar *et al.*, 2013). The accession numbers for YuaG (*B. subtilis*), YuaG (*B. halodurans*), flotillin-1, flotillin-2, SCO3607 and FloT (*S.*

lividans) are, in order: KIX81581.1, WP_010899631.1, AAC35387.1, AAV38285.1, NP_627802.1, WP_016326576.1.

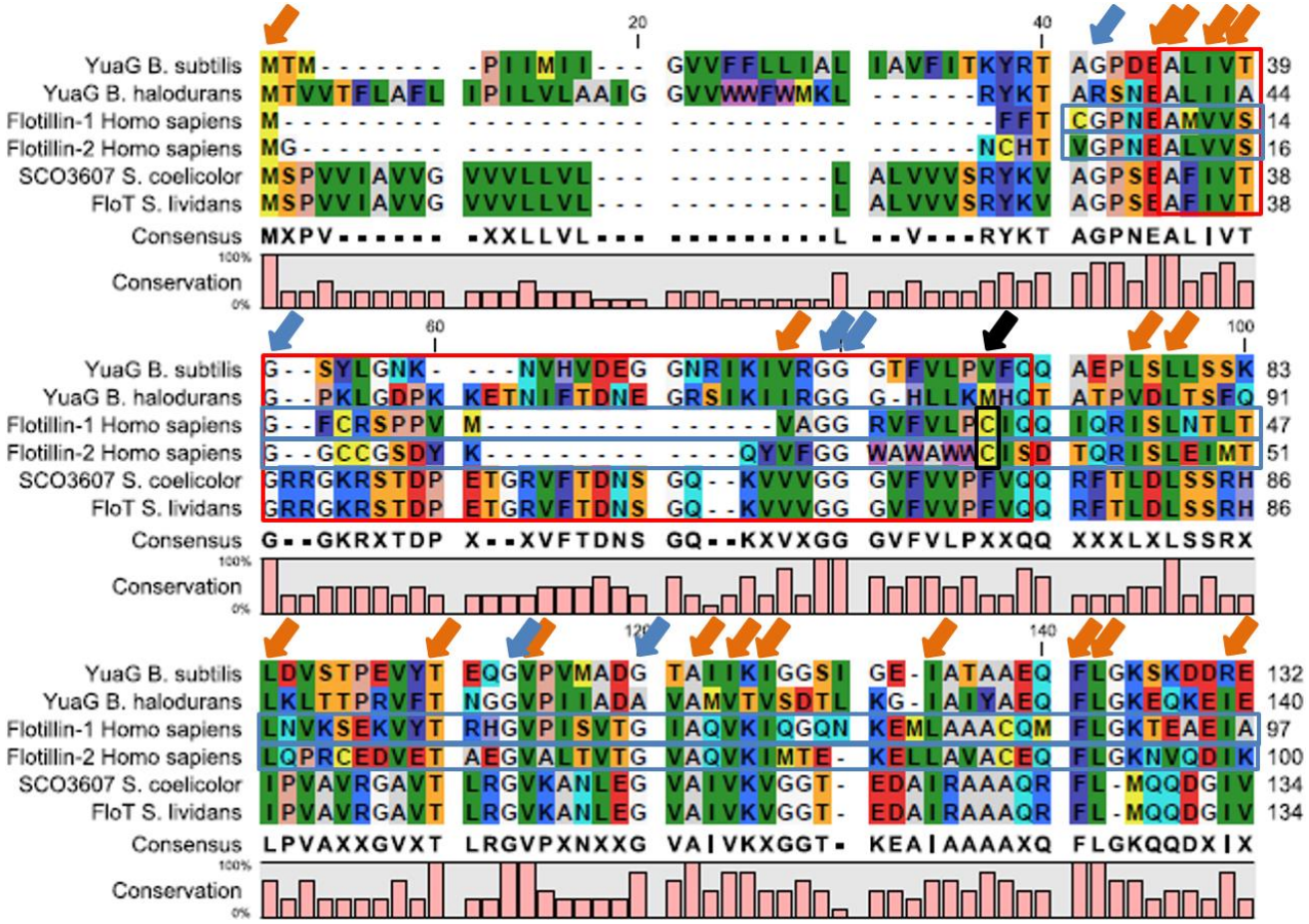

Fig3-2A. Multiple sequence alignment shows a large degree of flotillin conservation across several species. The protein sequences chosen were SCO3607 from *S. coelicolor*, FloT from *S. lividans*, flotillin-1 and -2 from *H. sapiens*, and YuaG from *B. subtilis* and *B. halodurans*. The N-terminal SPFH domains of flotillin-1 and -2 are indicated with blue boxes, C-terminal flotillin domains with orange boxes, hydrophobic membrane-associated regions with red boxes, palmitoylation sites with black boxes and a black arrow, and the coiled-coil protein interaction region in yellow (Morrow & Parton, 2005). Charge or residues conserved across all sequences are highlighted with orange arrows, glycine residues with a maximum of one change across all sequences are highlighted with a blue arrow. The SCO3607 protein sequence was retrieved from StrepDB, while the other protein sequences were retrieved from NCBI (Coordinators, 2017, Fernandez-Martinez *et al.*, 2011).

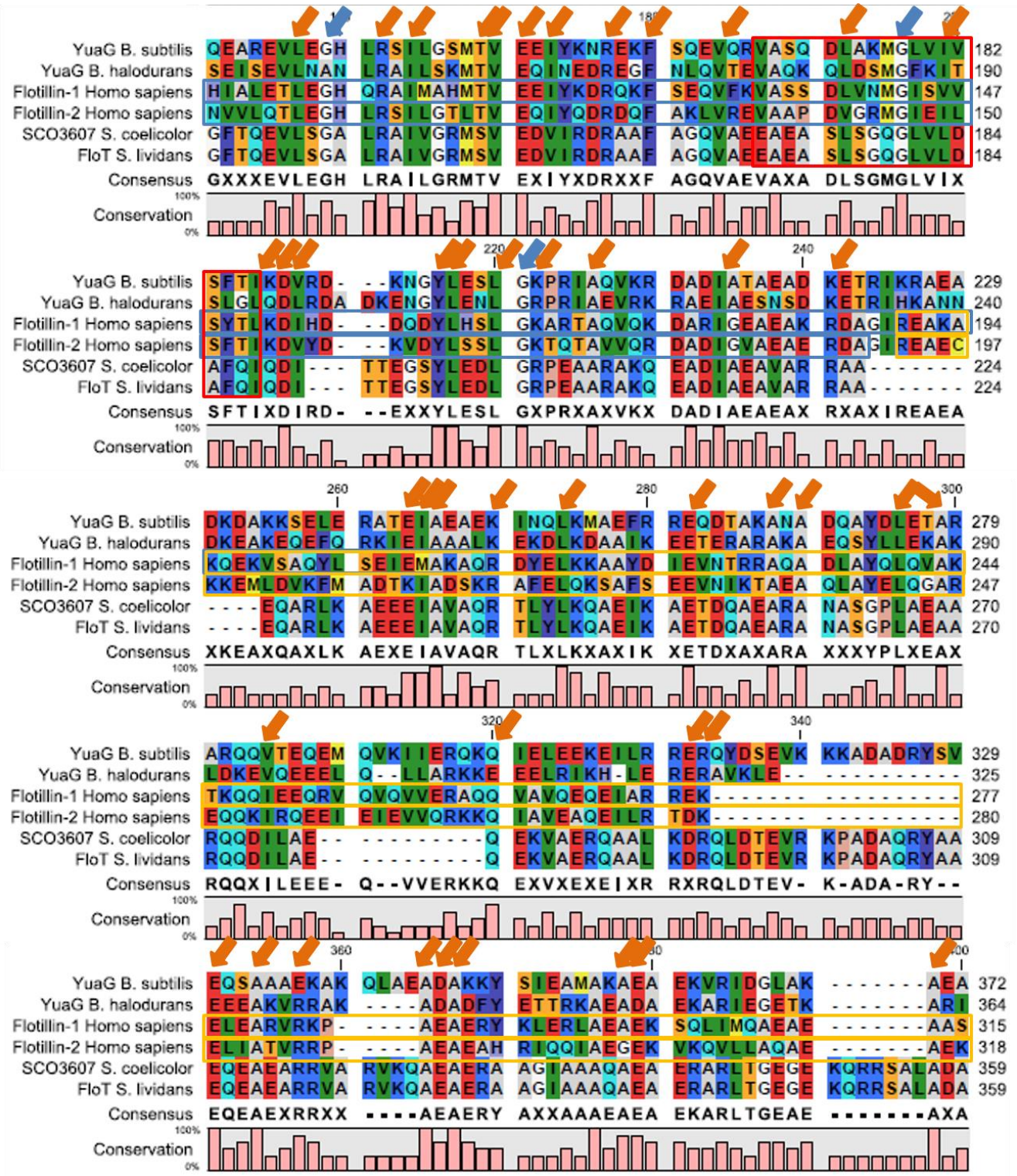

Fig3-2B. Multiple sequence alignment shows a large degree of flotillin conservation across several species.

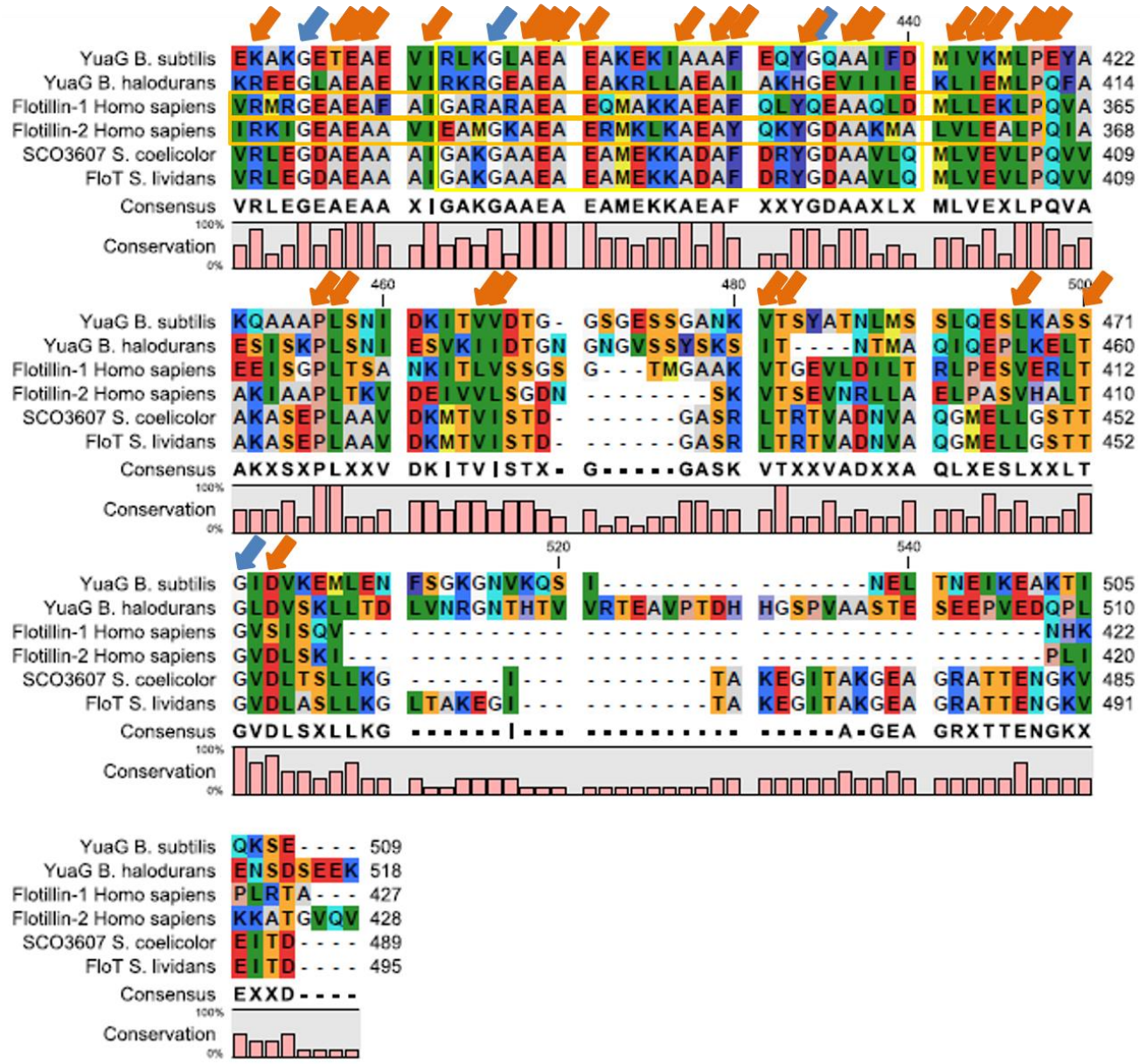

Fig3-2C. Multiple sequence alignment shows a large degree of flotillin conservation across several species.

A high degree of conservation across the various flotillins is obvious from the multiple sequence alignment (see Fig 3-2), but there are patches of even greater similarity, likely denoting regions of conserved function that has changed little. Specifically, the N-terminal SPFH domain, ranging from the 43-173rd residue, showed a higher degree of conservation than the C-terminal flotillin domain. The residues that were the best conserved were glutamate, alanine, and glycine, while charge was conserved in the hydrophobic valine/leucine/isoleucine residues, where they would be substituted by the other amino acids. There are also several EA-

motifs in the C-terminal flotillin domain, which are associated with coiled-coils and characteristic of flotillins (Schroeder *et al.*, 1994). There is additionally an AEAE-motif conserved across all species at the 377th residue of the *S. coelicolor* flotillin, though it could also be an unrelated alanine followed by EA repeats, as the motif is followed by a slightly less conserved alanine.

3.2.1.2. NfeD

A sequence alignment was then performed with SCO3608 of *S. coelicolor*, PH0471 of *P. hyrokoshii* and YuaF of *B. subtilis*. Accession numbers are NP_627803.1, BAA29559.1, and PLV35533.1, respectively. PH0471 and YuaF were chosen due to their partially known structure, thus allowing for better identification of residues relevant to function. Both of these proteins are missing the Clp-protease domain, making them more suited for alignment (Walker *et al.*, 2008, Kuwahara *et al.*, 2008). The OB-fold domain of the truncated NfeD of *P. horikoshii,* PH0471, is missing several key surface aromatic residues, W11, F18, F20, F31, H33, F34, and Y42. These are required for nucleotide binding in CspA of *E. coli*, a known OB-fold containing nucleotide-binding protein. While potentially a metal ion-binding domain, it is likely to be involved in protein-protein interactions due to similarities with toxic shock syndrome toxin-1 (TSST-1). TSST-1 binds to proteins of the Major Histocompatibility (MHC) class II through the following surface residues of its OB-fold: L30, I42, L44, I46, S53, and F83, part of the β3 sheet. These correspond to the E99, K110, I112, Y114, D116 and L133 residues of PH0471, making it unlikely it binds MHC class II proteins (Kuwahara *et al.*, 2008). However, the similarity between YuaF and PH0471 is poorly conserved, suggesting it may be the structure of the OB-fold that is important for binding (Walker *et al.*, 2008). Furthermore, *nfeD* readily evolves to lose its N-terminal protease domain and horizontal conjugation has further obfuscated the genetic lineage of the various *nfeD*s.

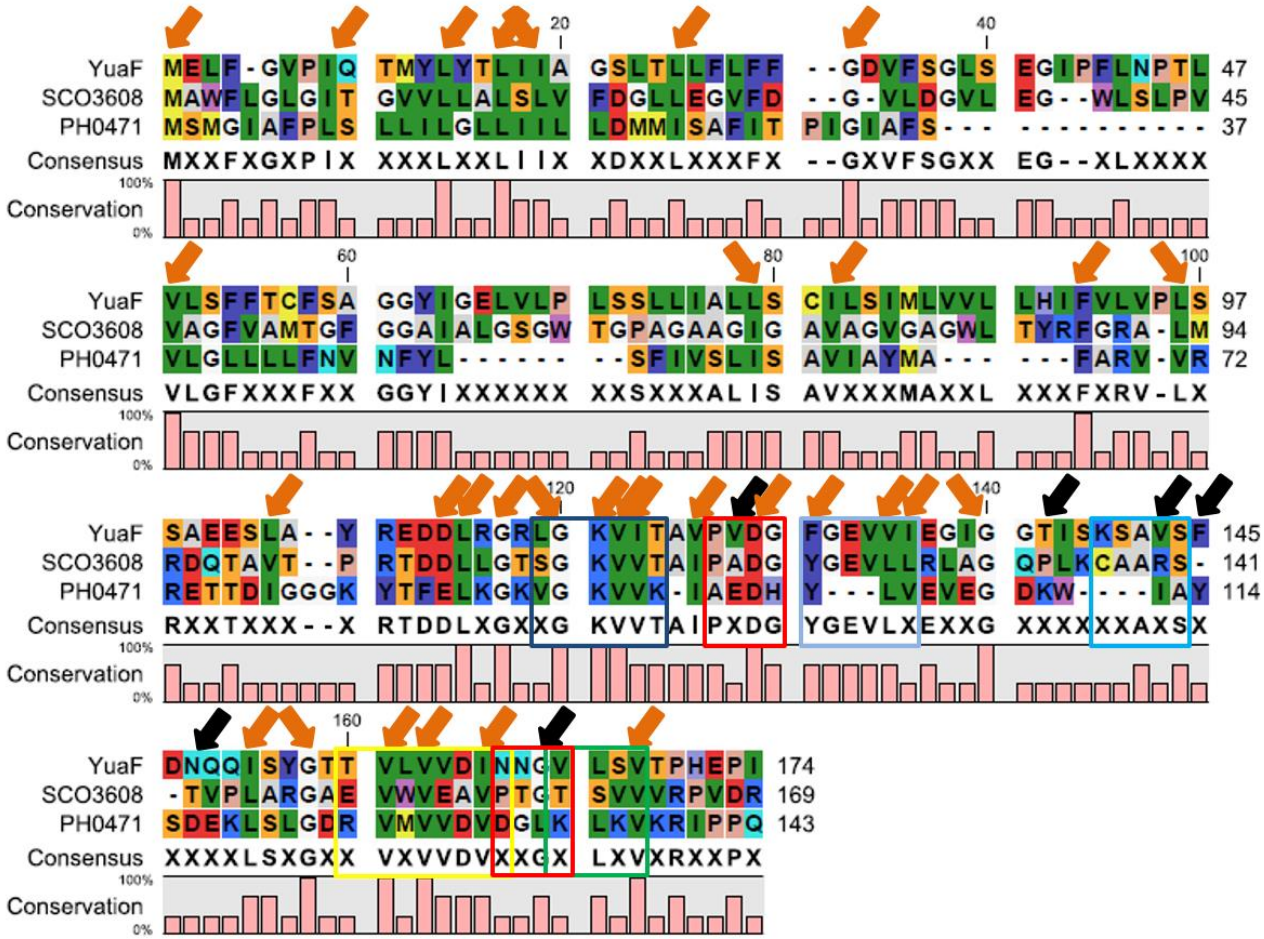

Fig3-3. Multiple sequence alignment shows a high degree of NfeD conservation between YuaF of *B. subtilis*, SCO3608 of *S. coelicolor*, and PH0471 from *P. hyrokoshii*. The surface residues of *P. hyrokoshii* corresponding to the residues involved in protein-protein interactions in TSST-1 have been annotated with black arrows. The β-sheets of the OB-fold have been annotated with blue, light blue, cyan, yellow, and green boxes, corresponding to the β-sheet colours in Fig3-1. Residues which are conserved throughout or which have the same charge have been annotated with orange arrows (Walker *et al.*, 2008). The SCO3608 protein sequence was retrieved from StrepDB, while the other protein sequences were retrieved from NCBI (Coordinators, 2017, Fernandez-Martinez *et al.*, 2011).

When comparing the sequences of the three proteins, a great deal of conservation in the C-terminal OB-fold was evident. In particular, the amino acids ranging from 114-140 showed very high levels of conservation and a four-amino acid stretch from a GKVV motif from 120-123 were identical but for a single valine to isoleucine substitution in YuaF. Valine and isoleucine are both similar hydrophobic residues which are readily substituted for each other. Otherwise, valine, leucine, and isoleucine residues are the conserved amino acids in the OB-

fold, similar to what was seen in flotillin (See Fig3-2).These are likely to form the inner hydrophobic core of the OB-fold (Walker *et al.*, 2008).

None of the residues required for protein-protein interactions in TSST-1 were present at the right positions in the three NfeDs, suggesting different residues involved in any potential protein-protein interactions.

3.2.2. Predicting domains to reveal potential structural similarities.

Protein domains were predicted using InterPro (Hunter *et al.*, 2012). Based on the amino acid structure of SCO3607 (accession number NP_627802.1), InterPro predicted it was indeed a band 7 protein of the flotillin family, with a band 7 domain stretching from the 29th to 219th residue. When viewed against the other flotillins in the multiple sequence alignment and the level of conservation, it is clear SCO3607 is indeed a flotillin. InterPro revealed an N-terminal flotillin domain, and when the entire protein was considered, the entire protein was predicted as an SPFH, thus mirroring the domain structure human flotillins (Browman *et al.*, 2007).

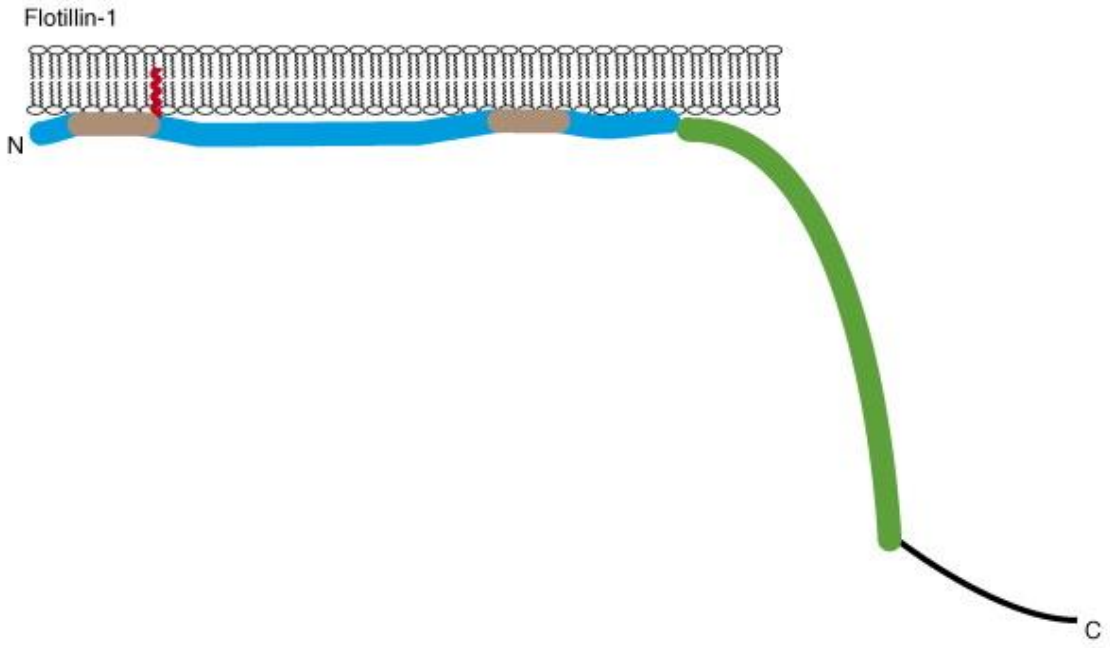

Fig3-4. The domain structure of SCO3607 is predicted to be similar to flotillin-1 of *Homo sapiens sapiens*. The grey membrane-associated hydrophobic sections intersect the blue SPFH domain, with the green C-terminal tail being the flotillin domain, with the red palmitate reside also enhancing membrane association. The image has been copied (Browman *et al.*, 2007).

When SCO3608 (accession number NP_627803.1) was analysed for protein domains InterPro predicted cytoplasmic region from the 88th residue to 169th, including an OB-fold from the 104th to 167th residue, in addition to 3 transmembrane helices at the N-terminal (see Fig3-5). This coincides with the largest degree of similarity in the protein. The OB-fold of YuaF differs from the standard OB-fold in many ways; it is missing an α-helix that connects the β3- and β4-strands is not present in the OB-fold of YuaF, β1 does not form an anti-parallel with the β4-strand, and it contains an extra α-helix that is likely to form a rigid spacer with the predicted transmembrane region (Walker *et al.*, 2008). Furthermore, OB-folds are generally oligosaccharide- or single-stranded nucleotide-binding proteins, with a few exceptions for protein binding (Theobald *et al.*, 2003, Bochkareva *et al.*, 2005).

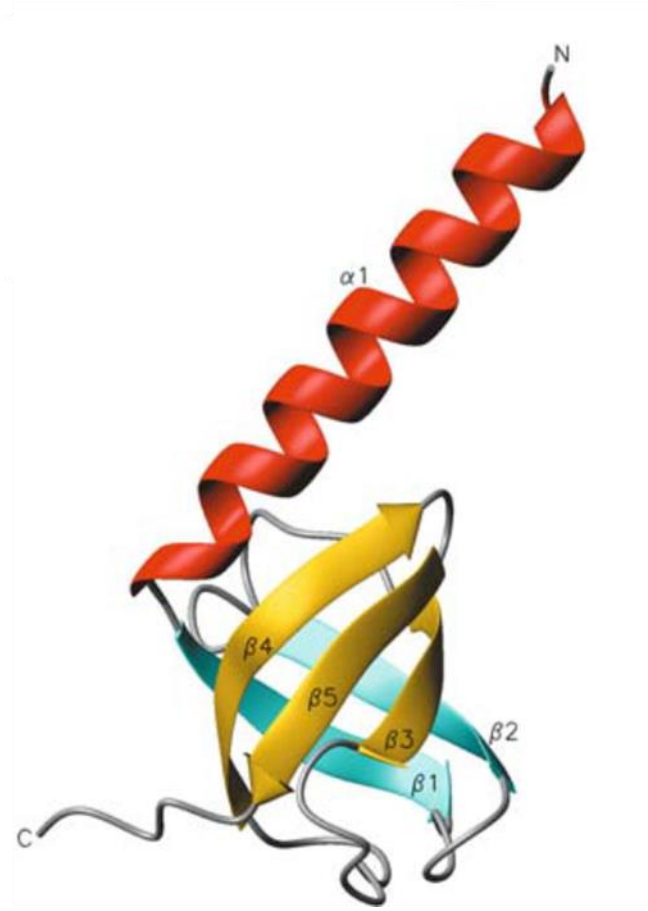

Fig3-5. The sYuaF structure contains an OB-fold. The residues visible are the 97-174 of full-length YuaF from *B. subtilis*. The five β-sheet barrel is the OB-fold, which was previously identified using NMR. The image has been copied (Walker *et al.*, 2008).

3.3 Investigating the co-evolutionary relationship of NfeD and SPFH proteins

3.3.1. The co-evolutionary relationship of NfeDs and SPFHs investigated using phylogenetic trees

The genetic link between NfeD and SPFHs-encoding genes is well documented, but their relationship with other genes less so, especially within Streptomycetes. Investigating genes close to *SCO3607* and *SCO3608*-homologues within Streptomycetes, it was clear there was little conservation of their neighbouring genes, suggesting their propagation within Streptomycetes was mediated by horizontal gene transfer. Furthermore, while a clear link between NfeDs and SPFH-encoding genes is established, the related nomenclature is conflicting and based on different systems of organisation (Green *et al.*, 2009, Hinderhofer *et al.*, 2009). While neither system of organisation is wrong, both describe a different aspect of their relationship. Phylogenetic trees available in the literature were too wide and focused on the evolution of the entire superfamily, so to clarify the relationship between the NfeD and SPFH three phylogenetic trees were constructed to investigate the evolutionary relationship between the SPFH superfamily, flotillin in particular, and NfeD. A selection of proteins from each major group was chosen to create a phylogenetic tree of manageable size. The first two trees were constructed from the chosen SPFHs and NfeDs, but the third was constructed from the C-terminal domains of the NfeDs. This was done to take into account the readily lost N-terminal serine protease domain, as the genetic lineage of NfeD is compounded not only by N-terminal serine protease domain, but also the amount of horizontal transfer and different amount of NfeD and SPFH proteins present in each organism (Green *et al.*, 2009).

The co-localisation of genes within a region of the genome is referred to as synteny, thus genes with a high degree of synteny can be found within the same region or cluster in several organisms. The level expression of the genes in these regions are also linked, irrespective of operons and strand (Junier & Rivoire, 2016). This conservation is often enhanced by the role of the genes encoded in specific stretch. Thus, if a gene is found in a specific locus or cluster, its wider role can often be deduced from its neighbours, such as secondary metabolite production (Cimermancic *et al.*, 2014). Thus, the degree of synteny can be used to investigate the evolutionary origins of a gene, such as the central core of *S. coelicolor* sharing a high degree of synteny with *Mycobacterium tuberculosis* and *Corynebacterium diphtheria* genomes (Bentley *et al.*, 2002).

Selecting streptomycetes with their gene organisation available on http://strepdb.streptomyces.org.uk, *SCO3607* and *SCO3608* were examined from this perspective. The accession numbers for the proteins encoded by the genes are found in Table 3-1. The immediate neighbouring genes within *S. avermitilis*, *S. scabiei*, *S. formicae*, and *S. griseus* are all different, with SCO3606 and SCO3605 homologues immediately upstream of *SCO3607* and *SCO3608* in *S. venezuela*, while *S. leeuwenhoekii*, and *S. lividans* had a SCO3609 homologue immediately downstream of the two gens. Additionally, in *S. griseus*, *SCO3607* and *SCO3608* are on the opposite strand, while *S. avermitilis* lacks a *SCO3608* homologue. The synteny of *SCO3607* and *SCO3608* and their neighbouring genes is thus low. This low degree of synteny suggests they are not part of a larger locus nor share a similar role with the genes in their region, and thus can be seen as somewhat isolated due to the lack of conserved neighbours. This means they are likely the result of horizontal gene transfer, which would be consistent with what has previously been suggested for *nfeD* (Adato et al., 2015, Green *et al.*, 2008).

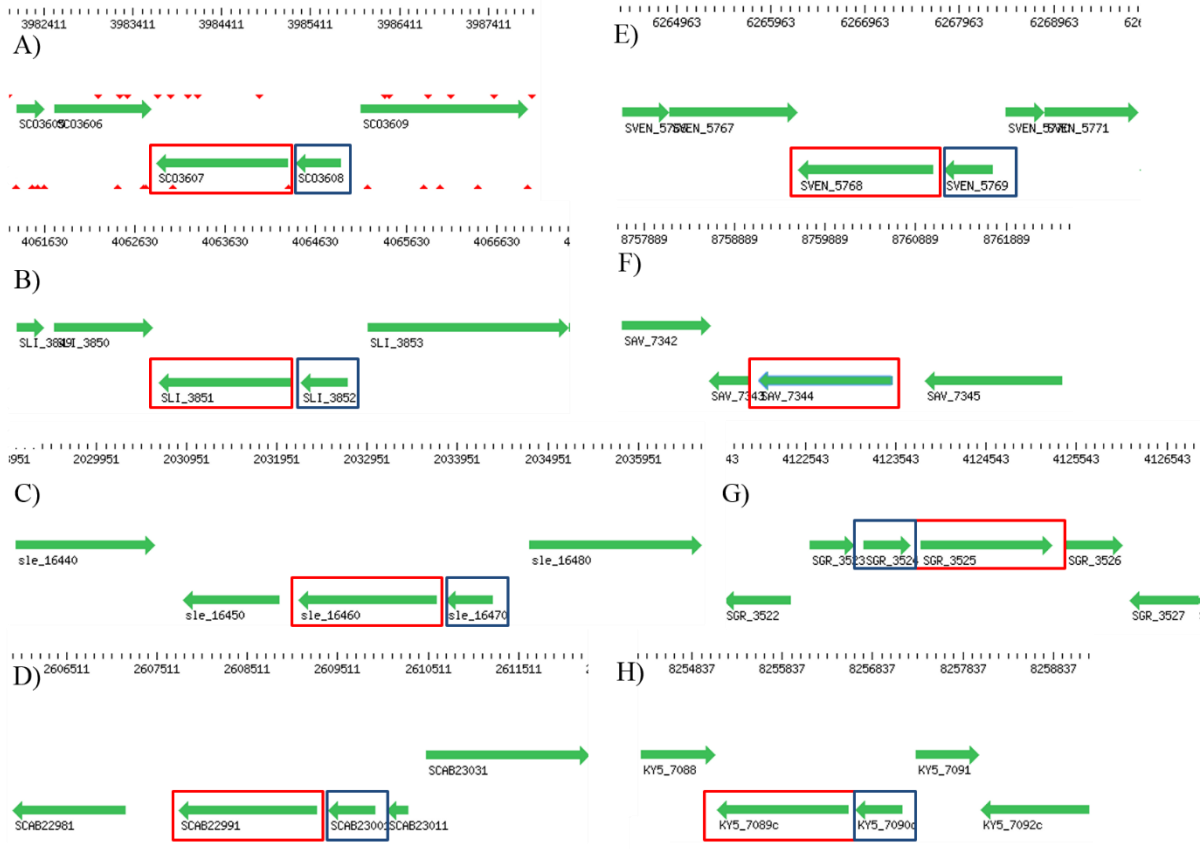

Fig3-6. *SCO3607* and *SCO3608* display low levels of synteny. *SCO3607* and its homologues are in red boxes and *SCO3608* and its homologues are in blue boxes. A) is *S. coelicolor*, B) is

S. lividans, C) is *S. leeuwenhoekii*, D) is *S. scabiei*, E) is *S. venezuelae*, F) is *S. avermitilis*, G) is *S. griseus*, and H) is *S. formicae*.

The SPFH proteins clustered predictably into two major branches – flotillins and stomatins/slipins. However, the plant and fungal flotillins clustered apart from the other eukaryotic flotillins, which clustered with the bacterial flotillins, especially those belonging to the bacilli. This was the case for the stomatins as well, which was where the HflCs of *S. coelicolor* clustered. Interestingly, though classified as HflC proteins based on their amino acid sequence, they are very similar to human stomatin, much more so than HflCs from other species. The eukaryotic SPFH proteins clustered separately was very surprising based on their species' evolutionary origins, and additionally as NfeD is not present in eukaryotes, which would suggest the eukaryotic stomatins and flotillins had separate ancestors that had both independently lost their NfeD partners.

Based on the NfeD phylogenetic tree, it is likely the flotillin-associated NfeDs are descended from the same NfeD that underwent a deletion event which resulted in the loss of the Clp-protease domain. While truncated NfeDs clustered together in a manner that mimicked flotillins, YuaF and YuaG of *B. halodurans* did not, and YuaG was the only flotillin of the selected proteins that had a full-length NfeD. The *S. coelicolor* protein sequence was retrieved from StrepDB, while the other protein sequences were retrieved from NCBI (Coordinators, 2017, Fernandez-Martinez *et al.*, 2011).

Table 3-1A. The list of proteins chosen for the phylogenetic trees used to elucidate the evolutionary relationship between proteins produced by genes with an adjacent *nfeD*. * Unknown taxology, order presented instead. **Class unknown, phylum presented instead. The first accession number is the SPFH family protein, while the second is the NfeD family protein.

Organism	**Domain**	**Class**	**Name**	**SPFH**	**Name**	**NfeD**	**Accession number**
Ajellomyces capsulatus	Eukarya	Eurotimycetes	FloT	Flotillin			EEH07732
Arabidopsis thaliana	Eukarya	Brassicales*	FLOT1A	Flotillin			OAO94680
Arabidopsis thaliana	Eukarya	Brassicales*	FLOT1B	Flotillin			NP_197908
Arabidopsis thaliana	Eukarya	Brassicales*	FLOT2	Flotillin			BAF00909

Table 3-1B. The list of proteins chosen for the phylogenetic trees used to elucidate the evolutionary relationship between proteins produced by genes with an adjacent *nfeD*. * Unknown taxology, order presented instead. **Class unknown, phylum presented instead. The first accession number is the SPFH family protein, while the second is the NfeD family protein.

Organism	Domain	Class	Name	SPFH	Name	NfeD	Accession number
Aspergillus nidulans	Eukarya	Eurotimycetes	FloA	Flotillin			EAA57963
Aspergillus nidulans	Eukarya	Eurotimycetes	StoA	Stomatin			CBF83280
B. subtilis	Bacteria	Bacilli	FloT/YuaG	Flotillin	YuaF	NfeD1b-5	KIX81581/ KIX81582
B. subtilis	Bacteria	Bacilli	YqfA	SPFH	YqeZ	NfeD1b-2	AGG61938/ BAA12472
B. cereus	Bacteria	Bacilli	FloT/YuaG	Flotillin	YuaF	NfeD1b-5	AUZ27599/ SME07005
B. halodurans	Bacteria	Bacilli	FloT/YuaG	Flotillin	YuaF	NfeD1b-2	WP_010899631
Calothrix parasitica	Bacteria	Cyanophyceae	Flotillin family protein	Flotillin			WP_096658968
Caulobacter crescentus	Bacteria	Caulobacterales	Flotillin	Flotillin			WP_058347757
Corynebacterium freiburgense	Bacteria	Actinobacteria		Flotillin		NfeD1b-5	WP_027011624/ WP_027011625
Corynebacterium glutamicum	Bacteria	Actinobacteria		Flotillin			WP_074495691
Daphnia magna	Eukarya	Crustacea	Flotillin-2	Flotillin			KZS07506
Deinococcus murrayi	Bacteria	Deinococci	FloT	Flotillin		NfeD	WP_034407892/ WP_027459434
Deinococcus proteolyticus	Bacteria	Deinococci	FloT	Flotillin		NfeD	WP_013614800/ WP_013614799
Drosophila melanogaster	Eukarya	Insecta	Flotillin-1a	Flotillin			NP_477358
Drosophila melanogaster	Eukarya	Insecta	Flotillin-2a	Flotillin			NP_727797
E. coli	Bacteria	Gammaproteobacteria	FloT/YqiK	Flotillin			OAC10723
Fischerella thermalis	Prokaryota	Cyanophyceae	Flotillin family protein	Flotillin			WP_102170920
Glycine max	Eukarya	Fabales*	Flotillin-like protein	Flotillin			XP_014632416
Homo sapiens	Eukarya	Mammalia	Flotillin-1	Flotillin			AAC35387

Table 3-1C. The list of proteins chosen for the phylogenetic trees used to elucidate the evolutionary relationship between proteins produced by genes with an adjacent *nfeD*. * Unknown taxology, order presented instead. **Class unknown, phylum presented instead. The first accession number is the SPFH family protein, while the second is the NfeD family protein.

Organism	**Domain**	**Class**	**Name**	**SPFH**	**Name**	**NfeD**	**Accession number**
Homo sapiens	Eukarya	Mammalia	Flotillin-2	Flotillin			AAV38285
Kitasatospora aureofaciens	Bacteria	Actinobacteria	Flotillin	Flotillin		NfeD	WP_052836443/ WP_052836446
Lactobacillus casei	Bacteria	Bacilli	Flotillin	Flotillin			EKQ12905
Macaca mulatta	Eukarya	Mammalia	Flotillin-1	Flotillin			NP_001098638
Macaca mulatta	Eukarya	Mammalia	Flotillin-2	Flotillin			XP_014974420
Macrophomina phaseolina	Eukarya	Dothideomycetes	FloT	Flotillin			EKG17859
Macrophomina phaseolina	Eukarya	Dothideomycetes	Band 7 Protein	Stomatin			EKG17836
Marchantia polymorpha	Eukarya	Marchantiopsida	Flotillin-like protein 1	Flotillin			OAE35509
Marchantia polymorpha	Eukarya	Marchantiopsida	Flotillin-like protein 2	Flotillin			OAE35510
Medicago truncatula	Eukarya	Fabales**	Flotillin-like protein 3	Flotillin			ADA83096
Medicago truncatula	Eukarya	Fabales**	Flotillin-like protein 4	Flotillin			ADA83097
Medicago truncatula	Eukarya	Fabales**	Flotillin-like protein 6	Flotillin			ADA83098
Micromonospora parva	Bacteria	Actinobacteria	Flotillin	Flotillin		NfeD1b-5	WP_030331832/ WP_030331830
Micromonospora purpureochromogenes	Bacteria	Actinobacteria	Flotillin	Flotillin			WP_030499487/ WP_088959687
Neurospora crassa	Eukarya	Sordariomycetes		Flotillin			XP_959457
Nocardia vinacea	Bacteria	Actinobacteria	Flotillin	Flotillin			WP_040692021
Physcomitrella patens	Eukarya	Funariales		Flotillin			PNR57783

Table 3-1D. The list of proteins chosen for the phylogenetic trees used to elucidate the evolutionary relationship between proteins produced by genes with an adjacent *nfeD*. * Unknown taxology, order presented instead. **Class unknown, phylum presented instead. The first accession number is the SPFH family protein, while the second is the NfeD family protein.

Organism	Domain	Class	Name	SPFH	Name	NfeD	Accession number
Populus trichocarpa	Eukarya	Malpighiales		Flotillin-2			XP_002324888
Populus trichocarpa	Eukarya	Malpighiales		Flotillin-1			XP_002309650
Pyrococcus horikoshii	Archaea	Thermococci	PH1511	Eoslipin	PH1510	NfeD1b-3	O59180/ O59179
Pyrococcus horikoshii	Archaea	Thermococci			PH0471	NfeD1b-2	BAA29559
Pyrobaculum aerophilum	Archaea	Thermoprotei	Eoslipin	Eoslipin	NfeD	NfeD1b-4	AAL63003/ AAL63002
Staphylothermus marinus	Archaea	Thermoprotei	Eoslipin	Eoslipin	NfeD	NfeD1b-4	ABN69269/ ABN69270
Shewanella violacea	Bacteria	Gammaproteobacteria	Eoslipin	Eoslipin	NfeD	NfeD1b-1	BAJ03851 / BAJ02557
S. albidoflavus	Bacteria	Actinobacteria	FloT	Flotillin		NfeD1b-5	WP_071337336/ WP_095710453
S. albus	Bacteria	Actinobacteria	FloT	Flotillin		NfeD1b-5	WP_064070887/ WP_032776657
S. ambofaciens	Bacteria	Actinobacteria	FloT	Flotillin		NfeD1b-5	WP_079155537/ WP_053134554
S. avermitilis	Bacteria	Actinobacteria	FloT	Flotillin			WP_037647117
S. bikiniensis	Bacteria	Actinobacteria	FloT	Flotillin		NfeD1b-5	WP_030211409/ WP_030211411
S. coelicolor	Bacteria	Actinobacteria	SCO3607	Flotillin	SCO3608	NfeD1b-5	NP_627802/ NP_627803
S. coelicolor	Bacteria	Actinobacteria	SCO1796	Slipin	SCO1797	NfeD1b-2	NP_626066/ NP_626067
S. coelicolor	Bacteria	Actinobacteria	SCO7227	Slipin	SCO7226	NfeD1b-2	NP_631283/ NP_631282
S. coelicolor	Bacteria	Actinobacteria	SCO6053	Slipin			NP_630163
S. formicae	Bacteria	Actinobacteria	KY5_7089c	Flotillin	KY5_7090c	NfeD1b-5	WP_016823599/ WP_015577837
S. griseus	Bacteria	Actinobacteria	FloT	Flotillin		NfeD1b-5	WP_037678300/ WP_037678297
S. kanamyceticus	Bacteria	Actinobacteria	FloT	Flotillin			WP_055556176/ WP_055556178
S. leeuwenhoekii	Bacteria	Actinobacteria	sle_16460	Flotillin	sle_16470	NfeD1b-5	CQR61108.1/ CQR61109.1/
S. lividans	Bacteria	Actinobacteria	FloT	Flotillin		NfeD1b-5	EFD68413/ WP_003975331
S. luteus	Bacteria	Actinobacteria	FloT	Flotillin		NfeD1b-5	WP_043371714/ WP_043376838

Table 3-1E. The list of proteins chosen for the phylogenetic trees used to elucidate the evolutionary relationship between proteins produced by genes with an adjacent *nfeD*. *Unknown taxology, order presented instead. **Class unknown, phylum presented instead. The first accession number is the SPFH family protein, while the second is the NfeD family protein.

Organism	Domain	Class	Name	SPFH	Name	NfeD	Accession number
S. pactum	Bacteria	Actinobacteria	FloT	Flotillin		NfeD1b-5	WP_079154983 / WP_070388667
S. scabiei	Bacteria	Actinobacteria	FloT	Flotillin	NfeD	NfeD1b-5	WP_086784257/ WP_086757412
S. venezuelae	Bacteria	Actinobacteria	FloT	Flotillin	NfeD	NfeD1b-5	WP_055640107/ WP_055644754
Synechocystis	Bacteria	Cyanobacteria**	Flotillin family protein	Flotillin		NfeD1b-4	WP_010871575/ BAA10836
Thermococcus barophilus	Archaea	Thermococci	Eoslipin	Eoslipin	NfeD	NfeD1b-3	WP_013467301/ WP_013467302
Vibrio harveyi	Bacteria	Gammaproteobacteria	Eoslipin	Eoslipin	NfeD	NfeD1b-1	WP_009700456/ WP_061009405
Zea mays	Eukarya	Poales	Flotillin-like protein 1	Flotillin			XP_008644764

The archaeal slipins, flotillins, and NfeDs were included to investigate where a manageable selction of archael proteins would cluster in relation to bacterial and eukaryotic proteins. PH0470 of *P. horikoshii* has been included, as it is an HflK protein, and quite a lot is known about its NfeD partner (Kuwahara *et al.*, 2009). The other proteins from *P. horikoshii* were included, as the NfeD PH1510 and the core domain of the stomatin PH1511 have been resolved by crystallisation and to see how the archael SPFHs cluster (Yokoyama *et al.*, 2008a, Yokoyama *et al.*, 2008b).

As most of the flotillin and NfeD research published concerns bacilli, *B. halodurans*, *B. subtilis*, and *B. cereus* were included. While the latter does not have any articles about its flotillin, it is a relevant organism based on its role in disease. YqfA/FloA of *B. subtilis*, another NfeD partner, is included in the table, and though one paper has included them in the SPFH superfamily, this is likely done due their proximity to NfeD rather than sequence similarity, as it is more similar to seryl-tRNA-synthetase superfamily (Yepes *et al.*, 2012, Hinderhofer *et al.*, 2009). One paper reported *yqfA* as restricted to Deinococci and Firmicutes, however, this paper failed to identify the presence of *nfeD* in actinobacteria, and similarly, *yqfA* homologues are present in actinobacteria, but only in two Streptomycetes, *S. regensis* and *S. ochraceiscloratus*

(Green *et al.*, 2009). This is the same for the reported *S. aureus* flotillin – it is not a flotillin, but a predicted seryl-tRNA-synthetase, and is thus not included, however, there is no NfeD present (Lopez & Kolter, 2010).Various flotillins were included from Streptomycetes, including slipins from *S. coelicolor*, to investigate their evolutionary relationship and form a more complete picture.

Other actinobacteria - *Corynebacteria*, *Micromonospora*, and *Nocardia* - were included to investigate the evolutionary relationship of the flotillins and NfeDs within the class. *C. glutamicum* is an industrially important bacterium, while *C. freiburgense* contained both an NfeD and a flotillin. *M. purpureochromogenes* is an industrial organism, while *M. parva* contained both an NfeD and a flotillin, and *N. vinacea* was included for the same reasons. There has been research published on the flotillin of the model organism *E. coli*, so it has been included as well (Lopez & Kolter, 2010). Several cyanobacteria were included as well to explore their flotillin and NfeDs' evolutionary relationship with that of the other organisms.

From eukarya, the human flotillins were included as they have far and beyond more articles published on them, in addition to the Rhesus Macaque, *Macaca mulatta*. The model organisms *Drosophila melanogaster* and *A. nidulans* were included due to the previously published research (Takeshita *et al.*, 2012). *A. capsulatus*, also known as *Histoplasma capsulatus*, is relevant to disease and adds to the fungal tree cluster, while *M. phaseolina* is a plant pathogen. *M. truncatula* is one of the more researched plant flotillins, and the model organism *A. thaliana* was the first plant to have its genome sequenced and is widely used for understanding plant genetics (Abdallah *et al.*, 2014, Arabidopsis Genome, 2000). Other model plant organisms were included.

Stomatins as a whole were included to investigate how full-length NfeDs, truncated NfeDs, flotillins, and stomatins would cluster on the two different trees, using the same reasoning for their inclusion. This includes SCO1796 and SCO7227 and their NfeD partners.

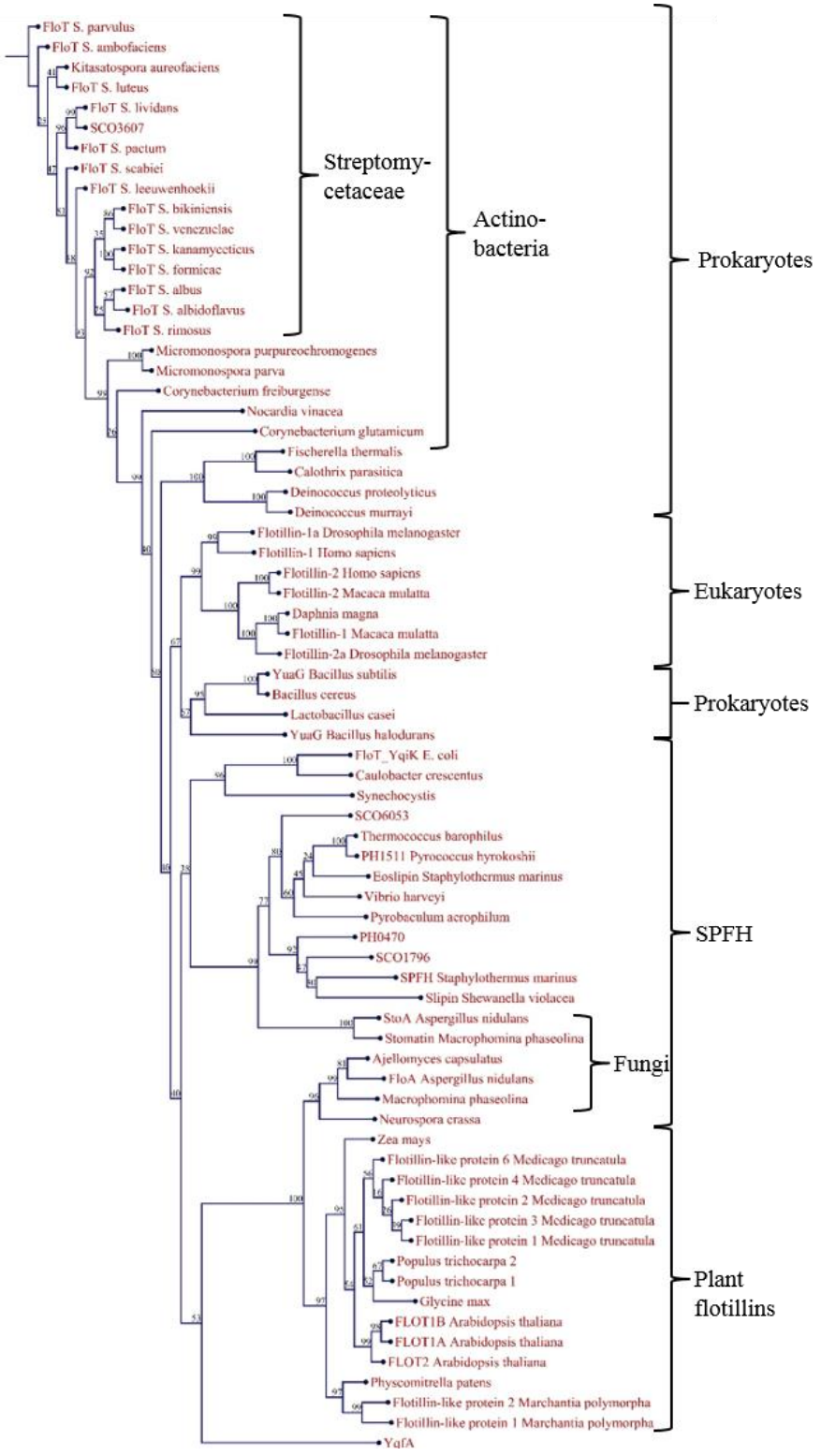

Fig 3-7. A phylogenetic tree of select proteins encoded by predicted SPFH genes across several model organisms and other representative organisms shows a closer relationship between animal flotillins and their eubacterial and bacterial counterparts than fungal and plant flotillins. Bootstraps values, in black, are expressed as percentages of 1000 repeats. Created with CLC Viewer 7.

The flotillin and stomatin phenotypic tree (see Fig3-6) showed a high degree of conservation, regardless of domain of life. The phylogenetic tree showed bacterial flotillins are a diverse group, with animal flotillins more similar to bacterial flotillins than other eukaryotic flotillins, such as fungal and plant flotillins. As expected, SCO3607 clustered with other flotillins from closely related species, which was repeated for most species. *Drosophila melanogaster* and mammalian flotillins clustered with those of *Bacillus* and *Lactobacillus*, but still more similar to Streptomycetes than other eukaryotes. Plant and fungal flotillins clustered separately, as did the did other SPFH proteins. YqfA, a predicted seryl-tRNA-synthetase categorised as a flotillin in one paper, formed its own separate branch (Green *et al.*, 2009).

Stomatins branched separately from the flotillins and the eukaryotic stomatins clustering in a manner that mimicked their flotillins, with human stomatin clustering with bacterial slipins and fungal stomatins clustering separately. SCO1796 and SCO7227, both categorised as HflCs based on genetic sequence, formed a branch within the other SPFHs.

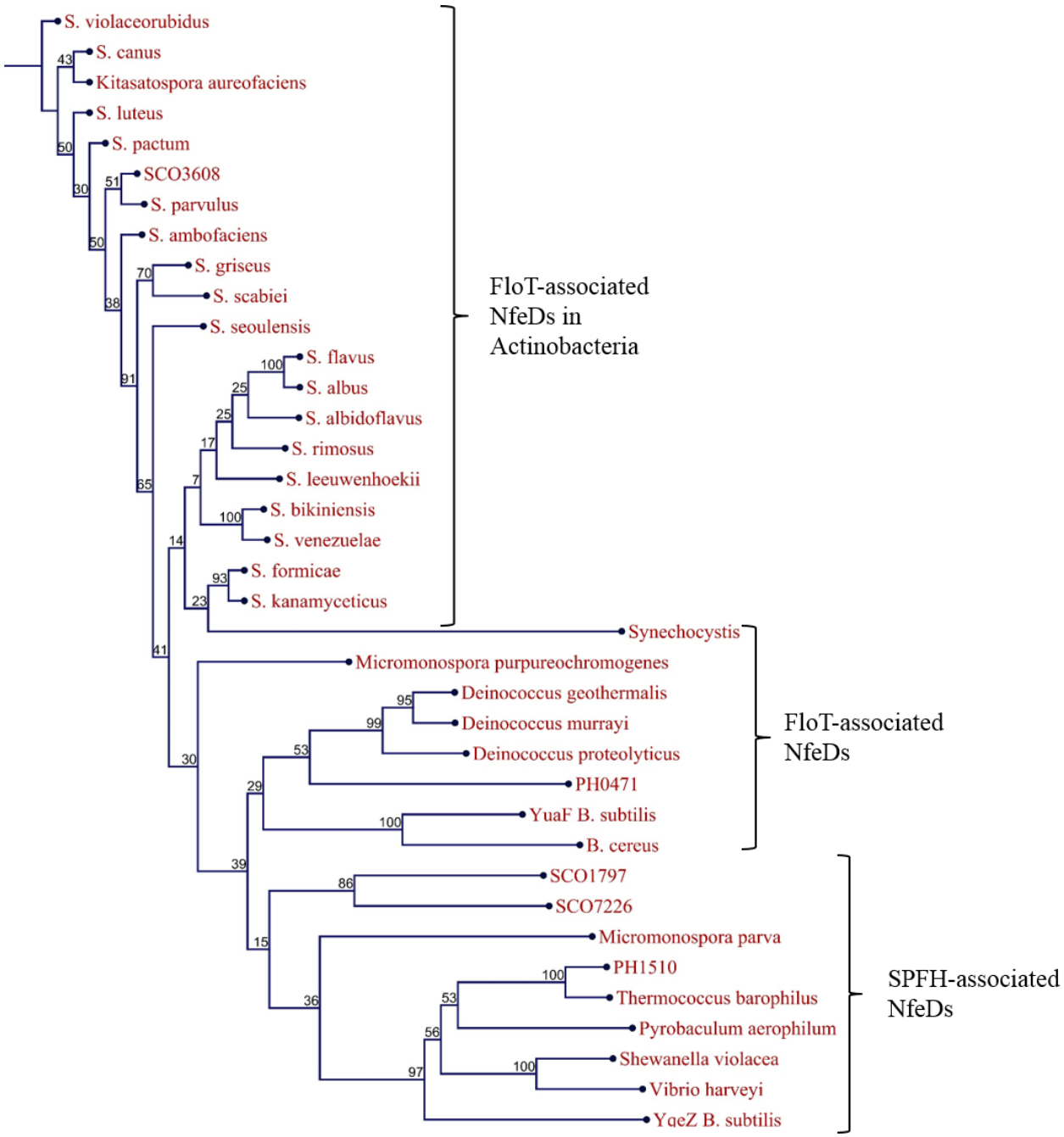

Fig 3-8. A phylogenetic tree of the C-terminus of full-length NfeD and entire sequence of truncated NfeDs affects the evolutionary origin of PH0471 and full-length NfeDs. Bootstraps values, in black, are expressed as percentages of 1000 repeats. Created with CLC Viewer 7.

SCO3608, the NfeD of *S. coelicolor*, clustered with other flotillin-associated streptomycete NfeDs, but also formed a greater cluster consisting of other flotillin-associated NfeDs. This confirms that the flotillin-associated NfeD of the streptomycetes had a common ancestor and at least of the surveyed ones, none were the result of a separate horizontal gene transfer event.

The eoslipin-associated NfeDs of *S. coelicolor* also formed their own branch, separate from the other NfeDs. SCO1797 and SCO7226 formed a separate branch, both of which are associated with HflCs. PH0471, an HflK-associated NfeD, had its own branch separate from flotillin-associated NfeDs, but was more similar to them than eoslipin-associated NfeDs.

YqeZ and YuaF, of *B. subtilis* and *B. halodurans*, respectively, are full-length NfeDs that formed their own branch. YqeZ is not associated with a flotillin, but rather with YqfA, a protein classified as either a member of the SPFH superfamily or the seryl-tRNA synthetase superfamily. YqfA clustered entirely separately from the bacterial SPFHs (see Fig3-6). YuaF of *B. halodurans* is associated with a flotillin that, while clustering with other flotillins, is separate from other Bacillaceae flotillins.

Furthermore, the clear clustering of the full-length and truncated NfeDs could be due to the emphasis placed on the presence of Clp-protease domain rather than differences in the more conserved C-terminal, which would be more indicative of the genetic lineage. A new phylogenetic tree was constructed, where only the overlapping C-terminals of the full-length NfeDs and the full length of the truncated NfeDs would be used, thus removing the Clp-protease domain from the genetic alignment. Parts of the sequences were overlapping prior to the exclusion of the N-terminal due to random chance, e.g. the first two residues of the N-terminal of both NfeDs were considered conserved by the software, but upon closer inspection was due to random chance not accounted for by the programme.

3.3.2. Predicting molecular adaption by using d_N/d_S ratios to calculate the effect of purifying pressure.

In order to assay the pressure on *SCO3607* and *SCO3608* to change, the d_N/d_S ratios were used to statistically model the purifying selection. Purifying selection is natural selection against harmful genetic mutations, and a method of measuring purifying selection is the d_N/d_S ratio. The d_N/d_S is the ratio of nonsynonymous (d_N) to synonymous (d_S) nucleotide substitutions, expressed as $\omega = d_N/ d_S$. If the substitution is neutral $\omega = 1$, but if the substitution is deleterious it will reduce the fixation rate, thus $\omega < 1$. If the amino acid change offers a selective advantage the fixation rate increases, thus $\omega > 1$ (Yang & Bielawski, 2000). From this it would seem obvious that most genes are $\omega < 1$, however the exception is when adaptive change is required, such as for immune system genes where they co-evolved alongside parasites, resulting in positive selection (Hurst, 2002). There are problems associated with the d_S/ d_N ratio; it ignores the transition/transversion rate bias and the "wobble" position, which are more likely to be

synonymous, leading to an underestimation of synonymous mutations and overestimation of nonsynonymous mutations. In essence, as there are 61 codons that code for amino acids (64 minus 3 stop codons), but less than 45 tRNAs, these tRNAs require broader specificity. This is achieved by the nucleotide at the 5' end of the anticodon loop, which often is a nucleotide of broader specificity, such as inosine, allowing for non-Watson-Crick pairings, which allows one tRNA to bind to several codons.

Nor does d_N/d_S take into account the time passed since the species diverged; a nucleotide may begin as an A, be replaced by C, and then changes to T, which would only result in one difference. Furthermore, it does not take into account issues that may be based in the genetic code, such as hairpin loops and translational efficiency (Yang & Bielawski, 2000). Examples of this in bacteria include hairpin loops in clustered, regularly interspaced, short palindromic repeats (CRISPR) in *Shigella* and *E. coli*, and the translational efficiency increase in *E. coli* genes containing the UAG codon upon addition of 3-iodo-L-tyrosine to the media (Kato, 2015, Yang *et al.*, 2015).

Genes were picked from several streptomycetes, as the method does not perform well with more distantly related genes due to the much greater difference between the genes and the nature of the calculations. *S. lividans* was picked due to its high similarity with *S. coelicolor*, which means its d_N/d_S ratio should be close to 0, so as to verify the soundness of the method. *S. avermitilis* was included as it did not include an NfeD homologue, suggesting very different evolutionary pressures. The ratios were calculated using the Yn00 program from PAML (Yang, 2007). *S. griseus*, *S. venezuelae*, and *S. scabiei* were then selected as suitable streptomycetes for variation. Accession numbers are available in Table 3-1.

Table 3-2. **The d_N/d_S ratios for *SCO3607* and its homologues show the flotillin of *S. avermitilis* was under the least evolutionary pressure, wheras *S. griseus* was under the most pressure to remain the same.**

Species	*S. coelicolor*	*S. venezuelae*	*S. avermitilis*	*S. lividans*	*S. griseus*	*S. scabiei*
S. venezuelae	0.08641					
S. avermitilis	0.23368	0.009677				
S. lividans	0.1311	0.096091	0.234405			
S. griseus	0.07697	0.068109	0.224511	0.104484		
S. scabiei	0.13082	0.155027	0.231508	0.128615	0.18116509	
Mean	0.13179	0.083062	0.186755	0.138939	0.13104682	0.16542602

The results show that the evolutionary pressure is highest on the flotillins of *S. venezuelae* and *S. griseus,* lowest on *S. avermitilis*, with *S. lividans, S. coelicolor*, and *S. scabiei* in the middle. It is important to observe that this is not the evolutionary relationship, but a measure of purifying selection. As a point of reference, using mean d_N/d_S ratios for measuring core genes conserved in *Synecococcus*, the strains CC9311 and CC9902 were 0.114 and 0.119, whereas accessory genes were 0.402 and 0.256 (Tai *et al.*, 2011).

Table 3-3. The d_N/d_S ratios for *SCO3608* and its homologues in closely related organisms show the homologue of *S. venezuelae* was under the least evolutionary pressure to change.

Species	*S. coelicolor*	*S. venezuelae*	*S. scabiei*	*S. griseus*	*S. lividans*
S. venezuelae	0.253782				
S. scabiei	0.076835	0.282025			
S. griseus	0.062217	0.252574	0.080759		
S. lividans	0	0.252939	0.074423	0.062224	
Mean	0.098209	0.26033	0.128511	0.114444	0.0973965

The results show *S. venezuelae* had the least pressure to remain the same, whereas the negative pressure was very high for the other strains examined. Using *Synecoccous* core and accessory gene d_N/d_S ratios as a point of reference (see above), NfeD is more akin to an accessory protein in *S. venezuelae*. *S. lividans* was under immense pressure to remain the same, which is consistent with the similiarity of the genome of *S. lividans* with *S. coelicolor*.

Pseudogenes can be used to provide reference numbers for d_N/d_S ratios, acting as a control for the statistical methods. Pseudogenes can be divided into two different origins; processed and nonprocessed. Processed pseudogenes occur by RNA retrontranspositioning into the genome, thus lacking start codons. Nonprocessed pseudogenes arise from duplication events and a gradual loss of function due to mutation (Torrents *et al.*, 2003). Three putative streptomycete pseudogenes were picked; *SCO0205*, a potential pyruvate formate-lyase activating enzyme, *SCO0448*, a transmembrane efflux protein, and *SCO4010*, a secreted protein (Reumerman, 2014). The d_N/d_S ratio of *SCO0205* was calculated against its orthologues in *S. venezuelae* and *S. scabiei*, as they were missing from the other streptomycetes. Its ratio was 1.1809, suggesting a positive selection for changing amino acids, and its missing codon suggesting it is a processed pseudogene. SCO0448 had only one orthologue, found in *S. lividans*. This made statistical testing difficult, but it had a d_N/d_S ratio of 0.268, probably due to how closely related *S. lividans* and *S. coelicolor* are. Such a low ratio does however suggest it is not a pseudogene. SCO4010

has orthologues in all sequenced streptomycetes, and its d_N/d_S ratio was 1.413, indicating a neutral/positive selection for new mutations.

Using the previously mentioned pseudogenes, it becomes clear that neither *SCO3607* nor *SCO3608* are pseudogenes and that the statistical model is sound.

3.4.1. Discussion

When examining the flotillin multiple sequence alignment glutamate, alanine, glycine residues, and AE repeats were conserved at a higher level. Human flotillin is characterised by its AE repeats, which is conserved throughout the other flotillins. These repeats are predicted to form coiled-coils (α-helices coiled around each other in a supercoil), which are required for oligomerisation (Bickel *et al.*, 1997, Rivera-Milla *et al.*, 2006). That these are conserved suggests the coiled-coils are conserved, which again suggests it oligomerises. Additionally, glutamate residues are negatively charged, polar amino acids which tend to be on the surface of the protein, though when they are inside a protein they are often involved in salt bridges by pairing with a positively charged amino acid to form a hydrogen bond, stabilising the protein. They are also often found to be involved in protein binding sites due to their charge. It is possible these conserved residues are involved in these structural functions, and thus potentially involved in dimerisation of flotillins. Alanine is a non-polar amino acid which tends towards being a non-reactive residue, and thus rarely involved directly in protein function. It can player a role in substrate recognition, especially of other non-reactive atoms, e.g. carbon.

Glycine often substitutes for alanine and vice versa, which can be seen in the few glycine mutations. Both are small amino acids, and due to glycine sidechain being a hydrogren atom rather than a carbon, it fits in much small places than other amino acids, and also allows it to bind phosphates. As there are many conserved glycine sites in flotillin, it is likely some of these are phosphorylation sites and others break up alpha helices.

Residues with valine, leucine, and isoleucine have a propensity to form alpha helices, in addition to being on the inside. In the case of SPFH proteins, the structure of the N-terminal SPFH domain, ranging from the 43rd to the 173rd residue, of flotillin-2 has been resolved, and is available in MMDB (Chen *et al.*, 2003). It contains four to five α-helices and six β-strands which form a globular structure. The structure of the C-terminal flotillin domain has not been resolved, but is predicted to contain several α-helices, which may form coiled-coils.

All SPFH proteins associate with the membrane through their N-terminal hydrophobic domains, such the transmembrane domain of prohibitin-1 and the intramembrane domains of stomatin, SLP-3 (a stomatin-like protein), and podocin (Tatsuta *et al.*, 2005, Wetzel *et al.*, 2007). Flotillin-1 is different in that palmitoylation is used to facilitate the N-terminal hydrophobic region membrane association, which is usually a reversible reaction where a palmitoyl group is covalently bound to an amino acid residue, usually cysteine, serine or

threonine. Flotillin-2 is palmitoylated and myristoylated, which is similar in all manners but that it is irreversible and a myristoyl group is added (Morrow & Parton, 2005, Langhorst *et al.*, 2005, Resh, 2013). Palmitoylation also occurs in stomatins and podocin, but are not involved in membrane attachment (Huber *et al.*, 2006).

Palmitoylation occurs in bacteria, such as palmitoylation of a fraction of lipid A, which is also myristoylated, by PagP results in both protection from the human immune system and a decrease in immune response (Bishop *et al.*, 2005). PagP is a lipid A palmitoyl transferase present in Gram-negatives, such as *E. coli*, *Salmonella*, and *Shigella* (Bishop *et al.*, 2000, Guo *et al.*, 1998). Though no PagP-like protein is present in the genome of *P. aeruginosa*, palmitoylation of lipid A still occurs (Stover *et al.*, 2000, Ernst *et al.*, 1999). Palmitoylation is increased in *E. coli* during biofilm formation, which *in vivo* improves the survival of the biofilm (Chalabaev *et al.*, 2014). PagP is generally regulated by a PhoQ/PhoP two-component system; PhoQ is an autophosphorylating sensor kinase which transfers its phosphogroup to the transcriptional regulator PhoP (Fields *et al.*, 1989, Miller *et al.*, 1989, Garcia Vescovi *et al.*, 1996).

The *S. coelicolor* protein most similar to PhoQ is RapA2, a predicted two-component sensor kinase, and the protein most similar to PhoP is KdpE, a predicted turgor pressure regulator. However, it is more likely the *S. coelicolor* homologues are PhoP and PhoR, which are also related (Strain *et al.*, 1985). When PhoP was knocked out of *S. lividans*, the culture was unable to grow on MM with low phosphate concentrations, unable to synthesise extracellular phosphatases, and had increased secondary metabolite production (Sola-Landa *et al.*, 2003). Due to the role of flotillin in biofilm formation in *B. subtilis*, it is tempting to suggest a link between PagP and flotillin, but there is no PagP in *S. coelicolor*, and of the mentioned bacteria with PagP, only *S. enterica* has a flotillin (Redenbach *et al.*, 1996). However, this does not mean palmitoylation does not occur in *S. coelicolor*; palmitoylation takes place in *P. aeruginosa*, though the proteins involved are not known, as even though there is a *phoPQ* operon, *pagP* is not found (Stover *et al.*, 2000). Flotillin-2, the flotillin most similar to the bacterial flotillin, is myristoylated at the Gly2 and palmitoylated at Cys4, though also to a lesser degree at Cys19 and Cys20 (Neumann-Giesen *et al.*, 2004). Flotillin-1 is not myristoylated, but is palmitoylated at Cys34, and possibly Cys5 and Cys17 (Morrow *et al.*, 2002). However, none of these are conserved in the bacterial flotillins, and compounded by the lack of any palmitoylation and myristoylation proteins in *S. coelicolor*, makes it unlikely they palmitoylated or myristoylated.

SPFH proteins form oligomers, and nine C-terminal residues (264-272) are essential for oligomerisation in stomatin (Umlauf *et al.*, 2006). This is not transferrable to flotillins, due to the different C-terminal domains. Though not as specific, oligomerisation of flotillins into homo- and heterotetramers is dependent on coiled-coil secondary structure in the C-terminal flotillin domain (Rivera-Milla *et al.*, 2006). Furthermore, in the absence of flotillin-2, flotillin-1 is rapidly degraded by the proteasome, but not vice versa, suggesting flotillin-2 prevents this degradation by binding to flotillin-1 (Solis *et al.*, 2007).

Examining the evolutionary relationship, *SCO3607* and *SCO3608* have low levels of synteny (see Fig3-6), suggesting its propagation throughout streptomycetes is due to horizontal gene transfer, consistent with what has been previously suggested (Green *et al*., 2008). In the phylogenetic trees, flotillins and eoslipins/stomatins all clustered predictably separately, though the most obvious piece of information gleaned from the phylogenetic tree is the high degree of similarity between the flotillins of the bacterial world and of humans (see Fig3-7). That human, Rhesus macaque, and *Drosophila melanogaster* flotillins would be more similar to bacterial flotillins was unexpected. Not only due to eukaryotes presumably being more similar to each other, but also that e. g. *A. nidulans* exploits the same niche as *S. coelicolor* and they superficially resemble each other. Plant and fungal flotillins also diverged considerably from the other flotillins, and instead clustered in a wider SPFH-containing branch of tree, suggesting a very ancient evolutionary origin, and possibly role.

It has previously been suggested that the flotillin of *B. subtilis* may provide a research model for human flotillins based on their shared structural and functional characteristics, as bacteria are far easier to work with than human tissue cultures (Mielich-Suss *et al.*, 2013). However, *S. coelicolor* would be even better suited than *B. subtilis* as a model for human flotillin and lipid raft research due to its tissue-specific expression, though the FloT of *B. subtilis* is genetically closer to human flotillin (Kelemen *et al.*, 2001). There is still more to be found out about SCO3607 with regards to recruitment of protein and lipid rafts, but based on the similarities between human flotillin, YuaG, and SCO3607 demonstrated in this chapter (see Fig3-2 and 3-7), it is likely perform similar molecular roles in *S. coelicolor*, making it a viable option.

HflC-, eoslipin-, and flotillin-associated NfeDs clustered separately in the phylogenetic tree, but YuaF of *B. halodurans*, a full-length flotillin-associated NfeD, clustered with YqeZ, another full-length NfeD, yet *yqeZ* is adjacent to *yqfA*, which is not a member of the SPFH family; YqfA is seryl-tRNA-synthetase which homologue is only present in *S. regensis* and *S. ochraceiscloratus* within *Streptomyces*, though is widely distributed within actinobacteria. The

difference between YuaF of *B. halodurans* and SCO3608 is much greater than the difference between *B. halodurans* YuaG and SCO3607, which in itself is not surprising granted that full-length NfeD1b proteins have evolved to lose their ClpP serine protease domain (Green *et al.*, 2009). However, YuaF was the only full-length NfeD associated with flotillin of the proteins surveyed, while other NfeDs from the bacilli and actinobacteria clustered with the other flotillin-associated NfeDs. What is thus likely, when one includes the data from the phylogenetic tree, is that a common ancestor of the Streptomycetaceae and Bacillaceae *nfed1b-flotillin* operon contained a full-length NfeD protein and that the *B. halodurans* operon diverged by retaining the serine protease domain while the others lost it.

The most surprising result from Fig3-7 is PH0471 when seen in relation to PH0470 (see Fig3-7 and Fig3-8). PH0470 is an HflK and formed part of the SPFH superfamily branch in Fig3-6. PH0471, the truncated NfeD, which gene is adjacent to PH0470 on the *P. horikoshii* genome, clustered with the full-length *Deinococcus* and *Bacillus* NfeDs. This is different from PH1510, which is a full-length NfeD associated with an eoslipin in the same organism that clusters with other full-length NfeDs associated with eoslipins. However, investigating the evolutionary relationship of HflKs and other members of the SPFH superfamily with NfeD is outside the scope of this body of work.

Judging by the d_N/d_S ratios, the ratios may seem somewhat counterintuitive. The highest and lowest purifying selection is on the flotillin and NfeD of *S. venezuelae*, respectively. All this really means is the residues of the flotillin are much more important for the role it plays in *S. venezuelae*, but not for the NfeD, suggesting the residues of NfeD may not be quite as important for its role. This role may be dependent on its structure, specifically its OB-fold with the missing conserved residues. This might suggest that the structure itself, rather than the residues, is most important for its function, so as long as the changes do not alter the structure of the fold, it can tolerate a certain amount of substitutions. That NfeD so readily loses its serine protease domain suggests that this function is redundant for flotillin, though not for the stomatins of the SPFH family, where it is conserved to a much larger degree. *S. avermitilis*, which does not have an NfeD homologue, had the least purifying pressure on its flotillin, suggesting a lesser role (see Table 3-2 and 3-3). When measured against the d_N/d_S ratios of known genes, most of the flotillin-like encoding genes of the assayed streptomycetes have a ratio of that of core genes, while *S. scabiei* and *S. avermitilis*, which genome does not encode an *nfed*, having somewhat high ratios. For the *nfed*-encoding genes, they all had the ratios of

known core genes, bar that of *S. venezuelae*, which had the ratio of an accessory gene (Tai *et al.*, 2011).

For flotillin this suggests the residues themselves are crucial, which is consistent with the palmitoylation and myristoylation demonstrated in the human flotillins (Morrow *et al*., 2002, Neumann-Giesen *et al.*, 2004). In light of the research in human flotillin, this is likely due to the residues being involved in protein-protein interactions. The flotillin genes are in general subject to substantial purifying pressure, especially when seen in light of pseudogenes.

This work tentatively proposes a new group of NfeD proteins, based on their association with flotillin-like protein and the phylogenetic information available, which includes *SCO3608*. The designation proposed is NfeD1b-5, and based on sequence similarity it is more likely have evolved from NfeD1b than NfeD1A. This is consistent with earlier literature assigning truncated NfeD1b names based on phyla, of which one did not exist for actinobacteria. It has previously been suggested they evolved on separate occasions from full-length NfeD1b proteins, losing the Clp-protease domain in the process, but this is controversial as they kept their conserved gene neighbour. The defining feature of the group is a common ancestor which neighboured the ancient flotillin rather than exact sequence similarity, which due to high degrees of mutations and horizontal gene transfer is problematic. The new group fits well with the previous designated groups, as over 85% of NfeD proteins have an immediate SPFH neighbour.

The use of the SPFH superfamily is here doubtfully used correctly; YqfA is included in the trees, and even though one paper has included them in the SPFH superfamily as SPFH5, with flotillins being SPFH2 and stomatins being SPFH1, this is at least in part due their proximity to NfeD rather than the very low sequence similarity (Hinderhofer *et al.*, 2009). While they have sequence similarity, they are much less conserved. One paper claims YqfA is restricted to Deinococci and Firmicutes, however, this body of work demonstrates that is not the case (Green *et al.*, 2009). Furthermore, a homologous seryl-tRNA synthetase in *S. aureus*, SA1402, was also grouped as an SPFH protein (Lopez & Kolter, 2010). This grouping is particularly puzzling, as there is neither sequence similarity between SA1402 and flotillin or an *nfed* in *S. aureus*. Presumably, this classification is based on its similarity to YqfA.

However, the group proposed is not perfect; it is not reserved for either truncated or full-length proteins; an example of a non-truncated NfeD in this group is YuaF of *B. halodurans*, though this is the exception rather than the rule. Additionally, it is more closely related to the other

NfeDs, yet its immediate neighbour is the FloT of *B. halodurans*. The group may well be incorrect based on more extensive phylogenetic information, but as a practical catchall for flotillin-associated NfeD it is very useful.

3.4.2. Conclusion and future work

In conclusion, it is clear SCO3607 and SCO3608 are a flotillin and truncated NfeD, respectively. Flotillins show high degrees of conservation, and SCO3607 is very similar to both human and the flotillin of *B. subtilis*, which are the best characterised flotillins. It is unlikely to be myristoylated or palmitoylated, but it retains the AE repeats associated with coiled-coil secondary structure in its C-terminal flotillin domain.

SCO3608 evolves more readily than SCO3607. Additionally, a new group of flotillin-associated NfeDs have been suggested – NfeD1b-5. This draws on both existing systems of nomenclature, as it uses both genetic and associative traits. The evolutionary pressure was higher for flotillin to retain its specific amino acids, suggesting the structure of NfeD is more important than flotillins, where the overall shape matters more. When aligned against other flotillins, there appeared to be conserved genetic stretches across the species. It is also likely to have spread throughout *Streptomyces* by way of horizontal gene transfer.

Future work which is outside the scope of this study includes investigating relationship between HflK/HflC and NfeD, a wider study into the SPFH and NfeD genetic lineage as previous literature omits several important proteins, and comparing YuaG/YuaF of *B. halodurans* with the flotillin/NfeD of other Bacillacaea. Tidying up the nomenclature, which in several cases includes seryl-tRNA synthetases as a flotillin, is work that should be performed as well.

4. Genotypic and macroscopic analysis of *SCO3607* and *SCO3608* mutants in *S. coelicolor*.

4.1. Introduction

4.1.1 Gene disruption of *SCO3607*

Determining the function of a protein can be conducted through several methods, such as a biochemical assay or mutagenesis of the gene encoding the protein. The aim of this chapter is to assess the mutant phenotype of *SCO3607* and *SCO3608*. Previous results from *B. subtilis* showed defects in biofilm formation in response to a *floT* null mutant (Yepes *et al.*, 2012). Furthermore, common macroscopic phenotypes related to differentiation in *S. coelicolor* are the *whi* and *bld* phenotypes. Arising from the inability to form spores and aerial hyphae, respectively, these two phenotypes are possible consequences of disruption of these two genes (Flardh & Buttner, 2009, McCormick & Flardh, 2012)

There are two ways of achieving this; gene disruption and gene deletion. Gene disruption is based on the insertion of an antibiotic resistance gene into the gene to be disrupted and gene deletion is based on the excision of the relevant gene, normally through replacement with an antibiotic resistance gene.

Gene disruption in *S. coelicolor* is achieved through *in vitro* transposon mutagenesis. A cosmid, carrying the relevant gene with a Tn*5062* insertion, is transferred into *S. coelicolor* by intergeneric conjugation. Through homologous recombination, a single or a double crossover event may take place leading to either the entire cosmid integrating into the chromosome, or a double crossover event takes place, causing the Tn*5062*-carrying gene to replace the chromosomal gene (see Fig4-1). Antibiotic screening can be used to detect whether one or two of these events have occurred as shown in Fig4-1 D) and F), which result in the disruption of the gene or complete incorporation of the cosmid respectively. Transposon insertions of Tn5 derivatives in *S. coelicolor* genes are available from the ordered cosmid library used to sequence the *S. coelicolor* genome, and the inclusion of the *oriT* from the IncP-group plasmid RP4 (RP1/RP2) in the transposon allows for conjugation into *S. coelicolor* from *E. coli* (Bishop *et al.*, 2004).

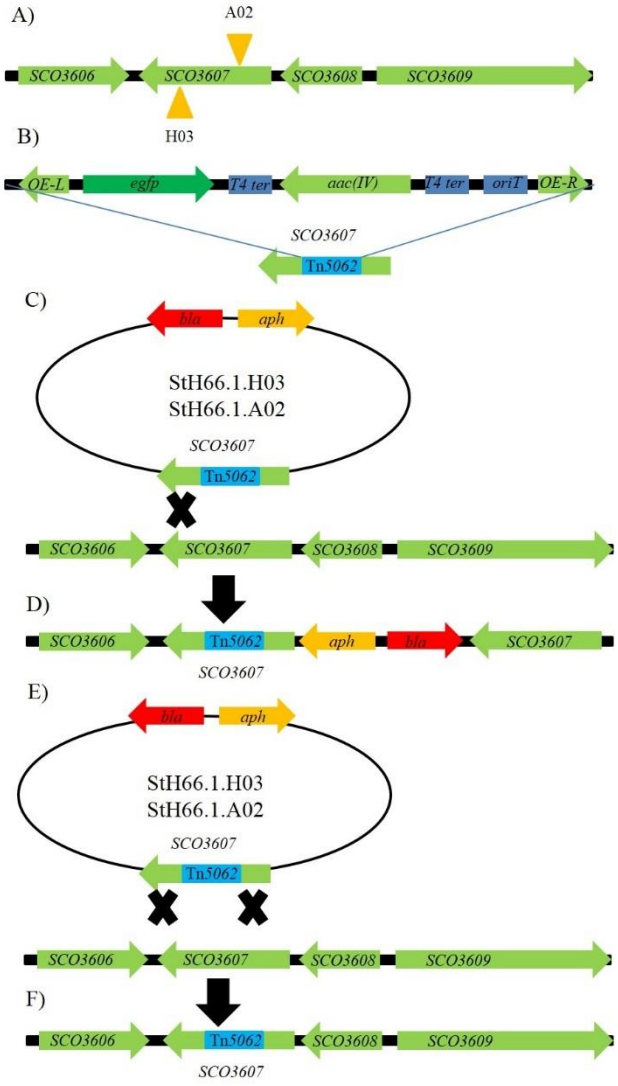

Fig4-1. Diagram explaining Tn*5062* transposon insertions in *SCO3607*. A) displays the two Tn*5062* transposon insertion sites used in this chapter, showing the strand and the approximate sites within *SCO3607*. B) is a genetic map of the Tn5062 transposon, containing an apracmycin resistance gene in the form of *aac(IV)*. C) shows a single crossover event between StH66.1.A02 or StH66.1.H03 and *SCO3607*. It also displays the cosmids complete with the Tn*5062* transposon inserted in *SCO3607* and the two antibiotic resistance genes, *aph* and *bla*. These genes confer resistance to kanamycin and ampicillin, respectively. D) displays the genetic alterations that have occur after a single crossover even between the aforementioned cosmids and *S. coelicolor*. where the entire cosmid is inserted into *SCO3607*.E) shows a double crossover event between StH66.1.A02 or StH66.1.H03 and *SCO3607*. F) displays the genetic alterations that have occur after a single crossover even between the aforementioned cosmids and *S. coelicolor*, where only the Tn*5062* transposon is inserted into *SCO3607*.

The potent methyl-specific restriction system of *S. coelicolor* needs to be overcome for the conjugation to be successful. To this end, *E. coli* ET12567, a strain defective in methylation due to a mutation in *dam*, is used, which greatly improves the conjugation efficiency. pUZ8002 is used as the mobilisation plasmid, as it contains the mobilisation gene *tra*, allowing for the conjugation of plasmids or cosmids from *E. coli* ET12567 (pUZ8002) into *S. coelicolor* (Bishop *et al.*, 2004). There are also several advantages to using *E. coli* as a conjugative donor organism, as it does not require protoplasts, restriction barriers are easily overcome through the use of non-methylating strains and vectors allowing for site-specific or insert-directed chromosomal integration (MacNeil *et al.*, 1992).

SCO3607 encodes the predicted flotillin of *S. coelicolor* and contains several Tn*5062* transposon insertion sites; however, *SCO3608*, the *nfeD* homologue, does not contain any Tn*5062* transposon insertion sites. Transposon insertions in *SCO3607* thus provide a way of elucidating whether it is required for growth and what a mutant phenotype it might have.

4.1.2. Gene deletion by PCR targeted mutagenesis of *SCO3607* and *SCO3608*

PCR targeted mutagenesis offers a simple, yet elegant, way of replacing a chromosomal fragment with an antibiotic resistance marker, and potentially flipping the marker out in the future, leaving a genomic "scar." Bacteria are not readily transformed with linear DNA due to their exonucleases that degrade the linear DNA, so there are two key issues in making a recombination strain: avoiding exonuclease activity and increasing recombination frequency. With regards to avoiding exonuclease activity, it appears that strains lacking exonuclease V of the *redBCD* cluster are transformable with linear DNA (Lorenz & Wackernagel, 1994, Cosloy & Oishi, 1973). For recombination to occur, *recB* or *recC* must carry a suppressor mutation in the form of either *sbcA* or *sbcB*, which activate the RecET recombinase of the Rac prophage or enhances recombination by activating the RecF pathway, respectively, allowing for linear DNA to recombine directly with the *E. coli* chromosome (Clark & Sandler, 1994, Winans *et al.*, 1985). Furthermore, *recD* mutants are recombinase proficient and lack the exonuclease V, which makes it an attractive tool for site-directed mutagenesis (Amundsen *et al.*, 1986). Utilising the homologous recombination systems of bacteriophages is another way of increasing recombination; λ Red increases the rate of recombination to greater than that of the *recBC, sbcB,* or *recD* mutants when transforming cells with linear DNA (Datsenko & Wanner, 2000, Smith, 1988, Murphy, 1998).

The method outlined here uses the λ RED system, which contains three relevant proteins: Gam, Bet and Exo. Gam inhibits the host RecBCD system and Bet and Exo enhance recombination efficacy in the presence of arabinose. *E. coli* BW25113 is used for the recombination as it is an *araBAD* and *hsdR*, the operon that encodes the proteins required for arabinose catabolism and an exonuclease, respectively, which greatly enhances the rate of recombination (Datsenko & Wanner, 2000). First, a PCR product containing an antibiotic resistance marker and *oriT*-containing cassette flanked by FRT (FLP recognition target), which are again flanked by sequences matching the regions flanking the genetic region to be removed is synthesised. This PCR product is then transformed into *E. coli* BW25113, which also carries the cosmid containing the gene to be removed. A double crossover event takes place between the cosmid and the PCR product, replacing the sequence to be deleted with the PCR product. The altered cosmid, with an antibiotic resistance gene in place of the gene, can then be introduced into *S. coelicolor* by conjugation, which requires passaging the cosmid through the methylation-deficient *E. coli* ET12567 (pUZ8002) to avoid the methylation-specific restriction system of *S. coelicolor*, and using antibiotics to test for transconjugants that have undergone double crossover events.

The disruption cassette is flanked by FRT sites, which are recognised by *E. coli* recombinase FLP. If so desired, FLP recombinase is then used to remove the resistance cassette from the modified cosmid, resulting in an 81 bp genetic "scar." This scar-bearing cosmid can then be introduced into the previously modified *S. coelicolor*, where a genetic crossover event takes place. Antibiotic selection can then be used to select double crossovers, which will now neither contain the gene or the disruption cassette, but rather the 81bp scar. This differs from earlier, as it is sensitivity to antibiotics that is being assayed. This can then be confirmed with either Southern blot or PCR. In this particular experiment, *SCO3607*, *SCO3608*, and *SCO3607* and *SCO3608* were replaced with a deletion cassette containing *aac3(IV)*, which confers apramycin resistance.

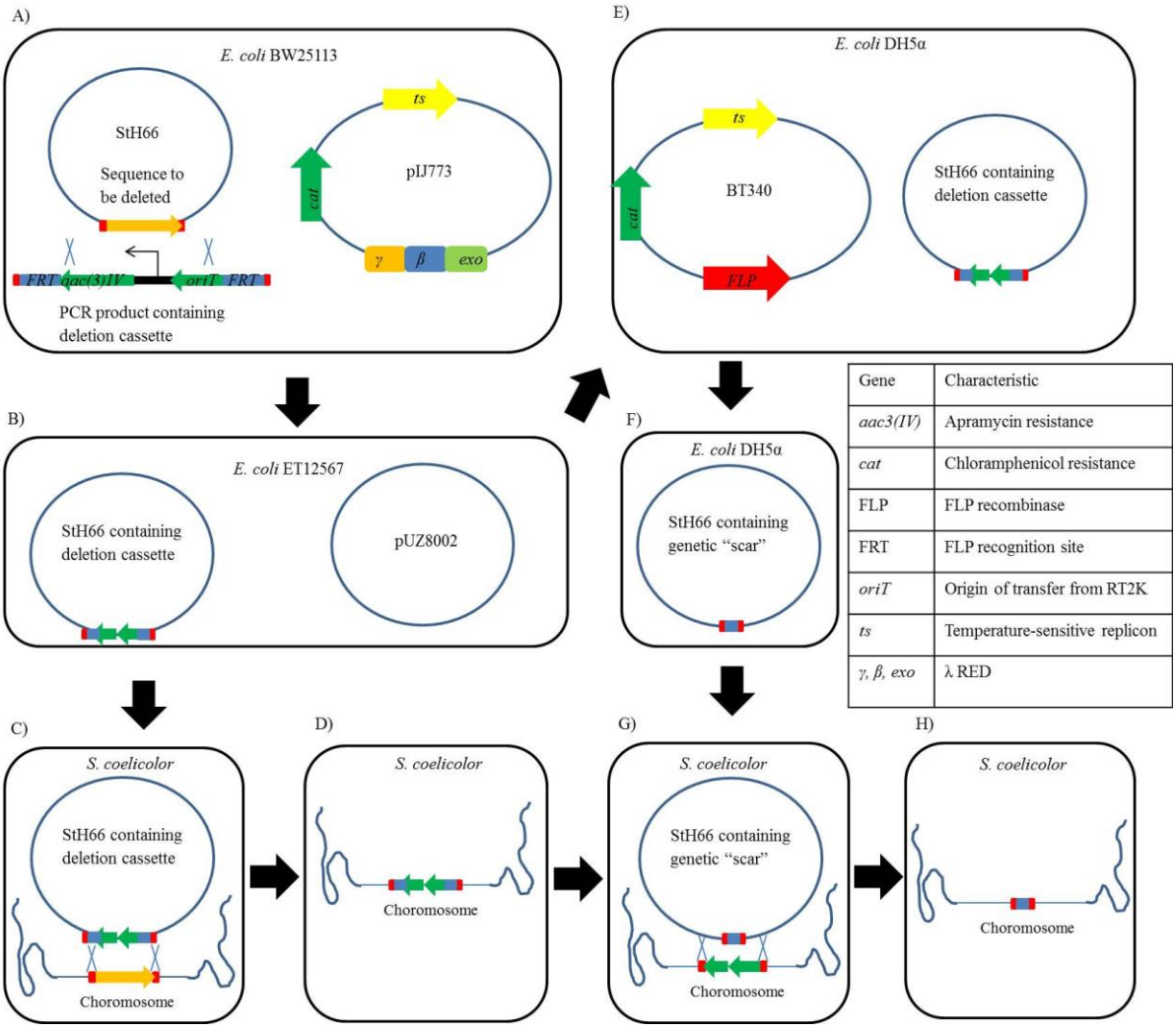

Gene	Characteristic
aac3(IV)	Apramycin resistance
cat	Chloramphenicol resistance
FLP	FLP recombinase
FRT	FLP recognition site
oriT	Origin of transfer from RT2K
ts	Temperature-sensitive replicon
γ, β, exo	λ RED

Fig4-2. Gene deletion of *SCO3607* and *SCO3608* by PCR targeted mutagenesis flowchart using a disruption cassette containing *aac3(IV)*. A) shows the double crossover event taking place in BW25113 leading to the generation of the deletion cassette-containing StH66. B) shows the altered StH66 after it has been passed into *E. coli* ET12567 (pUZ8002). C) shows the double crossover event between the chromosome and the altered StH66 cosmid in *S. coelicolor*. D) shows the *S. coelicolor* genome after the *aac3(IV)* containing deletion cassette has replaced the gene. E) shows the activation of FLP to excise the deletion cassette. F) shows the altered StH66 after the deletion cassette has been excised, with only the FRT and flanking regions left. G) shows the double crossover event which results in the excision of the deletion cassette. H) shows the final chromosomal configuration, with the gene and *aac3(IV)* containing deletion cassette replaced with the genetic scar.

4.1.3. Genetic complementation and verification

To verify that the correct gene was disrupted, and that a phenotype is not caused by an unlinked mutation, it is important to be able to restore wild-type phenotype through complementing the mutant with the disrupted gene with a fully functional gene. To this end, phage integrases are used to reintroduce a wild-type copy of the disrupted gene into chromosome. Normally, bacteriophages infect bacteria and subvert the host cell machinery to produce more phage and then lyse the cell to release the phage into the environment. If growth conditions are poor, the phage may integrate into the bacterial chromosome where it will lay dormant and when the conditions improve sufficiently it will excise and continue the cycle (Groth & Calos, 2004).

Phage mediate integration through an integrase enzyme that facilitates a recombination event between the phage attachment site, *attP*, a short viral DNA sequence, and the bacterial attachment site *attB*, a short stretch of bacterial DNA. Upon integration, the *attP* and *attB* sites are split in two, resulting in the phage being flanked by *attL* and *attR* sites, comprising *attP* and *attB* hybrid sequences. Integrases are divided into two families depending on which amino acid catalyses the strand-cleaving recombination event, the tyrosine recombinases and the serine recombinases. Tyrosine recombinases generally recognise longer *attP* sites, and serine recombinases recognise the shorter *attP* sites. Furthermore, some integrases act autonomously while some require other phage proteins and/or bacterially encoded host factors (Groth & Calos, 2004).

Phage integrases can be exploited to introduce fully functional genes. In *S. coelicolor*, there is an *attB* site within *SCO4848*, which can be utilised by the integration vector pMS82. This plasmid contains an *attP* site and a phage integrase, and thus will be integrated into *SCO4848* on the chromosome (Gregory *et al.*, 2003). It is then possible to introduce other genes into pMS82 to allow complementation.

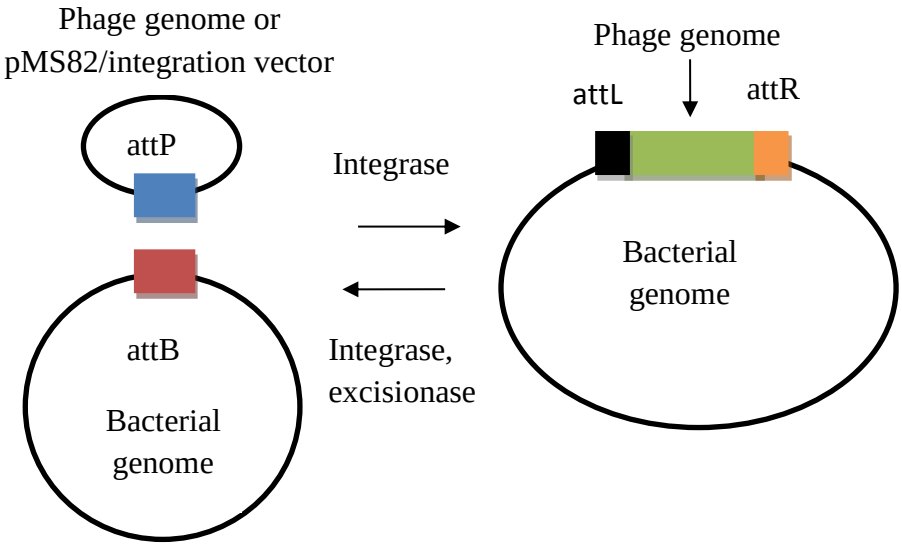

Fig4-3. Integration and excision genetic events mediated by phage integrases. The blue represents the *attP* site, red *attB* site, the green the phage genome, the black square the hybrid *attL* site and the orange square the hybrid *attR* site. Reproduced from (Groth & Calos, 2004).

4.1.4. Aims and goals

Determining whether a gene is essential is the first step in elucidating the function of a gene. Gene disruption is a quick method of establishing this, while gene deletion offers a more thorough option. The generation of Tn*5062* gene disrupted mutants also provides strains with, depending on the strand where the integration occurred, a gfp-tagged protein under the same promoter as the disrupted gene. Not all genes contain Tn*5062* insertion sites, the retention of incomplete functionality may also serve to partially mask effects, and polar effects of downstream genes, thus it is not always practical to rely solely on the Tn*5062* insertions. In this particular case, there are no Tn*5062* insertion sites in *SCO3608*. Therefore, *SCO3607* was disrupted at both StH66.1.A02 and StH66.1.H03 sites (see Fig4.2), thus allowing insertion on both strands, while *SCO3607* and *SCO3608* will be knocked out, both together and separately. The genes were also complemented to ensure the observed phenotype is due to the disruption or deletion.

Based on previous disruption and null mutants of flotillin and NfeD experiments in *B. subtilis*, *SCO3607* and *SCO3608* Tn*5062* and null mutations are predicted to be viable (Donovan & Bramkamp, 2009, Lopez & Kolter, 2010, Dempwolff *et al.*, 2012). However, *S. coelicolor* forms arthrospores while *B. subtilis* forms endospores, and the spore formation processes are

very different, so this is not an entirely correct comparison and they may play very different roles. Disruption and deletion will first help establish whether the genes are essential for growth, then, if the mutation is viable, if a phenotype becomes evident. The two most common macroscopic phenotypes for *S. coelicolor* are bald (*bld*), due to an inability to form aerial hyphae, and white (*whi*), due to an inability to form spores, so *whi* mutants are predicted due to the problems with sporulation in *B. subtilis* following deletion of the flotillin gene (Flardh & Buttner, 2009, McCormick & Flardh, 2012, Donovan & Bramkamp, 2009).

If Tn*5062* and null strains can be generated, they will be complemented and plated out on a variety of agars. *S. coelicolor* does not sporulate in liquid culture, so agar was chosen instead (van Keulen *et al.*, 2003). The agars to be used are SFM, R5, MM, and 3MA (see Table 2-3). SFM is used to rapidly induce sporulation and is a standard *S. coelicolor* growth medium, but it has been known to supress mutant phenotypes (Nodwell *et al.*, 1996). *S. coelicolor* produces more antibiotics when grown on R5, and is thus a good agar for visually assaying secondary metabolite production. Phenotypes observed in response to growth on R5 include reduction of actinorhodin production in a *SCO5812* null mutant (McArthur & Bibb, 2008). Minimal medium supplemented with mannitol suppresses some *bld* phenotypes, while glucose suppresses others (Willey *et al.*, 1991, van Wezel *et al.*, 1997). Poor growth has also been observed in some mutant strains (Kim *et al.*, 2012). Additionally, if a mutant phenotype was identified, complementation of wild-type phenotype could be attempted using different carbon sources or amino acids.

Different concentrations of KCl to assay for phenotypes in reaction to different growth conditions. *S. coelicolor* mutant strains have shown phenotypes in response to osmolarity (de Jong *et al.*, 2012, Bennett *et al.*, 2007, Keijser *et al.*, 2003). Salinity is also as a potential growth condition due to the induction of the *yuaFGI* operon of *B. subtilis*, which is under control of σ^w, which is induced by envelope stress, often caused by salt concentrations (Wiegert *et al.*, 2001, Huang *et al.*, 1999).

In summary, the goals of this Chapter is:

1) To ascertain whether *SCO3607* and *SCO3608* are essential for viability in *S. coelicolor*, both as single and double mutants, through the use of disruption and deletion mutatations.

2) To render *SCO3607* and *SCO3608* non-functional, both as single and double mutants, through the use of disruption and deletion cassettes so as to be able to investigate any potential mutant phenotype for information about its role, for example *bld* or *whi* phenotypes.
3) To investigate whether there are conditional mutant phenotypes based on media.
4) To generate strains for further downstream microscopic experiments.

4.2. Results

4.2.1. Transposon disruption and complementation of *SCO3607*

To determine whether *SCO3607* was an essential gene, *SCO3607* would be attempted disrupted using Tn*5062* transposon disruption cassettes. Two cosmids containing *S. coelicolor* chromosomal fragments with Tn*5062* transposon disruption cassette at two different sites in *SCO3607* were obtained, StH66.1.H03 and StH66.1.A02. The orientation of the *S. coelicolor* chromosomal fragments were determined. The cosmids were conjugated into *S. coelicolor* M145. Double crossovers had their *SCO3607* replaced with a *SCO3607* with a Tn*5062* transposon disruption cassette and were selected using antibiotic selection. Complemented strains were also generated for further downstream applications. As Tn*5062* transposon insertion strains were obtained with inserts at both sites, this demonstrates *SCO3607* is not an essential gene when cultured on SFM.

First, the orientation of the *S. coelicolor* fragments containing Tn*5062* transposon disruption cassettes in *SCO3607* in the cosmids, were determined. As the chromosome fragments are blunt ended when cloned into the vector, two possible orientations are possible (Fernandez-Martinez *et al.*, 2011). In order to generate accurate maps of the transposed cosmids it was necessary to determine the orientation that the *S. coelicolor* genomic fragments were originally cloned into the Supercos vector (Redenbach *et al.*, 1996). It was found they were of the "B" orientation (See Fig 4-4).

StH66.1.A02 and StH66.1.H03 were then isolated using a Bioline MiniPrep Kit from the *E. coli* JM109 stocks (available from Paul Dyson) containing the cosmids, then transformed into electro-competent *E. coli* ET12456/pIJ8002, before conjugation into *S. coelicolor* M145 (See sections 2.1.8., 2.3.2., and 2.3.9.). Double crossovers were selected for with antibiotic selection for both conjugations (Fernandez-Martinez *et al.*, 2011). As a single crossover event would result in a strain both apr^r and kan^r, apr^r and kan^s colonies were selected for as in described in section 2.1.8. Several apr^r kan^s strains were obtained, in addition to one apr^r kan^r strain. The apr^r kan^s strains derived from StH66.1.H03 were named CFW3607A, CFW3607B, CFW3607C, CFW3607D, CFW3607E, CFW3607F, CFW3607G, CFW3607H, and CFW3607I. CFW3607J contains a single crossover and is thus apr^r kan^r. The apr^r kan^s strains derived from StH66.1.A02 were named CFW3607K, CFW3607L, and CFW3607M (See Table 2-1). PCR was used to verify the Tn*5062* disruption cassette had been correctly inserted into *SCO3607* in CFW3607A and CFW3607M (See Fig4-6).

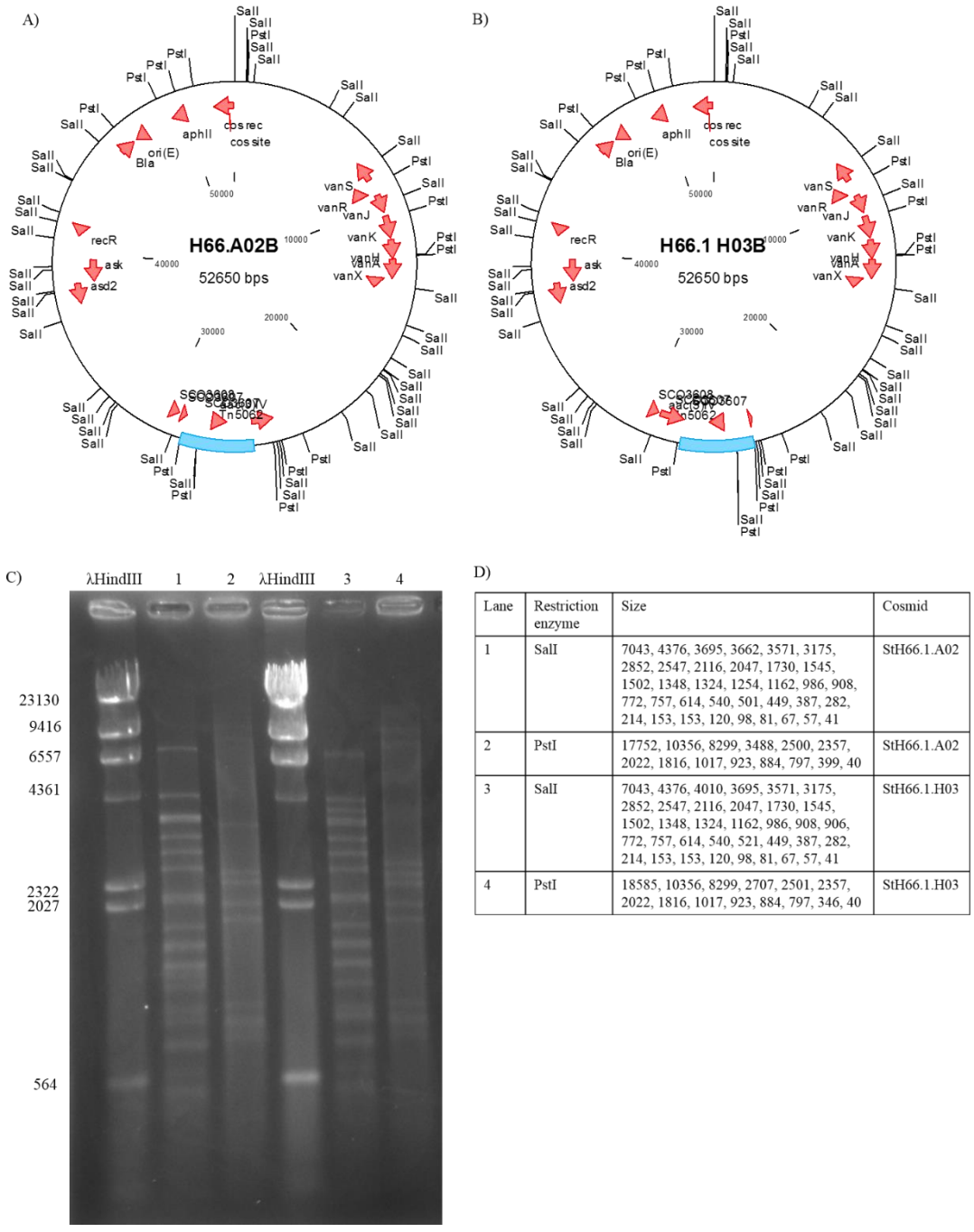

Lane	Restriction enzyme	Size	Cosmid
1	SalI	7043, 4376, 3695, 3662, 3571, 3175, 2852, 2547, 2116, 2047, 1730, 1545, 1502, 1348, 1324, 1254, 1162, 986, 908, 772, 757, 614, 540, 501, 449, 387, 282, 214, 153, 153, 120, 98, 81, 67, 57, 41	StH66.1.A02
2	PstI	17752, 10356, 8299, 3488, 2500, 2357, 2022, 1816, 1017, 923, 884, 797, 399, 40	StH66.1.A02
3	SalI	7043, 4376, 4010, 3695, 3571, 3175, 2852, 2547, 2116, 2047, 1730, 1545, 1502, 1348, 1324, 1162, 986, 908, 906, 772, 757, 614, 540, 521, 449, 387, 282, 214, 153, 153, 120, 98, 81, 67, 57, 41	StH66.1.H03
4	PstI	18585, 10356, 8299, 2707, 2501, 2357, 2022, 1816, 1017, 923, 884, 797, 346, 40	StH66.1.H03

Fig4-4. Gel electrophoresis confirmation of StH66.1.A02 and StH66.1.H03 orientation. A) and B) are cosmid maps constructed of the B orientation of StH66.1.A02 and StH66.1.H03. The Tn*5062* insertion is in blue. C) Is the 1% agarose gel electrophorese image of StH66.1.A02B and StH66.1.H03B digested with PstI or SalI, with HindIII cut λ phage as standard confirming the orientation. D) is the key for the gel, and contains the different enzymes and expected fragment sizes.

To confirm the correct insertion of the Tn*5062* transposon disruption cassette into *SCO3607* in CFW3607A and CFW3607M a PCR was performed. Genomic DNA from CFW3607A, CFW3607M, M145 was then isolated along with StH66.1.C09, StH66.1.H03, and StH66.1.A02 using a Bioline MiniPrep Kit (See sections 2.3.2. and 2.3.3.). The PCR primers A02F2, A02R2, H03F, and H03R were designed. These were used to amplify specific regions unique to the different strains and cosmids in combination with the primers EZR1 and EZL2. The regions amplified and their bands from the different templates are summarised in Fig 4-5 and Fig4-6 (See section 2.3.7. and Table 2-5 for primer sequences). The PCR reactions were performed using MyTaq while M145, StH66.1.C09, StH66.1.H03, and StH66.1.A02 were used as templates in the control experiments. Some of the larger PCR reactions did not work, likely due to the size of the PCR product, but they were attempted. Regardless, the correct insertion of the Tn*5062* transposon disruption cassette into *SCO3607* was confirmed.

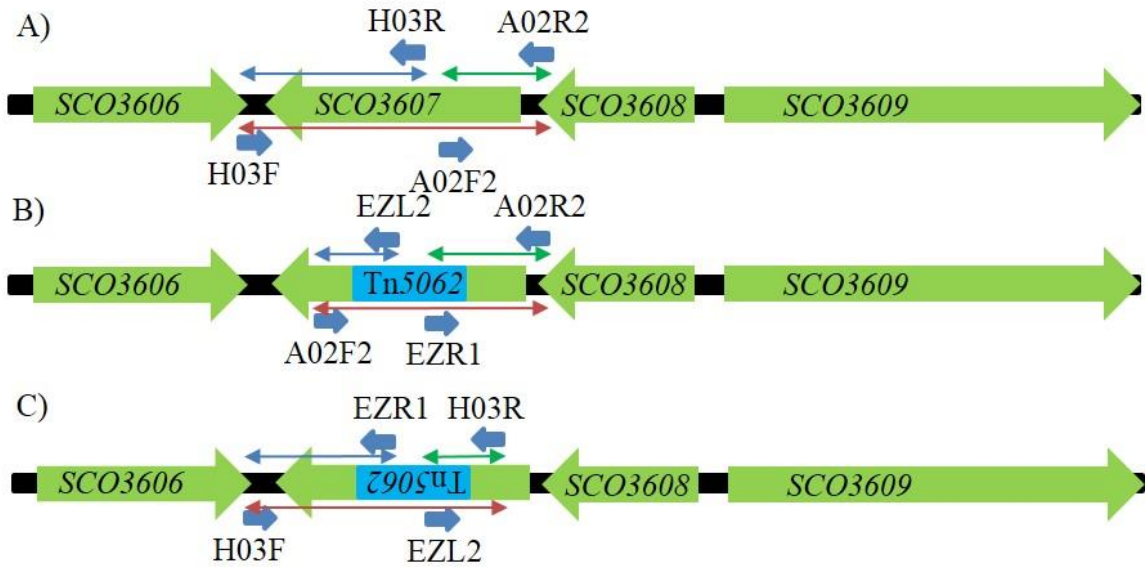

Fig4-5. Diagram displaying regions amplified by PCR in confirmation of the disrupted strains. A) shows which sections would be amplified by PCR using the aforementioned PCR primers in *S. coelicolor* M145, StH66.1.C09, and StH66.1.D07. The cosmids have Tn*5062* insertions in *SCO3609* and *SCO3606*, respectively, but they do not affect the PCR. Blue arrow represents the H03R and H03F band (1150bp), the green arrow represents the A02F2 and A02R2 band (1432bp). B) shows which sections are amplified in *S. coelicolor* CFW3607M and StH66.1.A02. The blue arrow shows the region amplified using EZL2 and A02F2 (1302bp), the green arrow shows the region amplified by A02R2 and EZR1 (400bp), and the red arrow shows the region amplified by A02R2 and A02F2 (4883bp). C) shows the regions amplified in *S. coelicolor* CFW3607A and StH66.1.H03. The blue arrow displays the region amplified by EZR1 and H03F (968bp), the green arrow displays the region amplified by H03R and EZL2 (452bp), and the red arrow displays the region amplified by H03F and H03R (4601bp). The Tn*5062* disruption insertion cassette has been inverted in C) to illustrate the H03 Tn*5062* insertion site being on the opposite strand. It has not been drawn to scale.

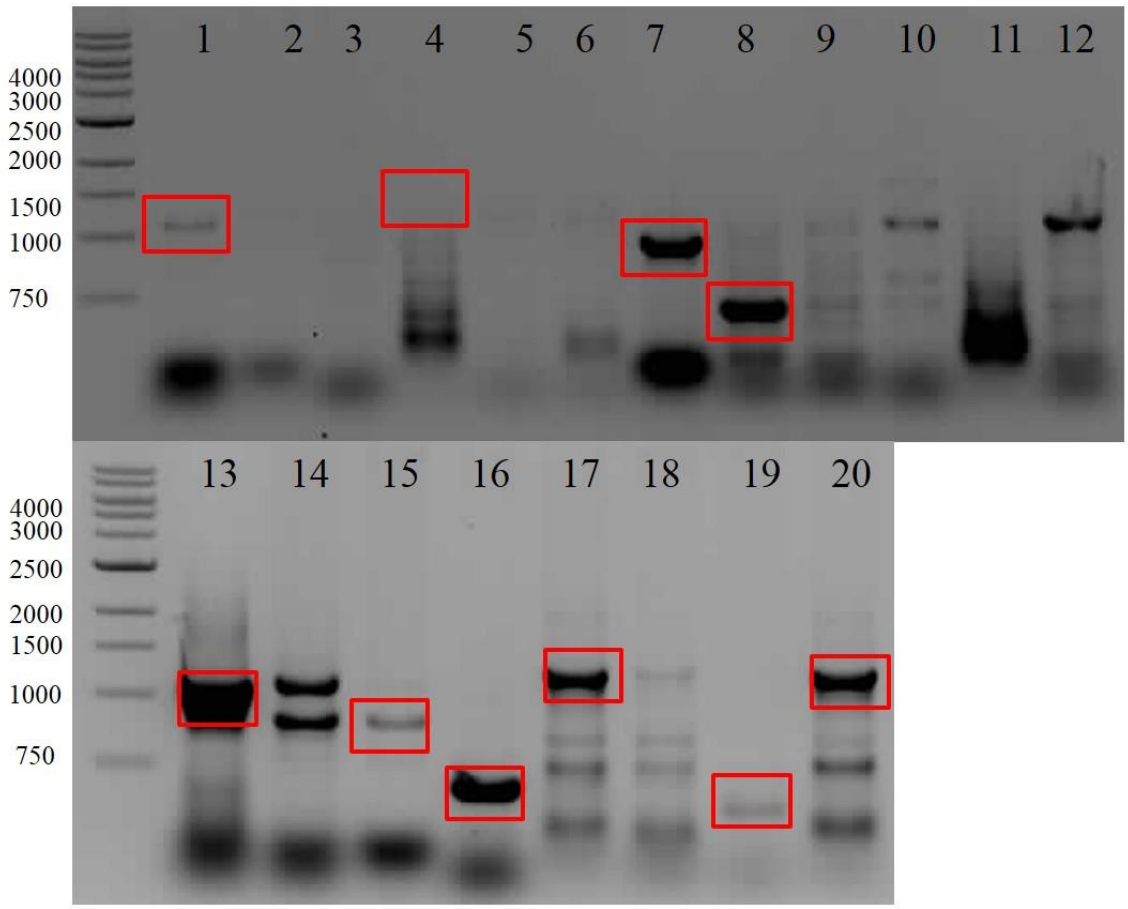

Well	Template	Primers	Product size
1	M145	H03F+H03R	1150
2	M145	H03F+EZR1	-
3	M145	H03R+EZL2	-
4	M145	A02F2+A02R2	1432
5	M145	A02F2+EZL2	-
6	M145	A02R2+EZR1	-
7	CFW3607A	H03F+EZR1	968
8	CFW3607A	H03R+EZL2	452
9	CFW3607A	H03F+H03R	4601
10	CFW3607M	A02R2+EZR1	400

Well	Template	Primers	Product size
11	CFW3607M	A02F2+EZL2	1302
12	CFW3607M	A02F2+A02R2	4883
13	StH66.1.C09	H03F+H03R	1150
14	StH66.1.H03	H03F+H03R	4601
15	StH66.1.H03	H03F+EZR1	968
16	StH66.1.H03	H03R+EZL2	452
17	StH66.1.D07	A02F2+A02R2	1432
18	StH66.1.A02	A02F2+A02R2	4883
19	StH66.1.A02	A02F2+EZL2	400
20	StH66.1.A02	A02R2+EZR1	1302

Fig4-6. PCR confirms CFW3607A and CFW3607M contain the Tn*5062* disruptions cassettes in *SCO3607*. The relevant PCR product in each experiment is highlighted with a red box. Some primer dimers and non-specific PCR products are visible.

The generation of a complementation vector is one of way of ensuring the phenotype is due to the genetic change introduced and not due to an unlinked mutation. Furthermore, the restoration of wild-type phenotype functions a control for downstream experiments, such as growth on different types of agar. To this end, a complementation vector, pCFW104, was generated from

StH66.1.C09 by subcloning a fragment containing both *SCO3607* and *SCO3608* into pMS82 (See Fig4-7 and Fig4-11). This was then conjugated into CFW3607A and CFW3607M to create the complemented strains CFW3607AC and CFW3607MC, respectively.

StH66.1.C09 was isolated from JM109 stocks and its orientation was checked, as was conducted for StH66.1.A02 and StH66.1.1H03 (see Fig4-4). It was then digested with BglII and EcoRI while pUC19 was digested with BamHI and EcoRI. StH66.1.C09 has a Tn*5062* transposon insertion cassette in *SCO3609*, but the fragment does not contain any part of the Tn*5062* transposon insertion cassette. The StH66.1.C09 fragment containing *SCO3607* and *SCO3608* was isolated by agarose gel DNA extraction. This was then ligated into the restriction enzyme digested pUC19 to create pCFW102 (see Fig4-8). Once pCFW102 was constructed, it and pBGS19 were digested with XbaI and HindIII. The *SCO3607* and *SCO3608* fragment from pCFW102 was isolated by agarose gel DNA extraction and ligated into pBGS19. The new plasmid was labelled pCFW103 (See Fig4-9). Again, this was restriction enzyme digested with SmaI, while pMS82 was restriction enzyme digested with EcoRV. The *SCO3607* and *SCO3608* fragment from pCFW103 was isolated by agarose gel DNA extraction and blunt-end ligated into pMS82 to make pCFW104 (See Fig 4-10). As this was a blunt-end subcloning the orientiation of the insert was checked. *E. coli* DH5α was used to propagate each of these plasmids. This entire cloning strategy is summarised in Fig4-7.

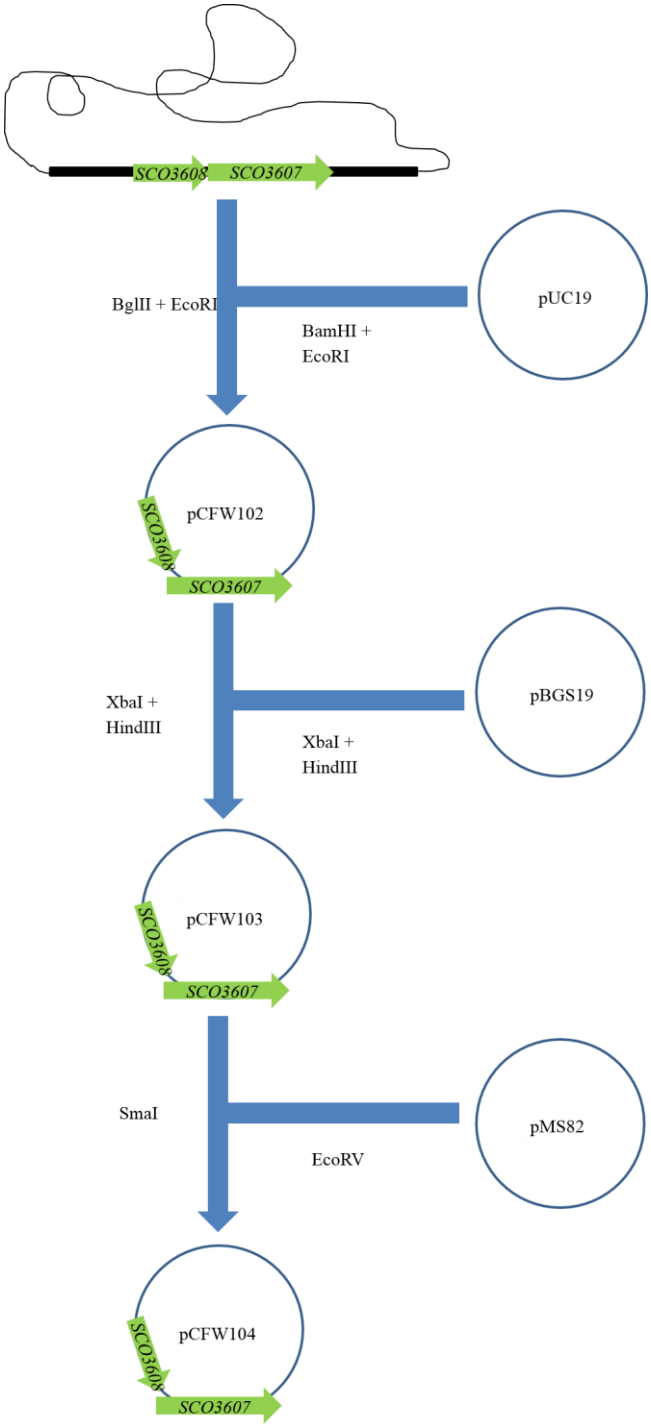

Fig4-7. Subcloning strategy flowchart for the generation of a complementation vector for CFW3607A and CFW3607M. StH66.1.C09 was digested with BglII and EcoRI and the 5.7kb fragment containing SCO3607 and SCO3608 was subcloned into pUC19, previously digested with BamHI and EcoRI to make pCFW102. pCFW102 and pBGS19 were digested with XbaI and HindIII and the gene-containing fragment from pCFW102 was subcloned into pBGS19 to make pCFW103. pCFW103 was further digested with SmaI and blunt-end subcloned into pMS82 to make pCFW104.

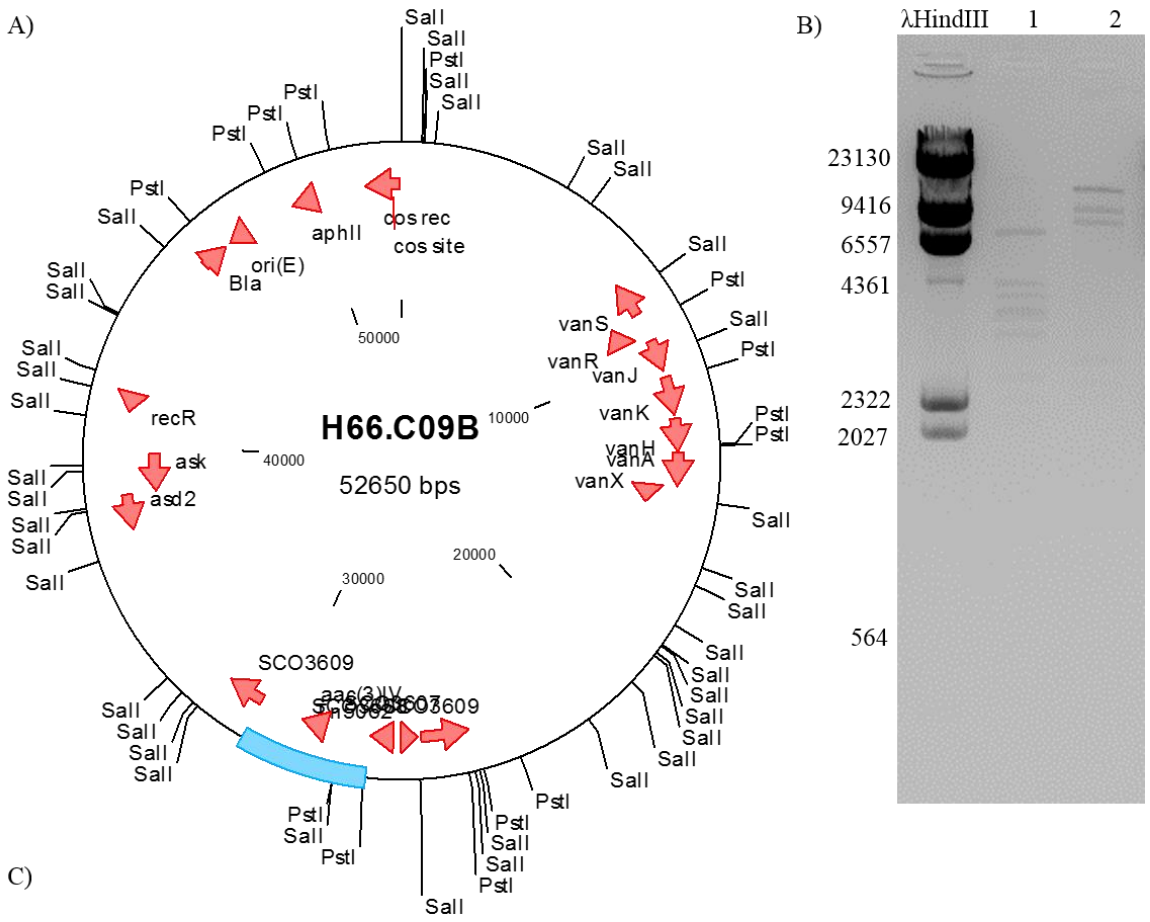

Lane	Restriction enzyme	Size	Cosmid
1	SalI	7043, 4376, 4030, 3695, 3571, 3175, 2547, 2273, 2047, 1730, 1545, 1502, 1465, 1348, 1324, 1162, 986, 908, 772, 757, 614, 540, 501, 449, 387, 282, 214, 153, 153, 120, 98, 81, 67, 57, 41	StH66.1.A02
2	PstI	18461, 10356, 8299, 2799, 2500, 2357, 2022, 1816, 1017, 923, 884, 797, 399, 40	StH66.1.A02

Fig4-8 Confirmation of StH66.1.C09. A) is a cosmid map constructed of the B orientation of StH66.1.C09. B) Confirmation of the 1% agarose gel electrophorese image of StH66.1.C09 digested with PstI or SalI, with HindIII cut λ phage as standard. C) is the key for the gel, and contains the different enzymes and expected fragment sizes.

A)

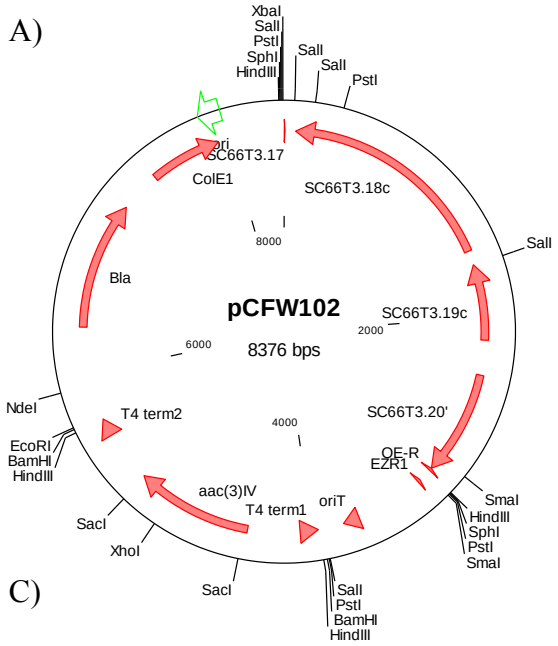

B)

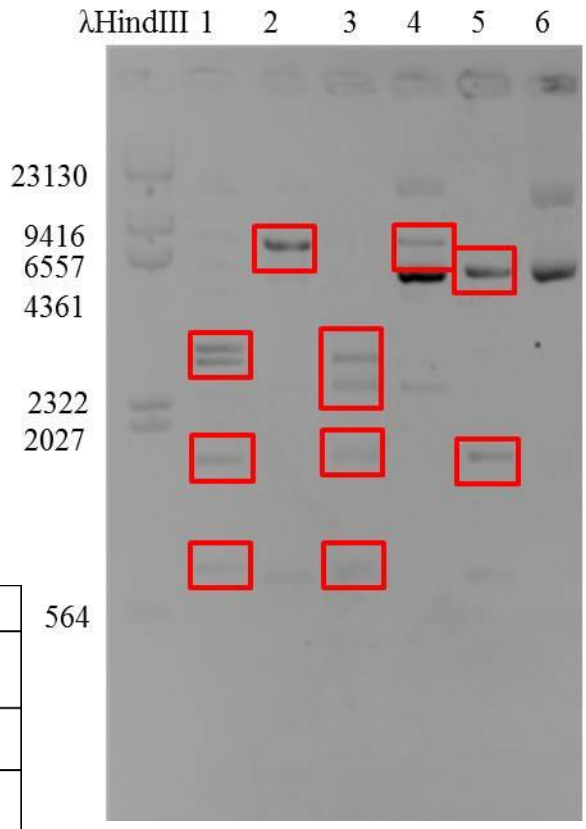

C)

Well	Restriction enzymes	Fragment size
1	HindIII	3147, 2667, 1721, 841
2	EcoRI	8376
3	HindIII+EcoRI	3147, 2635, 1721, 841, 32
4	XbaI	8376
5	BamHI	6613, 1763
6		Undigested

Fig4-9. Confirmation of pCFW102. A) pCFW102 map was constructed by ligating a BglII and EcoRI restriction enzyme digested StH66.1.C09 fragment into BamHI and EcoRI restriction enzyme digested pUC19. The clone contains a functional copy of *SCO3607* and *SCO3608*. B) Confirmation of the 1% agarose gel electrophorese image of pCFW102 digested with: HindIII, EcoRI, HindIII and EcoRI, XbaI, BamHI, and HindIII cut λ phage as a standard. C) is the key for the gel, and contains the different enzymes and expected fragment sizes.

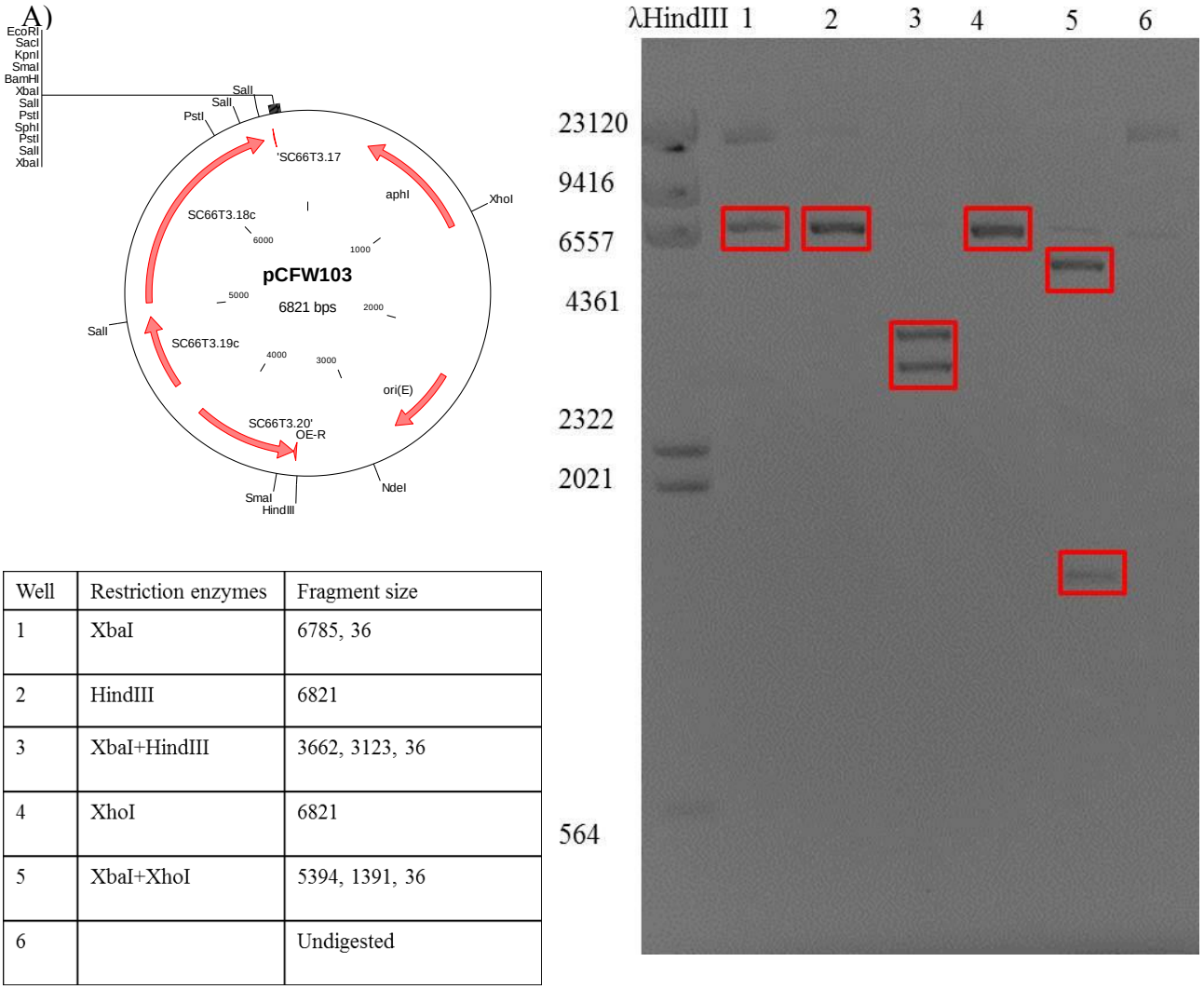

Well	Restriction enzymes	Fragment size
1	XbaI	6785, 36
2	HindIII	6821
3	XbaI+HindIII	3662, 3123, 36
4	XhoI	6821
5	XbaI+XhoI	5394, 1391, 36
6		Undigested

Fig4-10 Confirmation of pCFW103. A) pCFW103 map was constructed by ligating a XbaI and HindIII restriction enzyme digested pCFW102 fragment into XbaI and HindIII restriction enzyme digested pBGS19. The clone contains a functional copy of *SCO3607* and *SCO3608*. B) Confirmation of the 1% agarose gel electrophorese image of pCFW102 digested with: XbaI, HindIII, XbaI and HindIII, XhoI, XbaI and XhoI, and HindIII cut λ phage as a standard. C) is the key for the gel, and contains the different enzymes and expected fragment size

A)

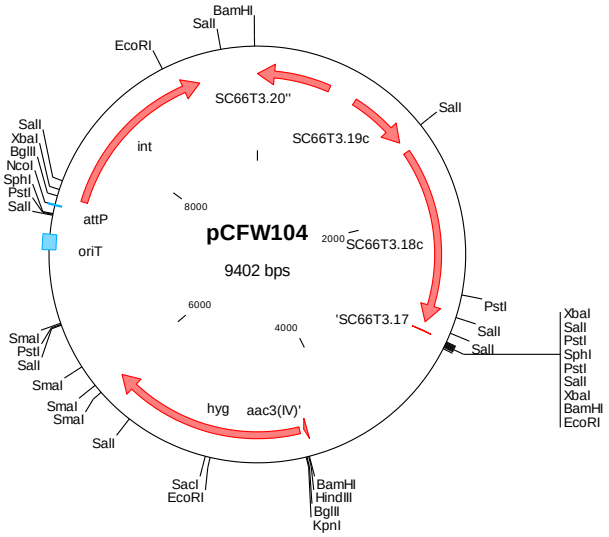

B)

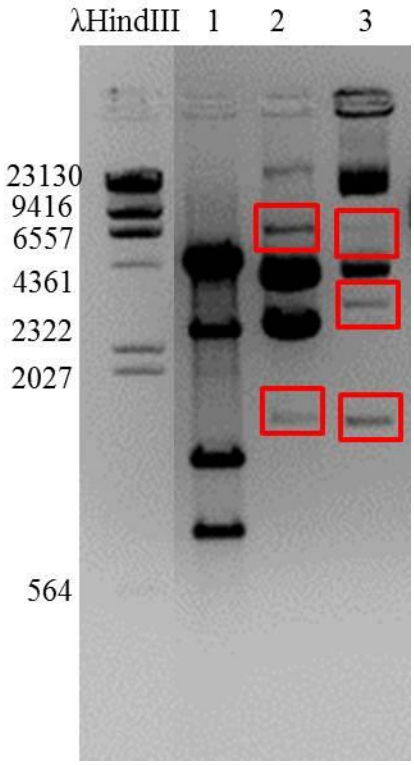

C)

Lane	Restriction enzymes	Fragment size
1	Undigested	-
2	XbaI+XhoI	5394, 1391, 36
3	BamHI	5059, 3061, 1282

Fig4-11. Confirmation of pCFW104 by restriction enzyme digest. A) is the pCFW104 map, which was constructed by blunt-end ligating the *SCO3607*-containing SmaI fragment from pCFW103 into an EcoRV restriction enzyme digested pMS82. B) is the restriction enzyme digested confirmations run on a gel electrophoresis gel with the relevant bands highlighted. There are considerable amounts of undigested DNA. Additionally, due to that the samples were run on a gel with non-relevant samples, these were cut out and account for the slight change in colour. C) is the key for the gel, and contains the different enzymes and expected fragment sizes.

Once the complementation vector pCFW104 was generated, it was isolated and conjugated into *S. coelicolor* CFW3607A and CFW3607M. The strains were labelled CFW3607AC and CFW3607MC.

4.2.2. Screening for morphological phenotypes

To ascertain whether SCO3607 had any macroscopic effects, such as the *whi* or *bld* phenotypes which would suggest SCO3607 plays a role in forming spores or aerial hyphae, respectively, strains containing disrupted *SCO3607* were plated out on several types of media to ensure any potential mutant phenotype was not supressed by the media (Flardh & Buttner, 2009, McCormick & Flardh, 2012, Nodwell *et al.*, 1996). To this end, CFW3607A, CFW3607AC, CFW3607M, CFW3607MC, and M145 were plated out on 3MA, MM, SFM, and R5 media and incubated at 30^{o} degrees for 6 days. Pictures were taken every 24 hours to assay for any morphological changes. The results showed no apparent phenotypic changes due to the Tn*5062* disruption cassette.

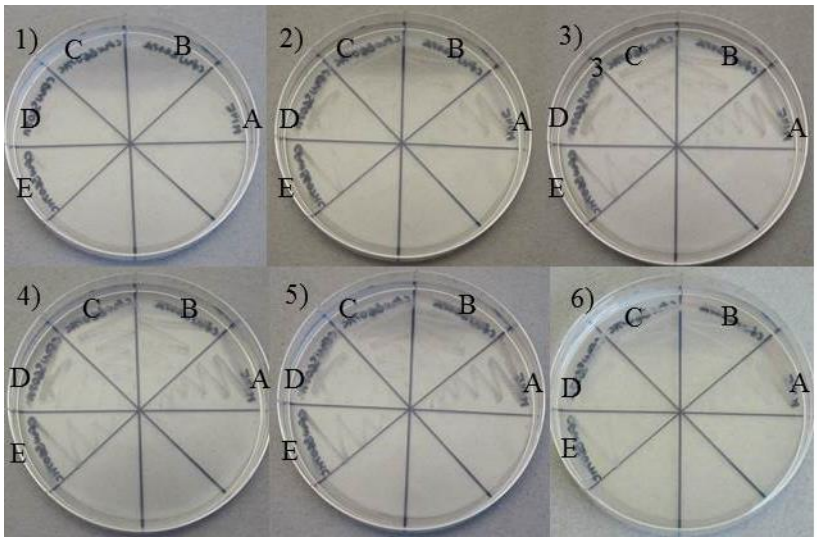

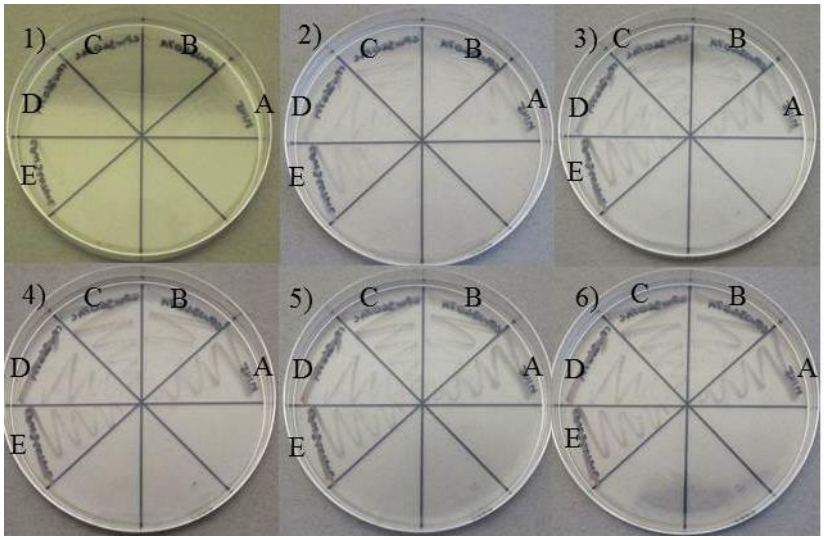

Key	Strain
A	M145
B	CFW3607A
C	CFW3607AC
D	CFW360M
E	CFW3608MC

Fig4-12. Tn*5062*-disrupted *SCO3607* mutants grown on 3MA (above) and MM (below) at 30º for 6 days display no particular phenotype. Number of days grown is indicated in the top left corner of each picture.

Much less biomass was visible when the strains were grown on 3MA and MM. Little to no growth was visible after 24 hours. White aerial hyphae were visible on 3MA after 6 days. Small amounts of undecylprodigiosin, a red antibiotic, were visible after 4 days.

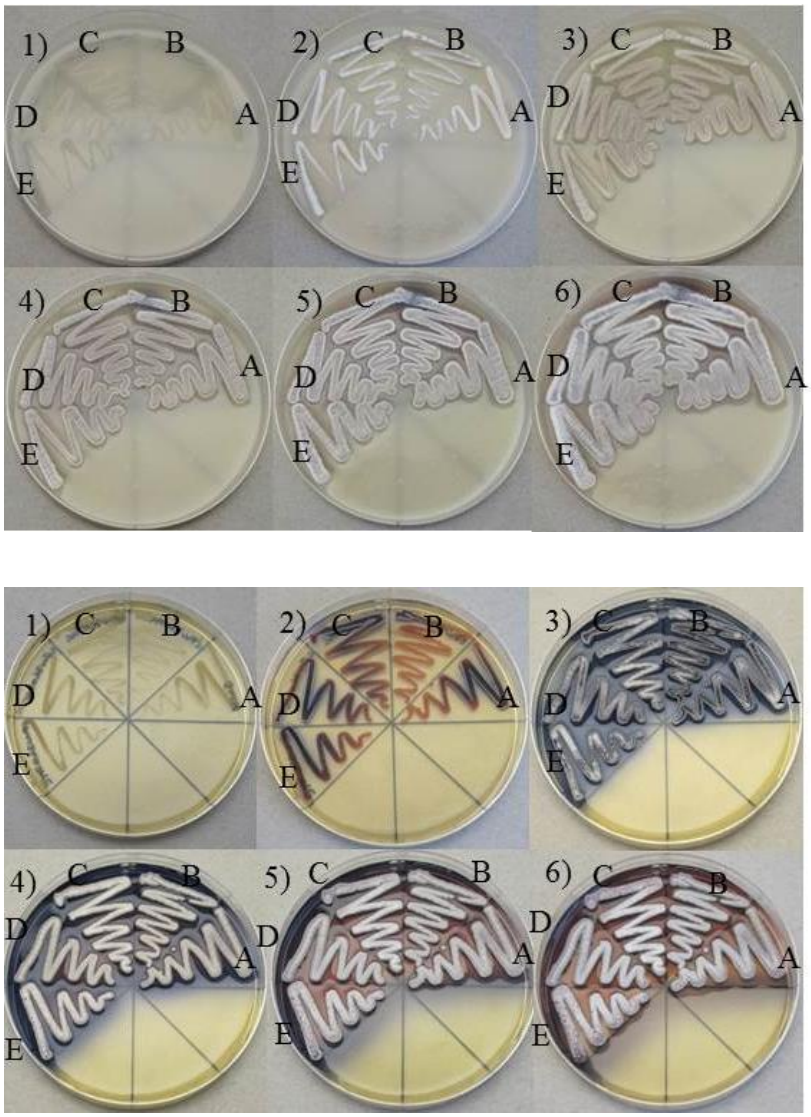

Key	Strain
A	M145
B	CFW3607A
C	CFW3607AC
D	CFW360M
E	CFW3608MC

Fig4-13. Tn*5062*-disrupted *SCO3607* mutants grown on SFM (above) and R5 (below) at 30º for 6 days display no particular phenotype. Number of days grown is indicated in the top left corner of each picture.

When the strains were grown on SFM, strains grew as vegetative hyphae after 24 hours, aerial hyphae had formed after 48 hours, visible due to the white pigment. Spores had formed after 72 hours and continued to mature until the end of the experiment, visible due to the grey colour. Increased antibiotic production was evident in all strains when grown on R5 medium due to the red and blue pigments, consistent with previous literature (McArthur & Bibb, 2008). These two pigments, which are red and blue, are undecylprodigiosin and actinorhodin, respectively. Antibiotic production was visible to a minor degree in all strains after 24 hours, but it did not fully begin to be produced until 48 hours after inoculation. CFW3607A appeared to possibly produce less actinorhodin. Aerial hyphae were visible after 72 hours, visible due to the white

colouring of the culture, and after 96 hours, grey spores were visible and maturation continued until 6 days after inoculation.

4.2.3. Screening for a morphological phenotype in response to osmotic stress

To investigate the role of SCO3607 in response to osmotic stress, SCO3607A, SCO3607AC, SCO3607M, SCO3607MC, and M145 were plated out on 3MA containing either 0.1M, 0.2M, 0.3M, 0.4M or 1M KCl to assay for morphological changes. The plates were incubated at 30^{o}C degrees for 6 days and pictures were taken every 24 hours. No phenotype was apparent, suggesting that even though FloT of *B. subtilis* is activated by σ^{w}, which in turn is activated by osmotic stress, this is not the case in *S. coelicolor* (Huang *et al.*, 1999). It does not affect antibiotic production either as undecylprodigiosin is visible on all plates. There was no difference in aerial hyphae formation either.

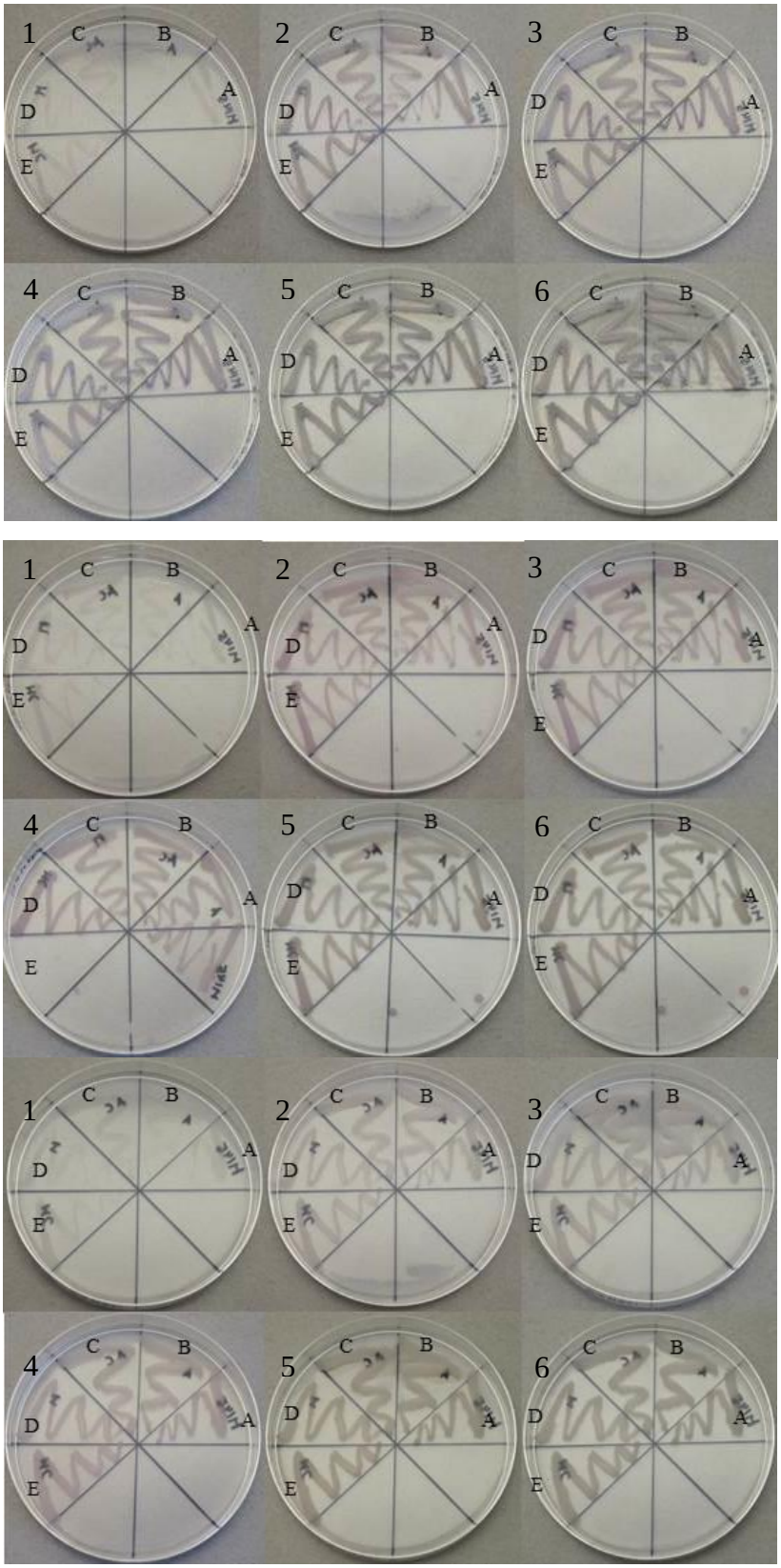

Key	Strain
A	M145
B	CFW3607A
C	CFW3607AC
D	CFW360M
E	CFW3608MC

Fig4-14. Tn*5062*-disrupted *SCO3607* mutants grown on 3MA with 0.1M (above), 0.2M (middle) and 0.3M KCl (below) at 30º for 6 days display no particular phenotype. Number of days grown is indicated in the top left corner of each picture.

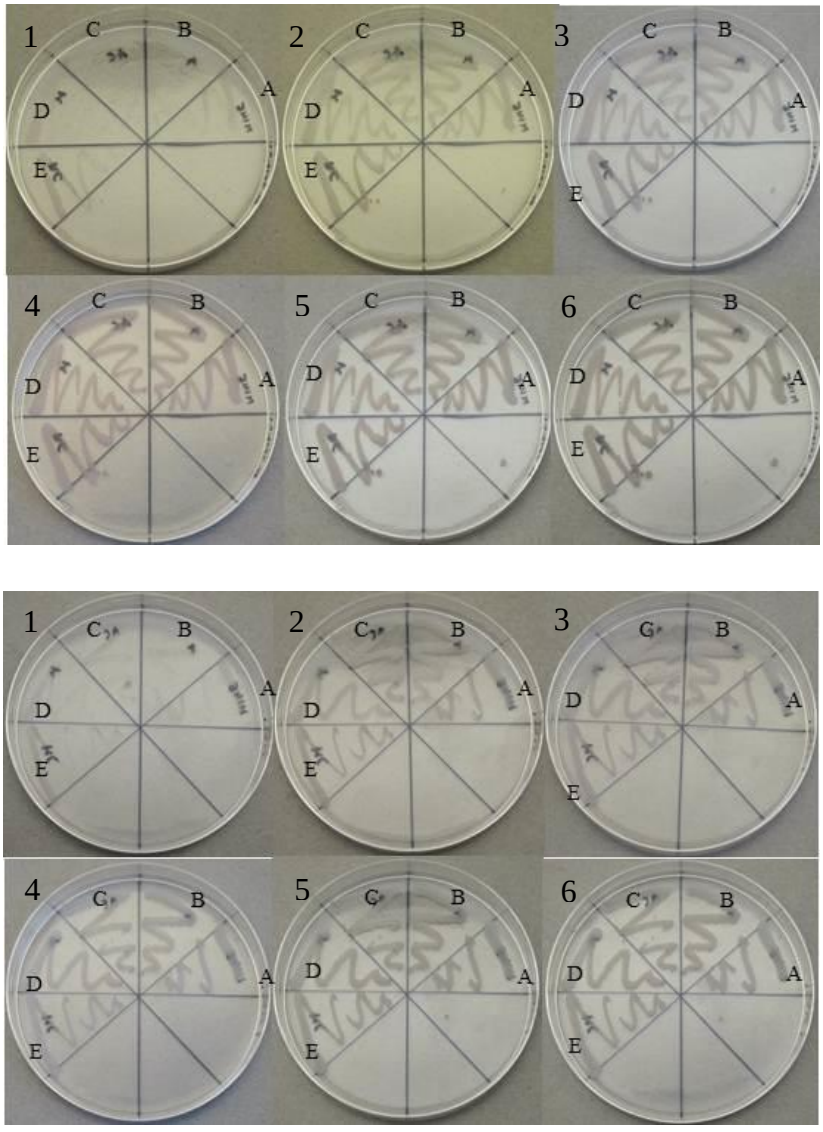

Key	Strain
A	M145
B	CFW3607δ
C	CFW3607δC
D	CFW3608δ
E	CFW3608δC
F	CFW3607/8δ
G	CFW3607/8δC

Fig4-15. Tn*5062*-disrupted *SCO3607* mutants grown on 3MA with 0.4M (above) and 1M (below) KCl at 30º for 6 days display no particular phenotype. Number of days grown is indicated in the top left corner of each picture. There was no obvious phenotype for any of the Tn*5062* disruption strains, regardless of time and osmotic stress.

On all plates undecylprodigiosin production was visible after 2 days, with the strongest production was visible on the 0.2M KCl plate. White aerial hyphae were visible after 3 days on the 0.1M KCl plate, but not on the other plates.

4.2.4. Construction of *SCO3607* and *SCO3608* null strains

To gain further insight into the macroscopic effects of SCO3607 and begin the investigation of the role of SCO3608, three null strains were constructed using PCR targeted mutagenesis (See Fig4-3). Three cosmids were constructed from StH66; StH66C3, StH66C4 and StH66C5. StH66C3 lacked *SCO3607*, StH66C4 lacked *SCO3608*, and StH66C5 lacked *SCO3607* and *SCO3608*. These were then conjugated into *S. coelicolor* M145 and double crossovers were selected; CFW3607δ, CFW3608δ, and CFW3607/8δ, which lacked *SCO3607*, *SCO3608*, and both *SCO3607* and *SCO3608*, respectively. The strains were confirmed by PCR (See Fig4-21 and Fig4-22). The previously constructed complementation vector pCFW104 (See Fig4-10) was conjugated into CFW3607δ, CFW3608δ, and CFW3607/8δ to generate the complemented strains CFW3607δC, CFW3608δC, and CFW3607/8δC, respectively. That it was possible to make null mutants of *SCO3607*, *SCO3608*, *SCO3607* and *SCO3608* demonstrated neither gene is essential, alone or together.

Long PCR primers were designed (See Materials and Methods), with 39 nucleotides at the 5' end of the primer identical to the flanking region of the gene to be deleted and 19 or 20 nucleotides at the 3' end matching the left or right end of the disruption cassette to be inserted (See Table 2-5). The primers used to perform the PCR were SCO3607DELF and SCO3607DELR for SCO*3607*, SCO3608DELF and SCO3608DELR for *SCO3608*, and SCO3608DELF and SCO3607DELR for the double knockout cosmid (See Fig4-16). pIJ790 was used as a template and the PCR product was purified.

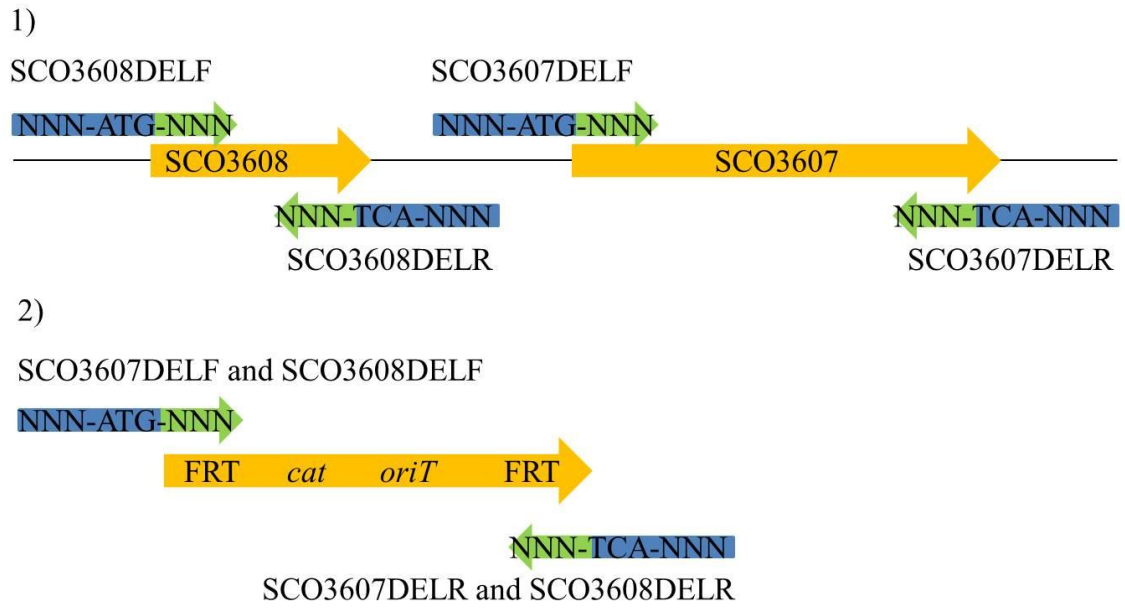

Fig4-16. Diagram describing the sequences amplified by PCR and where the flanking regions are on the primers. The 39 nucleotide 5' end of the primer that matches the flanks of the sequence to be deleted is highlighted in blue on each primer, while the 19 and 20 nucleotide 3' ends of the primers are highlighted in green on each primer. *SCO3607* and *SCO3608* are highlighted with orange, as is the antibiotic resistance cassette. 1) shows where the 39' 5 end of the primer anneals on the chromo and 2) shows where it anneals on pIJ790. When pIJ790 then is used to amplify the cassette, the ends of the PCR product will match the flanking regions of the gene(s) to be deleted, allowing for the double crossover event switching out the gene with the antibiotic resistance cassette.

The purified PCR products were then transformed into *E. coli* BW25113/pIJ790/StH66 as per the PCR targeted mutagenesis protocol (See Materials and Methods) and double crossovers were selected for with chloramphenicol, kanamycin, and apramycin. The temperature-sensitive recombination plasmid pIJ790 was deliberately lost to allow for this selection. The three new StH66 derived cosmids were labelled StH66C3, StH66C4, and StH66C5, which lacked *SCO3607*, *SCO3608*, and both, respectively, and stored in *E. coli* DH5α. The cosmids were then confirmed by restriction enzyme digest and gel electrophoresis (See Figs4-18-20). StH66C3, StH66C4, and StH66C5 were then transformed into *E. coli* ET12567/pUZ8002 and conjugated in *S. coelicolor* M145. Double crossover strains would be chl^r, kan^s and colonies were screened for this. The new strains were named CFW3607δ, CFW3608δ, and CFW3607/8δ, which lacked *SCO3607*, *SCO3608*, and both, respectively. These were then

confirmed by PCR (See Fig4-21). All three strains were then complemented with pCFW104 by conjugating the plasmid into the strains.

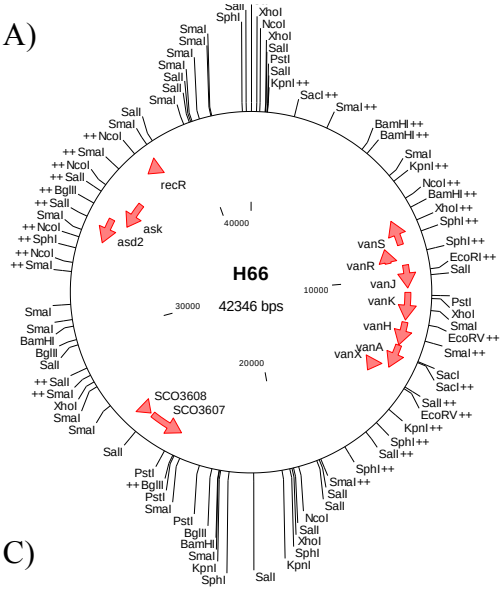

B)

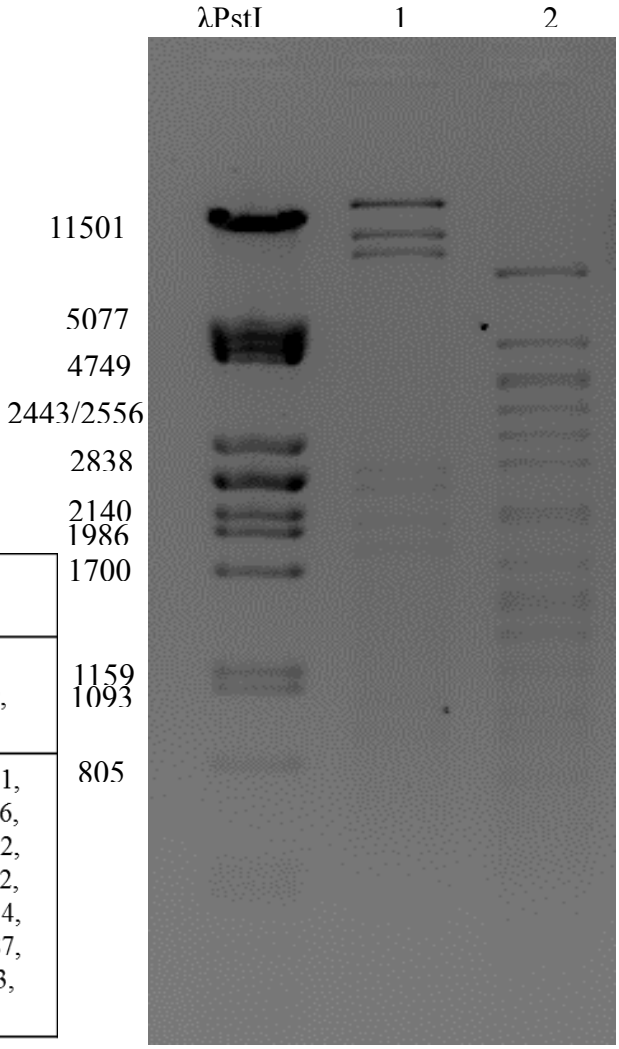

C)

Well	Restriction enzymes	Fragment size
1	PstI	18397, 10356, 8299, 2022, 1816, 1017, 399, 40
2	SalI	7043, 4376, 3695, 3571, 3175, 2852, 2547, 2116, 2047, 1730, 1545, 1502, 1465, 1348, 1324, 1162, 986, 908, 772, 757, 614, 540, 521, 501, 449, 387, 282, 214, 190 153, 153, 120, 98, 81, 67, 57, 41

Fig4-17. Confirmation of StH66. A) StH66 cosmid map. The cosmid contains a functional copy of *SCO3607* and *SCO3608*. B) Confirmation of the 1% agarose gel electrophorese image of StH66 digested with: PstI and SalI, and PstI cut λ phage as a standard. C) is the key for the gel, and contains the different enzymes and expected fragment sizes.

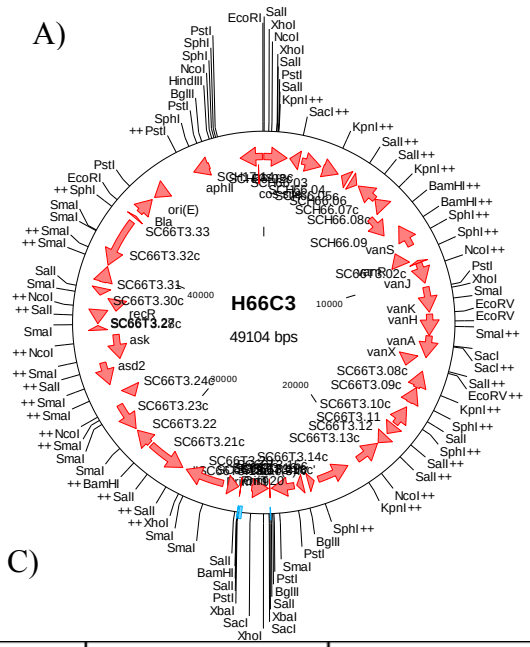

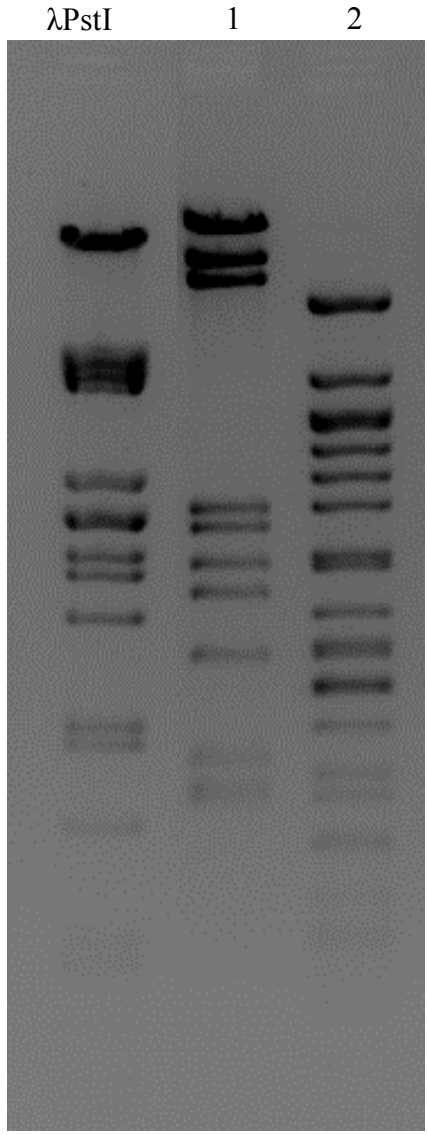

C)

Well	Restriction enzymes	Fragment size
1	PstI	17416, 10356, 8299, 2501, 2357, 2022, 1816, 1473, 1017, 923, 884, 40
2	SalI	7043, 4376, 3695, 3571, 3175, 3175, 2852, 2116, 2047, 1730, 1545, 1502, 1368, 1348, 1324, 1162, 986, 908, 772, 757, 614, 540, 521, 501, 449, 387, 282, 214, 153, 153, 120, 98, 81, 67, 57, 41

Fig4-18. Confirmation of StH66C3. A) StH66C3 cosmid map. The cosmid contains a functional copy of *SCO3608*, but *SCO3607* is not present. B) Confirmation of the 1% agarose gel electrophorese image of StH66C3 digested with: PstI and SalI, and PstI cut λ phage as a standard. C) is the key for the gel, and contains the different enzymes and expected fragment sizes.

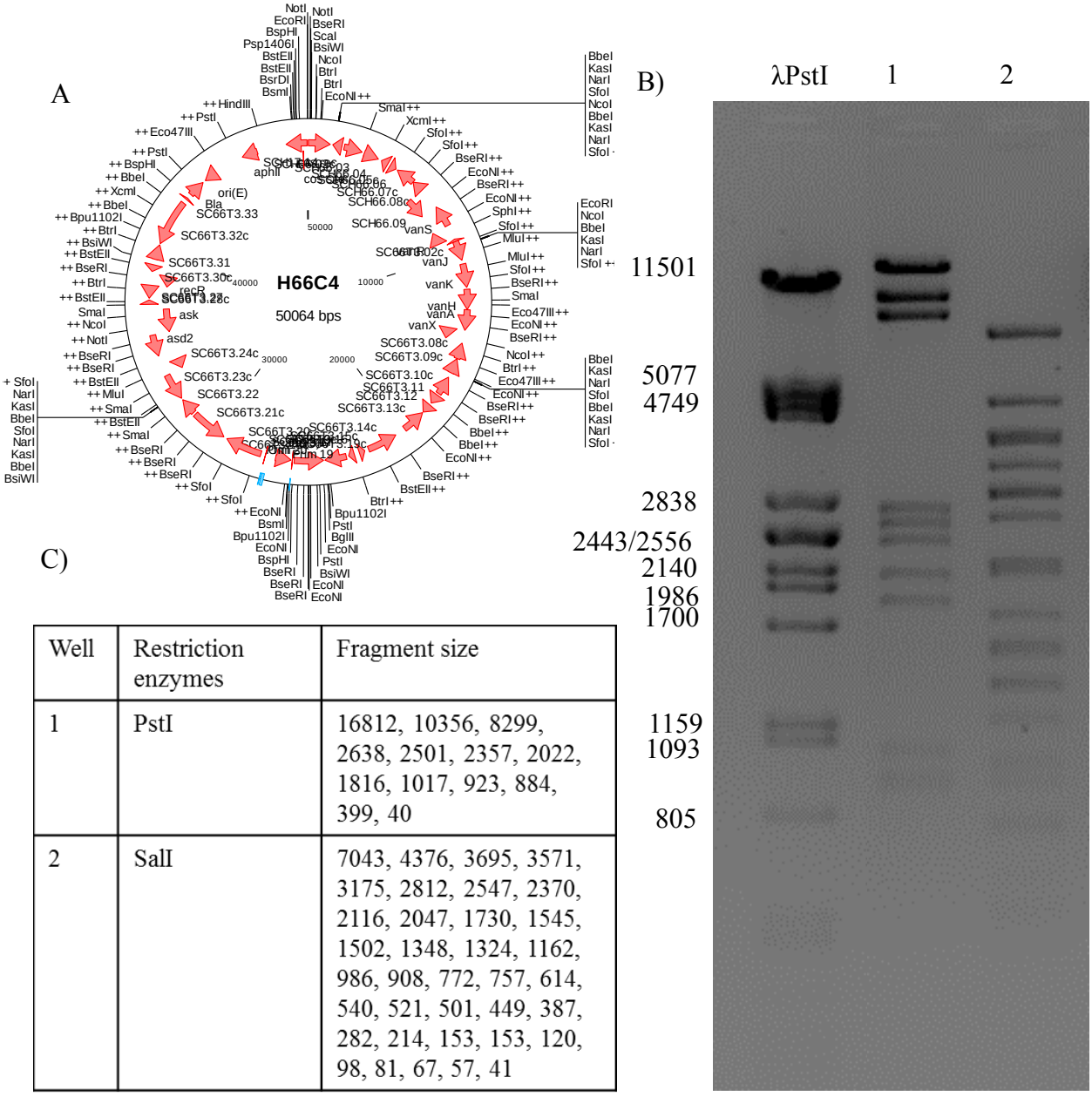

Well	Restriction enzymes	Fragment size
1	PstI	16812, 10356, 8299, 2638, 2501, 2357, 2022, 1816, 1017, 923, 884, 399, 40
2	SalI	7043, 4376, 3695, 3571, 3175, 2812, 2547, 2370, 2116, 2047, 1730, 1545, 1502, 1348, 1324, 1162, 986, 908, 772, 757, 614, 540, 521, 501, 449, 387, 282, 214, 153, 153, 120, 98, 81, 67, 57, 41

Fig4-19. Confirmation of StH66C4. A) StH66C4 cosmid map. The cosmid contains a functional copy of *SCO3608*, but *SCO3607* is not present. B) Confirmation of the 1% agarose gel electrophorese image of StH66C4 digested with: PstI and SalI, and PstI cut λ phage as a standard. C) is the key for the gel, and contains the different enzymes and expected fragment sizes.

A)

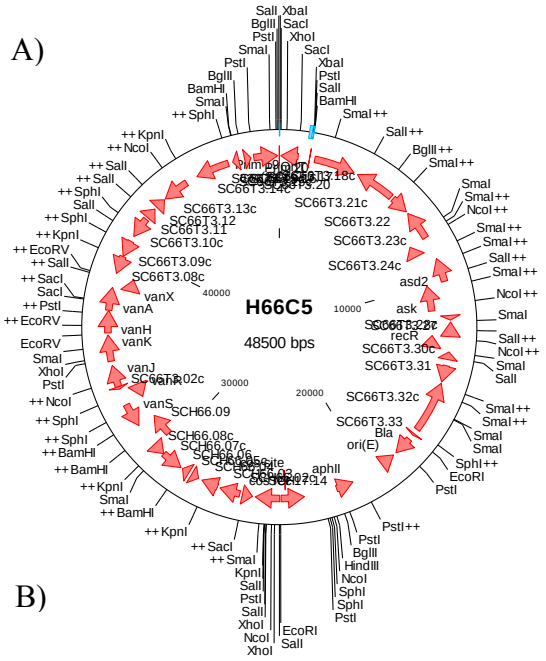

B)

Well	Restriction enzymes	Fragment size
1	PstI	16812, 10356, 8299, 2638, 2501, 2357, 2022, 1816, 1017, 923, 884, 46
2	SalI	7043, 4376, 3695, 3571, 3175, 2547, 2370, 2116, 2047, 1730, 1545, 1502, 1368, 1348, 1162, 986, 908, 772, 757, 614, 540, 521, 521, 449, 387, 282, 214, 153, 153, 98, 81, 67, 57, 41

C)

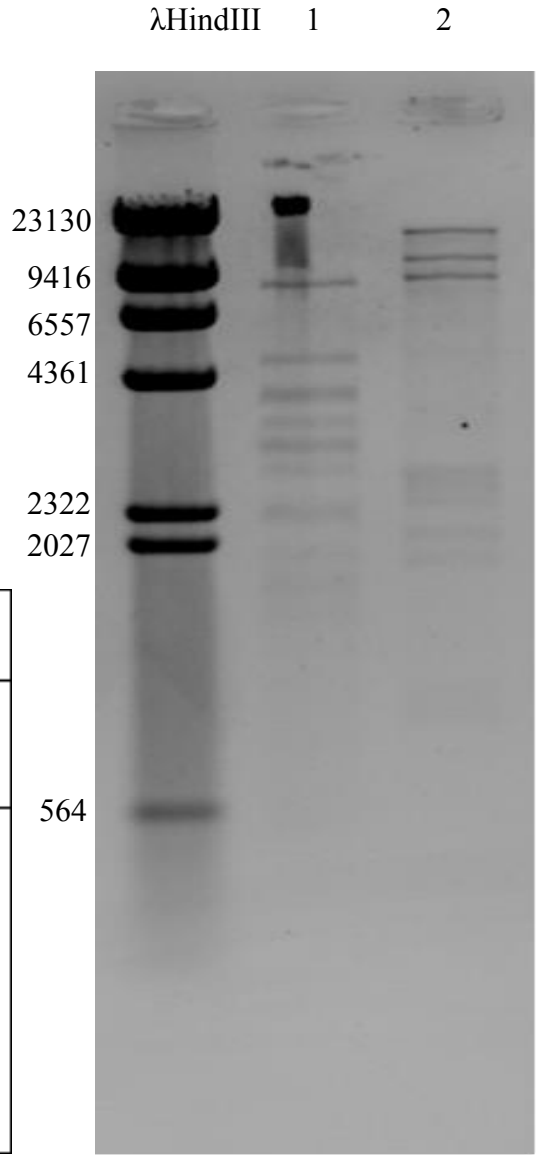

Fig4-20. Confirmation of StH66C5. A) StH66C5 cosmid map. The cosmid contains neither a functional copy of *SCO3608* or *SCO3607* is not present. B) Confirmation of the 1% agarose gel electrophorese image of StH66C5 digested with: PstI and SalI, and HindIII cut λ phage as a standard. C) is the key for the gel, and contains the different enzymes and expected fragment sizes.

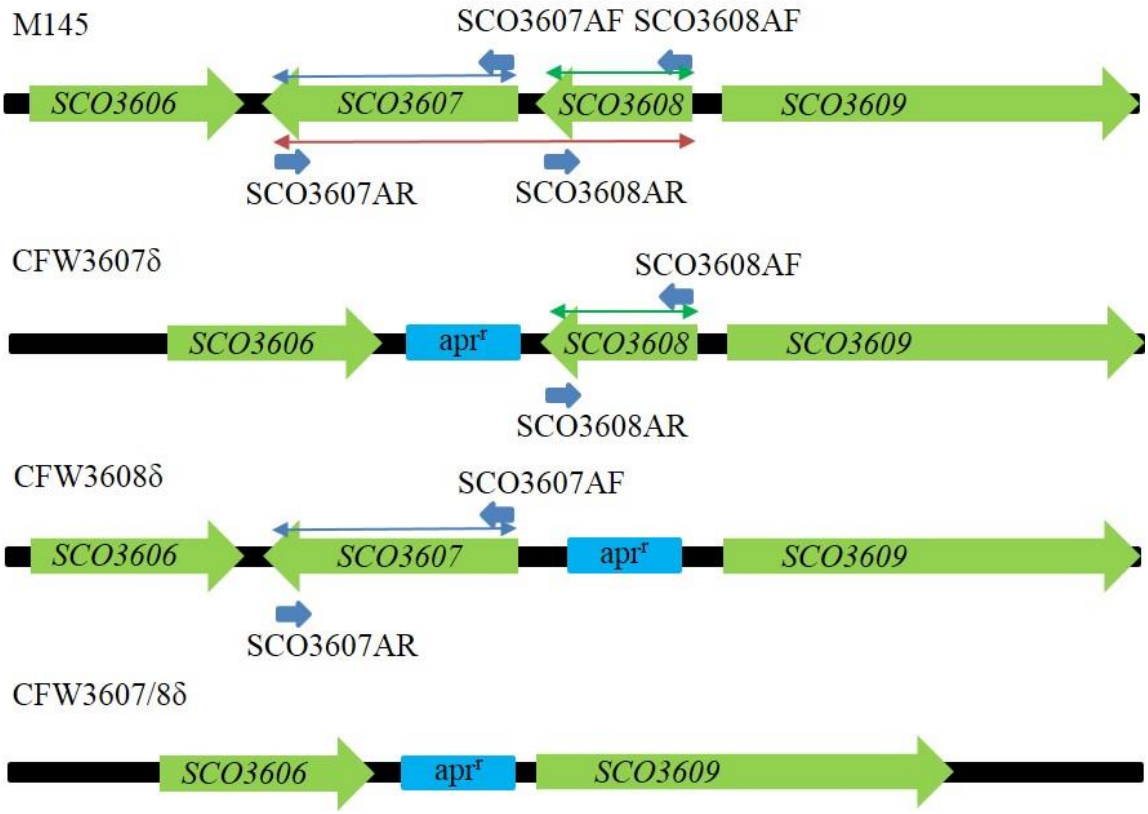

Fig4-21. Diagram displaying regions amplified by PCR in confirmation of the deletion strains. The blue arrow represents the SCO3607AF and SCO3607AR band (1469bp), the green arrow represents the A02F2 and A02R2 band (509bp), and the red arrow displays the region amplified by SCO3607AR and SCO3608AF (2073bp). The regions amplified have been labelled on the strains where it will be amplified. It has not been drawn to scale

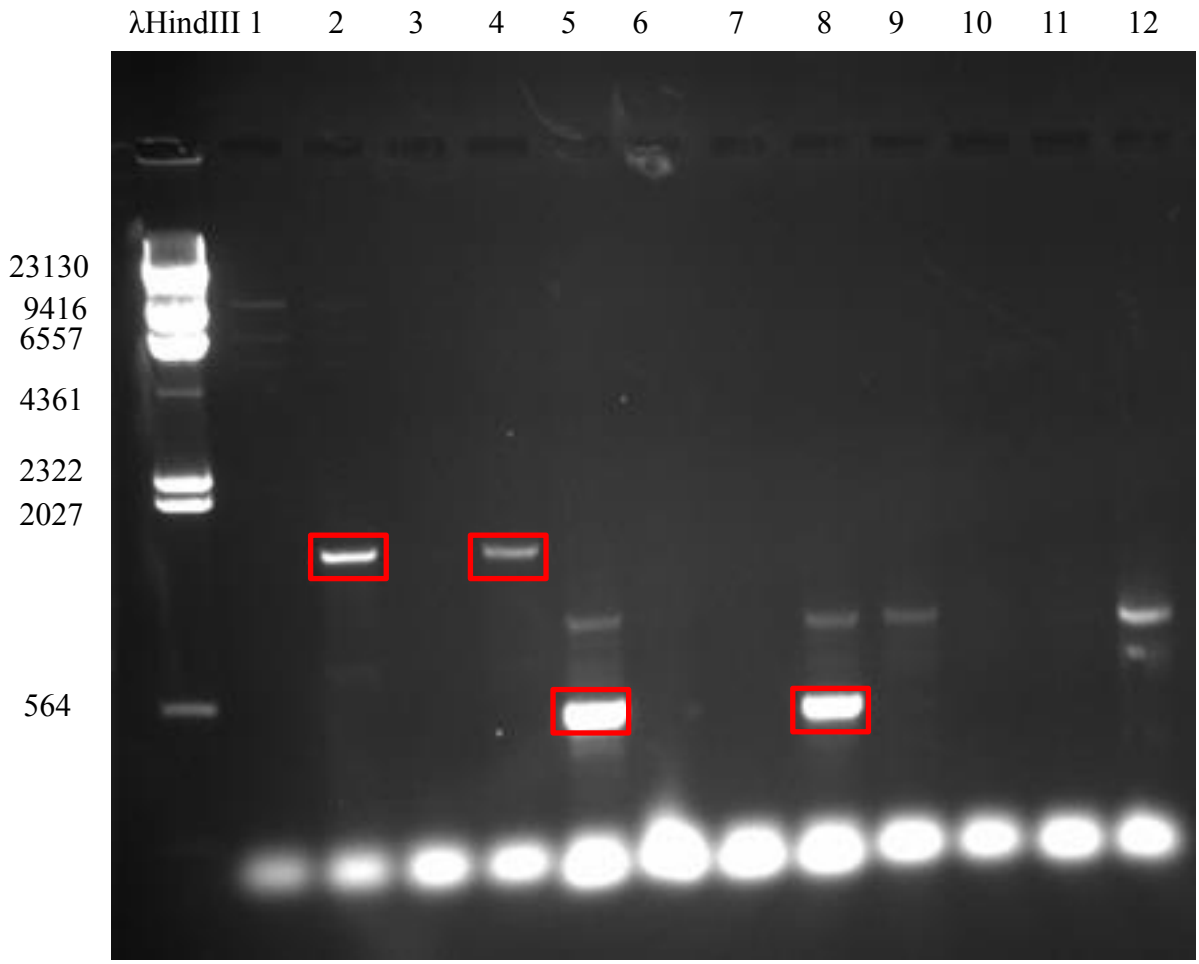

Well	Template	Primers	Product size
1	CFW3607δ	SCO3607AF + SCOF3607AR	-
2	CFW3608δ	SCO3607AF + SCOF3607AR	1469
3	CFW3607/08δ	SCO3607AF + SCOF3607AR	-
4	M145	SCO3607AF + SCOF3607AR	1469
5	CFW3607δ	SCO3608AF + SCOF3608AR	509
6	CFW3608δ	SCO3608AF + SCOF3608AR	-
7	CFW3607/08δ	SCO3608AF + SCOF3608AR	-
8	M145	SCO3608AF + SCOF3608AR	509
9	CFW3607δ	SCO3608AF + SCOF3607AR	-
10	CFW3608δ	SCO3608AF + SCOF3607AR	-
11	CFW3607/08δ	SCO3608AF + SCOF3607AR	-
12	M145	SCO3608AF + SCOF3607AR	2073

Fig4-22. PCR confirmation gel of knockout strains. The primers use stretches inside the gene rather than outside. It was not possible to get both genes amplified with the primers, but the presence and/or absence of the other products confirm it regardless. Some primer dimers and non-specific bands are visible.

4.2.5. Screening for morphological phenotypes

To ascertain whether the absence of SCO3607 and SCO3608 had any macroscopic effects, such as the *whi* or *bld* phenotypes which would suggest SCO3607 or SCO3608 plays a role in forming spores or aerial hyphae, respectively, strains lacking *SCO3607, SCO3608,* or both were plated out on several types of media to ensure any potential mutant phenotype was not supressed by the media (Flardh & Buttner, 2009, McCormick & Flardh, 2012, Nodwell *et al.*, 1996). To this end, CFW3607δ, CFW3607δC, CFW3608δ, CFW3608δC, CFW3607/8δ, CFW3607/8δC, and M145 were plated out on 3MA, MM, SFM, and R5 media and incubated at 30^{o} degrees for 6 days. Pictures were taken every 24 hours to assay for any morphological changes. Similar to the results in section 4.2.2., the results showed no major phenotype, though it appeared all the complemented null mutants produced slightly less undecylprodigiosin.

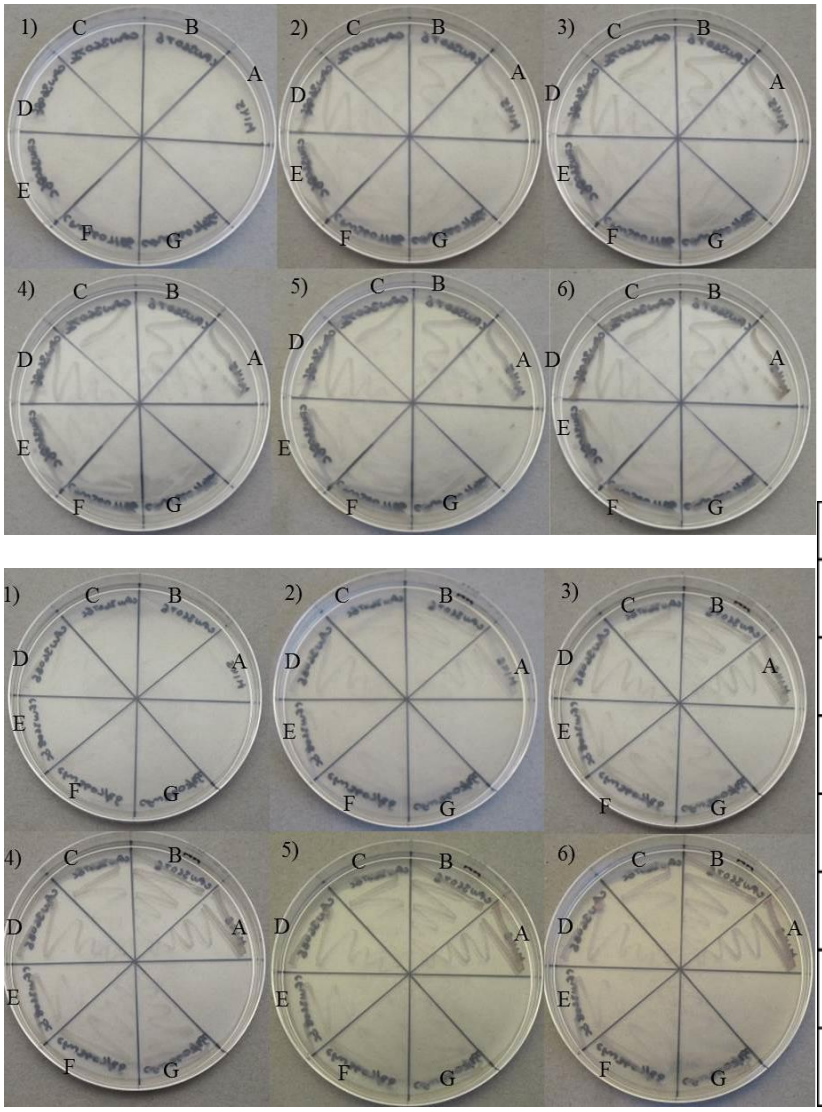

Key	Strain
A	M145
B	CFW3607δ
C	CFW3607δC
D	CFW3608δ
E	CFW3608δC
F	CFW3607/8δ
G	CFW3607/8δC

Fig4-23. *SCO3607* deletions mutants grown on 3MA (above) and MM (below) at 30º for 6 days display no particular phenotype. Number of days grown is indicated in the top left corner of each picture.

Much less biomass was visible when the strains were grown on 3MA and MM. Little to no growth was visible after 24 hours. Small amounts of undecylprodigiosin were visible after 6 days in cultures on 3MA agar. However, when grown on MM, slightly less undecylprodigiosin was visible for the mutant strains, including the complemented strains, after 6 days when compared to wild-type

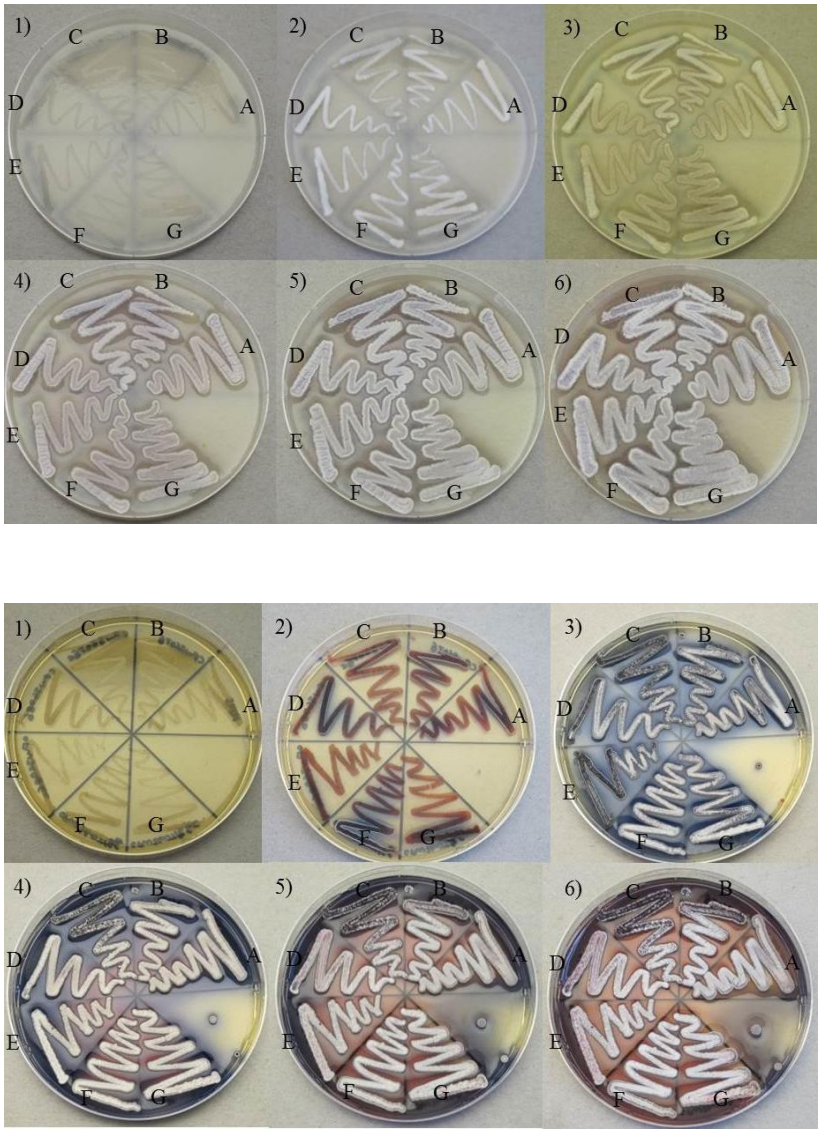

Key	Strain
A	M145
B	CFW3607δ
C	CFW3607δC
D	CFW3608δ
E	CFW3608δC
F	CFW3607/8δ
G	CFW3607/8δC

Fig4-24. *SCO3607* deletions mutants grown on SFM (above) and R5 (below) at 30º for 6 days display no particular phenotype. Number of days grown is indicated in the top left corner of each picture.

When the strains were grown on SFM, strains grew as vegetative hyphae after 24 hours, aerial hyphae had formed after 48 hours, visible due to the white pigment. Spores began forming after 72 hours and continued to mature until the end of the experiment, visible due to the grey colour.

Antibiotic production was visible to a minor degree in all strains grown on R5 after 24 hours, but it did not fully begin to be produced until 48 hours after inoculation. All complemented mutant strains appeared to produce slightly less undecylprodigiosin when compared to wild-type and the complemented strains. Aerial hyphae were visible after 72 hours, but it appeared

to possibly be slightly delayed in CFW3607δC and CFW3608δC. Sporulation began after 4 days.

4.2.6. Screening for morphological phenotypes in response to osmotic stress

To investigate the role of SCO3607 and SCO3608 in response to osmotic stress, CFW3607δ, CFW3607δC, CFW3608δ, CFW3608δC, CFW3607/8δ, CFW3607/8δC, and M145 were plated out on 3MA containing either 0.1M, 0.2M, 0.3M, 0.4M or 1M KCl to assay for morphological changes. The plates were incubated at 30^{o}C degrees for 6 days and pictures were taken every 24 hours. No phenotype was apparent, suggesting that even though FloT of *B. subtilis* is activated by σ^{w} which in turn is activated by osmotic stress, this is not the case in *S. coelicolor* (Huang *et al.*, 1999).

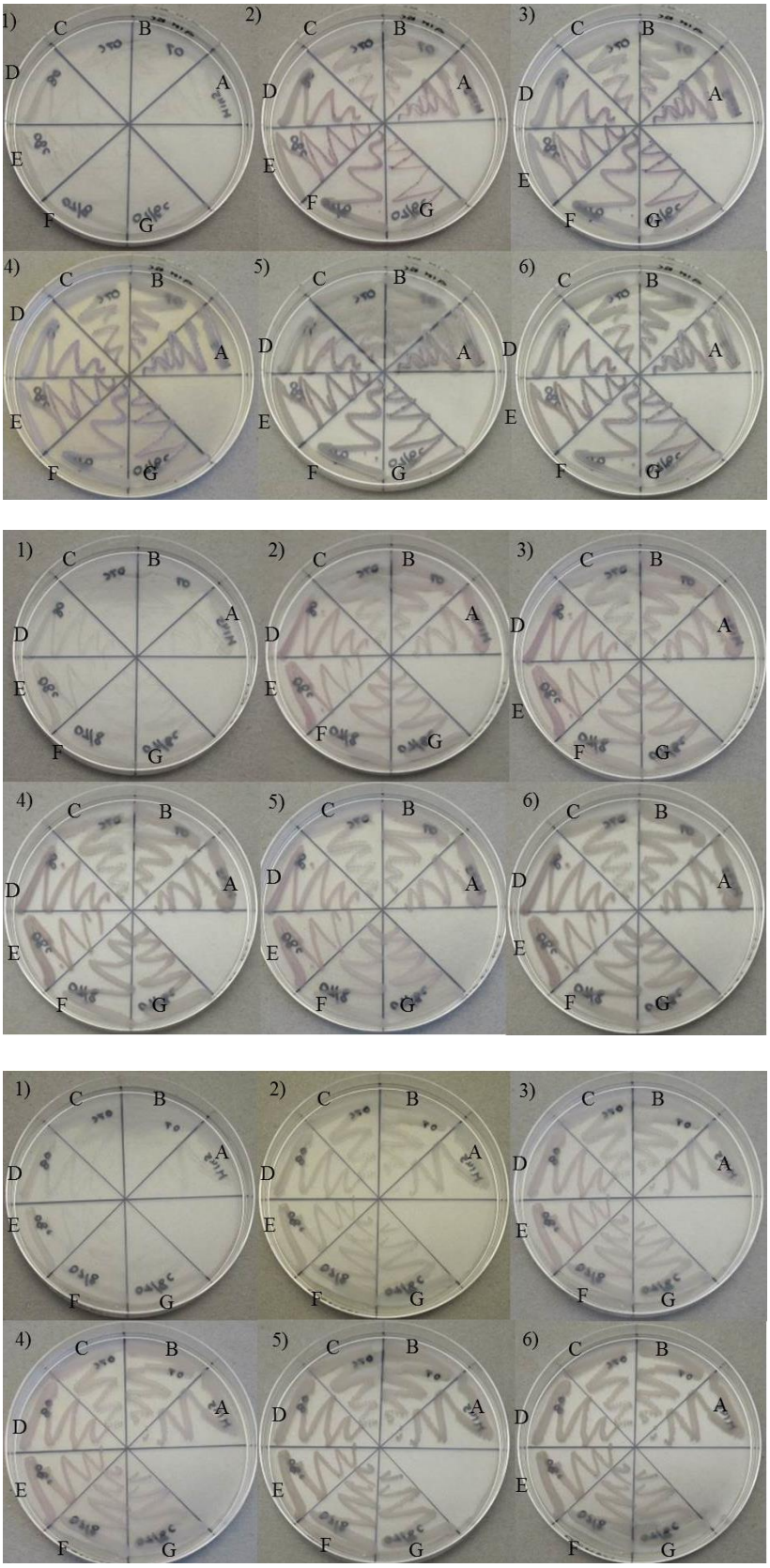

Key	Strain
A	M145
B	CFW3607δ
C	CFW3607δC
D	CFW3608δ
E	CFW3608δC
F	CFW3607/8δ
G	CFW3607/8δC

Fig4-25. *SCO3607* deletions mutants grown on 3MA containing 0.1M KCl (above), 0.2M KCl (middle), and 0.3M KCl (below) at 30º for 6 days display no particular phenotype. Number of days grown is indicated in the top left corner of each picture.

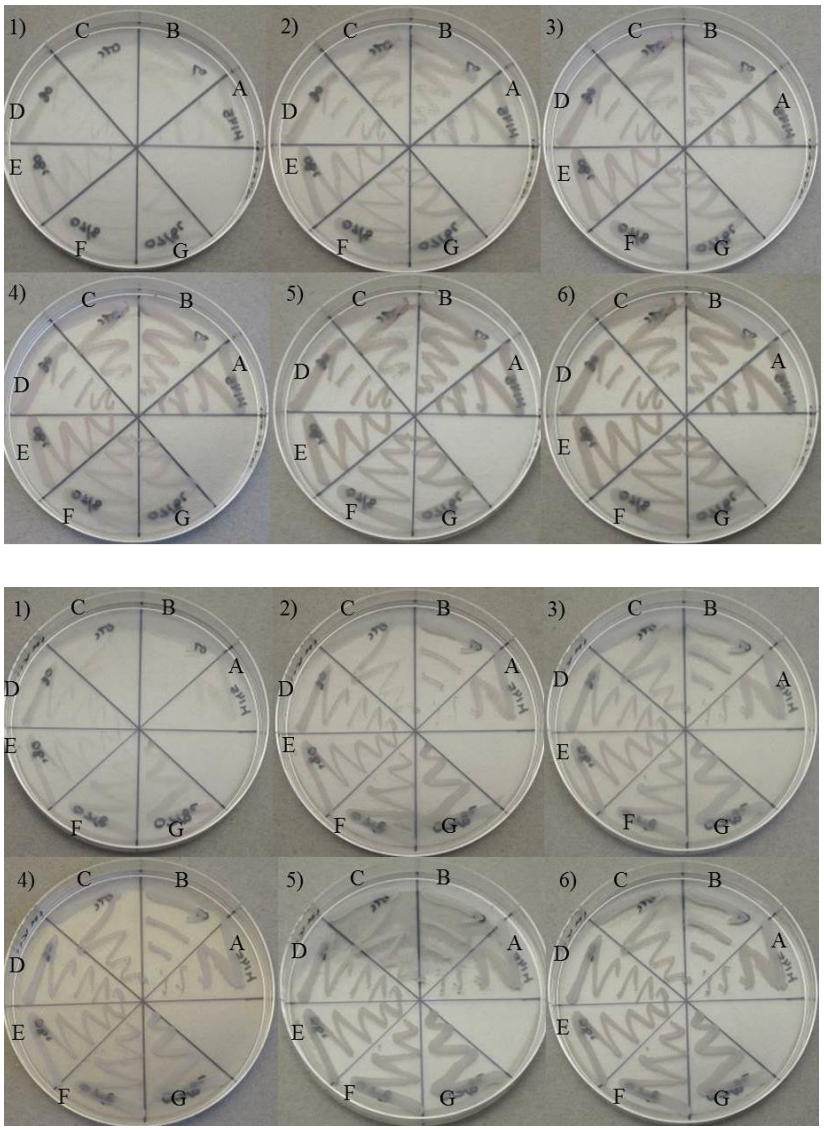

Key	Strain
A	M145
B	CFW3607δ
C	CFW3607δC
D	CFW3608δ
E	CFW3608δC
F	CFW3607/8δ
G	CFW3607/8δC

Fig4-26. *SCO3607* deletions mutants grown on 3MA containing 0.4M KCl (above) and 1M KCl (below) at 30º for 6 days display no particular phenotype. Number of days grown is indicated in the top left corner of each picture.

Undecylprodigiosin production became weaker the higher the KCl molarity rose, but stronger depending on time since inoculation. White aerial hyphae began to from after 4 days on all plates. No difference in phenotype was identified.

4.3.1. Discussion

The goals of these experiments were to elucidate whether *SCO3607* and *SCO3608* were essential genes and determine any phenotypic morphological effects following disruption and deletions. As it was possible to knock out both *SCO3607* and *SCO3608*, both separately and together, and also disrupt *SCO3607*, which demonstrates that both genes are non-essential. CFW3607δ, CFW3608δ, CFW3607/8δ, which lack *SCO3607*, *SCO3608*, and both, respectively, in addition to CFW3607A and CFW3607M, which contained a Tn*5062* disruption cassette in *SCO3607*, were screened for morphological effects on various agars with different concentrations of KCl.

The strains exhibited almost no differences when grown on 3MA, MM, R5 or SFM. CFW3607A may be producing slightly less actinorhodin on R5. All complemented null mutant strains possibly produced slightly less undecylprodigiosin and aerial hyphae may be slightly delayed in CFW3607δC and CFW3608δC. All of these phenotypes were considered to be so minor they were likely due to inoculum amount.

B. subtilis suffered a delayed sporulation phenotype and spore viability issues when its flotillin was disrupted, this was of some interest, as the results show the *S. coelicolor* homologue does not affect this (Donovan & Bramkamp, 2009). However, a later paper was not able to replicate this. Indeed, no phenotype was observed in a *B. subtilis floT* knockout other than lower motility, which would not affect *S. coelicolor* though potentially it may have had other effects., and a change in flotillin-associated NfeD localisation from colocalisation with flotillin to dispersion throughout the membrane (Dempwolff *et al.*, 2012). Additionally, as *S. coeliolor* and *B. subtilis* form two different kinds of spores, arthrospores and endospores, respectively, a mutant phenotype related to spores was not expected. Thus, the lack of a phenotype from the generation of a Tn*5062* disruption mutant or a null mutant was not unexpected. Additionally, the deletion of either full-length *nfeD* or flotillin-associated *nfeD* did not affect the macroscopic phenotype of *B. subtilis*.

While no meaningful phenotype was observed in a *floT* or *nfeD* knockout in *B. subtilis*, this was not the case in *B. subtilis* when both *floA* and *floT* were deleted, and a *floT floA* double knockout strain suffered severe morphological defects in sporulation, spore viability, gene transfer, and biofilm formation (Dempwolff *et al.*, 2012, Lopez & Kolter, 2010). While some previous papers claim *floA* and *floT* are related, this does not appear to be the case as almost

no sequence similarity exists and *floA* appears to be more similar to a seryl-tRNA-synthase (Donovan & Bramkamp, 2009, Lopez & Kolter, 2010).

While the localisation pattern of the flotillin-associated NfeD was dependent on FloT, YqeZ, the FloA-associated NfeD, localised independently of both FloA and FloT in *B. subtilis* (Dempwolff *et al.*, 2012). While there are no additional *nfed*-like genes present in the *S. coelicolor* genome, *scy* bears a high genetic resemblance to FloT. Scy is a cystoskeletal protein which forms a multi-protein complex with FilP and DivIVA, and interacts with ParA, thus it is involved in both cell polarity and chromosome segregation. However, though both FilP and DivIVA are essential, Scy is not an essential protein, but a null mutant suffered irregular branching, hyphae and spores, in addition to uneven DNA distribution (Ditkowski *et al.*, 2013, Holmes *et al.*, 2013). A double knockout of *scy* and *SCO3607* may provide a phenotype more similar to what has been observed in *B. subtilis*, especially as the phenotype associated with *Δscy* mimicked that of a double *floA/floT* knockout in *B. subtilis*. (Dempwolff *et al.*, 2012). However, it cannot be discounted that one of the stomatins of *S. coelicolor* does not partially compensate for the loss of SCO3607 though very unlikely.

When seen in relation to the d_N/d_S ratio (See Table 3-3) it shows the purifying pressure is on *SCO3607* and *SCO3608* to retain their residues for protein functionality and not for cell viability. It is not likely that there are any proteins that compensate for the loss of either protein, as there are no other NfeD proteins in the genome, and the three other SPFH proteins are stomatins and thus likely perform different roles.

However, there was no macroscopic phenotype in response osmolarity, which suggests a slightly different role for NfeD and flotillin in *S. coelicolor*.

Though there was no macroscopic phenotype in response to osmolarity, it is worthwhile to investigate potential similarities and differences and how they compare between *S. coelicolor* and *B. subtilis* in relation to flotillins and NfeD. In *B. subtilis*, alkaline shock, pH, and toxic peptides induce σ^w, which in turn switches on expression of *floT* and its neighbouring *yuaF*, suggesting a role in the cell envelope stress response, and in a *sigW* mutant transcription of *yuaFGI* was downregulated (Wiegert *et al.*, 2001, Zweers *et al.*, 2012). σ^E, a σ-factor involved in secondary metabolism and cell wall responses to antibiotic stress, is the σ-factor closest to σ^W in *S. coelicolor* (Paget *et al.*, 1999, Santos-Beneit *et al.*, 2014).

Another possibility is the alternative stress response σ-factor σ^H, whose disruption affects growth in high ionic-strength condition and sporulation (Sevcikova *et al.*, 2001). *ssgB* and the glutamate synthase *gltB* are two genes under control of σ^H (Kormanec & Sevcikova, 2002a, Kormanec & Sevcikova, 2002b). The gene encoding σ^H, *sigH*, is located in an operon encoding two other proteins, UshY and UshX, the latter which is a σ^H anti-σ-factor which binds σ^H (Sevcikova & Kormanec, 2002). *ushX* is immediately upstream of *sigH*, and *ushY* is again upstream of *ushX*. Upstream of *ushY* is the constitutive promoter *sigH*-P1, but three other promoters, *sigH*-P2, *sigH*-P3, *sigH*-P4 are upstream of *ushX*. *sigH*-P2 is a σ^H promoter, similar to an σ^B promoter, induced by salt stress, and *sigH*-P3 is a BldD promoter induced by heat-shock (Kormanec *et al.*, 2000, Kelemen *et al.*, 2001). This suggests a dual role for σ^H in development and stress response. However, an σ^H-P2 promoter is not found upstream of either *SCO3607* or *SCO3608* (Buttner *et al.*, 1988, Lonetto *et al.*, 1994). Furthermore, the *S. coelicolor* σ-factor σ^H, though the *S. coelicolor* σ-factor most similar to σ^W, is more closely related to the *B. subtilis* σ-factor σ^X (Paget *et al.*, 1999). It is worth bearing in mind there is overlap between σ^X and σ^W promoters (Huang *et al.*, 1998).

In disrupted *floT* mutants in *B. subtilis*, one of the phenotypes observed was inefficient activation of σ^E and cells with prespore compartments at both poles were observed, which are normally only seen in σ^E mutants (Donovan & Bramkamp, 2009). This suggests there may be σ-factors involved further into the growth cycle in *S. coelicolor*.

A different type of stress, such as detergents or toxic peptides, might result in a different phenotype. The σ-factors involved in the osmotic stress response in *S. coelicolor* are also involved in sporulation, and it would thus be interesting to see if any of these control expression of the two genes in question. This kind of conditional *bld* and *whi* phenotypes are not uncommon, and have also been supressed by media (Kelemen *et al.*, 2001, Lee *et al.*, 2005, Ditkowski *et al.*, 2013). However, this is not likely, as the phenotypic tests were rigorous enough to ensure that mutant phenotypes were not easily missed.

4.3.2. Conclusion

SCO3607 and *SCO3608* were both knocked out and complemented, and the former was disrupted at two different sites and complemented. This confirms they are not essential for viability. No phenotype was observed on any media nor in response to salt concentrations which had induced *floT* and *yuaF* expression in *B. subtilis* (Wiegert *et al.*, 2001). This might be due to redundancy from other proteins, though this is unlikely due to the highly conserved

nature of the proteins hinting at high amino acid similarity required for function. Additionally, there are no genes of very high similarity, though *scy* is somewhat similar to *SCO3608*. However, this was also the case for *floT* and *yuaF* knockout mutants in *B. subtilis* (Dempwolff *et al.*, 2012). Alternatively, it can be a conditional mutation and require other experiments to elucidate. Assaying spore viability and their heat resistance, growth in liquid culture, in addition to assaying secondary metabolite production are all potential experiments.

Other experiments that could be performed would be to assay for the absence of other proteins involved in signalling, molecule trafficking, or protein secretion by western blotting in the DRM in a *SCO3607* and *SCO3608* null mutant. Furthermore, RT-PCR experiments could potentially reveal the exact time of induction of *SCO3607* and *SCO3608.*

5. Microscopic analysis of *SCO3607* and *SCO3608* mutants in branch and cross-wall formation

5.1.1. Introduction

Fluorescence microscopy is one of the most commonly used methods for investigating and quantifying morphological changes in bacteria. Proteins can be fused translationally with fluorophores such as the red mCherry or the green GFP, membranes and specific lipids can be stained with the orange NAO. Propidium iodide (PI) is a frequently used DNA dye, and the green wheat germ agglutinin (WGA) and fluorescent antibiotic derivatives are used to dye cell walls (Pogliano *et al.*, 1995, Daniel & Errington, 2003, Mileykovskaya & Dowhan, 2000, Shaner *et al.*, 2004, Phillips, 2001, Suzuki *et al.*, 1997, Schwedock *et al.*, 1997). More complex staining methods include Förster resonance energy transfer (FRET) combined with fluorescence lifetime imaging microscopy (FLIM), which the measures the distance between two fluorophores, and immunofluorescence microscopy, which uses fluorophore-tagged antibodies (Alexeeva *et al.*, 2010, Buddelmeijer *et al.*, 1998, Willemse *et al.*, 2011).

Performing time-lapse microscopy on streptomycetes is more challenging than performing it on other bacteria due to the streptomycetes' aerobic lifestyle and morphology. The morphology of *S. coelicolor* thus leads to problems growing the organism between a microscope slide and a microscope slip and hyphae readily growing out of focus at 100x magnification. This makes the use of time-lapse fluorescence microscopy harder, but it has still been used to investigate the growth and sporulation of *S. coelicolor* (Jyothikumar *et al.*, 2008). Due to these issues, static images are easier to achieve, and fluorescence microscopy in a variety of forms is widely used in *S. coelicolor*.

Prodigiosin and similar autofluorescing molecules have been used in confocal microscopy to monitor initiation of secondary metabolism (Tenconi *et al.*, 2013). A combination of the two fluorophores mCherry and GFP were used in investigating conjugation taking place in the lateral cell walls in *S. lividans* (Thoma *et al.*, 2016). mCherry has been used as a reporter for WhiH and was used in elucidating the localisation of the lipoprotein SspA to the septum, but the most commonly used fluorophore is GFP (Persson *et al.*, 2013, Tzanis *et al.*, 2014). The GFP-tag has been used to reveal FtsZ dynamics and localisation, Tat pathway components, expression patterns of the undecylprodigiosin regulator RedD, the spore maturation sigma factor σ^F, and two HU proteins to mention a few (Willemse *et al.*, 2012, Sun *et al.*, 1999,

Salerno *et al.*, 2009). The FtsZ dynamics were also studied with immunofluorescence (Grantcharova *et al.*, 2005). Fluorescence microscopy has also been used to elucidate the lack of ordered chromosome segregation in *ssgB* null mutants by using PI and Syto-82 Orange, which stains the membrane (Xu *et al.*, 2009). Fluorescent vancomycin derivatives to demonstrate *S. coelicolor* incorporates peptidoglycan at the cell tip (Daniel & Errington, 2003).

The use of wheat germ agglutinin (WGA) to stain *N*-acetylglucosamine and *N*-acetylmuramic acid in cell wall and septa was originally done in *B. subtilis*, but was later adapted for use in *S. coelicolor* (Pogliano *et al.*, 1995). Combined with PI, it allows for visualisation of the two main cell components in bacteria. This method, the Schwedock stain, has previously been used in concert with immunofluorescence microscopy in *S. coelicolor*, which demonstrated the ladder-like structural arrays of FtsZ (Schwedock *et al.*, 1997). FtsZ has also been used in concert with fluorophore; foci of pre-Z-ring FtsZ in the septa was discovered using a GFP tag in combination with a Schwedock stain (Willemse & van Wezel, 2009). PI and SYTO9, a green DNA-binding fluorophore, have also been used to determine whether *S. coelicolor* spores are dead or alive (Ladwig *et al.*, 2015).

5.1.2. Fluorescence analysis of flotillin and NfeD

YuaG/FloT, YuaF/NfeD, and other related proteins have previously been studied using fluorescence microscopy in *B. subtilis*. As a note on nomenclature, FloA/YqfA has erroneously been annotated as a flotillin-like protein, but it is adjacent to an NfeD protein containing the signature serine protease domain of a full-length NfeD (see section 1.2.6). YuaG will be referred to as FloT, while YqfA will be referred to as FloA. Their associated NfeD proteins will be referred to as YuaF and YqeZ, respectivelly (Dempwolff *et al.*, 2012).

The first FloT fluorescence experiments found FloT-GFP to localise in a punctate pattern in the cell membrane. A FloT-YFP (Yellow fluorescent protein) fusions was also created, as both previously constructed strains had their FloT-fluorophore artificially induces by xylose. When placed under the native promotor, only a few foci were visible during the exponential phase, but a large increase in foci occurred during the stationary phase. Time-lapse microscopy demonstrated that these foci reorganised dynamically. Co-localisation with CL in *B. subtilis* was studied using NAO and a FloT-YFP fusion protein. Almost all CL localises to the pre-spore compartment during sporulation, but the FloT-YFP fusion, and FloT-GFP fusion when repeated, localised to the cell membrane of the mother cell. Strains were constructed with *GFP* with σ^F and σ^E-controlled promoters and loss of YuaG lead in both cases to a decrease in GFP

expression. σ^F-driven GFP expression occurred only in the prespore compartment, while σ^E-driven GFP expression only occurred in the mother cell. When combined with the FloT disruption mutant it lead to a decrease in GFP expression, demonstrating the asymmetric septum is not as efficient at separating the two compartments (Donovan & Bramkamp, 2009).

In another experiment in *B. subtilis*, KinC was translationally fused to YFP, and YFP monoclonal antibodies only bound to components of the DRM fraction, but were absent in a *yisP* null mutant. YisP is a squalene synthase (see section 1.2.6). As FloT is co-isolated with the DRM fraction, the authors repeated and confirmed the previous localisation experiments, in addition to revealing that there are on average 6 FloT-YFP loci in the bacterial membrane. When YisP was inhibited by zaragozic acid, these loci were abolished and FloT-YFP no longer localised to the membrane. FloA-CFP (Cyan fluorescent protein) and FloT-YFP translational fusions were found to co-localise (Lopez & Kolter, 2010).

However, later experiments using total internal reflection fluorescence microscopy could not repeat the co-localisation of FloA and FloT, and that the deletion of one did not alter the patterns of localisation of the other. It was also found that localisation patterns of FloA-YFP were different when cultured in rich or poor media, with 10 and more foci in poor media. This was also the same for FloT-YFP, but to a more limited extent. Truncated YFP versions of FloT were constructed, lacking either the C-terminal domain or the C-terminal and the flotillin domain. The localisation pattern changed only in the mutant lacking both domains and was uniformly distributed throughout the membrane. Two other variants were then generated: FloT lacking the flotillin domain in a *floA* null mutant background and a FloA lacking its supposed flotillin domain in a *floT* null mutant background. This abolished the dynamic foci and a double knockout phenotype was observed (Dempwolff *et al.*, 2012).

A YFP translation fusion of the NfeD associated with FloT showed the same expression and localisation patterns as FloT, with an increase in dynamic membrane foci during the stationary phase and a decrease on rich media. A FloT-CFP and NfeD-YFP mutant with the FloT-CFP under a xylose-inducible loci and the NfeD translational fusion under the native promoter showed a 90% co-localisation frequency. However, FloT-CFP in an *yuaF* null mutant background formed more dynamic foci, but when done with the YuaF-YFP mutant in a *floT* null mutant, the YuaF-YFP was now spread evenly throughout the cell membrane instead of localising in a punctate pattern, suggesting FloT recruits YuaF to the membrane. The localisation pattern of FloA-YFP was unaffected in a *yqeZ* null background. When *yqeZ* was

translationally fused with YFP it showed a membrane pattern different from the FloA, FloT, and YuaF punctate patterns and formed patches throughout the cell membrane. Additionally, YqeZ-YFP was found to localise to all completed septa, whereas FloT and FloA were only found there occasionally. The deletion of *floA*, *floT*, or *yqeZ* did not affect the localisation of any other the localisation of the proteins encoded by any other genes, and the deletion of *yuaF* did not affect the localisation of FloA (Dempwolff *et al.*, 2012).

FloT-YFP was also expressed in S2 cells from *Drosophila* flies, where it accumulated in the cell membrane in its normal punctate manner, showing it does not need any of the other proteins for its localisation, and FloA-CFP and FloT-YFP did not show co-localisation and often accumulated separately in the cell membrane (Dempwolff *et al.*, 2012). Fluorescence microscopy has also been used to on mammalian flotillin. To mention a few, a digoxigenin-labelled cRNA probe was used to demonstrate transcription in rat ganglion cells and immunofluorescence was used to elucidate the localisation pattern, and GFP-tagged flotillin was discovered to display a polar pattern in cell membrane distribution (Lang *et al.*, 1998, Rajendran *et al.*, 2009, Rajendran *et al.*, 2003).

In previously constructed disrupted *floT* mutants in *B. subtilis*, sporulation was delayed in addition to the production of alkaline phosphatase. The delay in sporulation was caused by a delay in formation of the asymmetric septum and by the formation of an inefficient asymmetric septum. This is turn lead to a delay and inefficient activation of σ^E in a *floT* mutant. This again delayed *spoIVA* transcription due to being transcribed from a σ^E-dependent promoter, which lead to the delay in sporulation. There was also an increase in cells with prespore compartments at both cell poles. The disporic cell phenotype is normally only observed in σ^E mutants. Furthermore, heat-resistant spores suffered a 66% drop in spore viability (Donovan & Bramkamp, 2009).

The issues with the asymmetric septum formation may be due to the delocalisation of the protease FtsH, and fluorescence microscopy demonstrated some colocalisation and his-tagging experiments demonstrated binding. Fluorescence microscopy revealed FtsH-RFP (red fluorescence protein), FloT-YFP, and YqfA-GFP localised to the division septa, and his-tagged YqfA and FloT were eluted alongside FtsH. It was noted that HflC and HflK are required for oligomerisation of FtsH in *E. coli*, and as *B. subtilis* lacks HflC and HflK, it is tempting to suggest that FloT and FloA, of which the former belongs to the SPFH family, might be perform a similar function in FtsH oligomerisation (Yepes *et al.*, 2012).

Later experiments with a *floT* and *floA* null mutant in *B. subtilis* abolished KinC-dependent biofilm formation, in addition to causing the absence of several proteins from the DRM (Lopez & Kolter, 2010). Another study failed to replicate the delayed sporulation phenotype observed in *B. subtilis* with a disrupted *floT* in a null mutant background. The motility of a *floT* null mutant suffered slightly, whilst the deletion of *yuaF* showed no apparent phenotype. A *floT floA* null mutant grew slowly, grew as single and curved cells of different sizes instead of growing as straight chains, and gene transfer machinery was misplaced, leading impaired gene transfer, and motility was impaired. No particular phenotype was observed for a *yqfB floT* double mutant (Dempwolff *et al.*, 2012).

Many other developmental mutant phenotypes have been observed in *S. coelicolor*, with the foremost being those resulting from mutations to *bld*, *whi*, *chp*, and *ram* genes (see section 1.3.3.). Microscopy has been used to investigate phenotypes on a cellular level. A *parA* null mutant did not result in any change to vegetatively growing hyphae, but aerial hyphae had severe septal and chromosome segregation alterations (Jakimowicz *et al.*, 2007). A *crp* null mutant resulted in delayed germination and bigger spores, due to a doubling of the cell wall width, which is probably the reason for the delayed germination (Piette *et al.*, 2005). The spores of an *sspA* null mutant were longer and more square when grown on minimal media supplemented with mannitol, suggesting immature spores (Tzanis *et al.*, 2014).

5.1.3. Aims and Goals

As no macroscopic phenotype was evident when CFW3607δ, CFW3608δ, CFW3607/8δ, CFW3607A, or CFW3607M were grown under a variety of growth conditions (see Chapter 4), assaying for microscopic changes became the next step. As earlier experiments with flotillin and NfeD in *B. subtilis* showed issues with asymmetric septum formation, this served as a rationale to investigate cross-wall formation in *S. coelicolor* (Dempwolff *et al.*, 2012). However, *B. subtilis* and *S. coelicolor* form different spores, as the former forms endospores while the latter forms arthrospores. This compounds predicting phenotypes, but from the phenotypes observed in *B. subtilis*, several assumptions can be made. A *SCO3608* mutant is not likely to have as severe an impact as a *SCO3607* mutant, due to the high similarities between the *S. coelicolor* genes and *B. subtilis* genes, the localisation of YuaF was affected in a *floT* mutant but not vice versa, and a *yuaF* mutants did not display a phenotype in *B. subtilis* (Dempwolff *et al.*, 2012, Donovan & Bramkamp, 2009). Thus a *SCO3608* phenotype is likely to be mild as the only serious phenotypes were in response to a double knockout strain lacking

floT and *floA*. As the main expression of YuaF and FloT occurred in the stationary stage and the effects deletions and disruptions have had on cell morphology and sporulation, an involvement in the later stages of the life cycle is likely. Additionally, as there is no FloA equivalent in *S. coelicolor*, there is no other known gene which deletion would cause such a severe phenotype as seen in *B. subtilis*. As inefficient septum formation during sporulation was the main driver behind the more severe phenotype, in addition to diasporic cells, and the *sspA* mutant which had aberrant spores similar to a *floT* disruption mutant, suggested measuring cross-wall to cross-wall and tip to cross-wall distances were good tests to ascertain any issues with septum and spore formation (Dempwolff *et al.*, 2012, Donovan & Bramkamp, 2009, Tzanis *et al.*, 2014).

Other potentially related phenotypes observed in *B. subtilis* were several proteins going missing from the DRM, delocalisation of YuaF, and cell polarity issues resulting in aberrant diasporic spores (Dempwolff *et al.*, 2012, Lopez & Kolter, 2010). Extrapolating from this, it is possible FloT may be responsible or related to the localisation of DivIVA in lieu of the growing amount of evidence that it localises to regions of negative curvature, which can be caused by e. g. CL (see 1.1.2.1.). As DivIVA is found at growing tips, it is possible that FloT is somehow involved the *S. coelicolor* polarisome (Multiprotein complexes involved in cell polarity), which would potentially result in changes in hyphal branching (Flardh *et al.*, 2012). To measure changes related to polarisome localisation, measuring branch to branch and tip to branch distances were deemed suitable measurements.

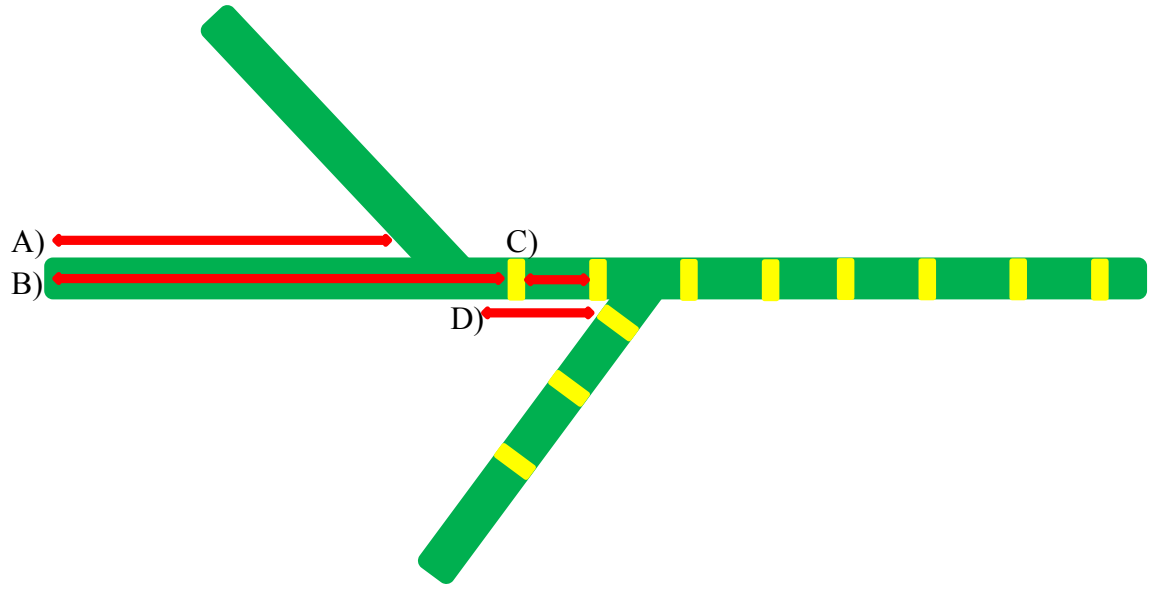

Fig5-1. Microscopic measurements performed on the different *S. coelicolor* strains. *S. coelicolor* is in green and its cell walls are in yellow. Red arrows signify the measurement being performed. A) is the tip to branch measurement, B) is the tip to cell wall measurement, C) is the cell wall to cell wall measurement, and D) is the branch to branch measurement.

As the aim was to elucidate what microscopic changes had occurred in cross-wall and branch formation, this was investigated in vegetative hyphae, aerial hyphae, and spores by culturing the bacteria on SFM agar and taking samples after 24, 48, and 72 hours. A Schwedock stain was used to visualise the different compartments. In summary, the measurements performed were the distance from branch to branch, tip to branch, cross-wall to cross-wall, and tip to cross-wall (see Fig5-1). The data from these measurements was expressed as a histogram of the distribution. Including both disrupted and null mutants was also of interest, as there are phenotypical differences between these in *B. subtilis* (Dempwolff *et al.*, 2012, Donovan & Bramkamp, 2009).

Based on what was observed in *B. subtilis* and Chapter 5, a severe phenotype was not expected for any of the strains, as *S. coelicolor* lacked a FloA homologue. However, changes to cross-wall to cross-wall and tip to cross-wall distances were likely, both from interference with septum formation which would potentially result in missing septa, resulting in a longer cell-wall to cell-wall distance after 72 hours. This could be compounded by changes to the polarisome, resulting in changes to cross-wall and branch distribution if cell polarity was disturbed. If the cell polarisome was affected, branches would likely form closer to the tip,

more tips would form and potentially also abortive branches, which would result in a smaller distance between branches. The phenotypes based on these predictions would likely occur in the strains lacking a fully functional *SCO3607*, and possibly more pronounced in the strain lacking *SCO3607* and *SCO3608*. The strain lacking *SCO3608* would not likely show much of a phenotype based on earlier experiments in *B. subtilis*, but based on the intrinsic differences between the spore formation and cellular signalling, this may not be correct.

In summary, the goals of this Chapter are the following:

1) To investigate any morphological and developmental changes in response to the deletion or disruption of *SCO3607* and/or *SCO3608* through assaying changes to tip to branch, tip to cross-wall, branch to branch, and cross-wall to cross-wall distances.
2) To ascertain whether the presence of *SCO3607* and/or *SCO3608* affects the spore formation.

5.2.1. Disruption and deletion *SCO3607* and *SCO3608* affect cell polarity

5.2.1.1. Deletion and disruption of *SCO3607* shortens tip to branch and cross-wall distances in vegetative *S. coelicolor*.

To investigate phenotypes related to branch and cross-wall formation in *S. coelicolor*, CFW3607A, CFW3607M, and CFW3607δ were, along with their complemented counterparts and M145, subjected to a Schwedock stain (see section 2.5). The measurements performed were tip to cross-wall, tip branch, cross-wall to cross-wall, branch to branch. A few mutant phenotypes were observed; shorter tip to cross-wall distances until 72 hours (p-values for CFW3607A and M145 were 0.0000 after both 24 and 48 hours, CFW3607M and M145 0.0000, 0.2228, and 0.0054 at the respective time-points, and 0.0000 and 0.0.0988 between CFW3607δ and M145 after 24 and 72 hours), in addition to shorter tip to branch distances for all strains (the p-values were 0.0077 and 0.0928 for CFW3607A and M145 after 24 and 72 hours, 0.000 CFW3607M and M145 after 24 and 48 hours, and 0.000, 0.0000, and 0.0109 for CFW3607δ and M145). While the two strains containing the disrupted *SCO3607* copy did not display a marked difference from wild-type in either cross-wall to cross-wall or branch to branch distances, CFW3607δ displayed much shorter cross-wall to cross-wall and branch to branch distances. All the statistical data has been included in the appendix.

Table 5-1. Number of tip to cross-wall measurements per *SCO3607*-mutant strain. The number of measurements is indicated in each column.

Strain	24 hours	48 hours	72 hours
CFW3607A	128	84	109
CFW3607AC	97	95	103
CFW3607M	85	85	93
CFW3607MC	85	103	104
CFW3607δ	125	101	144
CFW3607δC	93	91	79
M145	109	88	87

Table 5-2. Number of tip to branch measurements per *SCO3607*-mutant strain. The number of measurements is indicated in each column.

Strain	**24 hours**	**48 hours**	**72 hours**
CFW3607A	128	129	108
CFW3607AC	127	90	82
CFW3607M	85	85	93
CFW3607MC	85	103	104
CFW3607δ	115	85	114
CFW3607δC	95	111	77
M145	107	86	83

Table 5-3. Number of cross-wall to cross-wall measurements per *SCO3607*-mutant strain. The number of measurements is indicated in each column.

Strain	**24 hours**	**48 hours**	**72 hours**
CFW3607A	116	119	133
CFW3607AC	116	94	127
CFW3607M	85	119	133
CFW3607MC	116	94	127
CFW3607δ	77	217	149
CFW3607δC	101	130	132
M145	136	117	251

Table 5-4. Number of branch to branch measurements per *SCO3607*-mutant strain. The number of measurements is indicated in each column.

Strain	**24 hours**	**48 hours**	**72 hours**
CFW3607A	123	134	111
CFW3607AC	130	145	117
CFW3607M	112	162	106
CFW3607MC	112	136	102
CFW3607δ	111	208	147
CFW3607δC	159	116	119
M145	146	143	136

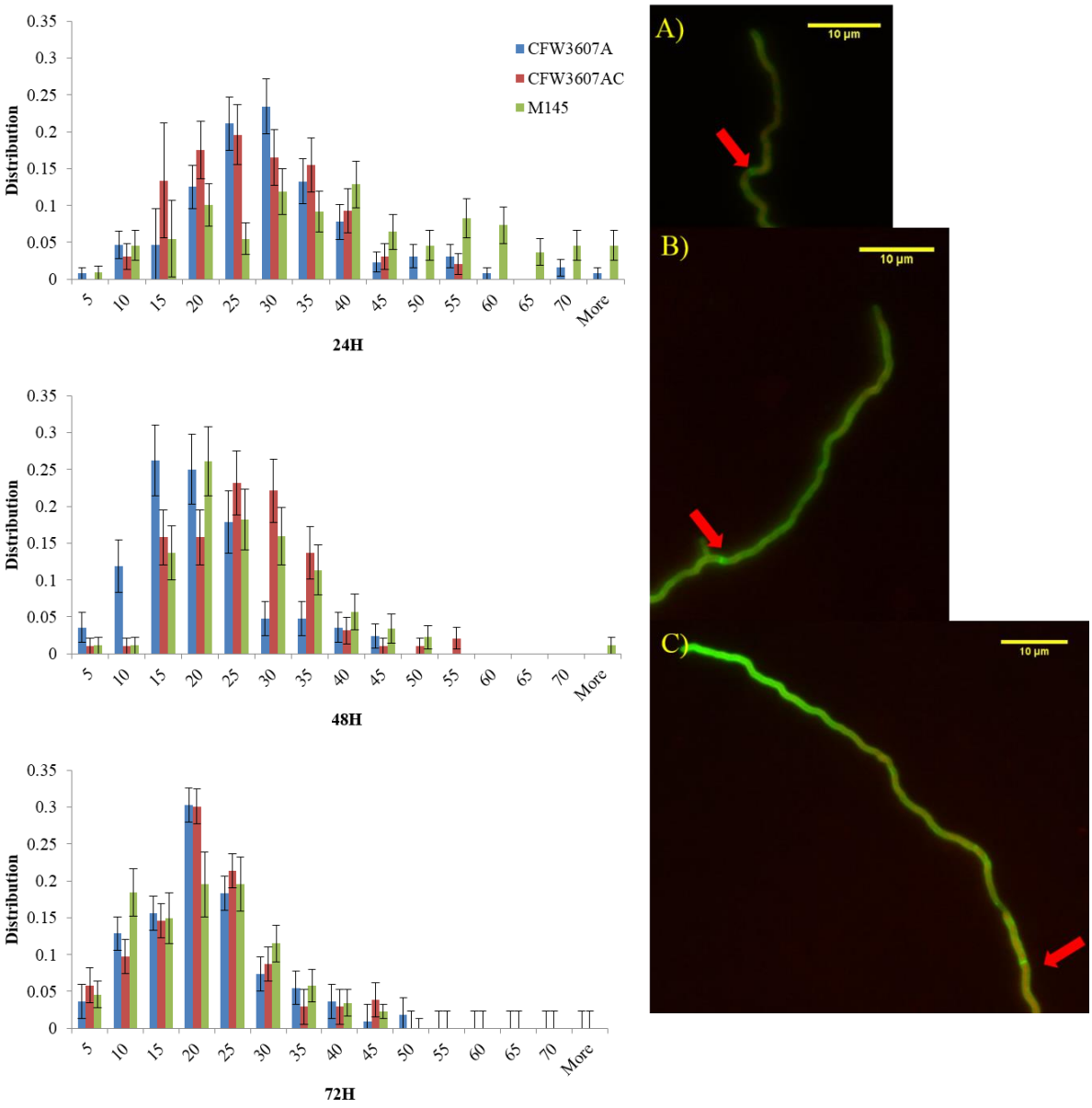

Fig 5-2. Tip to cross-wall distance for CFW3607A, CFW3607AC, and M145. The information is displayed as a histogram in µm. The average distances were 27.9µm, 18.88µm, and 18.9µm for CFW3607A, 24.72µm, 23.93µm, and 18.79µm for CFW3607AC, and 37.98µm, 24.10µm, and 18.58µm for M145, respective of the time-points. The sample sizes were 128 for CFW3607A, 97 for CFW3607AC, and 109 for M145 after 24 hours, 84 for CFW3607A, 95 for CFW3607AC, and 88 for M145 after 48 hours, and 109 for CFW3607A, 103 for CFW3607AC, and 87 for M145 after 72 hours. The images show cross-wall formation after 24 hours in A) CFW3607A, B) CFW3607AC, and C) M145.

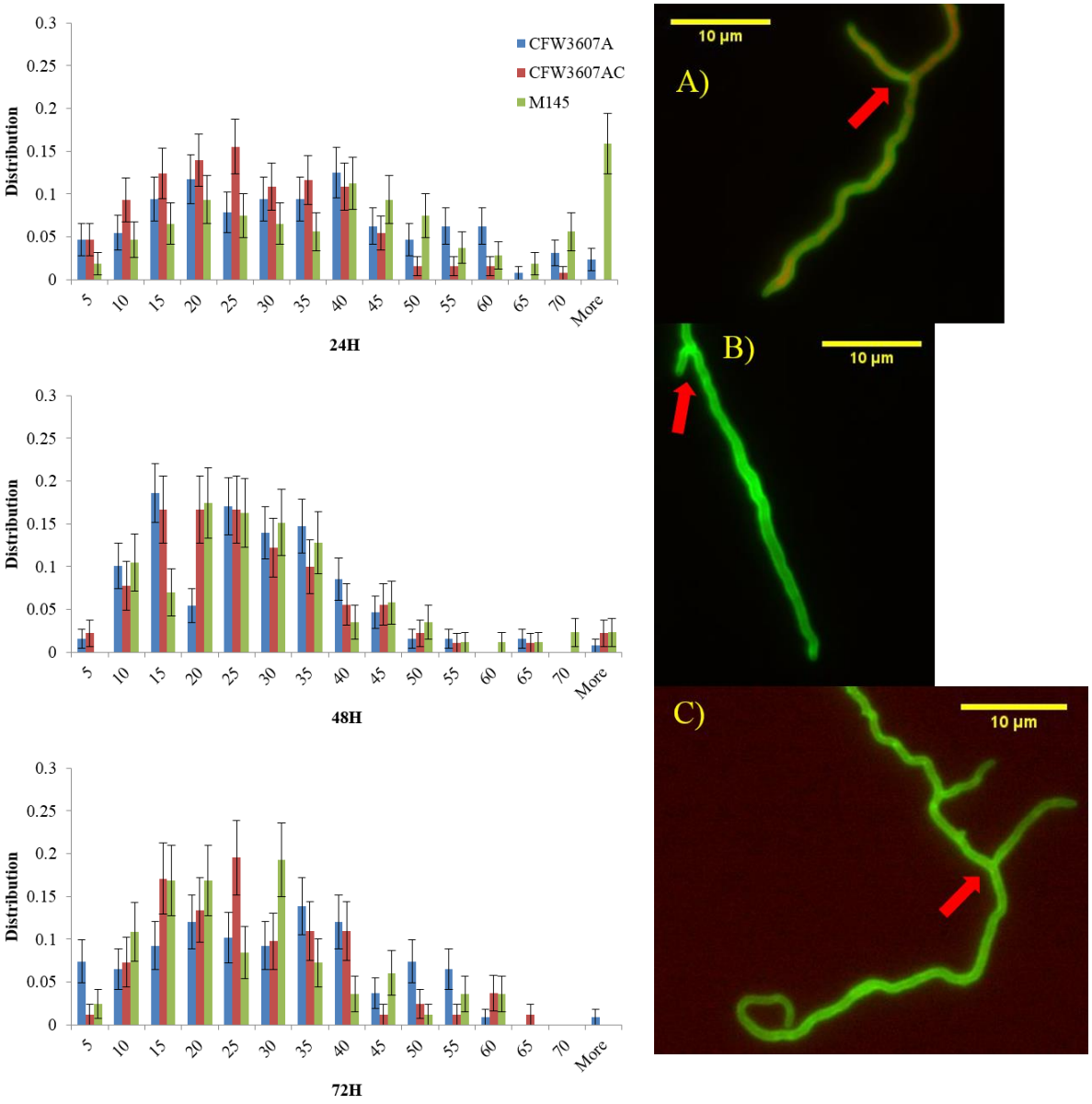

Fig 5-3. Tip to branch distance for CFW3607A, CFW3607AC, and M145. The information is displayed as a histogram in µm. The average distances were 32.35µm, 24.96µm, and 27.62µm for CFW3607A, 24.29µm, 24.48µm, and 25.23µm for CFW3607AC, and 41.60µm, 28.37µm, and 23.86µm for M145, respective of the time-points. The sample sizes were 128 for CFW3607A, 127 for CFW3607AC, and 107 for M145 after 24 hours, 129 for CFW3607A, 90 for CFW3607AC, and 86 for M145 after 48 hours, and 108 for CFW3607A, 82 for CFW3607AC, and 83 for M145 after 72 hours. The images show branch formation after 48 hours in A) CFW3607A, B) CFW3607AC, and C) M145.

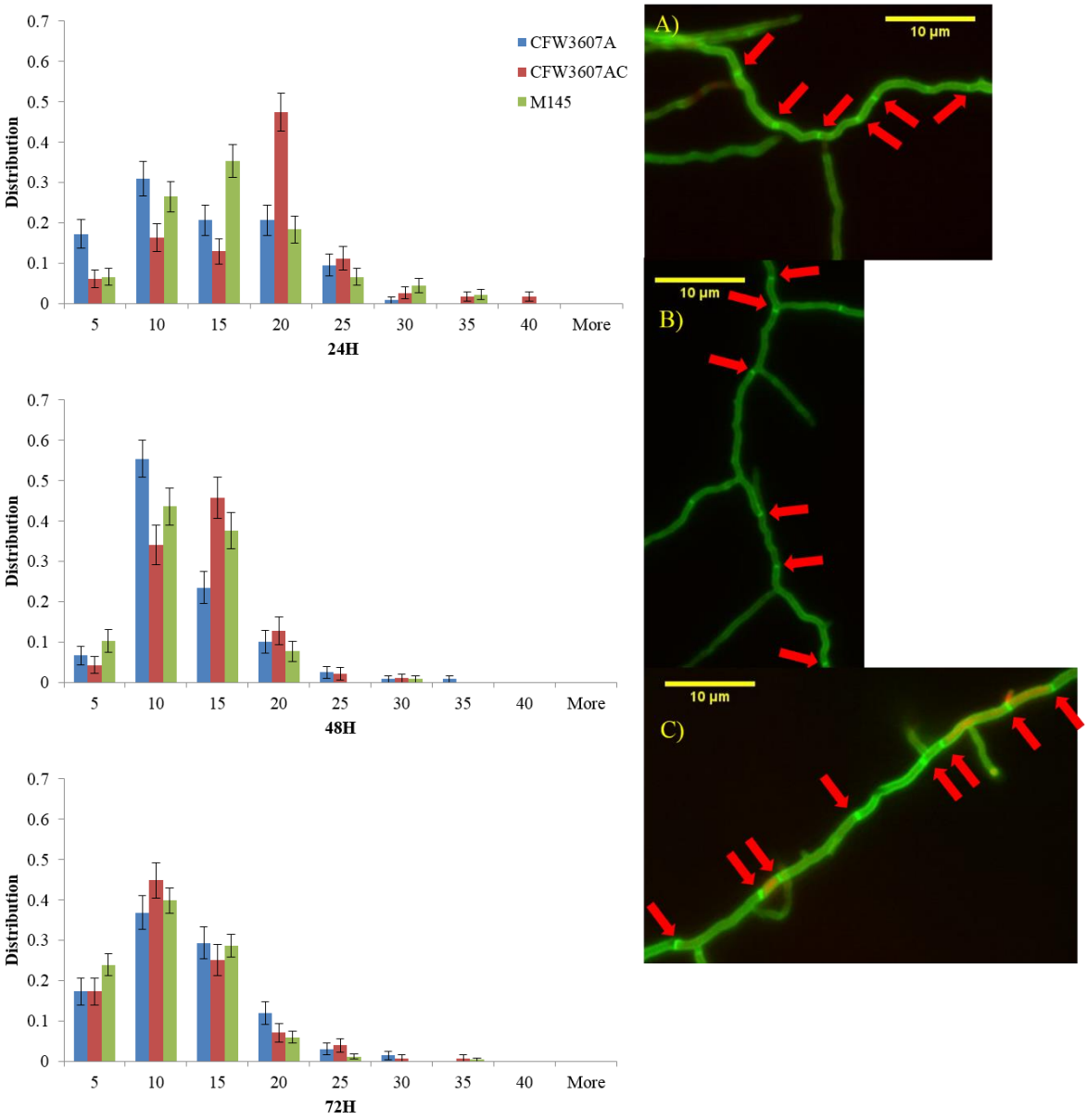

Fig 5-4. Cross-wall to cross-wall distance for CFW3607A, CFW3607AC, and M145. The information is displayed as a histogram in µm. The average distances were 11.29µm, 10.11µm, and 9.90µm for CFW3607A, 15.50µm, 11.49µm, and 9.38µm for CFW3607AC, and 13.28µm, 9.55µm, and 8.61µm for M145, respective of the time-points. The sample sizes were 116 for CFW3607A, 116 for CFW3607AC, and 136 for M145 after 24 hours, 119 for CFW3607A, 94 for CFW3607AC, and 117 for M145 after 48 hours, 133 for CFW3607A, 127 for CFW3607AC, and 251 for M145. The images show cross-wall formation after 72 hours in A) CFW3607A, B) CFW3607AC, and C) M145

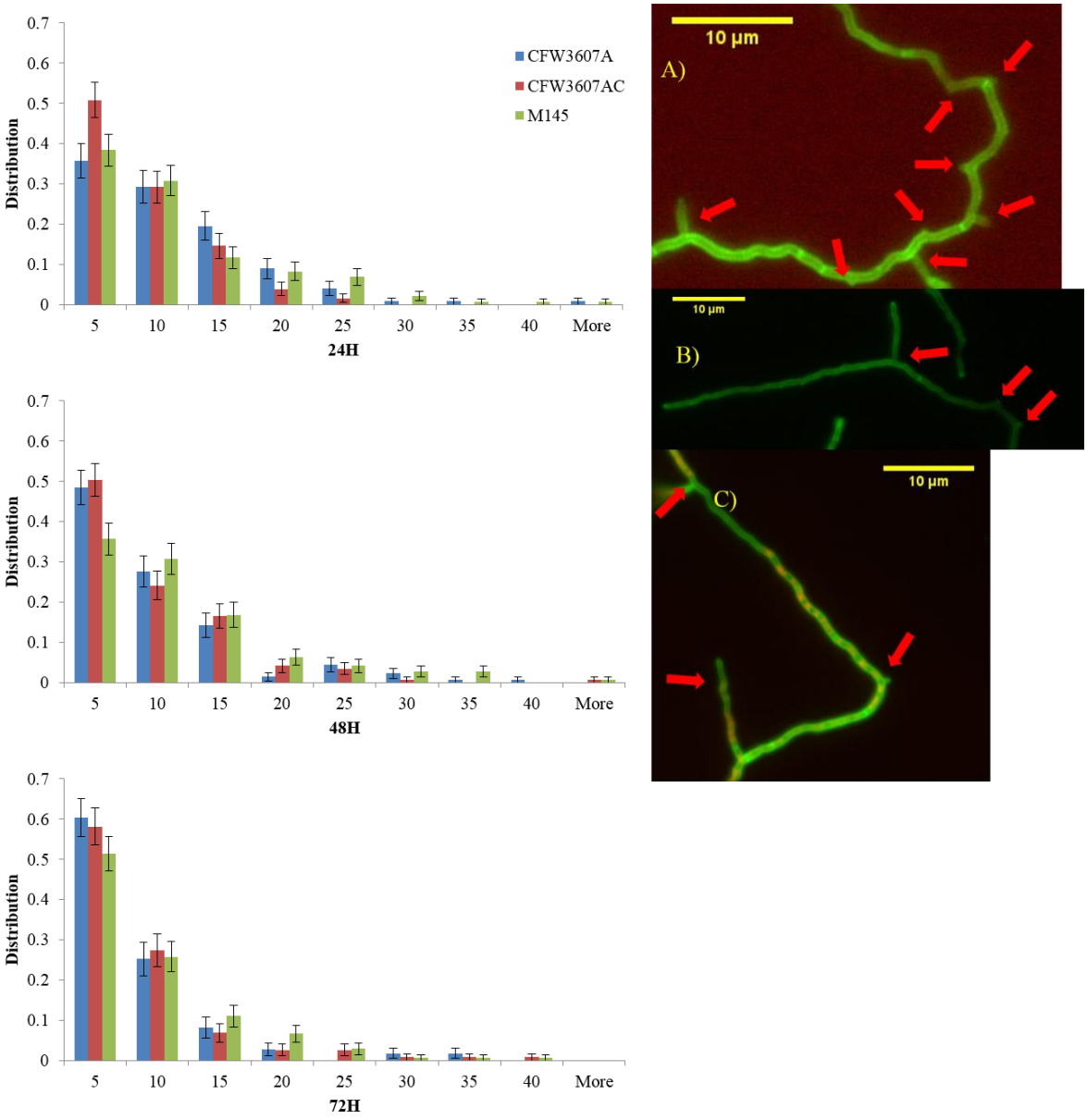

Fig 5-5. Branch to branch distance for CFW3607A, CFW3607AC, and M145. The information is displayed as a histogram in µm. The average distances were 8.96µm, 9.30µm, and 5.75µm for CFW3607A, 6.00µm, 6.95µm, and 6.15µm for CFW3607AC, and 8.86µm, 9.37µm, and 7.01µm for M145, respective of the time-points. The sample sizes were 123 for CFW3607A, 130 for CFW3607AC, and 146 for M145 after 24 hours, 134 for CFW3607A, 145 for CFW3607AC, and 143 for M145 after 48 hours, and 111 for CFW3607A, 117 for CFW3607AC, and 136 for M145 after 72 hours. The images show branch formation after 48 hours in A) CFW3607A, B) CFW3607AC, and C) M145.

In summary, the tip to cross-wall distance was on average shorter for CFW3607A until 72 hours, with complementation failing to restore wild-type after 24 hours, but restored wild-type distances after 48 hours. This marked difference was due to a different distribution of tip to cross-wall distances, with the cross-walls concentrating at 20-39µm away from the tip, with wild-type having a much more even spread. The average tip to branch distance was also shorter for CFW3607A after 24 hours, a phenotype exacerbated by complementation, but slightly longer after 72 (see Fig5-2 and Fig5-3). This was due to a large number of wild-type branches forming further away than 70µm from the tip. Both cross-wall to cross-wall and branch to branch distances were similar to that of wild-type, but both were slightly shorter after 24 hours in the mutant strain (see Fig5-4 and Fig5-5). Cross-wall to cross-wall distances were partially restored by complementation after 24 hours, but not so for the very small difference in branch to branch distances.

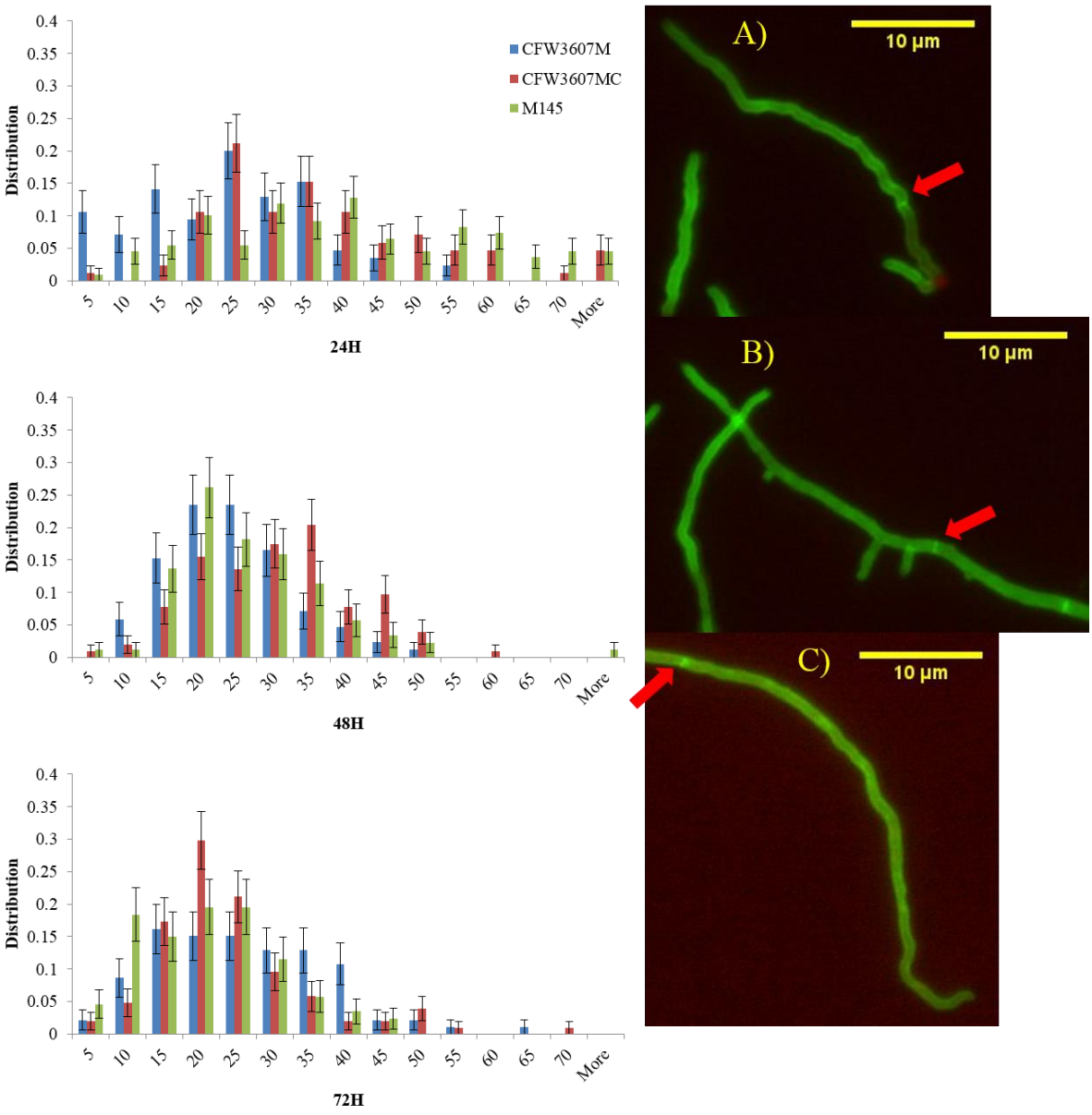

Fig 5-6. Tip to cross-wall distance for CFW3607M, CFW3607MC, and M145. The information is displayed as a histogram in µm. The average distances were 21.61µm, 22.10µm, and 23.48µm for CFW3607M, 34.23µm, 28.06µm, and 21.57µm for CFW3607MC, and 37.98µm, 24.10µm, and 18.58µm for M145, respective of the time-points. The sample sizes were 85 for CFW3607M, 85 for CFW3607MC, and 109 for M145 after 24 hours, 85 for CFW3607M, 103 for CFW3607MC, and 88 for M145 after 48 hours, and 93 for CFW3607M, 104 for CFW3607MC, and 87 for M145 after 72 hours. The images show cross-wall formation after 24 hours in A) CFW3607M, B) CFW3607MC, and C) M145.

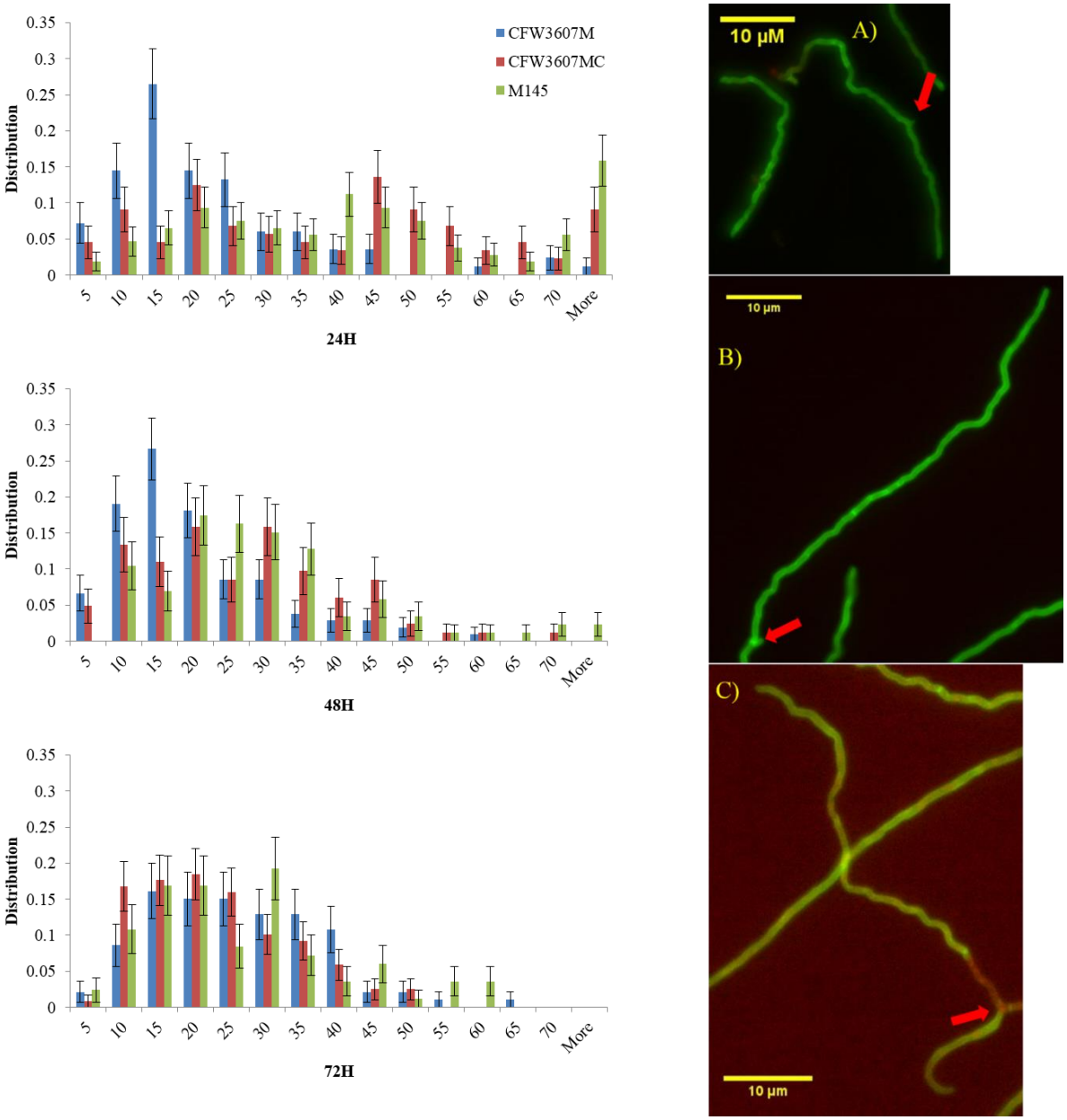

Fig 5-7. Tip to branch distance for CFW3607M, CFW3607MC, and M145. The information is displayed as a histogram in µm. The average distances were 20.54µm, 17.25µm, and 24.83µm for CFW3607M, 36.99µm, 24.24µm, and 20.64µm for CFW3607MC, and 41.60µm, 28.37µm, and 23.86µm for M145, respective of the time-points. The sample sizes were 85 for CFW3607M, 85 for CFW3607MC after 24 hours, 85 for CFW3607M, 103 for CFW3607MC, and 88 for M145 after 48 hours, and were 93 for CFW3607M, 104 for CFW3607MC, and 83 for M145 after 72 hours. The images show branch formation after 24 hours in A) CFW3607M, B) CFW3607MC, and C) M145.

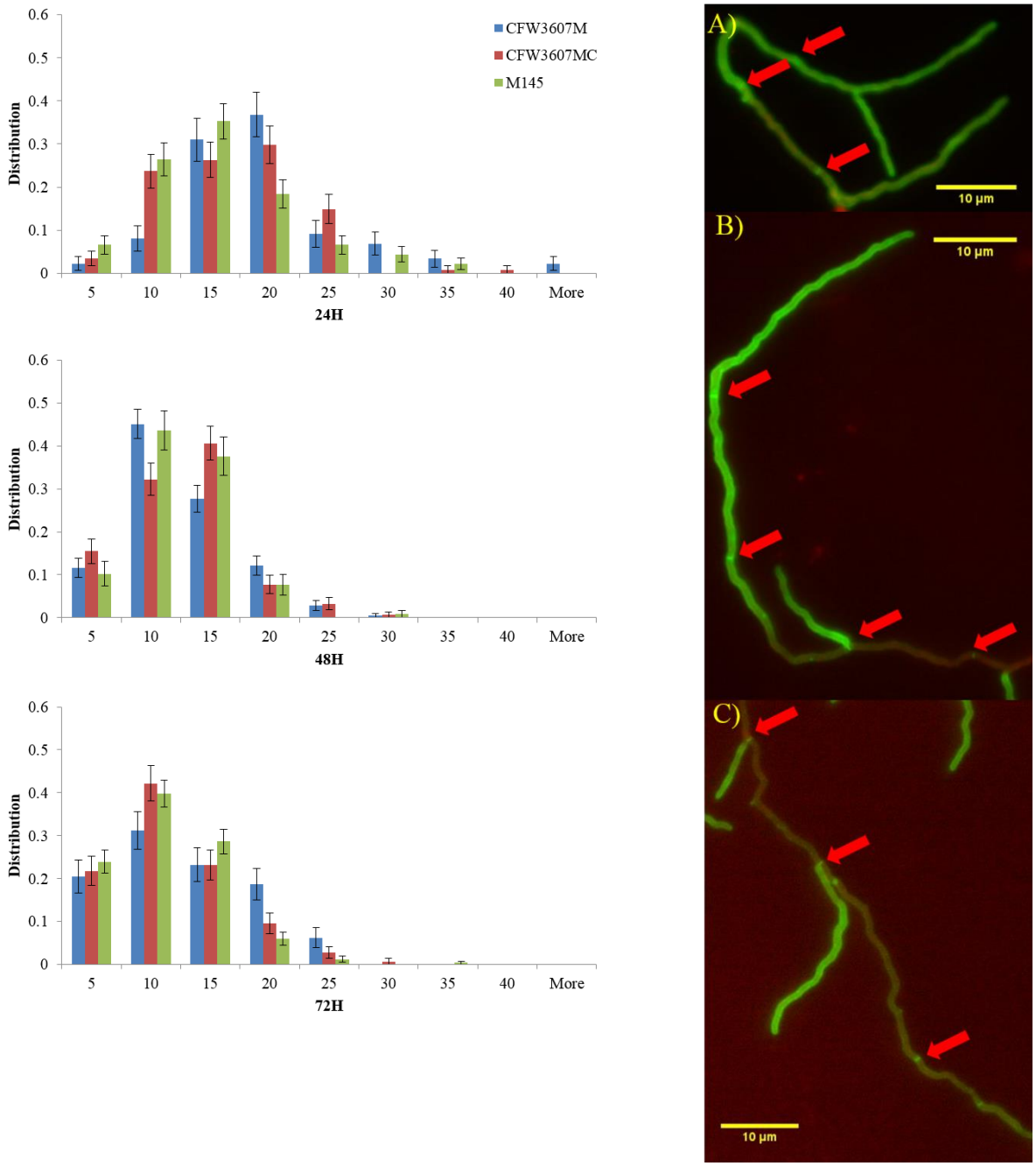

Fig 5-8. Cross-wall to cross-wall distance for CFW3607M, CFW3607MC and M145. The information is displayed as a histogram in µm. The average distances were 17.13µm, 10.08µm, and 10.49µm for CFW3607M, 14.44µm, 9.87µm, and 9.08µm for CFW3607MC, and 13.28µm, 9.55µm, and 8.61µm for M145, respective of the time-points. The sample sizes were 116 for CFW3607M, 116 for CFW3607MC, and 136 for M145 after 24 hours, 119 for CFW3607M, 94 for CFW3607MC, and 117 for M145 after 48 hours, 133 for CFW3607M, 127 for CFW3607MC, and 251 for M145. The images show cross-wall formation after 24 hours in A) CFW3607M, B) CFW3607MC, and C) M145.

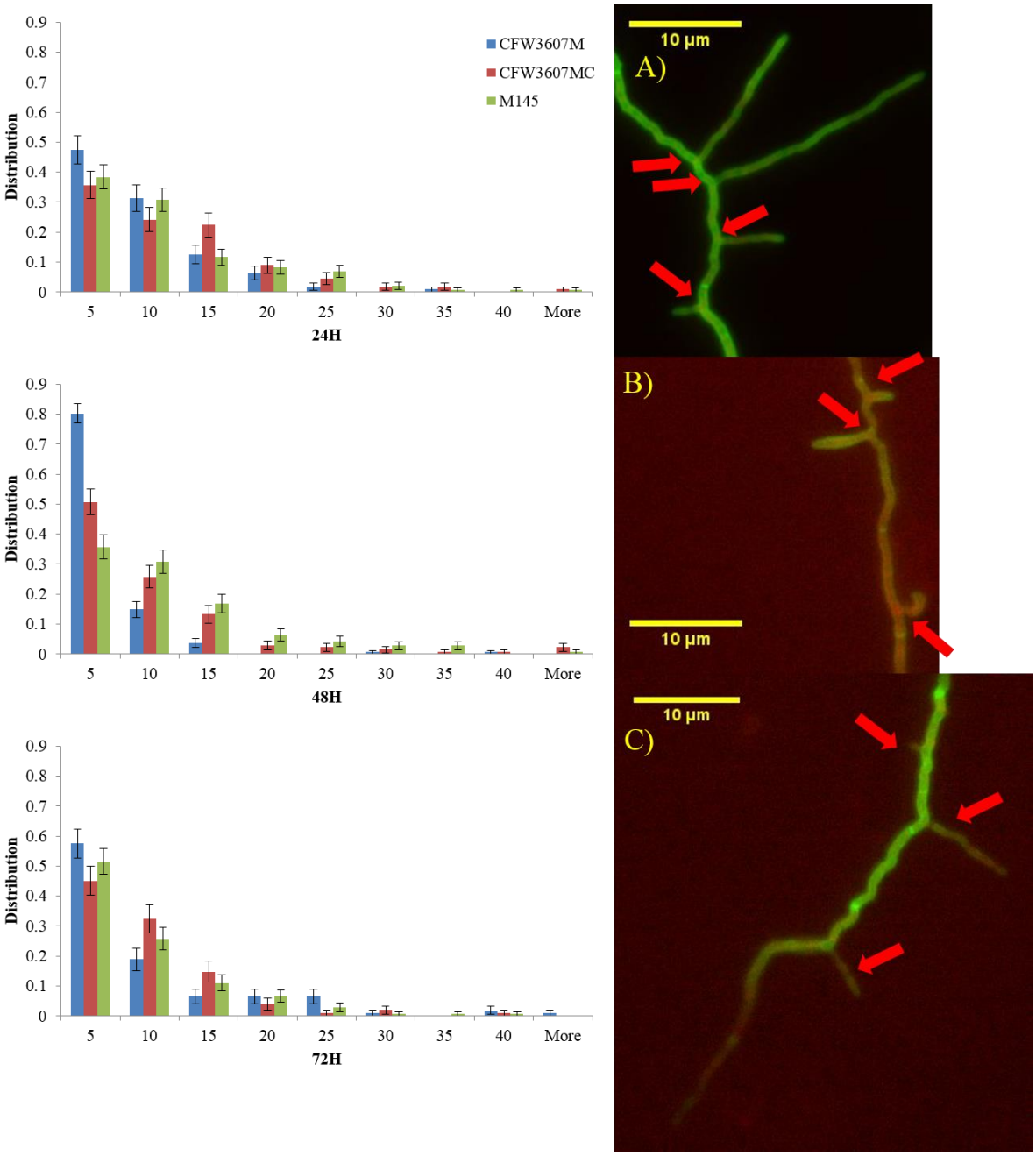

Fig 5-9. Branch to branch distance for CFW3607M, CFW3607MC, and M145. The information is displayed as a histogram in µm. The average distances were 6.92µm, 3.58µm, and 7.20µm for CFW3607M, 9.20µm, 7.82µm, and 7.06µm for CFW3607MC, and 8.86µm, 9.37µm, and 7.01µm for M145, respective of the time-points. The sample sizes were 112 for CFW3607M, 112 for CFW3607MC, and 146 for M145 after 24 hours, 162 for CFW3607M, 136 for CFW3607MC, and 143 for M145 after 48 hours, and 106 for CFW3607M, 102 for CFW3607MC, and 136 for M145 after 72 hours. The images show branch formation after 48 hours in A) CFW3607M, B) CFW3607MC, and C) M145.

The phenotype of CFW3607M was similar to that of CFW3607A. The average distance from the tip to the first cross-wall was much shorter for CFW3607M than wild-type after 24 hours, and wild-type phenotype was restored with complementation (see Fig5-6 and Table5-1). After 48 hours, the difference was much smaller, and after 72 hours, CFW3607M formed cross-walls only slightly further away from the tip, both of which were partially restored by complementation. When the distribution was examined, it became clear that wild-type had a much wider distribution, whereas the cross-walls of CFW3607M and its complemented version clustered much closer to the tip, specifically 20-39µm from the tip. The tip to branch distance after 24 hours was much shorter for CFW3607M compared to wild-type, with partial function distance restored by complementation (see Fig5-7 and Table5-2). When distribution was examined, it became obvious this was due to a different pattern. Wild-type had a much more even spread, while CFW3607M formed most of its branches at 0-25µm distance from the tip. This was similar to what had been observed in CFW3607A.

Cross-wall to cross-wall distances were slightly longer for CFW3607M after 24 hours, but wild-type and mutant distances were similar after that time point (see Fig 5-8). The branch to branch distance after 48 hours was much shorter for CFW3607M when compared to wild-type, with partial function distance restored by complementation (see Fig5-9 and Table5-4). When distribution was examined, wild-type had a much more even spread, while CFW3607M formed most of its branches at 0-10µm from each other, while wild-type had a much more even spread until 15µm.

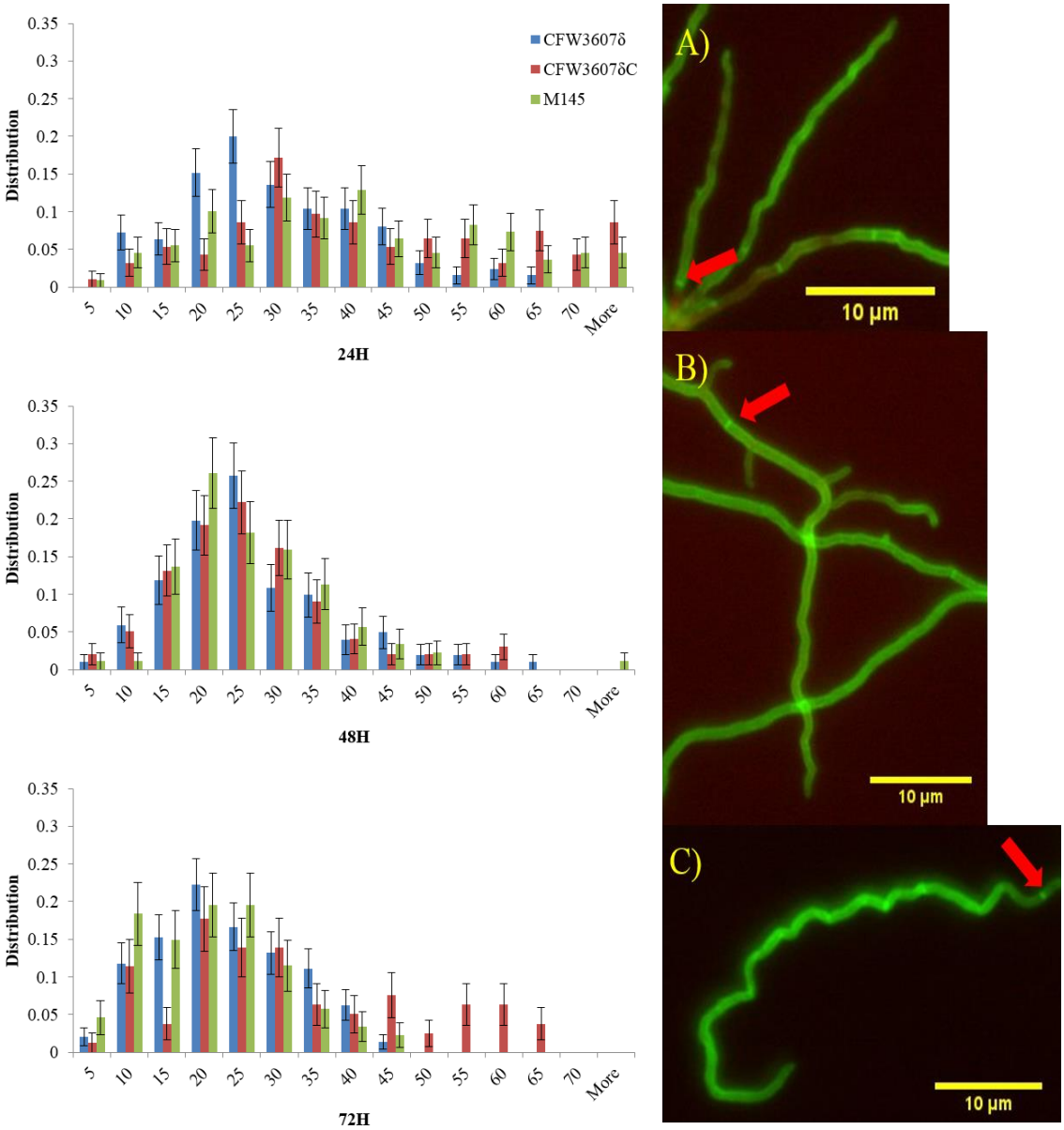

Fig 5-10. Tip to cross-wall distance for CFW3607δ, CFW3607δC, and M145. The information is displayed as a histogram in µm. The average distances were 27.55µm, 23.98µm, and 20.58µm for CFW3607δ, 40.06µm, 23.84µm, and 29.42µm for CFW3607δC, and 37.98µm, 24.10µm, and 18.58µm for M145, respective of the time-points. The sample sizes were 125 for CFW3607δ, 93 for CFW3607δC, and 109 for M145 after 24 hours, 101 for CFW3607δ, 91 for CFW3607δC, and 88 for M145 after 48 hours, and 144 for CFW3607δ, 79 for CFW3607δC, and 87 for M145 after 72 hours. The images show cross-wall formation after 24 hours in A) CFW3607δ, B) CFW3607δC, and C) M145.

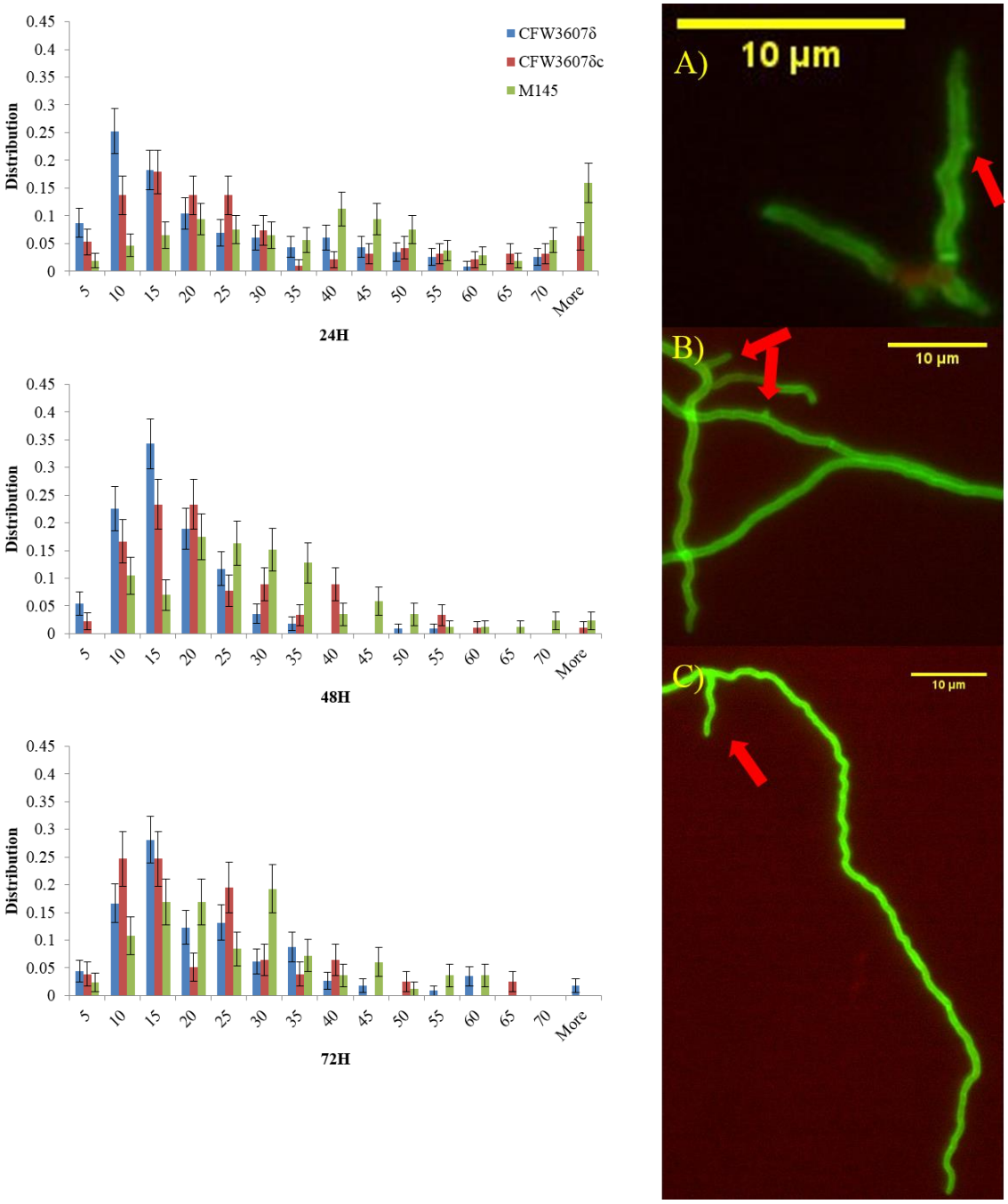

Fig5-11. Tip to branch distance for CFW3607δ, CFW3607δC, and M145. The information is displayed as a histogram in µm. The average distances were 20.31µm, 14.73µm, and 20.18µm for CFW3607δ, 27.55µm, 20.07µm, and 18.37µm for CFW3607δC, and 41.60µm, 28.37µm, and 23.86µm for M145, respective of the time-points. The sample sizes were 115 for CFW3607δ, 95 for CFW3607δC, and 109 for M145 after 24 hours, 85 for CFW3607δ, 111 for CFW3607δ, 90 for CFW3607δC, and 88 for M145 after 48 hours, and were 114 for CFW3607δ, 77 for CFW3607δC, and 83 for M145 after 72 hours. The images show branch formation after 24 hours in A) CFW3607δ, B) CFW3607δC, and C) M145.

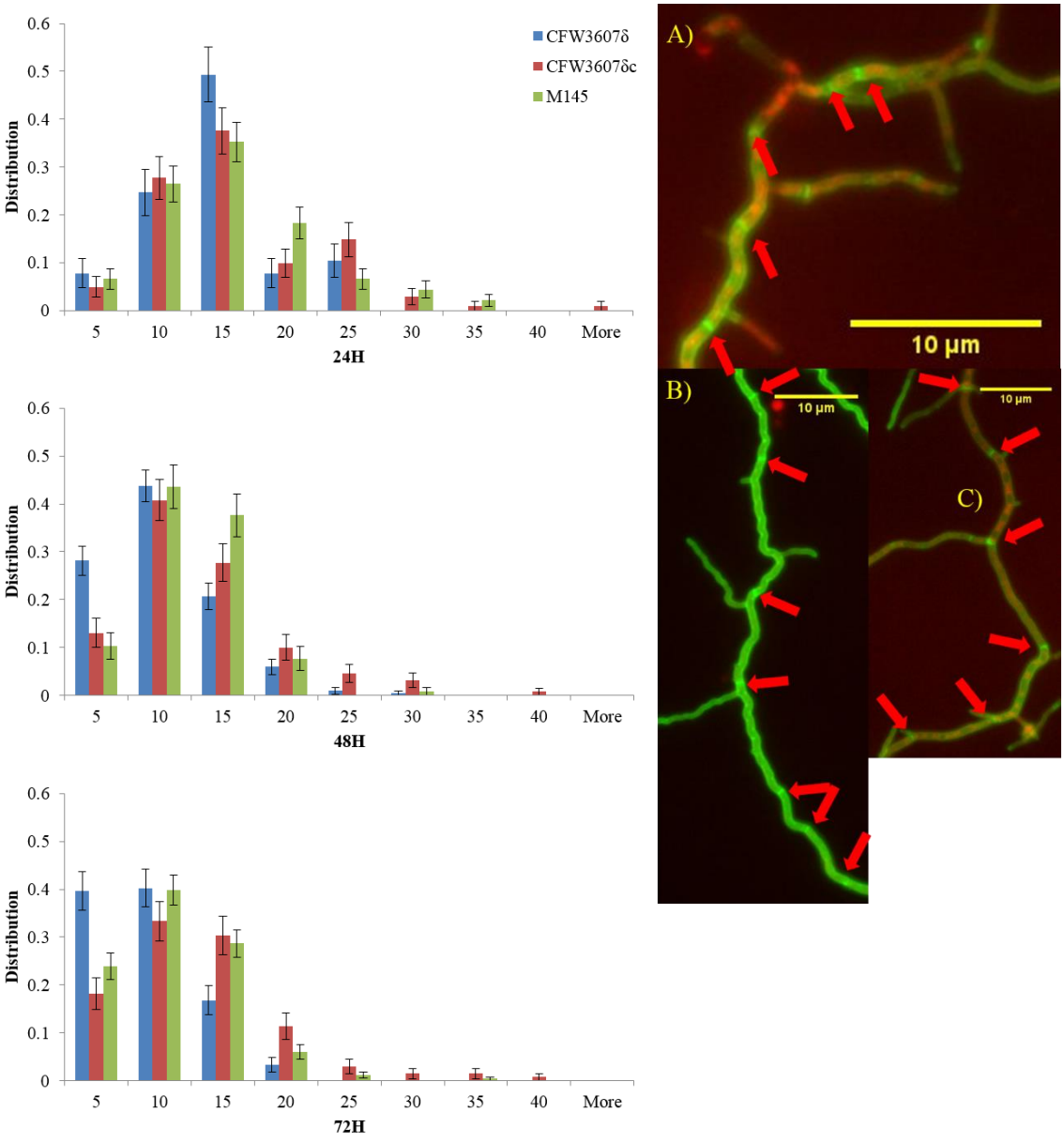

Fig5-12. Cross-wall to cross-wall distance for CFW3607δ, CFW3607δC, and M145. The information is displayed as a histogram in µm. 11.94µm, 7.83µm, and 6.67µm for CFW3607δ, 13.40µm, 10.78µm, and 10.43µm for CFW3607δC, and 13.28µm, 9.55µm, and 8.61µm for M145, respective of the time-points. The sample sizes were 77 for CFW3607δ, 101 for CFW3607δC, and 136 for M145 after 24 hours, 217 for CFW3607δ, 130 for CFW3607δ, and 117 for M145 after 48 hours, 149 for CFW3607δ, 132 for CFW3607δC, and 251 for M145. The images show cross-wall formation after 48 hours in A) CFW3607δ, B) CFW3607δC, and C) M145.

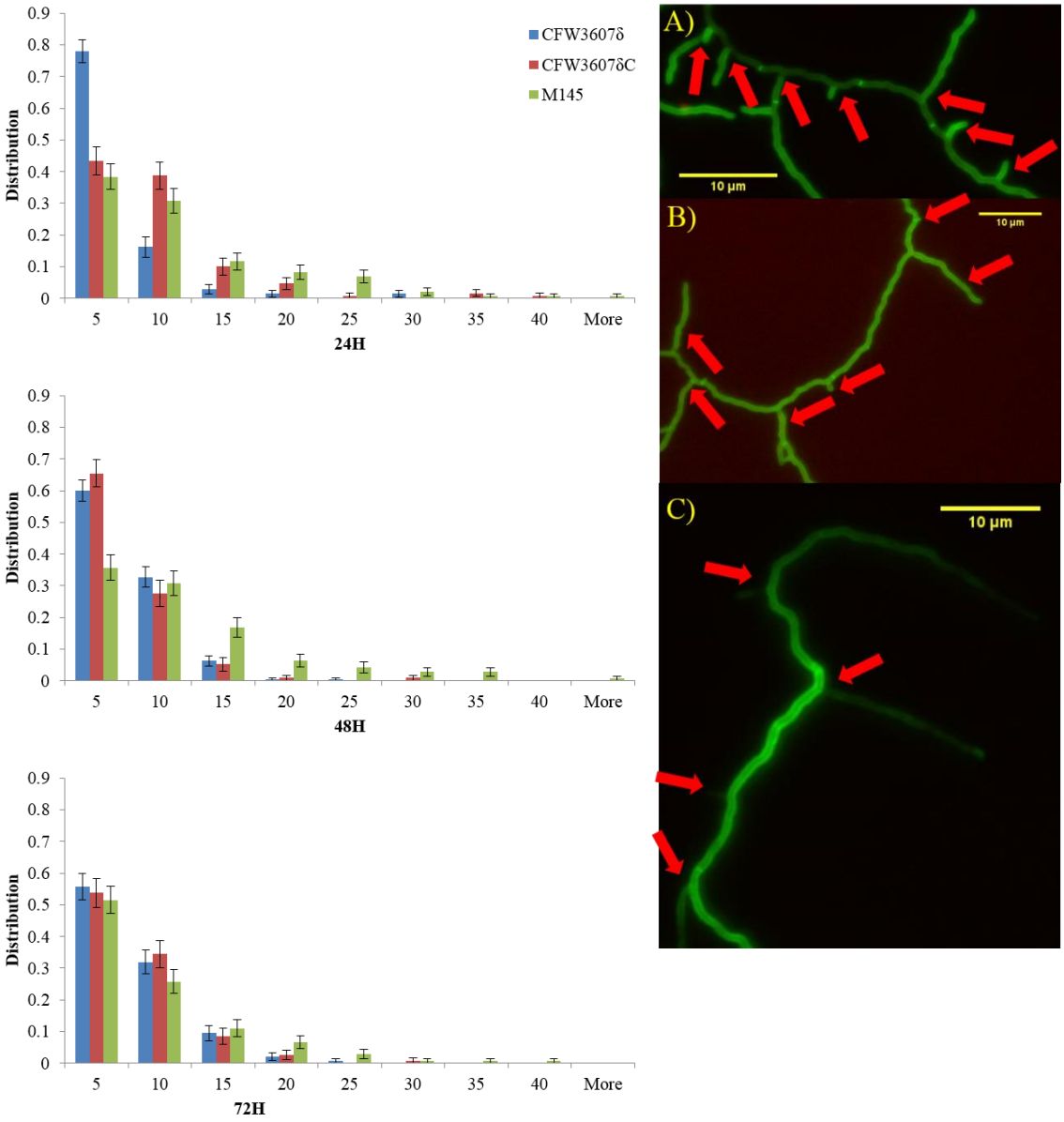

Fig5-13. Branch to branch distance for CFW3607δ, CFW3607δC, and M145. The information is displayed as a histogram in µm. The average distances were 3.92µm, 4.56µm, and 5.08µm for CFW3607δ, 6.82µm, 4.56µm, and 5.31µm for CFW3607δC, and 8.86µm, 9.37µm, and 7.01µm for M145, respective of the time-points. The sample sizes were 111 for CFW3607δ, 159 for CFW3607δC, and 146 for M145 after 24 hours, 208 for CFW3607δ, 116 for CFW3607δC, and 143 for M145 after 48 hours, and 147 for CFW3607δ, 119 for CFW3607δC, and 136 for M145 after 72 hours. The images show branch formation after 24 hours in A) CFW3607δ, B) CFW3607δC, and C) M145.

In summary, the deletion of *SCO3607* had a more severe effect than a disruption did. The tip to cross-wall distance was significantly shorter for CFW3607δ after 24 hours, which was restored by complementation. After 48 hours, there was no statistically significant difference (see Fig5-10). When distribution was examined, it became obvious wild-type had a much more even spread, while CFW3607δ formed most of its cross-walls at 16-30µm distance from the tip. This was similar to what had been observed in CFW3607A and CFW3607M. The tip to branch distance was much shorter for CFW3607δ throughout the measured time period. Wild-type tip to branch distance was partially restored by complementation after 24 and 48 hours, and there was no difference between M145 and CFW3607δ after 72 hours (see Fig5-11). When distribution was examined, it became obvious wild-type had a much more even spread, while CFW3607δ formed most of its branches at 0-20µm distance from the tip. This was similar to what had been observed in CFW3607A and CFW3607M, but the distance from tip to branch was even shorter. The average cross-wall to cross-wall distance was slightly shorter for CFW3607δ after 72 hours, whilst the branch to branch distance after 24 and 48 hours was much shorter for CFW3607δ compared to wild-type (see Fig5-12 and Fig5-13). After 24 hours, the majority of the mutant strain distances fell into the range of 0-5µm, while after 48 hours, there had been a shift to 5-10µm as well. As opposed to wild-type, the branch to branch distances of M145 did not cluster in the 0-5µm range. The wild-type phenotype was restored in the complemented strain after 24 hours, but not after 48 hours.

5.2.1.2. SCO3608 plays a smaller role than SCO3607 in cell polarity

To investigate any potential changes to cell morphology and cell polarity due to *SCO3608* deletion, a Schwedock stain was performed on CFW3608δ, its complemented strain CFW3608δC, and M145, and tip to cross-wall, tip to branch, cross-wall to cross-wall, and branch to branch distances were measured. Similar to the *SCO3607* mutant strains, tip to cross-wall and tip to branch distances were shorter after 24 and 48 hours, but further away after 72 hours (p-values for tip to cross-wall distances were 0.0077, 0.0000, and 0.0073 at the respective timepoints, and tip to branch distance p-values were 0.0000, 0.0298, and 0.0237). Variation was observed in cross-wall to cross-wall distances, where they were shorter until 72 hours, when they were slightly longer (p-values were 0.3139, 0.1513, 0.0000 in order of time-points). Branches formed closer together after 24 hours, further apart after 48 hours, with no difference after 72 hours (p-values were 0.1678 and 0.0000 after 24 and 48 hours). These phenotypes, probably also associated with cell polarity, were milder than their *SCO3607* counterparts. All the statistical data has been included in the appendix.

Table 5-5. Number of tip to cross-wall measurements per SCO3608-mutant strain. The number of measurements is indicated in each column.

Strain	**24 hours**	**48 hours**	**72 hours**
CFW3608δ	88	131	111
CFW3608δC	117	150	95
M145	109	88	87

Table 5-6. Number of tip to branch measurements per SCO3608-mutant strain. The number of measurements is indicated in each column.

Strain	**24 hours**	**48 hours**	**72 hours**
CFW3608δ	108	103	127
CFW3608δC	101	146	89
M145	107	86	83

Table5-7. Number of cross-wall to cross-wall measurements per strain. The number of measurements is indicated in each column.

Strain	**24 hours**	**48 hours**	**72 hours**
CFW3608δ	154	151	131
CFW3608δC	101	158	130
M145	136	117	251

Table5-8. Number of branch to branch measurements per strain. The number of measurements is indicated in each column.

Strain	**24 hours**	**48 hours**	**72 hours**
CFW3608δ	146	136	141
CFW3608δC	158	177	114
M145	146	143	136

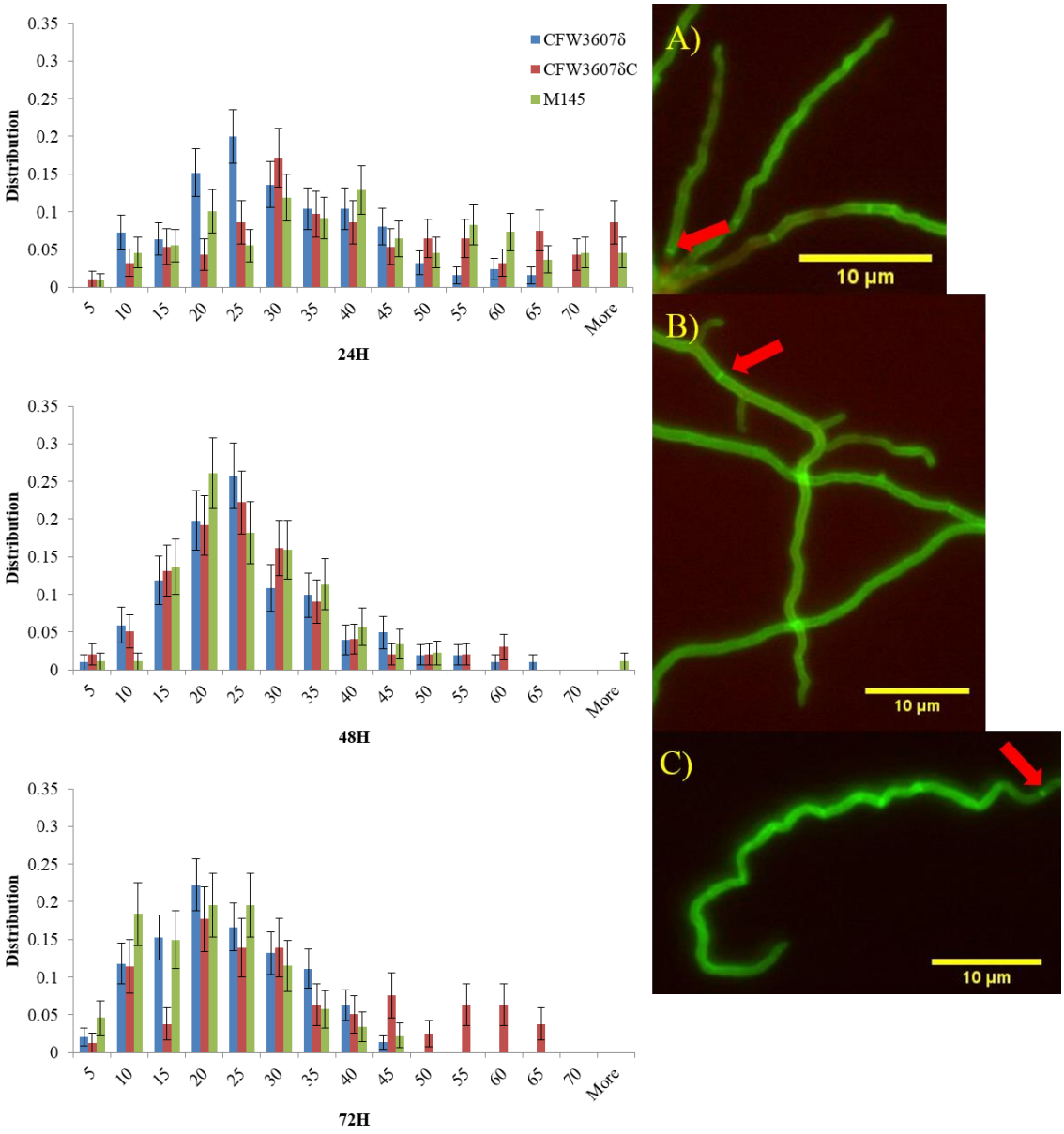

Fig5-14. Tip to cross-wall distance for CFW3608δ, CFW3608δC, and M145. The information is displayed as a histogram in µm. The average distances were 33.11µm, 18.43µm, and 23.09µm for CFW3608δ, 34.19µm, 24.86µm, and 21.29µm for CFW3608δC, and 37.98µm, 24.10µm, and 18.58µm for M145, respective of the time-points. The sample sizes were 88 for CFW3608δ, 117 for CFW3608δC, and 109 for M145 after 24 hours, 131 for CFW3608δ, 150 for CFW3608δC, and 88 for M145 after 48 hours, and 111 for CFW3608δ, 95 for CFW3608δC, and 87 for M145 after 72 hours. The images show cross-wall formation after 48 hours in A) CFW3608δ, B) CFW3608δC, and C) M145.

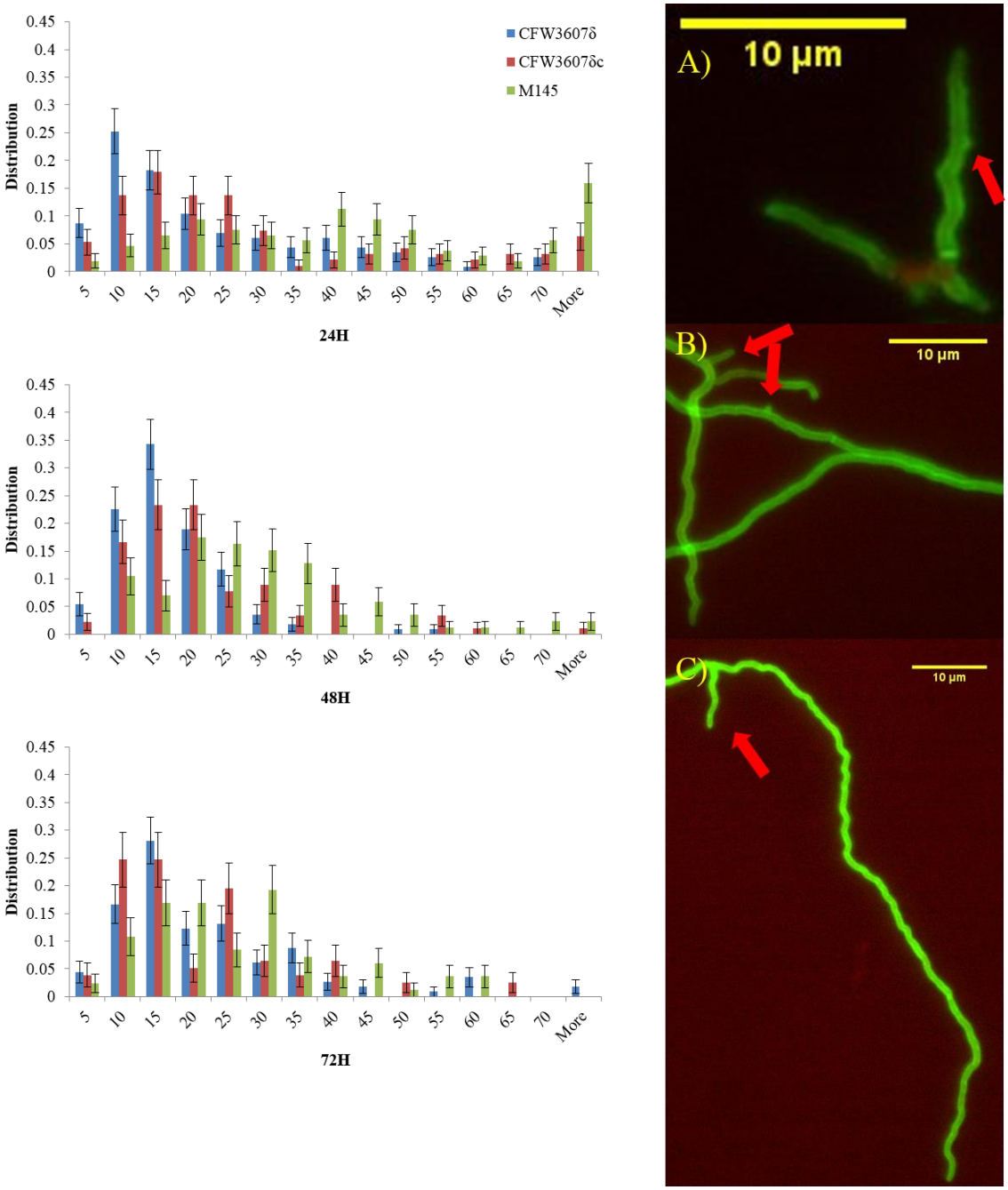

Fig5-15. Tip to branch distance for CFW3608δ, CFW3608δC, and M145. The information is displayed as a histogram in µm. The average distances were 31.40µm, 22.90µm, and 28.34µm for CFW3608δ, 29.48µm, 21.64µm, and 31.73µm for CFW3608δC, and 41.60µm, 28.37µm, and 23.86µm for M145, respective of the time-points. The sample sizes were 108 for CFW3608δ, 101 for CFW3608δC, and 109 for M145 after 24 hours, 103 for CFW3608δ, 146 for CFW3608δC, and 88 for M145 after 48 hours, and were 127 for CFW3608δ, 89 for CFW3608δC, and 83 for M145 after 72 hours. The images show branch formation after 48 hours in A) CFW3608δ, B) CFW3608δC, and C) M145

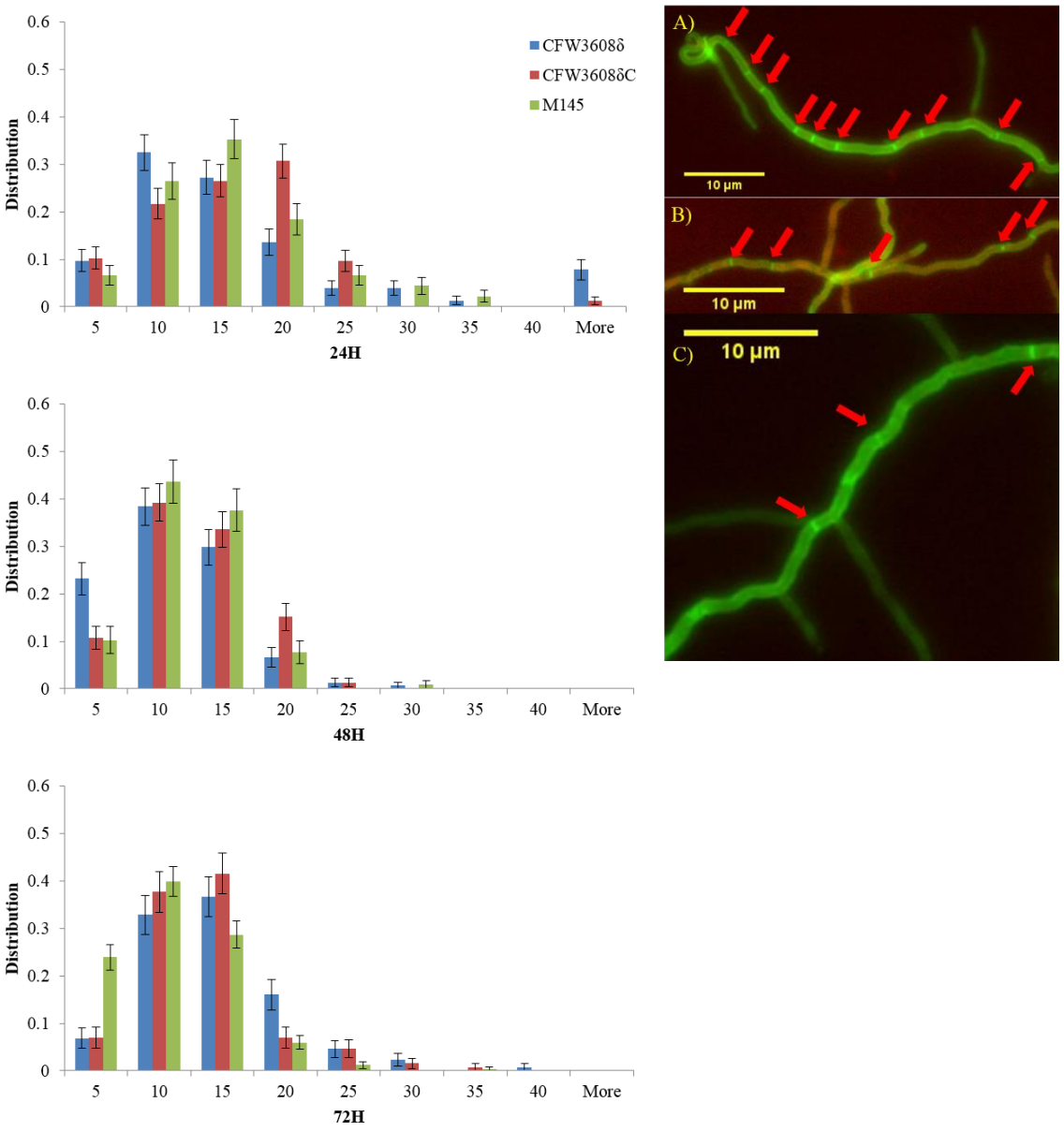

Fig5-16. Cross-wall to cross-wall distance for CFW3608δ, CFW3608δC, and M145. The information is displayed as a histogram in µm. The average distances were 16.33µm, 8.95µm, and 12.07µm for CFW3608δ, 13.44µm, 10.42µm, and 10.94µm for CFW3608δC, and 13.28µm, 9.55µm, and 8.61µm for M145, respective of the time-points. The sample sizes were 154 for CFW3608δ, 101 for CFW3608δC, and 136 for M145 after 24 hours, 151 for CFW3608δ, 158 for CFW3608δ, and 117 for M145 after 48 hours, 131 for CFW3608δ, 130 for CFW3608δC, and 251 for M145 after 72 hours. The images show cross-wall formation after 48 hours in A) CFW3608δ, B) CFW3608δC, and C) M145.

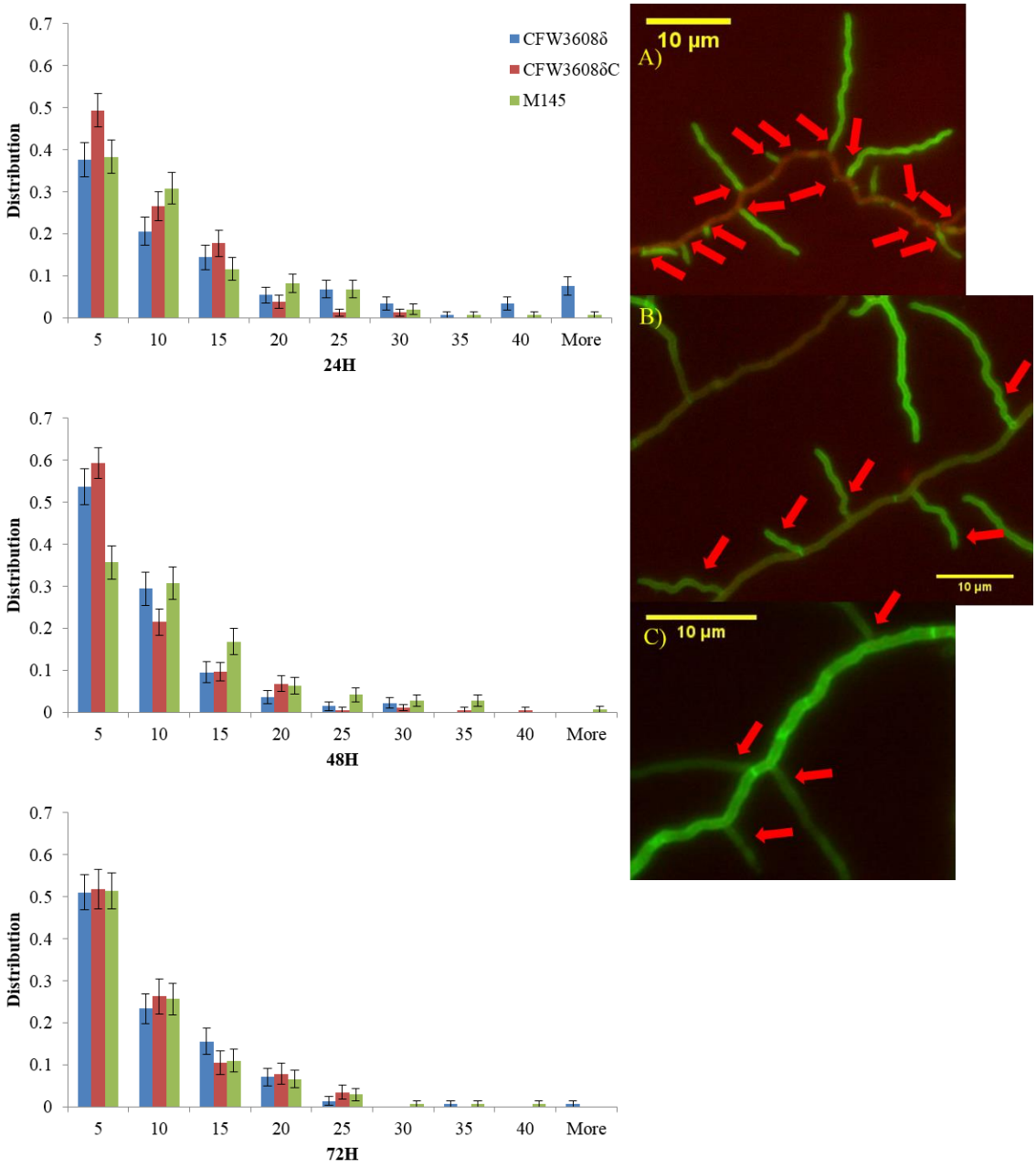

Fig5-17. Branch to branch distance for CFW3608δ, CFW3608δC, and M145. The information is displayed as a histogram in µm. The average distances were 13.86µm, 5.96µm, and 6.88µm for CFW3608δ, 6.54µm, 5.91µm, and 6.55µm for CFW3608δC, and 8.86µm, 9.37µm, and 7.01µm for M145, respective of the time-points. The sample sizes were 146 for CFW3608δ, 158 for CFW3608δC, and 146 for M145 after 24 hours, 136 for CFW3608δ, 177 for CFW3608δC, and 143 for M145 after 48 hours, and 141 for CFW3608δ, 114 for CFW3608δC, and 136 for M145 after 72 hours. The images show branch formation after 48 hours in A) CFW3608δ, B) CFW3608δC, and C) M145.

The tip to cross-wall distance for CFW3608δ is slightly different, with slightly shorter distances on average after 24 and 48 hours, and slightly longer after 72 hours, with the difference after 48 hours being very pronounced (see Fig5-14). The distribution was markedly different after 24 hours, with M145 measurements being much more evenly. Wild-type was restored after 24 hours and 48 hours, and partially after 72 hours. The branches formed closer to the tip in CFW3608δ after 24 and 48 hours, but further away after 72 hours, with complementation failing to restore wild-type phenotype at all time-points (see Fig5-15). The distribution after 24 hours for CFW3607δ relative to M145 is the same with regards to the distribution in the SCO3607 mutants, with branches generally forming much closer to the tip and M145 having a much higher percentage of its branches forming further away than 40µm. Cross-wall to cross-wall distances were marginally longer after 24 hours, slightly shorter after 48 hours, and slightly longer after 72 hours (see Fig5-16). Wild-type phenotype was restored by complementation after 24 and 48 hours, and partially after 72 hours. CFW3608 formed branches further apart after 24 hours, with complementation restoring wild-type (see Fig5-17). This reversed after 48 hours, where it formed branches closer together than wild-type, with complementation failing to restore wild-type phenotype. There was no difference after 72 hours.

5.2.1.3. A double knock-out mutant suffered from larger cross-wall compartments and issues with cell polarity

To elucidate the role of both SCO3607 and SCO3608 in cell morphology in vegetative hyphae, CFW36078δ, along with CFW36078δC and M145, were subjected to a Schwedock stain (see section 2.5) and tip to cross-wall, tip to branch, cross-wall to cross-wall, and branch to branch distances were measured. The data was presented as percentage histograms of the distribution, and statistical significance was demonstrated using p-values and F-tests (see appendix). The tip to cross-wall distance was shorter for CFW36078δ after 24 hours, but was slightly longer after 72 hours (p-values were 0.0000 for both). The tip to branch distance remained shorter for CFW36078δ until 72 hours (p-values were 0.0111, 0.0000, 0.2393). The cross-wall to cross-wall distance of CFW36078δ began to increase after 48 hours and was considerably longer than wild-type after 72 hours (p-values were 0.0125, 0.0636, 0.0000). Its branch to branch distance only differed from wild-type after 48 hours, when the branches formed slightly closer to each other (the p-value was 0.0089).

Table 5-9. Number of tip to cross-wall measurements per double mutant strain. The number of measurements is indicated in each column.

Strain	24 hours	48 hours	72 hours
CFW36078δ	111	105	106
CFW36078δC	114	86	151
M145	109	88	87

Table 5-10. Number of tip to branch measurements per double mutant strain. The number of measurements is indicated in each column.

Strain	24 hours	48 hours	72 hours
CFW36078δ	96	147	119
CFW36078δC	92	84	133
M145	107	86	83

Table 5-11. Number of cross-wall to cross-wall measurements per double mutant strain. The number of measurements is indicated in each column.

Strain	24 hours	48 hours	72 hours
CFW36078δ	137	136	112
CFW36078δC	143	149	117
M145	136	117	251

Table 5-12. Number of branch to branch measurements per double mutant strain. The number of measurements is indicated in each column.

Strain	24 hours	48 hours	72 hours
CFW36078δ	111	136	173
CFW36078δC	159	150	145
M145	146	143	143

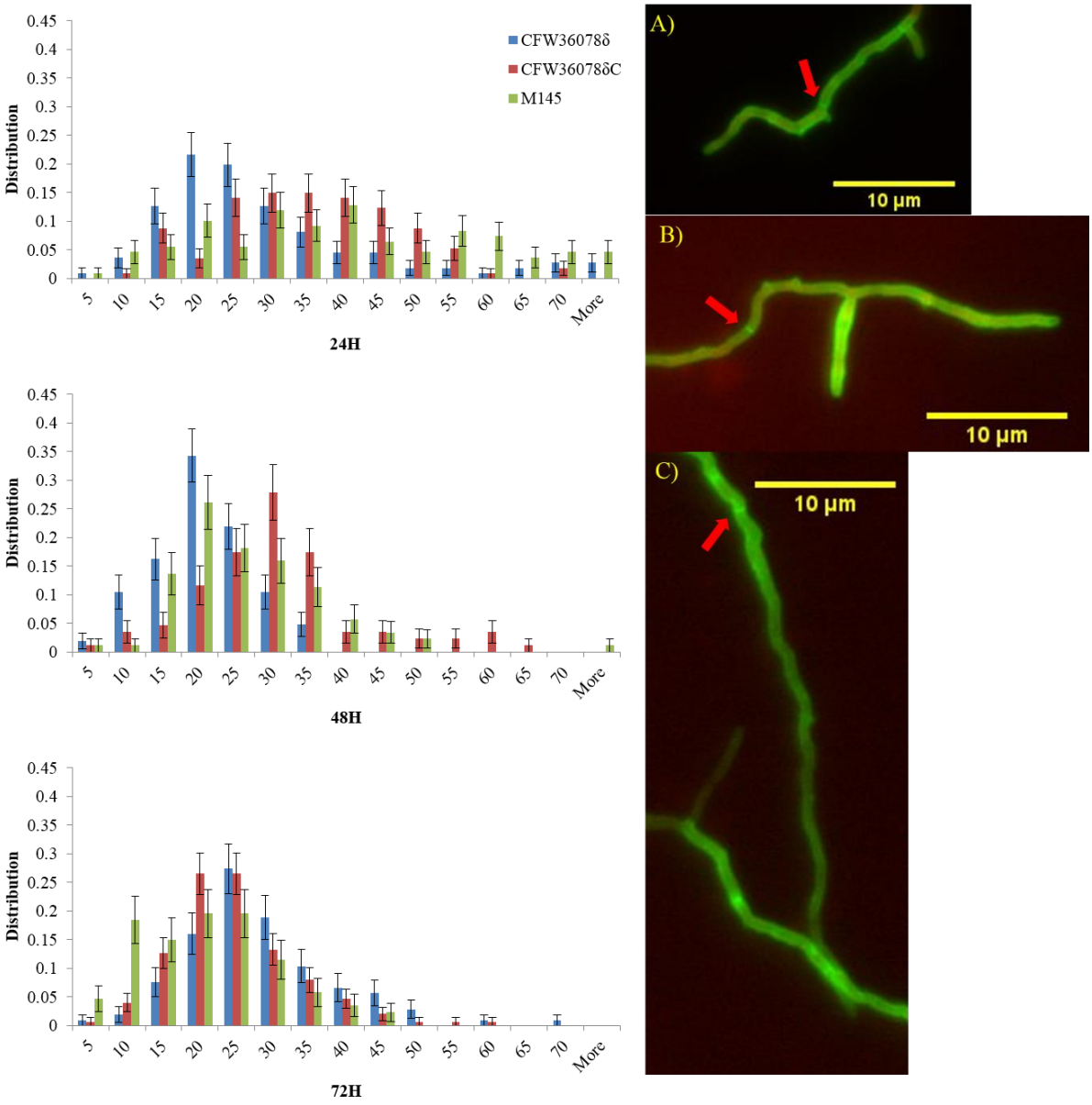

Fig5-18. Tip to cross-wall distance for CFW36078δ, CFW36078δC, and M145. The information is displayed as a histogram in µm. The average distances were 27.28µm, 18.40µm, and 25.93µm for CFW36078δ, 32.94µm, 28.15µm, and 22.50µm for CFW36078δC, and 37.98µm, 24.10µm, and 18.58µm for M145, respective of the time-points. The sample sizes were 111 for CFW36078δ, 114 for CFW36078δC, and 109 for M145 after 24 hours, 105 for CFW36078δ, 86 for CFW36078δC, and 88 for M145 after 48 hours, and 106 for CFW36078δ, 151 for CFW36078δC, and 87 for M145 after 72 hours. The images show cross-wall formation after 48 hours in A) CFW3608δ, B) CFW3608δC, and C) M145.

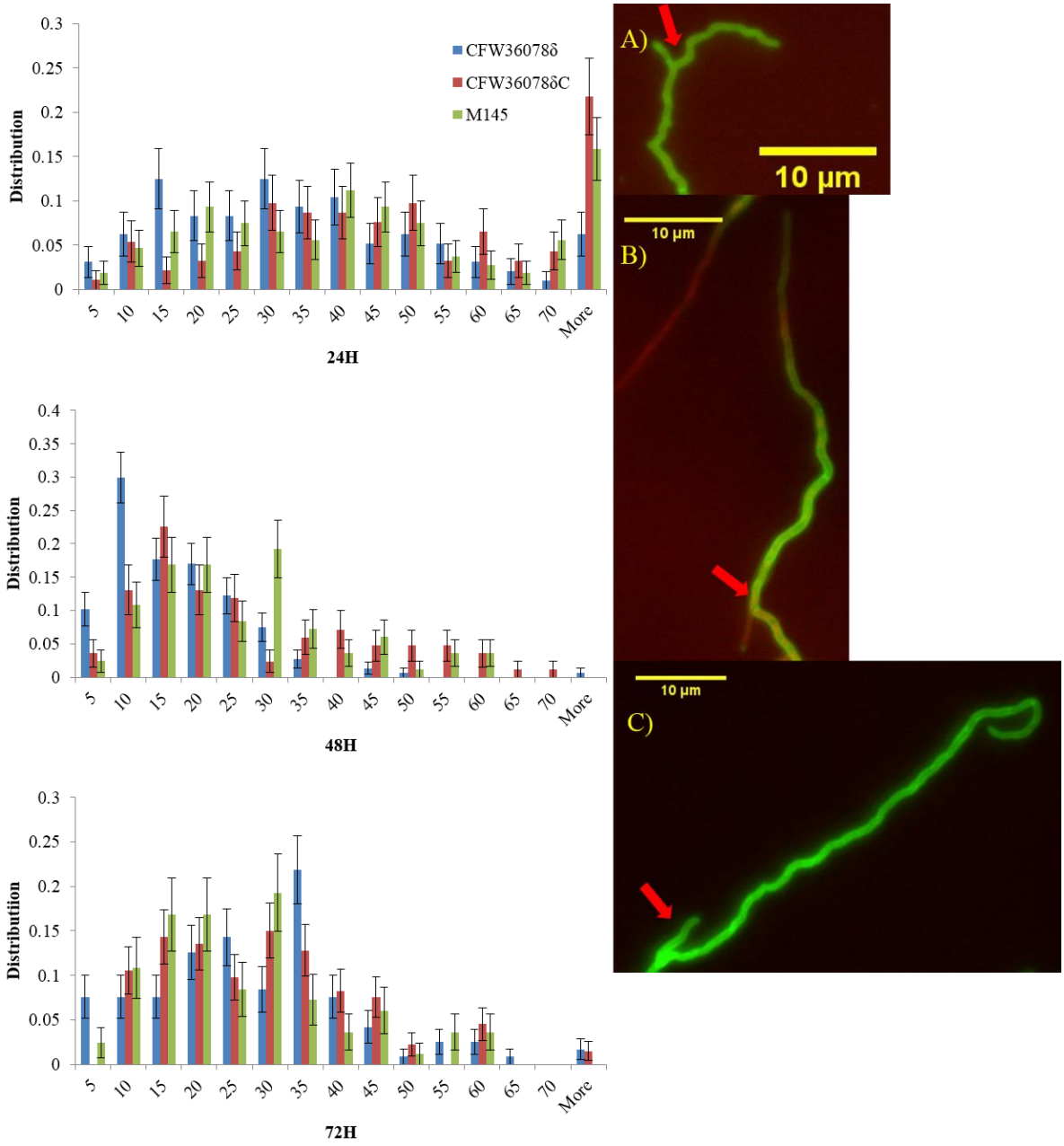

Fig5-19. Tip to branch distance for CFW36078δ, CFW36078δC, and M145. The information is displayed as a histogram in µm. The average distances were 32.63µm, 15.05µm, and 26.06µm for CFW36078δ, 47.02µm, 24.56µm, and 26.62µm for CFW36078δC, and 41.60µm, 28.37µm, and 23.86µm for M145, respective of the time-points. The sample sizes were 96 for CFW36078δ, 92 for CFW36078δC, and 109 for M145 after 24 hours, and 147 for CFW36078δ, 84 for CFW36078δC, and 88 for M145 after 48 hours, and were 119 for CFW36078δ, 133 for CFW36078δC, and 83 for M145 after 72 hours. The images show branch formation after 48 hours in A) CFW3608δ, B) CFW3608δC, and C) M145.

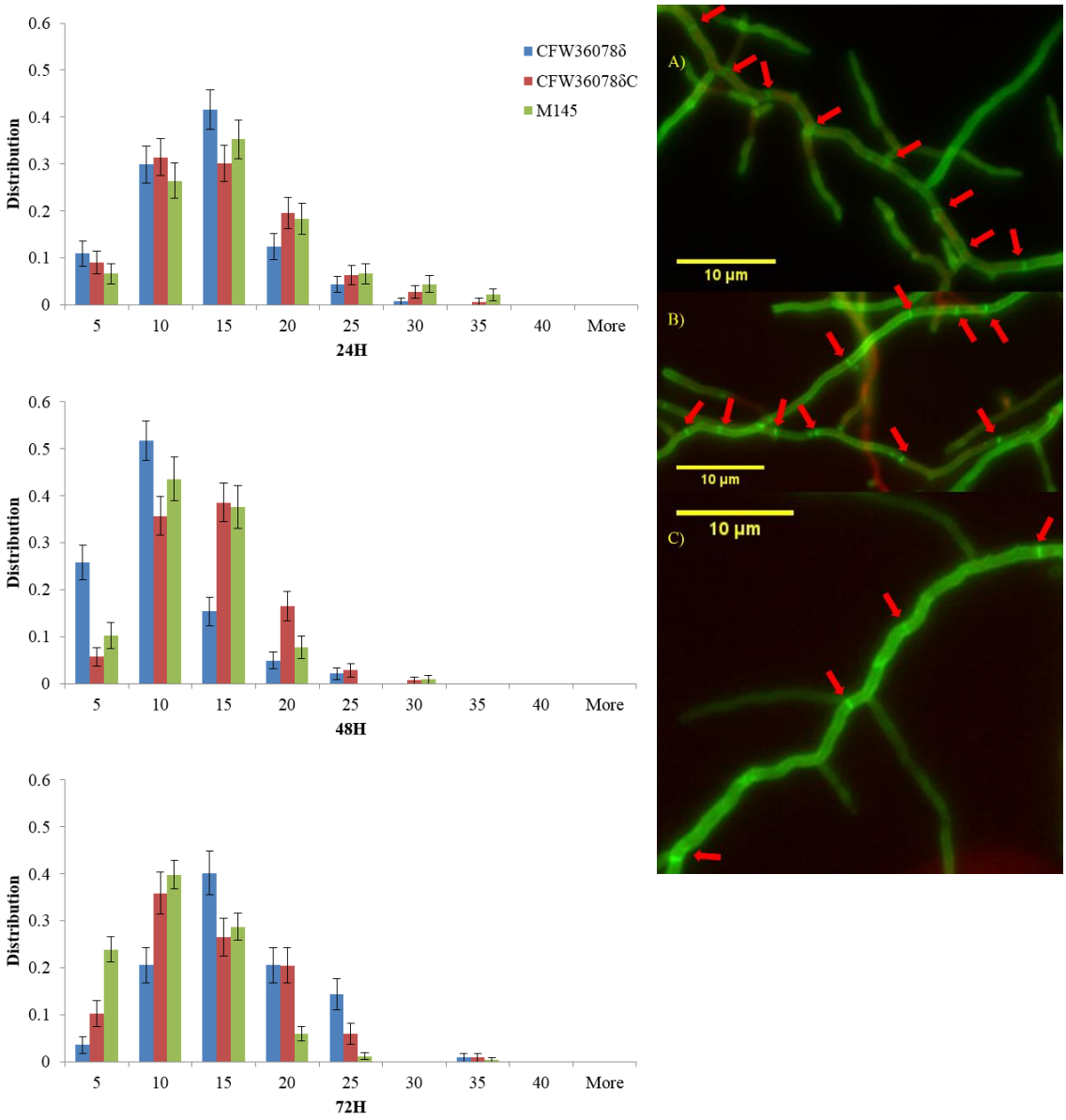

Fig5-20. Cross-wall to cross-wall distance for CFW36078δ, CFW36078δC, and M145. The information is displayed as a histogram in µm. The average distances were 11.08µm, 7.91µm, and 14.04µm for CFW36078δ, 12.15µm, 11.41µm, and 11.55µm for CFW36078δC, and 13.28µm, 9.55µm, and 8.61µm for M145, respective of the time-points. The sample sizes were 137 for CFW36078δ, 143 for CFW36078δC, and 136 for M145 after 24 hours, 143 for CFW36078δ, 149 for CFW36078δC, and 117 for M145 after 48 hours, 112 for CFW36078δ, 117 for CFW36078δC, and 251 for M145. The images show cross-wall formation after 48 hours in A) CFW3608δ, B) CFW3608δC, and C) M145.

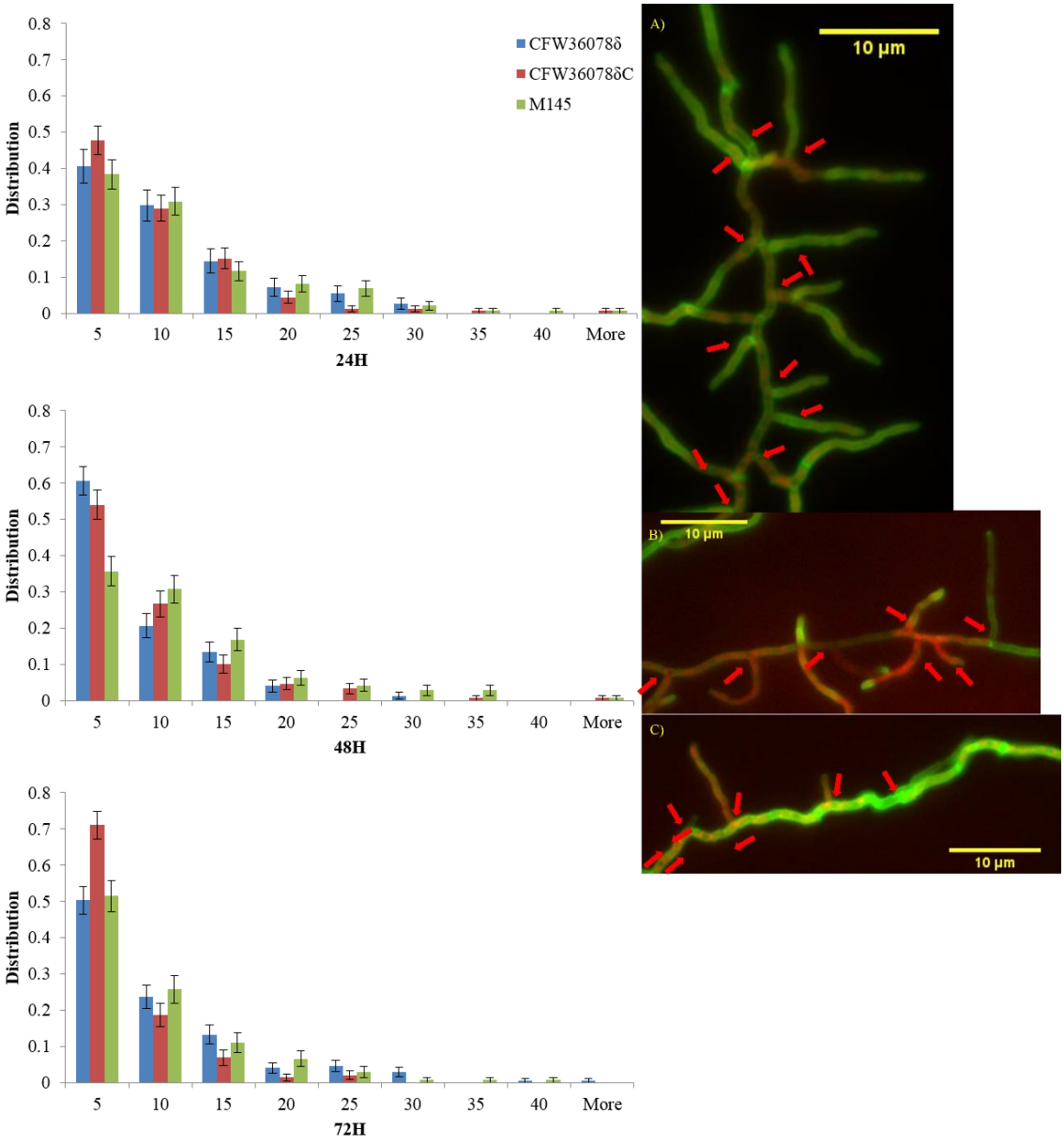

Fig5-21. Branch to branch distance for CFW36078δ, CFW36078δC, and M145. The information is displayed as a histogram in µm. The average distances were 7.98µm, 5.48µm, and 7.53µm for CFW3608δ, 7.13µm, 6.81µm, and 4.40µm for CFW3608δC, and 8.86µm, 9.37µm, and 7.01µm for M145, respective of the time-points. The sample sizes were 111 for CFW36078δ, 159 for CFW36078δC, and 146 for M145 after 24 hours, 136 for CFW3608δ, 150 for CFW36078δ, 150 for CFW36078δC, and 143 for M145 after 48 hours, and 173 for CFW36078δ, 145 for CFW36078δC, and 136 for M145 after 72 hours. The images show branch formation after 48 hours in A) CFW3608δ, B) CFW3608δC, and C) M145.

The distribution and average distance from the tip to the first cross-wall was much shorter for CFW36078δ after 24 hours, with complementation partially restoring the wild-type phenotype (see Fig5-18). When the distribution was examined, it became clear that wild-type had a wider distribution, whereas the cross-walls of CFW36078δ were mostly 11-30µm from the tip, whereas wild-type distance was distributed wider, with most being 11-55µm from the tip. The tip to cross-wall distance was also much shorter after 48 hours, with complementation increasing the tip to cross-wall distance beyond wild-type. CFW36078δ had a much narrower distribution, with almost 35% of its cross-walls 16-20µm from the tip, whereas M145 had less than 20% of its cross-walls from the tip. The distribution and average distance from the tip to the first cross-wall was slightly longer for CFW36078δ after 72 hours. When the distribution was examined, it became clear that it was due to a spike in cross-walls 6-10µm from the tip, but which was within the standard error. CFW36078δ still had a higher percentage of its tip to cross-wall distances from 21-25µm.

The tip to branch distance after 24 hours was much shorter for CFW36078δ compared to wild-type, with complementation failing to restore the mutant phenotype (see Fig5-19). When distribution was examined, it became obvious this was due to many a substantial number of branches more than 70µm away from the tip. Tip to branch distance is much shorter for CFW36078δ after 48 hours due to a much higher number of branches 6-10µm away from the tip, whereas wild-type had a much more even distribution of its tip to branch distance. Complementation restored wild-type phenotype after this time-point. After 72 hours, tip to branch distance was slightly longer for the mutant phenotype. Complementation did not restore wild-type phenotype.

Cross-wall to cross-wall distances were marginally shorter until 72 hours, where they were considerably longer (see Fig5-20). There percentage of cross-walls with up to 10µm between them is much lower for CFW36078δ, whereas this range represented the bulk of the wild-type distances. It is possible CFW36078δ is then failing to erect cross-walls. Complementation partially or fully restored wild-type phenotype at all time points. However, from the averages it would appear that the major difference after 72 hours arises from what could just be normal high and low values, as they are not dramatically different from measurements at other time-points.

Branch to branch distance is shorter for CFW36078δ after 48 hours due to a much higher number of branches between 6-10µm away from the tip, whereas wild-type had a much more

even distribution of its tip to branch distance (see Fig5-21). Complementation partially restored wild-type phenotype.

5.2.4. Spore size was enlarged in a strain lacking *SCO3607* and *SCO3608*

To further investigate potential morphological changes related to strains lacking the two genes, especially in lieu of what was observed in *B. subtilis* spores, spore analysis was performed to explore any similarities in phenotype (Donovan & Bramkamp, 2009). Statistical analysis of *S. coelicolor* M145, CFW3607A, CFW3607M, and CFW3607δ, CFW3608δ, CFW36078δ, in addition to their complemented strains, was performed on Schwedock-stained (see section 2.5) spores. The measurements and statistical analysis was average spore size (see Fig5-22 and Table 5-21), p-tests (Tables 5-22 through 24), and F-tests (Tables 5-25 through 27). The p-tests revealed there was a statistically significant increase in size for CFW36078δ when compared to wild-type ($1.50251E^{-5}$), with wild-type restored by complementation (0.1433). All the statistical data has been included in the appendix.

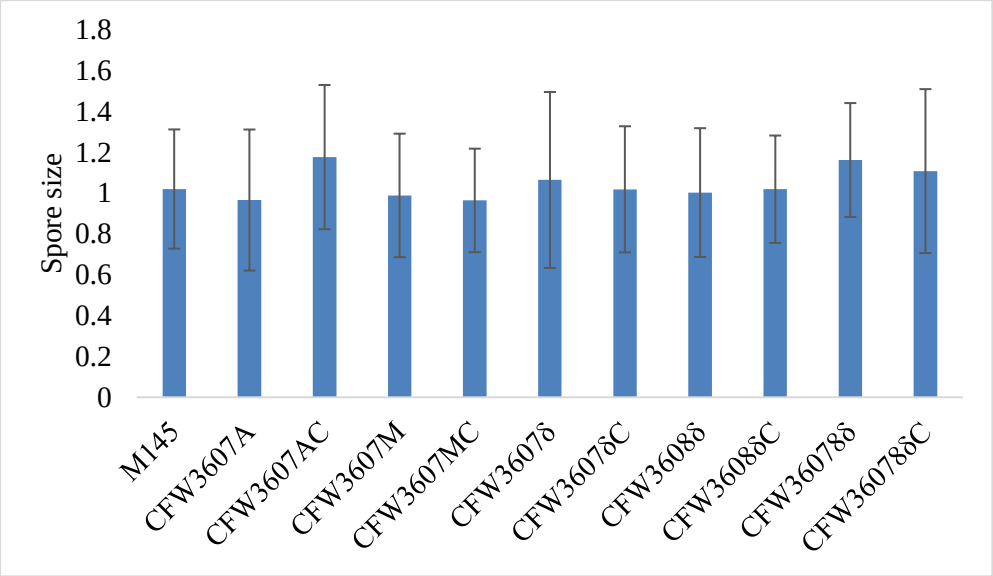

Fig5-22. CFW36078δ displayed enlarged spores. The information is displayed as a histogram, with spore size in µm. The samples sizes were 175 for M145, 233 for CFW3607A, 173 for CFW3607AC, 166 for CFW3607M, 181 for CFW3607MC, 187 for CFW3607δ, 181 for CFW3607δC, 145 for CFW3608δ, 141 for CFW3607δC, 154 for CFW36078δ, and 69 for CFW36078δC.

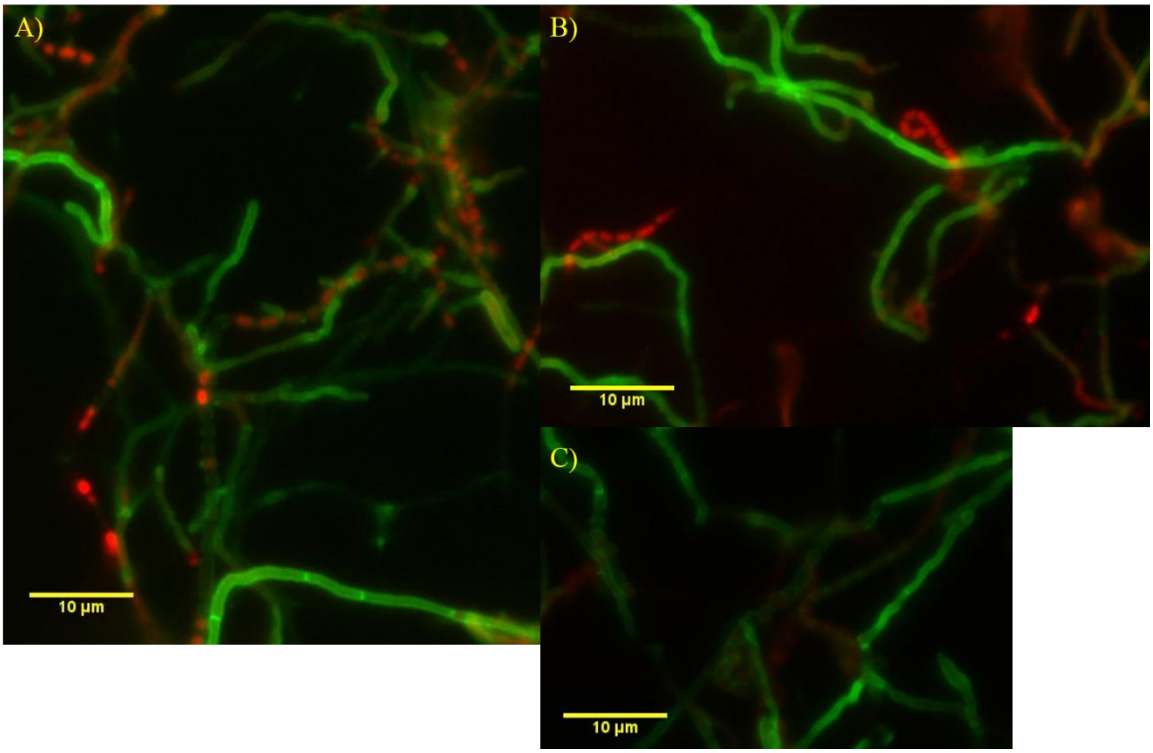

Fig 5-23. CFW36078δ displayed larger spores than wild-type. A) is M145, B) is CFW36078δ, C) is CFW36078δC.

The spore sizes were not affected by the lack of SCO3607 or SCO3608, but when both were knocked out, spore sizes were larger, with wild-type restored by complementation. Spore sizes were also larger for CFW3607AC. No other statistically significant measurements were observed.

5.3.1. Discussion

The average tip to cross-wall distance was similar for all strains lacking a functional *SCO3607*; it was consistently shorter after 24 hours, which lingered until for 48 hours for CFW3607A, though the average distance from tip to cross-wall was longer for CFW36078δ after 72 hours (see Fig5-2, Fig5-6, Fig5-10, and Fig5-18). However, the distribution of the distance from the tip to cross-wall is different and not just shorter; the wild-type distances are spread much more evenly than those of the mutant strains which clustered in spikes between 10µm and 40µm. Complementing the mutant strain partially restored the distance. That CFW3608δ was the least affected suggests a direct correlation between the absence of *SCO3607* and the formation of the vegetative cell walls nearer to the cell tip (see Fig5-14). A role for SCO3607, indirect or direct, would be similar to what was observed for the inefficient septum formation in *B. subtilis* (Donovan & Bramkamp, 2009).

Cross-wall formation may be preceded by the formation of large anionic phospholipid assemblies which cross the membrane. These large cross-membrane assemblies form in regions where DNA is absent, and 77% of them are impermeable, and thus partially compartmentalise the multicellular *S. coelicolor*, independent of cross-walls (Celler *et al.*, 2016). There may thus be a connection between the SCO3607 and SCO3608 and the formation of the septal membrane structures, which would fit with the punctate membrane localisation pattern of flotillin in *B. subtilis* (Donovan & Bramkamp, 2009).

There are a few oddities in the distribution of the distances as well, with the distribution of the distances from tip to branch more even in CFW36078δ when compared to the single *SCO3607* knockouts' spikes at 10-25µm. The tip to branch distance is much shorter for all mutant strains after 24 hours and 48 hours, but after 72 hours it is mostly within standard error of each other, bar the tip to branch distance for CFW3607A, which is longer than that of wild-type (see Fig5-2, Fig5-6, Fig5-10, and Fig5-18). This corroborates the results of the tip to cross-wall experiments, strongly suggesting the two proteins are involved in the hyphal growth.

The tip to branch and tip to cross-wall phenotypes occur mostly during the first 24 hours, though some effect lingers until 48 hours, suggesting *SCO3607* and *SCO3608* play a role in early vegetative hyphae polarity. The main cell polarity determinant of *S. coelicolor* is DivIVA, which forms part of the tip-organising complex (TIPOC), which also contains FilP and Scy (Ditkowski *et al.*, 2013, Celler *et al.*, 2016). If this cell polarity is in any way compromised,

by, for example, a destabilisation of TIPOC, this would lead to a weaker cell polarity, and thus the formation of cross-walls and branches closer to the tip.

If SCO3607 and SCO3608 indeed do interact or affect DivIVA, it may be involved in the localisation of DivIVA to negative curvature, potentially through lipid-protein interactions (Flardh, 2003a, Flardh, 2010). The obvious lipid to consider is CL, which localises to tip and branch points, both regions of negative curvature (Jyothikumar *et al.*, 2012). However, it is not likely, as no interaction between the flotillin or CL was demonstrated beyond colocalisation in *B. subtilis*, and correct localisation of flotillin occurred independently of CL (Donovan & Bramkamp, 2009). Other candidates include other anionic phospholipids, and DivIVA colocalises with large anionic lipid assemblies 27% of the time. However, this experiment used a general anionic lipid dye rather than targeting specific anionic lipids. These anionic lipid assemblies occurred both as septa and as blebs attached to the cell wall, a localisation pattern similar to DivIVA. It may be DivIVA, which is the earliest known protein to be recruited to the nascent branching sites, localises there in an anionic lipid-dependent manner, and this interaction is affected directly or indirectly by SCO3607 and SCO3608 (Hempel *et al.*, 2008). Two proteins have also been suggested to be involved: Scy and SsgA (Noens *et al.*, 2007, Holmes *et al.*, 2013). Alternatively, they may be affected by SCO3607 and SCO3608. If either SCO3607 or SCO3608 interacts with either of these proteins, or further unknown factors, it is possible this affects the stability or regulatory mechanisms preventing formation of branches and cross-walls forming compartments closer to the tip.

Previously, vegetative *S. coelicolor* M145 cross-wall to cross-wall were reported as forming 5-10µm apart, which was replicated in these experiments, with averages of 13.28µm, 8.61µm, and 9.55µm after 24, 48, and 72 hours, respectively (Celler *et al.*, 2016). Only CFW3607M and CFW36078δ showed any non-wild type phenotype, where the former displayed larger cross-wall compartments after 24 hours, though they were generally at least slightly larger at all time-points (see Fig5-4, Fig5-8, Fig5-12, Fig5-16, and Fig5-20). For CFW36078δ, the cross-wall to cross-wall distances showed no significant changes until 72 hours, when the compartments were substantially bigger. As the three strains which lacked only a fully-functional *SCO3607* did not have more distance between cross-walls than wild-type, it seems this phenotype was caused by a lack of *SCO3608*, and not *SCO3607*. That CFW3608δ did not display as prominent a phenotype as CFW36078δ, this suggests in combination with the time-points, that *SCO3608*, in combination with *SCO3607*, affects late stage vegetative

compartmentalisation of *S. coelicolor*. That the mutant phenotype of a double knockout would be more severe, and that the two proteins could be involved in cross-wall formation was stated in section 5.1.3.

Branch to branch distance was shorter for all strains lacking SCO3607, including the double knockout, at various time-points (see Fig5-5, Fig5-9, Fig5-13, and Fig5-21). Branch to branch distance is actually greater for CFW3608δ after 24 hours due to a few distances greater than 40µm away (see Fig5-17). The main reason behind the shorter branch to branch distances were peptidoglycan depositions in the lateral cell walls, rather than fully-formed branches. These appear to be either nascent branches or abortive branches, and were observed with some regularity. These were included as branches in the measurements, as it was impossible to discern between abortive or nascent branches. If SCO3607 inhibits DivIVA disassociation or affects the lipid membranes that may play a role in its recruitment, knocking it out allows for potentially stronger DivIVA foci, thus increasing the rate of branching.

A protein that has a different function in *S. coelicolor* when compared to *B. subtilis* is the actin homologue MreB. MreB recruits penicillin binding proteins (PBPs) to the lateral cell walls for inserting peptidoglycan (PG) into the cell wall during rapid cylindrical extension, and orchestrates chromosome segregation and cell polarity (Kawai *et al.*, 2009, Kruse & Gerdes, 2005). During sporulation, insertion of PG into the cell wall is done by Mbl, an MreB-like protein (Daniel & Errington, 2003). In contrast, peptidoglycan deposition and cell elongation takes place at the tip in an MreB-independent manner in *S. coelicolor* (Heichlinger *et al.*, 2011b). Peptidoglycan deposition, cell polarity, and determination of nascent branching sites in *S. coelicolor* instead seem to be orchestrated by DivIVA (Hempel *et al.*, 2008, Flardh, 2003a). DivIVA also supplants the role of MreB in mycobacteria and corynebacteria, so this is not restricted to streptomycetes (Letek *et al.*, 2008, Kang *et al.*, 2008). The MreB and FtsZ examples illustrate the difference in how cell division and life cycle occurs on a molecular level between *B. subtilis* and *S. coelicolor*, suggesting that even though both *S. coelicolor* and *B. subtilis* genomes encode conserved *floT* and *nfeD* genes, suggestion a conserved molecular function, their role in relation to the life cycle and cell division may be divergent.

When spore size was assayed, CFW36078δ, the double knock-out strain, displayed an enlarged phenotype (see Fig5-22, Fig5-23, and Table 5-21 and 5-24). *B. subtilis* spore size has not been assayed in previous experiments, but disporic cells were identified in a *B. subtilis* strain with a disrupted *yuaG* (Donovan & Bramkamp, 2009). No such phenotype was observed in this piece

of work. This phenotype is similar to what has been observed in *mre*-mutants, though the visible phenotype was much less severe when compared to the bloated spores of *mre*-mutants (Kleinschnitz *et al.*, 2011a). This does however suggest a minor role in sporulation and possible interactions with the products of the *mre*-cluster. Another difference between *mre*-mutants and the strains used in this body of work, is *mre*-mutants were sensitive to alkaline conditions (see Chapter 4). The larger spore sizes of the double knock-out are consistent with disruptions to cell polarity and peptidoglycan machinery seen with the increased cross-wall distances. Being the only strain to show a mutant phenotype is also consistent with it displaying the most deviant phenotype described earlier in this chapter (see Fig5-51 through 21).

It is worth bearing in mind that the increase was minor, and no other strong phenotype was observed. Additionally, it was within standard error (see Fig5-22). One of the complemented strains, CFW3607AC, also displayed a statistically significant size increase when measured against wild-type.

In summary, the goal was to observe what microscopical changes occurred in response to disruption and deletion of FloT and NfeD. The results showed a shortening of the distance from the tip to both branch and cross-wall, suggesting potentially a role in cell polarity strength during the vegetative stage of the life cycle of *S. coelicolor*, rather than what has been observed in *B. subtilis*, where FloT and NfeD played a role in sporulation (Donovan & Bramkamp, 2009).

There are several sources that may affect the statistical accuracy of the results, and they are thus worth mentioning. Shearing of cells during staining and preparing of slides may release proteins that degrade peptidoglycan and other cellular components, the dyeing may not be perfect or the image may be poor, thus resulting in missed branches or cross-walls compounded by human error.

5.3.2. Conclusion and future work

Based on the statistical evidence, cell polarity was affected by disruptions and deletions of *SCO3607* and *SCO3608*. This is in stark contrast to what was observed in *B. subtilis* (Donovan & Bramkamp, 2009). The *SCO3607* knock-out displayed shorter branch to branch distance, and strains with null mutants of *SCO3607* or containing a Tn*5062* disruption cassette displayed shorter tip to branch and tip to cross-wall distances. CFW36078δ and CFW3608δ both had longer distances between vegetative cross-walls.

While the results suggest activity of both proteins during the vegetative part of the growth cycle, this would benefit from investigating expression by qPCR or time-lapse microscopy. While mentioned in section 3.3.2., it is worth re-iterating that it would be beneficial to investigate any potential interactions with Scy, SsgB, DivIVA, and other associated TIPOC proteins. Fluorophore-tagged proteins would also be a fruitful endeavour in exploring localisation patterns and investigating whether DNA replicates closer to the cell pole. Experiments with zaragozic acid, which inhibits YisP, a squalene synthase, may also prove illuminating when combined with fluorophore-tagged SCO3607 or SCO3608, which may abolish localisation patterns, similar to what occurred in *B. subtilis* (Lopez & Kolter, 2010). Further investigating protein-lipid investigations with CL or other PLs is also an avenue that should be explored; specifically, FRET-FLIM (Alexeeva *et al.*, 2010, Buddelmeijer *et al.*, 1998).

With regards to spore assays, assaying for dead and empty spores, would be other logical assays to further pursue (Ladwig *et al.*, 2015). Investigating, potentially through BACTH experiments, the relationship between the *mre*-cluster and *SCO3607* and *SCO3608* is also a worthwhile endeavour in lieu of the observed phenotype.

6. Determination of SCO3607 and SCO3608 protein interactions

6.1.1. Introduction

Protein-protein interactions are physical interactions between two or more proteins. Many proteins assemble into complexes with other proteins or the same protein, forming hetero-oligomers or homo-oligomers, respectively. These can range in size from ribosomes of 2.5 mega daltons to the much smaller histone octamers, where the monomers range from 0.011400 to 0.015400 mega daltons (Bashan *et al.*, 2003, Luger, 2003). These can form through stable or transient reactions through covalent or non-covalent interactions (Jones & Thornton, 1996). Most multi-protein complexes are formed through non-covalent interactions, such as van der Waal's forces, ionic interactions, hydrophobic bonds, and hydrogen bonds (Westermarck *et al.*, 2013).

A minority do however form covalent bonds, and these can be through electron pairing and disulphide bonds (Kaiser *et al.*, 2011). An example of a covalent bond is ubiquitination of proteins, where one of seven lysine residues on ubiquitin binds to the protein being bound. Additionally, other ubiquitins can bind other ubiquitins, resulting in a chain of ubiquitin proteins attached to the original bound protein (Ciehanover *et al.*, 1978). Disulphide bonds are generally between cysteine residues, and the proteins containing internal sulphide bridges are generally destined for the extracellular environment, due to the prevalence of cytosolic reducing agents which would interfere with the bond (Reardon-Robinson & Ton-That, 2015). While most of these disulphide bonds are within the same protein, such as an *E. coli* alkaline phosphatase, it is also used to cross-link proteins such as MotB and FlgI of the bacterial flagellar motor (Sone *et al.*, 1997, Hizukuri *et al.*, 2010).

SCO3607 and *SCO3608* were previously concluded to be non-essential genes (See Chapter 4). Investigating the nature of potential protein-protein interactions was the next step in elucidating their molecular mechanisms, which might be important in understanding their role in *S. coelicolor* and other bacteria, but also in shedding light on the role of flotillin in disease as it may yield information about binding mechanisms. As flotillin interact with the aforementioned proteins Src kinases, actin, N-methyl-D-aspartate receptors, vinexins, CAP/ponsin, ArgBP2, and other flotillins, it stands to reason it is likely to interact with other proteins in bacteria as well (Ogura *et al.*, 2014, Langhorst *et al.*, 2007, Swanwick *et al.*, 2009, Solis *et al.*, 2007,

Kimura *et al.*, 2001). The logical two proteins to investigate for interactions first are the flotillin of *S. coelicolor* and its corresponding NfeD.

Direct interactions between flotillin and NfeD were demonstrated in *P. horikoshii*, where NfeD, a serine protease, cleaved a flotillin in the C-terminal hydrophobic region (Yokoyama & Matsui, 2005). As previously mentioned, flotillins consist of an N-terminal membrane-associated domain, a central SPFH domain, and a flotillin domain (Dempwolff *et al.*, 2012). Bacterial proteins containing the SPFH domain, such as flotillin and stomatins, form various oligomers; dimers, trimers, tetramers and multimers, even though it lacks the normal coiled-coils required for oligomerisation (Kuwahara *et al.*, 2009).

To elucidate the nature of the relationship between flotillin and NfeD in *S. coelicolor*, bacterial two-hybrid (BACTH) experiments were performed. This would yield information about whether they do interact, and potentially which parts of the proteins that mediate the interaction.

In essence, BACTH experiments bring together two parts of the catalytic domain of CyaA, T18 and T25. Each catalytic domain is translationally fused to one of the proteins being investigated, and produce cAMP when brought together (Goyard *et al.*, 1993, Karimova *et al.*, 1998). cAMP binds to catabolite activator protein (CAP), and the cAMP/CAP complex switches on expression of several genes, with the genes of interest being *mal* and *lac*, allowing the bacteria to grow utilise maltose and lactose, respectively, as a carbon source (Karimova *et al.*, 2000). Selective media can then be used to determine whether maltose or lactose is being used, thus determining whether the two catalytic domains are brought into proximity of each other by the protein(s) being tested.

One of the main virulence factors of *B. pertussis*, the causative agent of whooping coughs, is a secreted calmodulin-activated adenylate cyclase toxin (CyaA) (Weiss & Hewlett, 1986). CyaA is a 1706 amino-acid long protein with both adenylate cyclase activity, in the N-terminal 400 amino acids, and weak haemolytic activity in the C-terminal 1307 amino acids, due to its ability to form cation-selective channels in membranes (Goyard *et al.*, 1993, Glaser *et al.*, 1988a). The adenylate cyclase activity of CyaA is switched on by calmodulin, a eukaryotic protein, but it still remains active at a low level even without calmodulin (Glaser *et al.*, 1988b). The two fragments of the adenylate cyclase domain, T18 (residue 225-399) and T25 (reside 1-224), can together produce cAMP in the presence of the calmodulin *in vitro*, but not even residual cAMP

production takes place when the two fragments are expressed without calmodulin in *E. coli* (Ladant *et al.*, 1992, Ladant *et al.*, 1989, Karimova *et al.*, 1998). However, if they are fused to proteins that interact, the chimeric protein interaction allows the two fragments to interact and produce cAMP and the cells will display a Cya^+ phenotype. Furthermore, the strain used for BACTH experiments, *E. coli* BTH101, is *cya*-deficient (Karimova *et al.*, 1998).

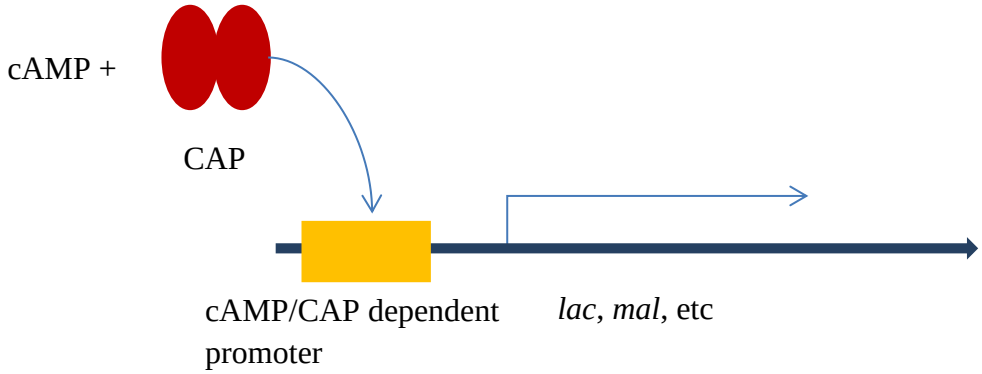

Fig 6-1. cAMP dependent gene expression. The diagram shows cAMP binding to CAP, which activates transcription of the *lac* and *mal* genes (Xiong *et al.*, 1991).

In *E. coli*, cAMP is a signalling molecule that binds to dimeric CAP, which regulates carbon utilisation through expression of genes encoding carbon utilisation enzymes, such as *lac* and *mal*, which are required for utilisation of lactose and maltose as a carbon source, respectively (Xiong *et al.*, 1991). cAMP increases the DNA affinity of CAP, which then binds to major grooves on the DNA, which opens up the DNA and activates transcription of the *lac* genes (Busby & Ebright, 1999, Schultz *et al.*, 1991). β-galactosidase is encoded on *lacZ*, which is able to cleave X-gal and utilise other carbon sources as well. X-gal consists of linked indole and galactose, and when cleaved by β-galactosidase produces a blue indole ester pigment (Kiernan, 2007). Thus, β-galactosidase activity can be used to assay qualitatively whether two proteins associate. Isopropyl-β-D-thiogalactopyranoside (IPTG) can be added to further increase expression of β-galactosidase, thus an optimal agar to assay for protein interaction contains both X-gal and IPTG (Horwitz *et al.*, 1964). MacConkey agar can also be used, but will turn the colonies red instead (Karimova *et al.*, 1998).

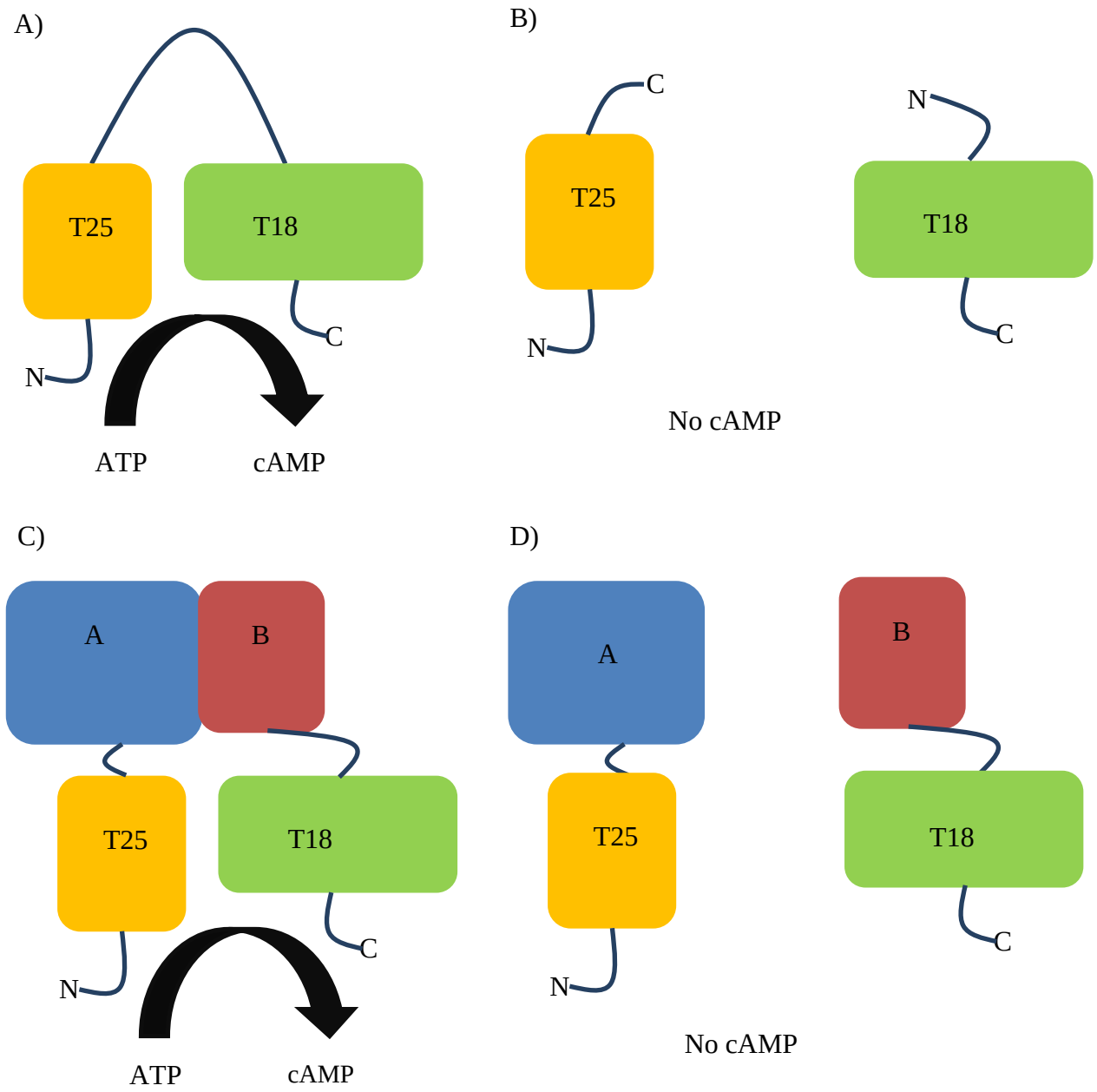

Fig 6-2. cAMP generation using the bacterial two-hybrid system. A) shows how the adenylate cyclase domain of CyaA converts ATP to cAMP. B) shows when the two fragments are not associated with each other no cAMP is produced. C) shows how the two fragments associate with each other when fused to two interacting proteins. D) shows how no cAMP is made when the two proteins the fragments are fused to do not interact.

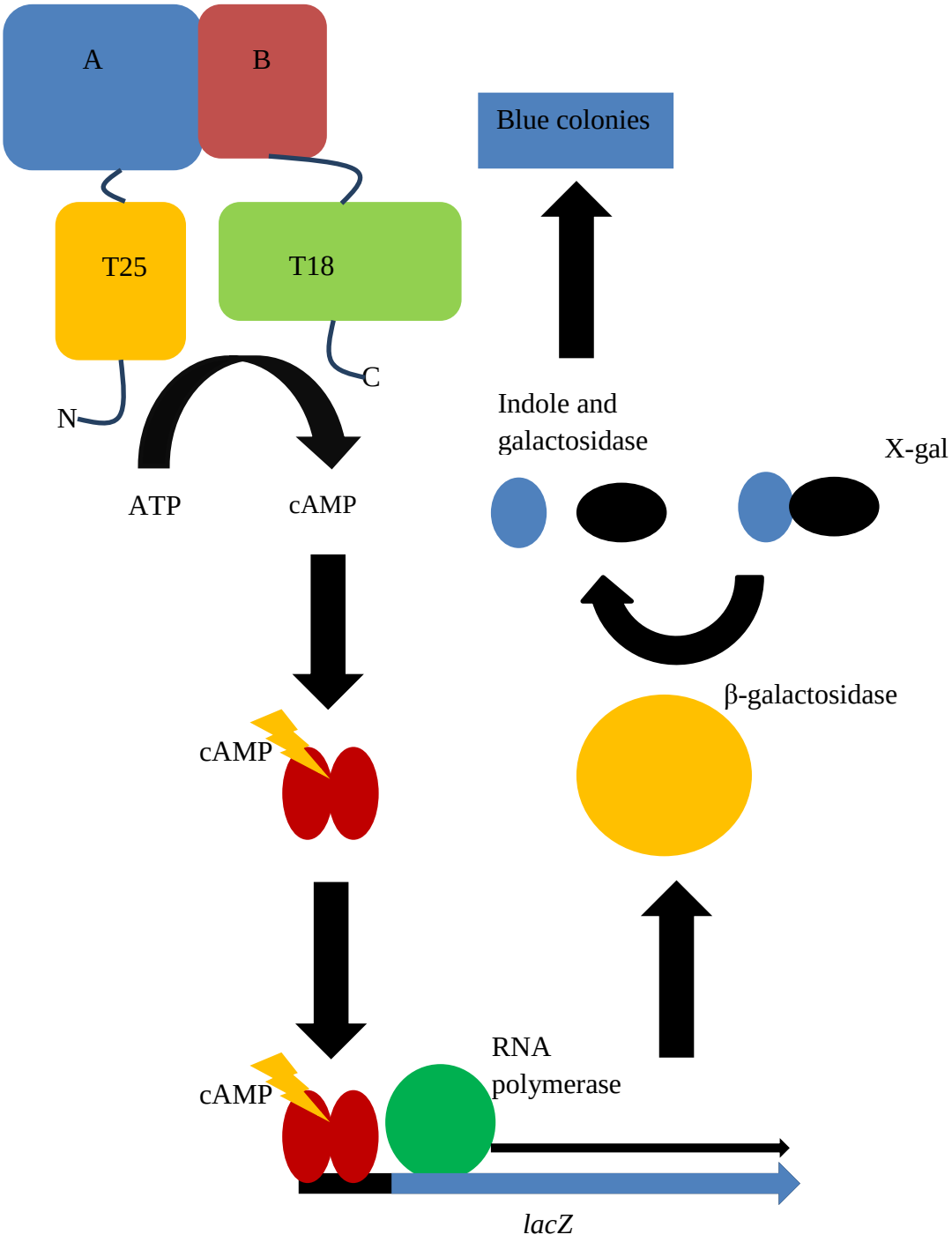

Fig 6-3. Full diagram of active BATCH experiment. The two CyaA cAMP catalytic domains are brought together by the associating proteins, producing cAMP. cAMP allows RNA polymerase to bind to *lacZ* and transcribe the gene, which leads to the synthesis of β-galactosidase. The substrate of this enzyme, X-gal, is then cleaved into indole and galactose. Indole is a blue pigment and turns the colony blue (Kiernan, 2007).

The bacterial two-hybrid system is however not perfect for showing the interaction between two proteins; the CyaA fragments may interfere with the binding, potentially abolishing any binding, though this does offer information about the method interaction itself.

In *S. coelicolor*, BACTH experiments have been used to elucidate the binding partners of several proteins. BACTH experiments were used to investigate the relationship between BldG and SCO3548, which interact with each other in addition to self-interaction (Parashar *et al.*, 2009). RodZ and MreB also interact when subject to BACTH experiments, and the same experiment showed that RodZ did not interact with the other MreB-like proteins of *S. coelicolor*; Mbl and SCO6166 (Heichlinger *et al.*, 2011b). BACTH experiments were also used to elucidate whether Scy interacted with FilP, ParA, and DivIVA (Holmes *et al.*, 2013). As a full-length Scy did not bind ParA, a truncated Scy was used. This truncated protein bound ParA, which was dependent on a coiled-coil domain. SCO3607 is genetically similar to Scy and the eukaryotic flotillins contain a C-terminal coiled-coil domain required for oligomerisation, suggesting that may be the region required for protein interactions in SCO3607 (Ditkowski *et al.*, 2013, Liu *et al.*, 2005, Rivera-Milla *et al.*, 2006).

6.1.2. Aims and goals

SCO3607 is the flotillin homologue of *S. coelicolor* and SCO3608 is the NfeD homologue. Their genomic adjacency and close proximity suggest they are in the same operon.

This is consistent with previous literature, suggesting at least an indirect interaction between the two proteins, and interactions occur in *P. hyrokoshii* (Green *et al.*, 2009, Yokoyama & Matsui, 2005). A more recent paper showed FloT was responsible for NfeD recruitment to focal assemblies in *B. subtilis* (Dempwolff *et al.*, 2012). Additionally, flotillin-flotillin interactions have been shown in humans, and due to the high degree of similarity between eukaryotic and prokaryotic flotillins, this potential interaction was also investigated (Babuke *et al.*, 2009).

The aims of the chapter is then:

1) To qualitatively investigate whether the *SCO3607* and *SCO3608* products interact with the other proteins.
2) To, dependent on the interactions, obtain information pertaining to the binding domains of the proteins in question.

6.2. Results

6.2.1. Cloning of *SCO3607* and *SCO3608*

To investigate the nature of the relationship between SCO3607 and SCO3608, elucidating whether they bind each other or self-interact, cloning the two genes into the pUT18, pUT18c, pKT25, and pKNT was done, bar cloning *SCO3608* into pUT18 and pKNT25. *SCO3607* and *SCO3608* were amplified using primers taking into account frameshift mutations and the addition of XbaI and KpnI restriction sites using StH66.C09 as a template (See Fig4.8), generating pCFW106 and pCFW108. Using the XbaI and KpnI restriction sites, these two genes were then subcloned into pUT18, pUT18c, pKT25, and pKNT25, bar SCO3608 into pUT18 and pKNT25. These two combinations were attempted several times, but it was not possible to clone the combinations. These results are illustrated in a flowchart below (See Fig3-4). The plasmids were then confirmed by restriction enzyme digestion.

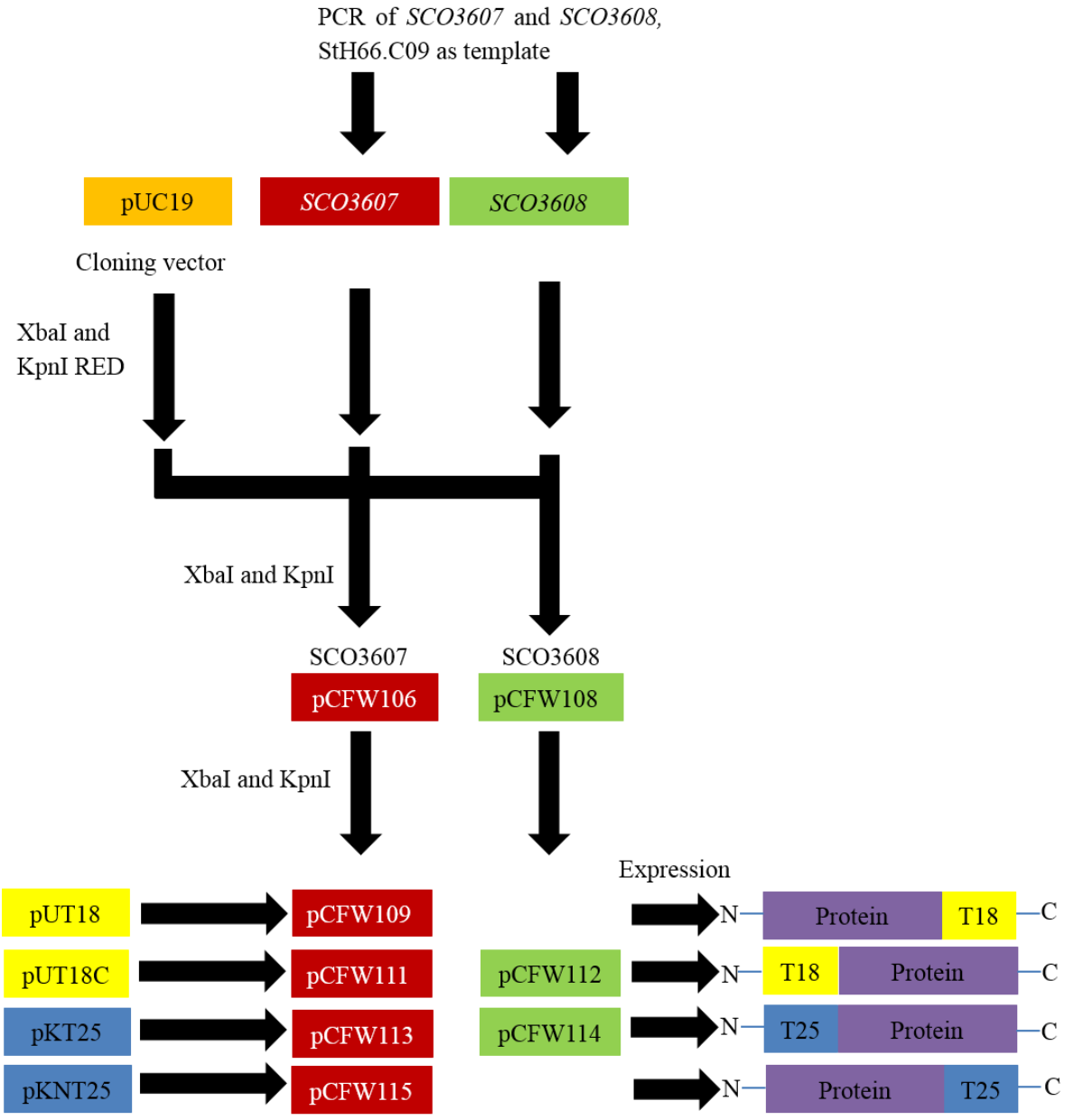

Fig 6-4. Flowchart representing BACTH generation cloning strategy. The cloning strategy was to amplify *SCO3607* and *SCO3608* from SH66.C09, digest the product and pUC19 with XbaI and KpnI, and ligated to create plasmids containing either gene. The genes were then then further subcloned into pKT25, pKNT25, pUT18, and pUT18c using KpnI and XbaI.

A)

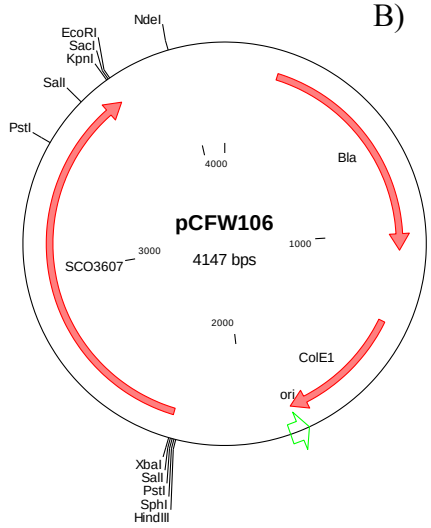

B)

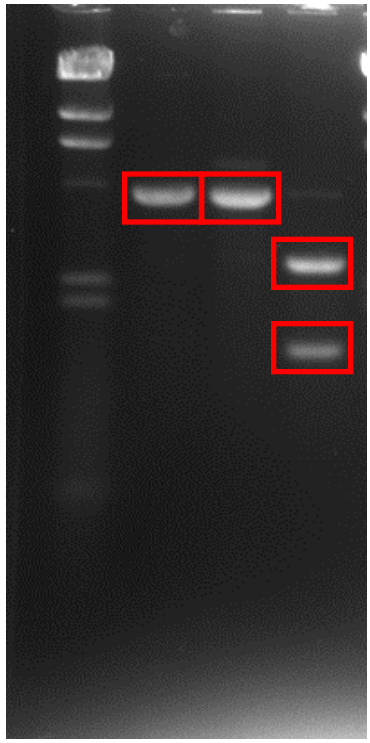

C)

Lane	Restriction enzymes	Size
1	XbaI	4147
2	KpnI	4147
3	XbaI + KpnI	1457, 2672

Fig 6-5. Confirmation of pCFW106. 1) pCFW106 plasmid was constructed by ligating XbaI and KpnI-flanked *SCO3607* fragment into pUC19. The clone contains a functional copy of *SCO3607*. B) Confirmation of the 1% agarose gel electrophorese image of pCFW106 digested with: XbaI, KpnI, and XbaI + KpnI, with a HindIII cut λ phage standard. C) is the key for the gel, and contains the different enzymes and expected fragment sizes.

A)

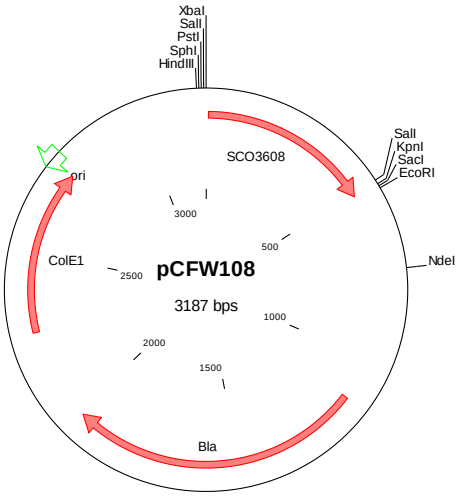

B)

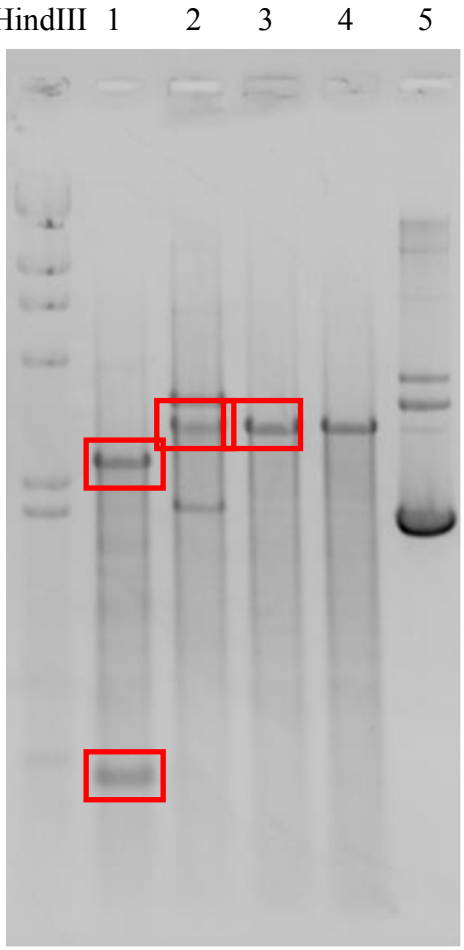

C)

Lane	Restriction enzymes	Size
1	SalI	2676, 511
2	EcoRI	3187
3	HindIII	3187
4	EcoRI + HindIII	2635, 552
5	Undigested	

Fig 6-6. Confirmation of pCFW108. A) pCFW108 plasmid was constructed by ligating XbaI and KpnI-flanked *SCO3608* fragment into pUC19. The clone contains a functional copy of *SCO3608*. B) Confirmation of the 1% agarose gel electrophorese image of pCFW108 digested with: SalI, EcoRI, HindIII, EcoRI + HindIII, and undigested with a HindIII cut λ phage standard. C) is the key for the gel, and contains the different enzymes and expected fragment sizes. Some residual DNA is visible.

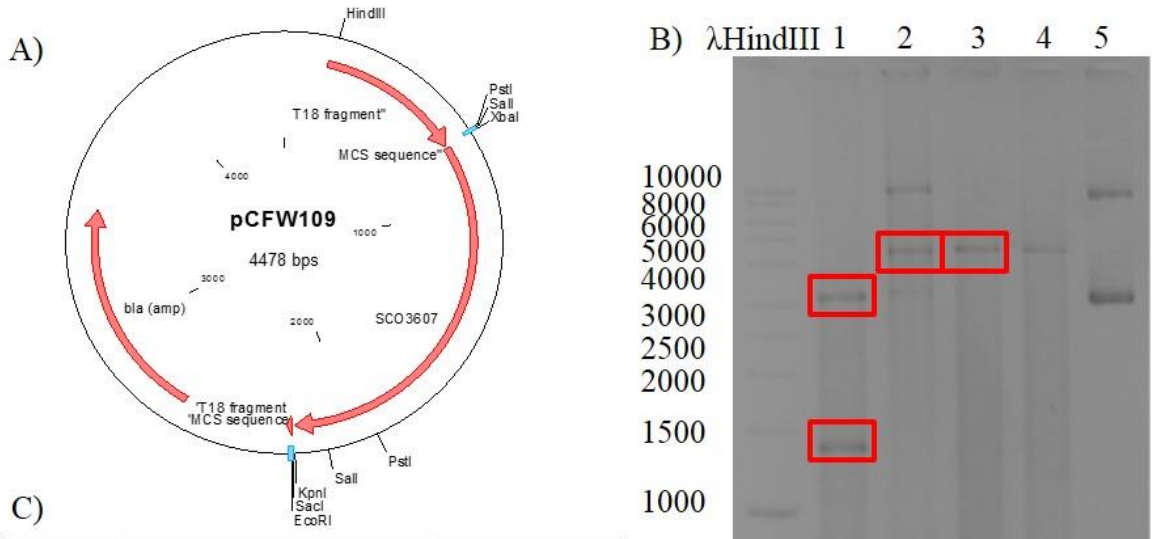

C)

Lane	Restriction enzymes	Size
1	SalI	3106, 1372
2	EcoRI	4478
3	HindIII	4478
4	EcoRI + HindIII	2444, 2034
5	Undigested	

Fig 6-7. Confirmation of pCFW109. A) pCFW109 plasmid was constructed by ligating XbaI and KpnI-flanked *SCO3607* from pCFW106 fragment into pUT18. The clone contains a functional copy of *SCO3607*. B) Confirmation of the 1% agarose gel electrophorese image of pCFW109 digested with: SalI, EcoRI, HindIII, EcoRI + HindIII, and undigested, with a 1000bp ladder. C) is the key for the gel, and contains the different enzymes and expected fragment sizes.

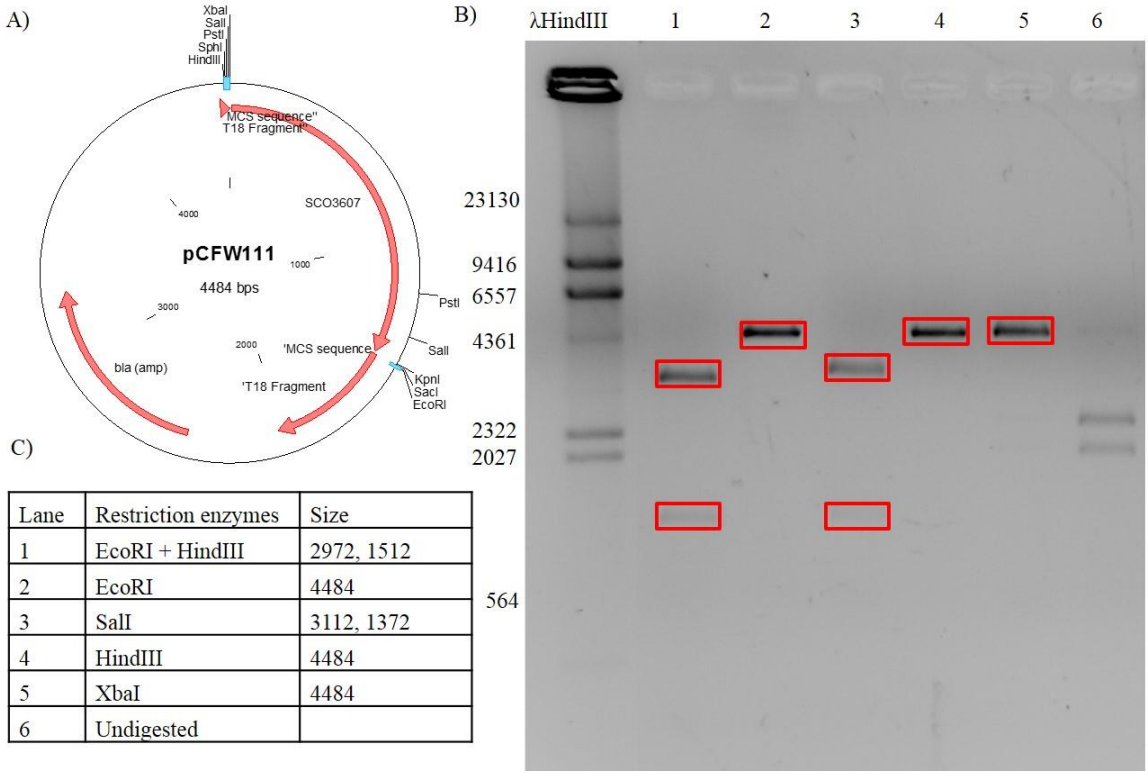

C)

Lane	Restriction enzymes	Size
1	EcoRI + HindIII	2972, 1512
2	EcoRI	4484
3	SalI	3112, 1372
4	HindIII	4484
5	XbaI	4484
6	Undigested	

Fig 6-8. Confirmation of pCFW111. A) pCFW111 map was constructed by ligating XbaI and KpnI-flanked *SCO3607* from pCFW106 fragment into pUT18c. The clone contains a functional copy of *SCO3607*. B) Confirmation of the 1% agarose gel electrophorese image of pCFW111 digested with: SalI, EcoRI, HindIII, EcoRI + HindIII, and undigested, with a HindIII cut λ phage standard. C) is the key for the gel, and contains the different enzymes and expected fragment sizes.

A)

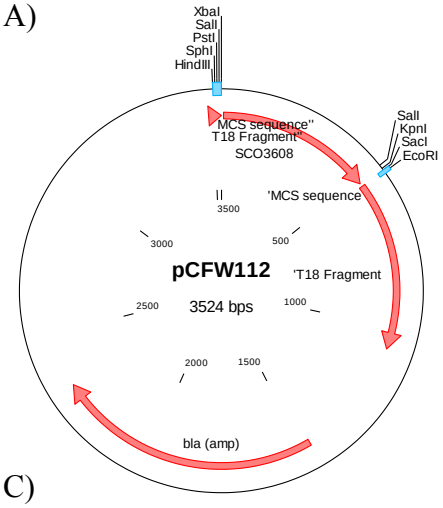

B)

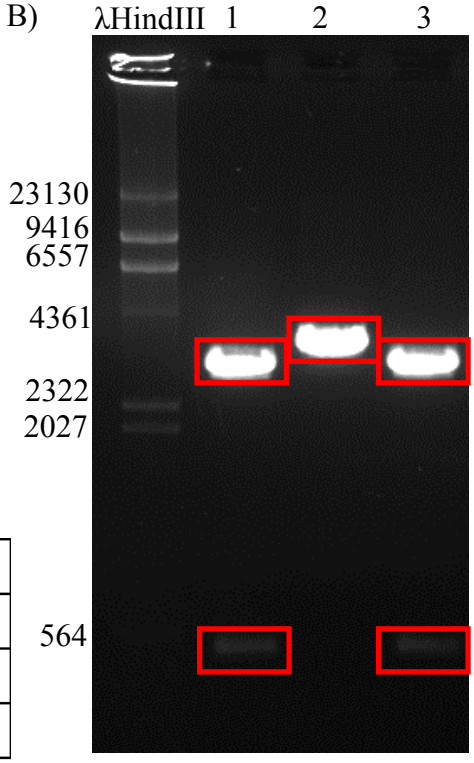

C)

Lane	Restriction enzymes	Size
1	SalI	3013, 511
2	XbaI	3524
3	SalI + XbaI	3013, 505, 6

Fig 6-9. Confirmation of pCFW112. A) pCFW112 plasmid was constructed by ligating XbaI and KpnI-flanked *SCO3608* from pCFW108 fragment into pUT18c. The clone contains a functional copy of *SCO3608*. B) Confirmation of the 1% agarose gel electrophorese image of pCFW112 digested with: SalI, XbaI, and SalI + XbaI, with a HindIII cut λ phage standard. C) is the key for the gel, and contains the different enzymes and expected fragment sizes.

A)

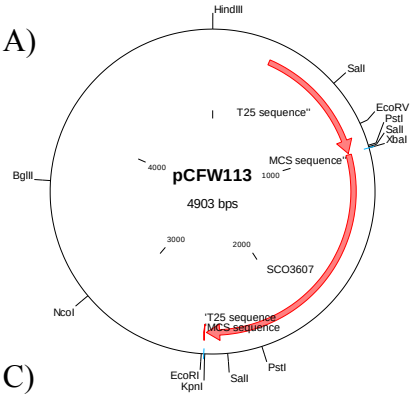

B)

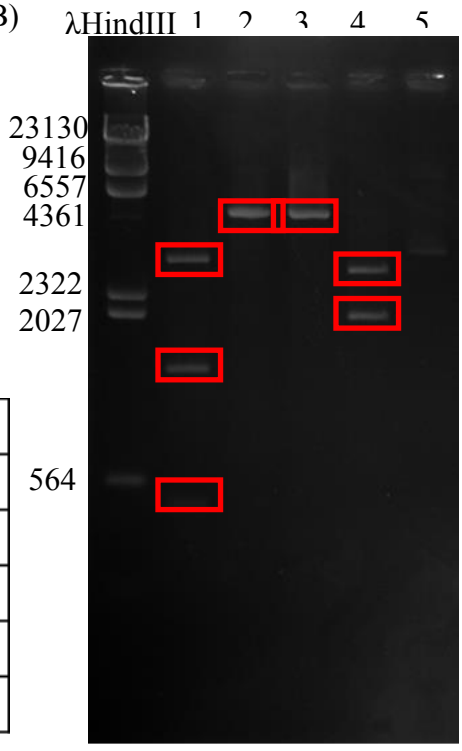

C)

Lane	Restriction enzymes	Size
1	SalI	3181, 1372, 350
2	NcoI	4903
3	XbaI	4903
4	NcoI + XbaI	2782, 2121
5	Undigested	

Fig 6-10. Confirmation of pCFW113. A) pCFW113 plasmid was constructed by ligating XbaI and KpnI-flanked *SCO3607* from pCFW106 fragment into pKT25. The clone contains a functional copy of *SCO3607*. B) Confirmation of the 1% agarose gel electrophorese image of pCFW113 digested with: SalI, XbaI, and SalI + XbaI, with a HindIII cut λ phage standard. C) is the key for the gel, and contains the different enzymes and expected fragment sizes.

A)

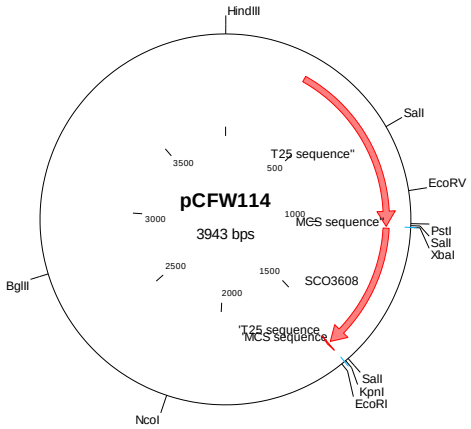

B)

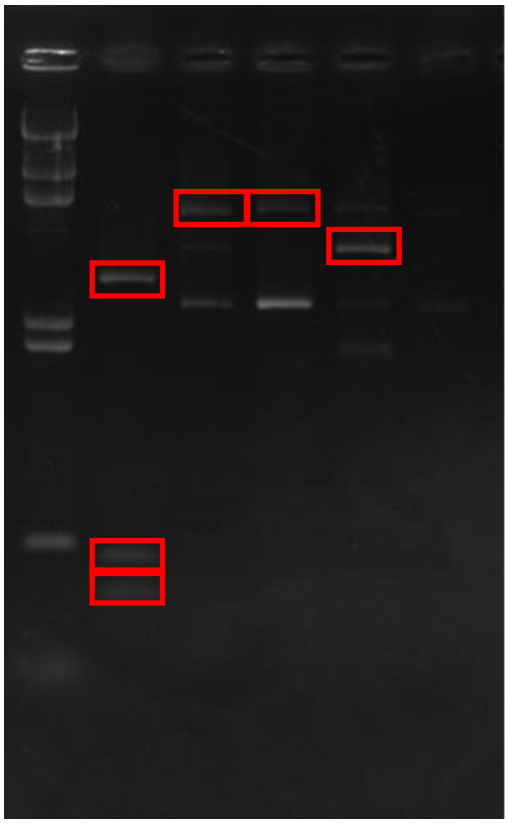

C)

Lane	Restriction enzymes	Size
1	SalI	3082, 511, 350
2	XbaI	3943
3	NcoI	3943
4	NcoI + XbaI	2782, 1161
5	Undigested	

Fig 6-11. Confirmation of pCFW114. A) pCFW114 plasmid was constructed by ligating XbaI and KpnI-flanked *SCO3608* from pCFW108 fragment into pKT25. The clone contains a functional copy of *SCO3608*. B) Confirmation of the 1% agarose gel electrophorese image of pCFW114 digested with: SalI, XbaI, NcoI, and NcoI + XbaI, with a HindIII cut λ phage standard. C) is the key for the gel, and contains the different enzymes and expected fragment sizes.

A)

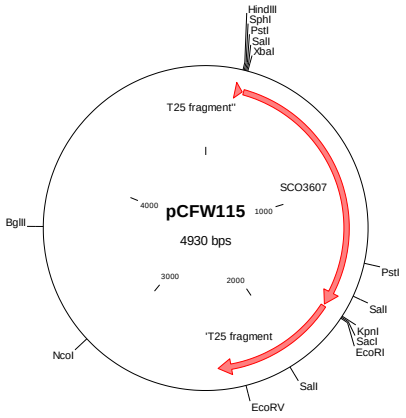

B)

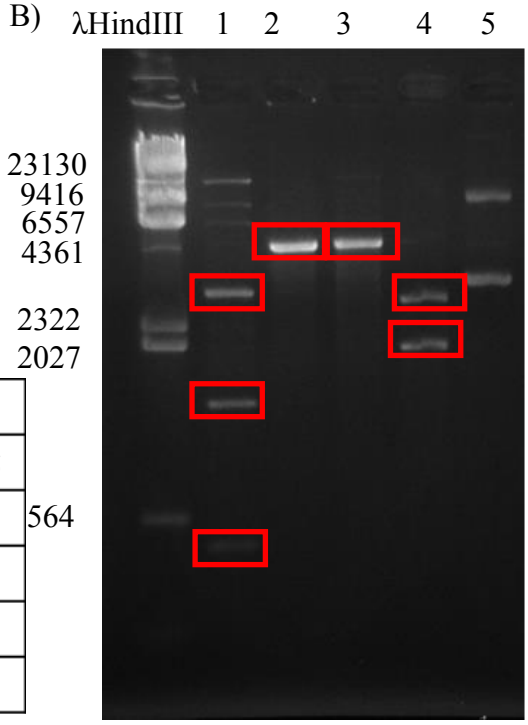

C)

Lane	Restriction enzymes	Size
1	SalI	3093, 1372, 465
2	NcoI	4930
3	XbaI	4930
4	NcoI + XbaI	2903, 2027
5	Undigested	

Fig 6-12. Confirmation of pCFW115. A) pCFW115 plasmid was constructed by ligating XbaI and KpnI-flanked *SCO3607* from pCFW108 fragment into pKNT25. The clone contains a functional copy of *SCO3607*. B) Confirmation of the 1% agarose gel electrophorese image of pCFW115 digested with: SalI, NcoI, XbaI, and NcoI + XbaI, with a HindIII cut λ phage standard. C) is the key for the gel, and contains the different enzymes and expected fragment sizes

6.2.2. Bacterial two hybrid experiments

The SCO3607 and SCO3608-containing plasmids were transformed into *E. coli* BTH101 with ampicillin and kanamycin selection (See Table 2-4). The following plasmid combinations were transformed into BTH101: pCFW109 and pCFW113, pCFW109 and pCFW114, pCFW109 and pCFW115, pCFW111 and pCFW113, pCFW111 and pCFW114, pCFW111 and pCFW115, pCFW112 and pCFW113, pCFW112 and pCFW114, pCFW112 and PCFW115, and the positive control plasmids pUT18-zip and pKNT25-zip. The two latter two plasmids encode T18 and T25 catalytic domains, respectively, translationally fused to a GCN4 leucine zipper which self-interacts (Karimova *et al.*, 1998). The different cultures were then plated onto an LB agar plate containing 0.5mM IPTG and 40µg/mL X-Gal, in addition to the aforementioned antibiotic selection, and incubated for 24 hours at 37^{o}C (for concentrations, see Table 2-4).

To elucidate whether SCO3607 and SCO3608 interacted with each other or self-interacted, the previously constructed plasmids were transformed into the same host. The *SCO3607* and *SCO3608*-containing plasmids were transformed into BTH101 and Cya activity was assayed for by plating the cultures onto IPTG and X-Gal containing LB agar plates. Two of the cultures containing only SCO3607-containing plasmids, pCFW109 + pCFW113 and pCFW109 + pCFW115, turned blue, showing the self-interaction. The products of pCFW115 and pCFW111 did not interact. The two latter plasmids have the adenylate cyclase subunits fused to the C-terminal of flotillin, suggesting this may be the binding site. That SCO3607 interacts with other SCO3607 proteins is unsurprising due to the human flotillins form tetramers, and the sequence similarity being so high between them and SCO3607 (Solis *et al.*, 2007). No interaction was observed in cultures with SCO3608-derived products, suggesting it does not interact with SCO3607 nor SCO3608. In conclusion, SCO3607 self-interacts, whereas SCO3608 does not (see Fig6-13).

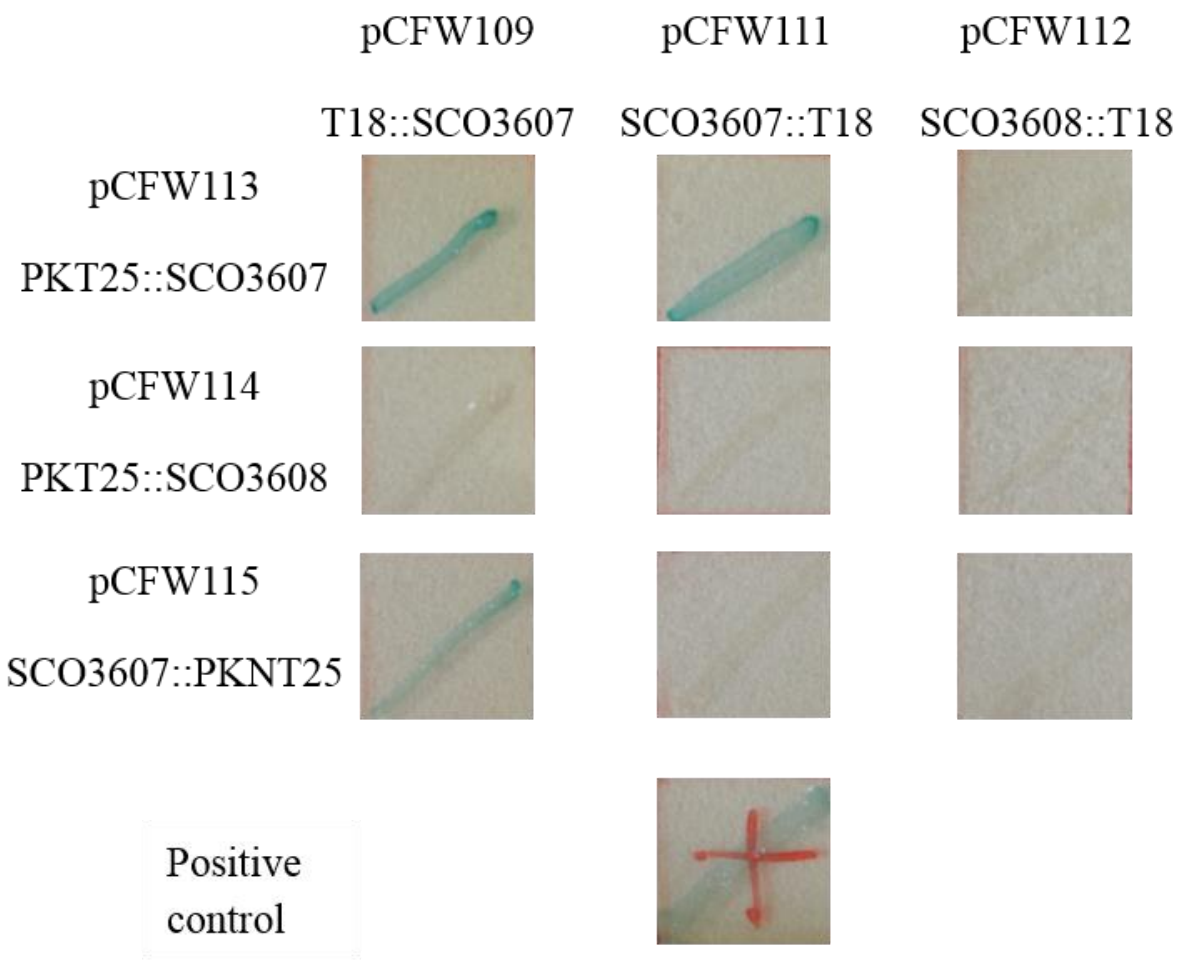

Fig 6-13. BACTH experiments demonstrate SCO3607-SCO3607 interactions. The *cyaA* T-18 domain containing plasmids (pCFW109, pCFW111, pCFW112) are horizontal across the top, while the *cyaA* T-25 domain containing plasmids (pCFW113, pCFW114, pCFW115) are vertical on the left. The positive control contains pUT18c-zip and pKNT-zip, which express T18 and T25 subunits. Blue colonies are strains where two proteins interact.

The BATCH experiment showed SCO3607-SCO3607 interactions, but it does not interact with SCO3608. However, when the adenylate cyclase domains were both fused to the C-terminus of SCO3607, interaction was abolished, suggesting this obscured the binding sites.

6.3.1. Discussion

The BACTH experiments demonstrated the self-interaction in SCO3607, though it did not interact with SCO3608, nor did SCO3608 display self-interaction (see Fig6-13). The self-interaction is not surprising, as the two human flotillins, flotillin-1 and flotillin-2, form homo- and heterotetramers (Solis *et al.*, 2007, Neumann-Giesen *et al.*, 2004). However, when both the T-18 and T-25 adenylate cyclase domains were fused to the C-terminal of SCO3607, interaction was abolished. A few possibilities are likely: either the binding of flotillin occurs at the C-terminal and the adenylate cyclase domains abolish the binding, or the binding occurs at the N-terminal and the two adenylate cyclase domains are too far apart to interact.

Oligomerisation is a common feature of SPFH family proteins, but the SPFH domain does not appear to be involved in oligomerisation, and it is the C-terminal flotillin domain that mediates the homo- and hetero-oligomerisation of the human flotillins. It is the second coiled-coil. and partially the first (residues 239-321 and 184-238, respectively, see Fig3.1), of flotillin-2 that mediates the tetramerisation of flotillin-1 and -2 in humans, and flotillin-2 is also required for the stabilisation of flotillin-1 in humans. Without the presence of flotillin-1, flotillin-2 undergoes proteosomal degradation in humans and *Drosophila melanogaster*, in addition to similar to what has been observed with other SPFH proteins, such as HflC/HlfK in *Saccharomyces cerevisia*e and prohibitins in humans (Solis *et al.*, 2007, Hoehne *et al.*, 2005, Berger & Yaffe, 1998, Nijtmans *et al.*, 2002). Of the two proteins, SCO3607 is overall most similar to flotillin-1, though this is marginal. The first coiled-coil is highly conserved throughout the organisms in Fig3-2, though the second coiled-coil is less conserved, with small stretches of the coiled-coil missing in the human flotillins compared to their bacterial counterparts. Thus, based on sequence similarity with known flotillins, it is likely binding takes place at the C-terminal and that SCO3607 tetramerises.

FloT has been shown to recruit NfeD in *B. subtilis*, but this experiment demonstrated no direct interaction between the two, suggesting flotillin-dependent recruitment of NfeD to focal assemblies in *B. subtilis* is indirect rather than the product of a direct interaction between the two proteins (Dempwolff *et al.*, 2012). However, in *P. horikoshii*, NfeD cleaved a stomatin, a protein closely related to flotillin (Yokoyama & Matsui, 2005). It is worth noting this NfeD is rather different, as it is a full-length NfeD as opposed to the truncated NfeD of *S. coelicolor* (See Fig3-6). This suggests there are other proteins involved, but what protein(s) or mechanism is unknown. One possibility is YuaI, an acyltransferase, which is in the *yuaFGI* operon in *B.*

subtilis, though there is no other gene in the *S. coelicolor* NfeD-flotillin operon, and the closest one genetically is *SCO6477*. However, *B. subtilis* appears to be the only organism with an acyltransferase in the same operon as flotillin. It is thus likely that the acyltransferase of *B. subtilis* does not play a role in the molecular role of flotillin and NfeD. There might also be additional proteins which are required for NfeD-flotillin or NfeD-NfeD interaction, which was touched upon with the acyltransferase YuaI being implicated, but that is not likely due to the aforementioned reasons. However, that many other proteins are likely to be involved due to the range of proteins eukaryotic flotillins interact with (Zhao *et al.*, 2011).

The Cya domains may obscure binding of NfeD, even though the translationally fused Cya domains were fused to either end of the protein. Alternatively, together they may obstruct interactions between NfeD and flotillin. It is worth noting that especially the T25 Cya domain is larger than the SCO3608. Furthermore, BACTH experiments occur in *E. coli*, so SCO3607 and SCO3608 are not in their native system, which could interfere with their molecular mechanism, creating false negatives. Special attention should be paid to the three different localisation patterns of flotillin in *B. subtilis*; helical, random, and dynamical foci (Lopez & Kolter, 2010, Donovan & Bramkamp, 2009). Correct localisation of flotillin is also required for NfeD recruitment to these foci, so it is possible that the differences in membrane from its native *S. coelicolor* interferes with this (Dempwolff *et al.*, 2012). This might be due to lipids causing a conformational change in the protein structure or be required for binding in some other way. The difference in phospholipid content could interfere with the localisation, as *S. coelicolor* contain six-fold more CL than *E. coli* (Raetz & Dowhan, 1990, Sandoval-Calderon *et al.*, 2009). This would be similar to cholesterol depletion abolishing Src-flotillin interaction (de Diesbach *et al.*, 2008). As there is a proposed link between bacterial lipid microdomains and flotillin this is not unlikely (Lopez & Kolter, 2010). Another potential reason for the lack of interaction is the different roles of proteins in *S. coelicolor*, such as the different role of MreB in S. coelicolor. This could be the same for NfeD and flotillin. This is somewhat unlikely due to the highly conserved nature of the flotillins.

6.3.2. Conclusion and further work

The results showed flotillin interacted with flotillin. Binding likely occurs at the C-terminal due to translationally fusing the larger CyaA cAMP domain abolished β-galactosidase activity. NfeD did not interact with NfeD, nor did it interact with flotillin. However, based on previous literature, it could be the non-native system disrupted the binding, as the membranes are very

different. Alternative methods of assaying protein-protein interactions, such as affinity mass spectrometry and co-immunoprecipitation.

The most obvious place to continue the experiments would be constructing the two omitted plasmids; pUT18c with *SCO3608* and pKNT25 with *SCO3608*. Further BACTH experiments to perform would include DivIVA, Scy, and ParA. The former is a heterogeneously distributed membrane protein which thus may be involved in bacterial lipid microdomains (Hempel *et al.*, 2008). Scy interacts with both DivIVA and ParA (Ditkowski *et al.*, 2013). MreB and Mbl, the bacterial actin homologues, and SCO6166, a similar protein missing the IB and IIB actin subdomains, are also potential interaction partners, as the human flotillins interact with F-actin through the SPFH domain (Langhorst *et al.*, 2007, Heichlinger *et al.*, 2011b). However, in *S. coelicolor*, these proteins have different roles than cell scaffolding; MreB and Mbl are used in sporulation, while SCO6166 is involved in the vegetative state, but is lacking several actin subdomains. Additionally, all three are non-essential proteins (Heichlinger *et al.*, 2011b).

S. aureus mutants lacking FloA, its flotillin homologue, had a less effective type vii secretion system (Mielich-Suss *et al.*, 2017). In *S. coelicolor*, the *esx*-locus encodes a type vii secretion system, which secretes EsxA and EsxB (Abdallah *et al.*, 2007). Forming heterodimers, EsxA and EsxB appear to play a role in cell division coordination. Mutant strains display pre-spore compartments of irregualar size with multiple nucleoids. This phenotype further deteriorates when combined with *smc*, *ftsK, parB* mutations (Akpe San Roman *et al.*, 2010). This makes them interesting for BACTH experiments, following the compartment irregularities observed in chapter 5.

There are also several Src kinases worth investigating in the *S. coelicolor* genome. Src kinases have previously been reported to phosphorylate mammalian flotillins, and are thus a potential interaction partner (Ogura *et al.*, 2014). There are no *S. coelicolor* homologues of N-methyl-D-aspartate receptors, vinexins, CAP/ponsin, or ArgBP2, so other proteins than their homologues should be investigated for interactions. Furthermore, FtsH has been shown to colocalise with FloT in *B. subtilis*, and a bacterial two-hybrid experiment with an equivalent protein would be of interest in *S. coelicolor* (Yepes *et al.*, 2012).

7. Discussion

The bioinformatics showed SCO3607 was a flotillin, while SCO3608 was a truncated NfeD. In a phylogenetic tree, SCO3607 was present in a wider cluster containing both human and *B. subtilis* flotillins, though the flotillins of *Streptomyces* formed a separate cluster of flotillins separate from those two within a larger cluster. SCO3607 was also highly conserved. SCO3608 was similar, though eukaryotic genomes do not encode *nfeD*s, and clustered predictably alongside the truncated NfeDs of *B. subtilis*. It was less conserved when compared to SCO3607; NfeDs tend to be less conserved and several mutations are known to occur, such as losing its N-terminal protease domain (Green *et al.*, 2009).

Performing research on flotillins, specifically protein-protein and protein-lipid interactions, in *B. subtilis* and extrapolating this to human research has previously been suggested (Mielich-Suss *et al.*, 2013). The reasoning behind lies within the intrinsic ease of working with bacteria compared to human cell lines, in addition to the similarities of the flotillins. The phylogenetic trees revealed the degree of similarity between human flotillin and SCO3607, and when taking the multicellularity of *S. coelicolor* into account, this is potentially a very good model for testing protein-protein and protein-lipid interactions in a better background.

Two separate ways of organising NfeDs have been proposed. One system was based on which *SPFH* was adjacent to the *nfeD* on the chromosome, while another organised into several groups based on truncation of the *nfeD* gene in question (see sections 1.2.6 and 3.4.1) (Green *et al.*, 2004, Hinderhofer *et al.*, 2009). In the former system, any flotillin-associated NfeD is given the designation NfeD2, irrespective of any potentially different genetic lineage. Notably, due to the high degree of horizontal gene transfer of the *SPFH-nfeD* operons and the several occasions upon which separate NfeD has lost its Clp-domain, exact phylogeny has been occluded. In the latter system, the NfeDs are grouped based on two types of NfeDs, NfeD1A, and NfeD1B, of which NfeD1B is split into truncated and full-length, and again split into 4 separate groups; NfeD1B-1 to -4. The groups previously characterised were based on whether they were found in Archae or Eubacteria, and whether they were upstream of *yqeZ* or downstream or upstream of an eoslipin (see section 1.2.6). The same papers had failed to identify any NfeDs within actinobacteria, so NfeDs within the actinobacteria are not assigned to any group, nor do they fit the previously organised groups (Green *et al.*, 2009, Green *et al.*, 2004). Furthermore, truncated NfeDs associated with flotillins had not been included, thus an

entirely new group is proposed; NfeD1b-5. This group would this include the entire flotillin-associated truncated NfeD1b lineage.

SCO3607 was disrupted using a Tn*5062* disruption cassete at two different sites on opposite strands, but neither mutant displayed a macroscopic phenotype. *SCO3607* and *SCO3608* were both deleted separately, in addition to a double knockout mutant being generated, of which none displayed a macroscopic phenotype. This was similar to what had been observed in previous experiments with *B. subtilis* (Dempwolff *et al.*, 2012, Donovan & Bramkamp, 2009, Bach & Bramkamp, 2013). No phenotype was observed in response to salt concentrations, which had previously induced *yuaG* and *yuaF* expression in B. subtilis. This difference strongly suggests a different role for flotillin and NfeD in *S. coelicolor* (Wiegert *et al.*, 2001).

Changes to branch and cross-wall formation in response to the deletion and disruption of SCO3607 and SCO3608 were investigated in the CFW3607A, CFW3607M, CFW3607δ, CFW3608δ, and CFW36078δ mutant strains. A Schwedock stain was performed after 24, 48, and 72 hours, and the distance from tip to cross-wall and branch, in addition to intra branch and cross-wall distances, were measured. In all strains, tip to cross-wall distances were shorter after 24 hours, though only moderately so for CFW3608δ, with shorter distances after 48 hours measured for CFW3607A, CFW3607M, and CFW3608δ. After 72 hours, the tip to cross-wall distances were longer for CFW3607δ, CFW3608δ, and CFW36078δ, but no difference observed for the other strains. Tip to branch distances were also shorter at both 24 and 48 hours for every strain, though after 72 hours it was longer for CFW3607A and CFW3608δ, but shorter for CFW3607δ. Cross-wall to cross-wall distances were also affected, with the distance slightly shorter for CFW3607A CFW3607δ, and CFW3608δ at both 24 and 48-hour time points. The average distance was longer for CFW3607M after 24 hours, but CFW3608δ it was slightly longer after 24 hours, but slightly shorter after 48 hours. For both CFW3608δ and CFW36078δ it was longer after 72 hours. Branch to branch distances were also affected, though not at all in CFW3607A. Branches formed slightly closer together in CFW3607M after 48 hours, but they formed consistently closer at all time points for CFW3607δ. For CFW3608δ they formed slightly further apart after 24 hours, closer after 48 hours, and no difference after 72 hours. For CFW36078δ, there only difference was after 48 hours, where they formed slightly closer.

From the microscopy, it became clear the genes played a role in cell polarity, as the strains formed branches and cross-walls closer to the tip after 24 hours, with only CFW3607δ and

CFW36078δ not forming cross-walls closer to the tip after 48 hours. Cross-wall to cross-wall distances were not affected to any large degree, though after 72 hours, cross-wall to cross-wall distances were shorter for CFW3607A and CFW3607δ, but longer for CFW3608δ and CFW36078δ. Essentially, strains without *SCO3608* suffered from larger compartments after 72 hours, including CFW36078δ, which lacked both *SCO3607* and *SCO3608*, while two of the strains lacking *SCO3607*, but not SCO3608, CFW3607A and CFW3607δ, had smaller compartments. The statistical significance was much stronger between larger compartments for CFW3608δ than for CFW36078δ, which reflected the lack of *SCO3607*. Furthermore, the statistical significance for CFW3607A, while there, was not very large, as opposed to CFW3607δ. While it is surprising there are differences within mutants lacking SCO3607, disruption and knockout variants have shown difference in B. subtilis.

Branch to branch distances were largely unaffected, but CFW3607δ formed branches much shorter apart. These were characterised by small peptidoglycan depositions in the cell wall, forming what appeared to be either nascent or aborted branches. This would further connect cell polarity with flotillin. It is possible that the lack of SCO3607 caused the peptidoglycan machinery to begin the synthesis of new cell wall material, but issues with cell polarity caused it to stop. It appears a lack of SCO3607 and SCO3608 results in morphological irregularities, possibly due to their on cell polarity, which would consistent with its role in *B. subtilis* (Ditkowski *et al.*, 2013, Donovan & Bramkamp, 2009). Alternatively, it may be involved with the EsX/type vii secretion system, as mutations to the *esxBA* operon resulted in irregular spore compartments and changes to the DNA content (Akpe San Roman *et al.*, 2010).

That most of the aberrant phenotypes occurred during the first 24 to 48 hours, which indicates the involvement of flotillin in the earlier stages of the life cycle, as opposed to *B. subtilis*, where flotillin was expressed during sporulation (Donovan & Bramkamp, 2009). This is altogether not entirely surprising due to their vastly different life cycles.

Another phenotype evident during fluorescence microscopy were the slightly enlarged spores of the double knock-out strain, CFW36078δ. While enlarged spores have previously been observed in *S. coelicolor* in reaction to mutations in the *mre*-cluster, the phenotype observed here was not as severe, nor was there any non-wild type macroscopic phenotype in reaction to alkaline growth conditions, which had strongly reduced the viability of the *mre*-mutants (Kleinschnitz *et al.*, 2011a).

BACTH experiments demonstrated SCO3607 interacting with SCO3607, which there is some circumstantial evidence for it to occur at the C-terminal based on the BACTH experiments. Neither NfeD-flotillin nor NfeD-NfeD interactions were evident based on the experiments performed. Further experiments, such as co-immunoprecipitation, are suggested to verify that the lack of interaction between NfeD and flotillin was not due to blocking of binding sites by the adenylate cyclate domains (see 3.2.2.). Further BACTH experiments do assay for any interactions with other proteins is also suitable; Scy, DivIVA, and ParA have all been translationally fused with the adenylate cyclase domains previously, and are thus possible candidates (Ditkowski *et al.*, 2013). MreB and Mbl, bacterial actin homologues, are also potential candidates, as human flotillin interacts with actin and mutations to the *mre*-cluster has previously been implicated in enlarged spores, which were observed during fluorescence microscopy (Langhorst *et al.*, 2007, Heichlinger *et al.*, 2011b, Kleinschnitz *et al.*, 2011a).

In conclusion, SCO3607 and SCO3608 appear to play a role in cell morphology and a minor role in spore formation. This work has begun to reveal its role, but more work is required before any definite conclusions can be drawn as to the mechanisms and potential partners, both lipid and protein, that the two proteins interact with.

8. References

Aaronson, L.R. & C.E. Martin, (1983) Temperature-induced modifications of glycosphingolipids in plasma membranes of *Neurospora crassa*. *Biochim Biophys Acta* **735**: 252-258.

Abachin, E., C. Poyart, E. Pellegrini, E. Milohanic, F. Fiedler, P. Berche & P. Trieu-Cuot, (2002) Formation of D-alanyl-lipoteichoic acid is required for adhesion and virulence of *Listeria monocytogenes*. *Mol Microbiol* **43**: 1-14.

Abanes-De Mello, A., Y.L. Sun, S. Aung & K. Pogliano, (2002) A cytoskeleton-like role for the bacterial cell wall during engulfment of the *Bacillus subtilis* forespore. *Genes Dev* **16**: 3253-3264.

Abdallah, A.M., N.C. Gey van Pittius, P.A. Champion, J. Cox, J. Luirink, C.M. Vandenbroucke-Grauls, B.J. Appelmelk & W. Bitter, (2007) Type VII secretion--mycobacteria show the way. *Nat Rev Microbiol* **5**: 883-891.

Abdallah, C., B. Valot, C. Guillier, A. Mounier, T. Balliau, M. Zivy, D. van Tuinen, J. Renaut, D. Wipf, E. Dumas-Gaudot & G. Recorbet, (2014) The membrane proteome of *Medicago truncatula* roots displays qualitative and quantitative changes in response to arbuscular mycorrhizal symbiosis. *J proteomics* **108**: 354-368.

Abhishek, A., A. Bavishi, A. Bavishi & M. Choudhary, (2011) Bacterial genome chimaerism and the origin of mitochondria. *Can J Microbiol* **57**: 49-61.

Adato, O., N. Ninyo, U. Gophna, S. Snir, (2015) Detecting Horizontal Gene Transfer between Closely Related Taxa. *PLoS Computational Biology*, **11**(10), e1004408.

Addinall, S.G. & J. Lutkenhaus, (1996) FtsZ-spirals and -arcs determine the shape of the invaginating septa in some mutants of *Escherichia coli*. *Mol Microbiol*. **22**: 231-237.

Agashe, V.R., S. Guha, H.C. Chang, P. Genevaux, M. Hayer-Hartl, M. Stemp, C. Georgopoulos, F.U. Hartl & J.M. Barral, (2004) Function of trigger factor and DnaK in multidomain protein folding: increase in yield at the expense of folding speed. *Cell* **117**: 199-209.

Akpe San Roman, S., P.D. Facey, L. Fernandez-Martinez, C. Rodriguez, C. Vallin, R. Del Sol & P. Dyson, (2010) A heterodimer of EsxA and EsxB is involved in sporulation and is secreted by a type VII secretion system in *Streptomyces coelicolor*. *Microbiology* **156**: 1719-1729.

Aktas, M. & F. Narberhaus, (2015) Unconventional membrane lipid biosynthesis in *Xanthomonas campestris*. *Environ Microbiol.*

Alami, M., I. Luke, S. Deitermann, G. Eisner, H.G. Koch, J. Brunner & M. Muller, (2003) Differential interactions between a twin-arginine signal peptide and its translocase in *Escherichia coli*. *Mol Cell* **12**: 937-946.

Alder, N.N. & S.M. Theg, (2003) Energetics of protein transport across biological membranes. a study of the thylakoid DeltapH-dependent/cpTat pathway. *Cell* **112**: 231-242.

Alexeeva, S., T.W. Gadella, Jr., J. Verheul, G.S. Verhoeven & T. den Blaauwen, (2010) Direct interactions of early and late assembling division proteins in *Escherichia coli* cells resolved by FRET. *Mol Microbiol* **77**: 384-398.

Altschul, S.F., W. Gish, W. Miller, E.W. Myers & D.J. Lipman, (1990) Basic local alignment search tool. *J Mol Biol* **215**: 403-410.

Amundsen, S.K., A.F. Taylor, A.M. Chaudhury & G.R. Smith, (1986) *recD*: the gene for an essential third subunit of exonuclease V. *PNAS* **83**: 5558-5562.

Anchisi, L., S. Dessi, A. Pani & A. Mandas, (2012) Cholesterol homeostasis: a key to prevent or slow down neurodegeneration. *Front Physiol* **3**: 486.

Andersson, S.G., A. Zomorodipour, J.O. Andersson, T. Sicheritz-Ponten, U.C. Alsmark, R.M. Podowski, A.K. Naslund, A.S. Eriksson, H.H. Winkler & C.G. Kurland, (1998) The genome sequence of *Rickettsia prowazekii* and the origin of mitochondria. *Nature* **396**: 133-140.

Angelini, R., P. Corral, P. Lopalco, A. Ventosa & A. Corcelli, (2012) Novel ether lipid cardiolipins in archaeal membranes of extreme haloalkaliphiles. *Biochim Biophysica Acta* **1818**: 1365-1373.

Arabidopsis Genome, I., (2000) Analysis of the genome sequence of the flowering plant *Arabidopsis thaliana*. *Nature* **408**: 796-815.

Arabolaza, A., M. D'Angelo, S. Comba & H. Gramajo, (2010) FasR, a novel class of transcriptional regulator, governs the activation of fatty acid biosynthesis genes in *Streptomyces coelicolor*. *Mol Microbiol* **78**: 47-63.

Arni, S., S.A. Keilbaugh, A.G. Ostermeyer & D.A. Brown, (1998) Association of GAP-43 with detergent-resistant membranes requires two palmitoylated cysteine residues. *J Biol Chem* **273**: 28478-28485.

Arora, A., H. Raghuraman & A. Chattopadhyay, (2004) Influence of cholesterol and ergosterol on membrane dynamics: a fluorescence approach. *Biochem Biophys Res Commun* **318**: 920-926.

Athenstaedt, K. & G. Daum, (1999) Phosphatidic acid, a key intermediate in lipid metabolism. *Eur J Biochem/ FEBS* **266**: 1-16.

Ayton, G.S., P.D. Blood & G.A. Voth, (2007) Membrane remodeling from N-BAR domain interactions: insights from multi-scale simulation. *Biophys* J **92**: 3595-3602.

Babuke, T., M. Ruonala, M. Meister, M. Amaddii, C. Genzler, A. Esposito & R. Tikkanen, (2009) Hetero-oligomerization of reggie-1/flotillin-2 and reggie-2/flotillin-1 is required for their endocytosis. *Cell Signal* **21**: 1287-1297.

Bach, J.N. & M. Bramkamp, (2013) Flotillins functionally organize the bacterial membrane. *Mol Microbiol* **88**: 1205-1217.

Baddiley, J., J.G. Buchanan, F.E. Hardy, R.O. Martin, U.L. Rajbhandary & A.R. Sanderson, (1961) The structure of the ribitol teichoic acid of *Staphylococcus aureus H. Biochim Biophysica Acta* **52**: 406-407.

Baddiley, J., J.G. Buchanan, U.L. Rajbhandary & A.R. Sanderson, (1962) Teichoic acid from the walls of *Staphylococcus aureus* H. Structure of the N-acetylglucosaminyl-ribitol residues. *Biochem J* **82**: 439-448.

Bagnat, M., S. Keranen, A. Shevchenko, A. Shevchenko & K. Simons, (2000) Lipid rafts function in biosynthetic delivery of proteins to the cell surface in yeast. *Proc Natl Acad Sci U.S.A.* **97**: 3254-3259.

Barak, I., K. Muchova, A.J. Wilkinson, P.J. O'Toole & N. Pavlendova, (2008) Lipid spirals in *Bacillus subtilis* and their role in cell division. *Mol Microbiology* **68**: 1315-1327.

Barak, I., P. Prepiak & F. Schmeisser, (1998) MinCD proteins control the septation process during sporulation of *Bacillus subtilis. J Bact* **180**: 5327-5333.

Bashan, A., R. Zarivach, F. Schluenzen, I. Agmon, J. Harms, T. Auerbach, D. Baram, R. Berisio, H. Bartels, H.A. Hansen, P. Fucini, D. Wilson, M. Peretz, M. Kessler & A. Yonath, (2003) Ribosomal crystallography: peptide bond formation and its inhibition. *Biopolymers* **70**: 19-41.

Baumann, C.A., V. Ribon, M. Kanzaki, D.C. Thurmond, S. Mora, S. Shigematsu, P.E. Bickel, J.E. Pessin & A.R. Saltiel, (2000) CAP defines a second signalling pathway required for insulin-stimulated glucose transport. *Nature* **407**: 202-207.

Becker, W.M., L.J. Kleinsmith & J. Hardin, (2006) The World of the Cell. Pearson Benjamin Cummings.

Bentley, S.D., K.F. Chater, A.M. Cerdeño-Tárraga, G.L. Challis, N.R. Thomson, K.D. James, D.E. Harris, M.A. Quail, H. Kieser, D. Harper, A. Bateman A, S. Brown, G. Chandra, C.W. Chen, M. Collins, A. Cronin, A. Fraser, A. Goble, J. Hidalgo, T. Hornsby, S. Howarth, C.H. Huang, T. Kieser, L. Larke, L. Murphy, K. Oliver, S. O'Neil, E. Rabbinowitsch, M.A. Rajandream, K. Rutherford, S. Rutter, K. Seeger, D. Saunders, S. Sharp, R. Squares R, S. Squares, K. Taylor, T. Warren, A. Wietzorrek, J. Woodward, B.G. Barrell, J. Parkhill, D.A. Hopwood, (2002) Complete Genome Sequence of the Model Actinomycete *Streptomyces coelicolor A3*(2). *Nature* **417**: 141-147.

Ben-Yehuda, S., D.Z. Rudner & R. Losick, (2003) RacA, a bacterial protein that anchors chromosomes to the cell poles. *Science* **299**: 532-536.

Bennett, J.A., R.M. Aimino & J.R. McCormick, (2007) *Streptomyces coelicolor* genes *ftsL* and *divIC* play a role in cell division but are dispensable for colony formation. *J Bacteriol* **189**: 8982-8992.

Berg, S., D. Kaur, M. Jackson & P.J. Brennan, (2007) The glycosyltransferases of Mycobacterium tuberculosis - roles in the synthesis of arabinogalactan, lipoarabinomannan, and other glycoconjugates. *Glycobiology* **17**: 35-56R.

Berger, K.H. & M.P. Yaffe, (1998) Prohibitin family members interact genetically with mitochondrial inheritance components in *Saccharomyces cerevisiae*. *Mol Cell Biol* **18**: 4043-4052.

Bergmann, S. & S. Hammerschmidt, (2006) Versatility of pneumococcal surface proteins. *Microbiology* 152: 295-303.

Berks, B.C., (1996) A common export pathway for proteins binding complex redox cofactors? *Mol Microbiol* **22**: 393-404.

Berks, B.C., F. Sargent, E. De Leeuw, A.P. Hinsley, N.R. Stanley, R.L. Jack, G. Buchanan & T. Palmer, (2000) A novel protein transport system involved in the biogenesis of bacterial electron transfer chains. *Biochim Biophysica Acta* **1459**: 325-330.

Bernal, P., J. Munoz-Rojas, A. Hurtado, J.L. Ramos & A. Segura, (2007) A *Pseudomonas putida* cardiolipin synthesis mutant exhibits increased sensitivity to drugs related to transport functionality. *Environ Microbiol* **9**: 1135-1145.

Bernhardt, T.G. & P.A. de Boer, (2003) The *Escherichia coli* amidase AmiC is a periplasmic septal ring component exported via the twin-arginine transport pathway. *Mol Microbiol* **48**: 1171-1182.

Bertsche, U., T. Kast, B. Wolf, C. Fraipont, M.E. Aarsman, K. Kannenberg, M. von Rechenberg, M. Nguyen-Disteche, T. den Blaauwen, J.V. Holtje & W. Vollmer, (2006) Interaction between two murein (peptidoglycan) synthases, PBP3 and PBP1B, in *Escherichia coli*. *Mol Microbiol* **61**: 675-690.

Bi, E. & J. Lutkenhaus, (1993) Cell division inhibitors SulA and MinCD prevent formation of the FtsZ ring. *J Bacteriol* **175**: 1118-1125.

Bibb, M.J., V. Molle & M.J. Buttner, (2000) sigma(BldN), an extracytoplasmic function RNA polymerase sigma factor required for aerial mycelium formation in *Streptomyces coelicolor* A3(2). *J Bacteriol* **182**: 4606-4616.

Bickel, P.E., P.E. Scherer, J.E. Schnitzer, P. Oh, M.P. Lisanti & H.F. Lodish, (1997) Flotillin and epidermal surface antigen define a new family of caveolae-associated integral membrane proteins. *J Biol Chem* **272**: 13793-13802.

Birnboim, H.C. & J. Doly, (1979) A rapid alkaline extraction procedure for screening recombinant plasmid DNA. *Nucleic Acids Res* **7**: 1513-1523.

Bishop, A., S. Fielding, P. Dyson & P. Herron, (2004) Systematic insertional mutagenesis of a streptomycete genome: a link between osmoadaptation and antibiotic production. *Genome Res* **14**: 893-900.

Bishop, R.E., H.S. Gibbons, T. Guina, M.S. Trent, S.I. Miller & C.R. Raetz, (2000) Transfer of palmitate from phospholipids to lipid A in outer membranes of Gram-negative bacteria. *EMBO J* **19**: 5071-5080.

Bishop, R.E., S.H. Kim & A. El Zoeiby, (2005) Role of lipid A palmitoylation in bacterial pathogenesis. *J Endotoxin Res* **11**: 174-180.

Blaudeck, N., P. Kreutzenbeck, M. Muller, G.A. Sprenger & R. Freudl, (2005) Isolation and characterization of bifunctional *Escherichia coli* TatA mutant proteins that allow efficient tat-dependent protein translocation in the absence of TatB. *J Biol Chem* **280**: 3426-3432.

Blaylock, B., X. Jiang, A. Rubio, C.P. Moran, Jr. & K. Pogliano, (2004) Zipper-like interaction between proteins in adjacent daughter cells mediates protein localization. *Genes Dev* 18: 2916-2928.

Block, R.C., E.R. Dorsey, C.A. Beck, J.T. Brenna & I. Shoulson, (2010) Altered cholesterol and fatty acid metabolism in Huntington disease. *J Clin Lipidol* **4**: 17-23.

Bochkareva, E., L. Kaustov, A. Ayed, G.S. Yi, Y. Lu, A. Pineda-Lucena, J.C. Liao, A.L. Okorokov, J. Milner, C.H. Arrowsmith & A. Bochkarev, (2005) Single-stranded DNA mimicry in the p53 transactivation domain interaction with replication protein A. *Proc Natl Acad Sci U.S.A.* **02**: 15412-15417.

Boonstra, M., I.G. de Jong, G. Scholefield, H. Murray, O.P. Kuipers & J.W. Veening, (2013) Spo0A regulates chromosome copy number during sporulation by directly binding to the origin of replication in *Bacillus subtilis*. *Mol microbiol* **87**: 925-938.

Borner, G.H., D.J. Sherrier, T. Weimar, L.V. Michaelson, N.D. Hawkins, A. Macaskill, J.A. Napier, M.H. Beale, K.S. Lilley & P. Dupree, (2005) Analysis of detergent-resistant membranes in *Arabidopsis*. Evidence for plasma membrane lipid rafts. *Plant Physiol* **137**: 104-116.

Borodina, I., P. Krabben & J. Nielsen, (2005) Genome-scale analysis of *Streptomyces coelicolor* A3(2) metabolism. *Genome Res* **15**: 820-829.

Botella, E., S.K. Devine, S. Hubner, L.I. Salzberg, R.T. Gale, E.D. Brown, H. Link, U. Sauer, J.D. Codee, D. Noone & K.M. Devine, (2014) PhoR autokinase activity is controlled by an intermediate in wall teichoic acid metabolism that is sensed by the intracellular PAS domain during the PhoPR-mediated phosphate limitation response of *Bacillus subtilis*. *Molecular Microbiol* **94**: 1242-1259.

Bottomley, A.L., A.F. Kabli, A.F. Hurd, R.D. Turner, J. Garcia-Lara & S.J. Foster, (2014) *Staphylococcus aureus* DivIB is a peptidoglycan-binding protein that is required for a morphological checkpoint in cell division. *Molecular Microbiol* **5**: 1041-1064.

Bouchek-Mechiche, K., L. Gardan, D. Andrivon & P. Normand, (2006) *Streptomyces turgidiscabies* and *Streptomyces reticuliscabiei*: one genomic species, two pathogenic groups. *Int J Syst Evol Microbiol* **56**: 2771-2776.

Bouchek-Mechiche, K., L. Gardan, P. Normand & B. Jouan, (2000) DNA relatedness among strains of *Streptomyces pathogenic* to potato in France: description of three new species, *S. europaeiscabiei sp. nov.* and *S. stelliscabiei sp. nov.* associated with common scab, and *S. reticuliscabiei sp. nov.* associated with netted scab. *Int J Syst Evol Microbiol* **50** Pt 1: 91-99.

Bourquin, F., H. Riezman, G. Capitani & M.G. Grutter, (2010) Structure and function of sphingosine-1-phosphate lyase, a key enzyme of sphingolipid metabolism. *Structure* **18**: 1054-1065.

Boylen, C.W. & J.C. Ensign, (1968) Ratio of teichoic acid and peptidoglycan in cell walls of *Bacillus subtilis* following spire germination and during vegetative growth. *J Bacteriol* **96**: 421-427.

Bramkamp, M. & D. Lopez, (2015) Exploring the existence of lipid rafts in bacteria. *Microbiol Mol Biol Rev* **79**: 81-100.

Broder, D.H. & K. Pogliano, (2006) Forespore engulfment mediated by a ratchet-like mechanism. *Cell* **126**: 917-928.

Broniatowski, M., M. Flasinski, K. Zieba & P. Miskowiec, (2014) Interactions of pentacyclic triterpene acids with cardiolipins and related phosphatidylglycerols in model systems. *Biochim Biophys acta* **1838**: 2530-2538.

Browman, D.T., M.B. Hoegg & S.M. Robbins, (2007) The SPFH domain-containing proteins: more than lipid raft markers. *Trends Cell Biol* **17**: 394-402.

Brown, D., (1994) GPI-anchored proteins and detergent-resistant membrane domains. *Braz J Med Biol Res* **27**: 309-315.

Brown, D.A. & E. London, (1998) Functions of lipid rafts in biological membranes. *Annu Rev Cell Dev Biol* **14**: 111-136.

Brown, D.A. & J.K. Rose, (1992) Sorting of GPI-anchored proteins to glycolipid-enriched membrane subdomains during transport to the apical cell surface. *Cell* **68**: 533-544.

Bruser, T., T. Yano, D.C. Brune & F. Daldal, (2003) Membrane targeting of a folded and cofactor-containing protein. *Eur J Biochem* **270**: 1211-1221.

Buddelmeijer, N., M.E. Aarsman, A.H. Kolk, M. Vicente & N. Nanninga, (1998) Localization of cell division protein FtsQ by immunofluorescence microscopy in dividing and nondividing cells of *Escherichia coli*. *J Bacteriol* **180**: 6107-6116.

Buddelmeijer, N. & J. Beckwith, (2004) A complex of the *Escherichia coli* cell division proteins FtsL, FtsB and FtsQ forms independently of its localization to the septal region. *Mol Microbiology* **52**: 1315-1327.

Bukhalid, R.A., S.Y. Chung & R. Loria, (1998) nec1, a gene conferring a necrogenic phenotype, is conserved in plant-pathogenic *Streptomyces* spp. and linked to a transposase pseudogene. *Mol Plant Microbe Interact* **11**: 960-967.

Burbulys, D., K.A. Trach & J.A. Hoch, (1991) Initiation of sporulation in *B. subtilis* is controlled by a multicomponent phosphorelay. *Cell* **64**: 545-552.

Burton, B.M., K.A. Marquis, N.L. Sullivan, T.A. Rapoport & D.Z. Rudner, (2007) The ATPase SpoIIIE transports DNA across fused septal membranes during sporulation in *Bacillus subtilis*. *Cell* **131**: 1301-1312.

Busby, S. & R.H. Ebright, (1999) Transcription activation by catabolite activator protein (CAP). *J Mol Biol* **293**: 199-213.

Busiek, K.K., J.M. Eraso, Y. Wang & W. Margolin, (2012) The early divisome protein FtsA interacts directly through its 1c subdomain with the cytoplasmic domain of the late divisome protein FtsN. *J Bacteriol* **194**: 1989-2000.

Buskirk, S.W. & E.R. Lafontaine, (2014) *Moraxella catarrhalis* expresses a cardiolipin synthase that impacts adherence to human epithelial cells. *J Bacteriol* **196**: 107-120.

Butcher, B.G. & J.D. Helmann, (2006) Identification of *Bacillus subtilis* sigma-dependent genes that provide intrinsic resistance to antimicrobial compounds produced by *Bacilli*. *Mol Microbiol* **60**: 765-782.

Buttner, M.J., A.M. Smith & M.J. Bibb, (1988) At least three different RNA polymerase holoenzymes direct transcription of the agarase gene (dagA) of *Streptomyces coelicolor* A3(2). *Cell* **52**: 599-607.

Camp, A.H. & R. Losick, (2009) A feeding tube model for activation of a cell-specific transcription factor during sporulation in *Bacillus subtilis*. *Genes Dev* **23**: 1014-1024.

Campanella, R., (1992) Membrane lipids modifications in human gliomas of different degree of malignancy. *J Neurosurg* **36**: 11-25.

Campo, N. & D.Z. Rudner, (2007) SpoIVB and CtpB are both forespore signals in the activation of the sporulation transcription factor sigmaK in *Bacillus subtilis*. *J Bacteriol* ***189***: 6021-6027.

Carmona-Salazar, L., M. El Hafidi, C. Enriquez-Arredondo, C. Vazquez-Vazquez, L.E. Gonzalez de la Vara & M. Gavilanes-Ruiz, (2011) Isolation of detergent-resistant membranes from plant photosynthetic and non-photosynthetic tissues. *Anal Biochem* **417**: 220-227.

Carniol, K., S. Ben-Yehuda, N. King & R. Losick, (2005) Genetic dissection of the sporulation protein SpoIIE and its role in asymmetric division in *Bacillus subtilis*. *J Bacteriol* **187**: 3511-3520.

Castaing, J.P., A. Nagy, V. Anantharaman, L. Aravind & K.S. Ramamurthi, (2013) ATP hydrolysis by a domain related to translation factor GTPases drives polymerization of a static bacterial morphogenetic protein. *Proc Natl Acad Sci USA* **110**: E151-160.

Celler, K., R.I. Koning, J. Willemse, A.J. Koster & G.P. van Wezel, (2016) Cross-membranes orchestrate compartmentalization and morphogenesis in *Streptomyces*. *Nat Commun* **7**: ncomms11836.

Cha, J.H. & G.C. Stewart, (1997) The *divIVA* minicell locus of *Bacillus subtilis*. *J Bacteriol* **179**: 1671-1683.

Chai, Y., R. Kolter & R. Losick, (2010) Reversal of an epigenetic switch governing cell chaining in *Bacillus subtilis* by protein instability. *Mol Microbiol* **78**: 218-229.

Chalabaev, S., A. Chauhan, A. Novikov, P. Iyer, M. Szczesny, C. Beloin, M. Caroff & J.M. Ghigo, (2014) Biofilms formed by Gram-negative bacteria undergo increased lipid a palmitoylation, enhancing *in vivo* survival. *mBio* **5**.

Champoux, J.J., F.C. Neidhardt, W.L. Drew & J.J. Plorde, (2004) Sherris Medical Microbiology.

Chapot-Chartier, M.P. & S. Kulakauskas, (2014) Cell wall structure and function in lactic acid bacteria. *Microb Cell Fact* **13** Suppl 1: S9.

Chater, K.F., (2001) Regulation of sporulation in *Streptomyces coelicolor* A3(2): a checkpoint multiplex? *Curr Opin Microbiol* **4**: 667-673.

Chater, K.F., S. Biro, K.J. Lee, T. Palmer & H. Schrempf, (2010) The complex extracellular biology of *Streptomyces*. *FEMS Microbiol Rev* **34**: 171-198.

Chen, J., J.B. Anderson, C. DeWeese-Scott, N.D. Fedorova, L.Y. Geer, S. He, D.I. Hurwitz, J.D. Jackson, A.R. Jacobs, C.J. Lanczycki, C.A. Liebert, C. Liu, T. Madej, A. Marchler-Bauer, G.H. Marchler, R. Mazumder, A.N. Nikolskaya, B.S. Rao, A.R. Panchenko, B.A. Shoemaker, V. Simonyan, J.S. Song, P.A. Thiessen, S. Vasudevan, Y. Wang, R.A. Yamashita, J.J. Yin & S.H. Bryant, (2003) MMDB: Entrez's 3D-structure database. *Nucleic Acids Res* **31**: 474-477.

Chiba, S., K. Ito & Y. Akiyama, (2006) The *Escherichia coli* plasma membrane contains two PHB (prohibitin homology) domain protein complexes of opposite orientations. *Mol Microbiol* **60**: 448-457.

Choi, J.Y., W.I. Wu & D.R. Voelker, (2005) Phosphatidylserine decarboxylases as genetic and biochemical tools for studying phospholipid traffic. *Anal Biochem* **347**: 165-175.

Choi, S.Y., P. Huang, G.M. Jenkins, D.C. Chan, J. Schiller & M.A. Frohman, (2006) A common lipid links Mfn-mediated mitochondrial fusion and SNARE-regulated exocytosis. *Nat Cell Biol* **8**: 1255-1262.

Christie, D.A., C.D. Lemke, I.M. Elias, L.A. Chau, M.G. Kirchhof, B. Li, E.H. Ball, S.D. Dunn, G.M. Hatch & J. Madrenas, (2011) Stomatin-like protein 2 binds cardiolipin and regulates mitochondrial biogenesis and function. *Mol Cell Biol* **31**: 3845-3856.

Ciehanover, A., Y. Hod & A. Hershko, (1978) A heat-stable polypeptide component of an ATP-dependent proteolytic system from reticulocytes. *Biochem Biophys Res Comms* **81**: 1100-1105.

Cimermancic P., M.H. Medema, J. Claesen, K. Kurita, L.C. Wieland Brown, K. Mavrommatis, A. Pati, P.A. Godfrey, M. Koehrsen, J. Clardy J, B.W. Birren, E. Takano, A. Sali, R.G. Linington, M.A. Fischbach, (2014) Insights into secondary metabolism from a global analysis of prokaryotic biosynthetic gene clusters. *Cell* **158**(2): 412-421.

Claessen, D., W. de Jong, L. Dijkhuizen & H.A. Wosten, (2006) Regulation of *Streptomyces* development: reach for the sky! *Trends Microbiol* **14**: 313-319.

Claessen, D., R. Emmins, L.W. Hamoen, R.A. Daniel, J. Errington & D.H. Edwards, (2008) Control of the cell elongation-division cycle by shuttling of PBP1 protein in *Bacillus subtilis*. *Mol Microbiol* **68**: 1029-1046.

Clark, A.J. & S.J. Sandler, (1994) Homologous genetic recombination: the pieces begin to fall into place. *Crit Rev Microbiol* **20**: 125-142.

Collins, L.V., S.A. Kristian, C. Weidenmaier, M. Faigle, K.P. Van Kessel, J.A. Van Strijp, F. Gotz, B. Neumeister & A. Peschel, (2002) *Staphylococcus aureus* strains lacking D-alanine modifications of teichoic acids are highly susceptible to human neutrophil killing and are virulence attenuated in mice. *J Infect Dis* **186**: 214-219.

Coordinators, N.R., (2017) Database Resources of the National Center for Biotechnology Information. *Nucleic Acids Res* **45**: D12-D17.

Corcelli, A., (2009) The cardiolipin analogues of Archaea. *Biochem Biophys Acta* **1788**: 2101-2106.

Cosloy, S.D. & M. Oishi, (1973) The nature of the transformation process in *Escherichia coli* K12. *Mol Gen Genet* **124**: 1-10.

Crane, J.M. & L.K. Tamm, (2004) Role of cholesterol in the formation and nature of lipid rafts in planar and spherical model membranes. *Biophys* J **86**: 2965-2979.

Cullis, P.R. & B. de Kruijff, (1978) The polymorphic phase behaviour of phosphatidylethanolamines of natural and synthetic origin. A 31P NMR study. *Biochim Biophys Acta* **513**: 31-42.

Cunningham, K.A. & W.F. Burkholder, (2009) The histidine kinase inhibitor Sda binds near the site of autophosphorylation and may sterically hinder autophosphorylation and phosphotransfer to Spo0F. *Mol Microbiol* **71**: 659-677.

Czyz, O., T. Bitew, A. Cuesta-Marban, C.R. McMaster, F. Mollinedo & V. Zaremberg, (2013) Alteration of plasma membrane organization by an anticancer lysophosphatidylcholine analogue induces intracellular acidification and internalization of plasma membrane transporters in yeast. *J Biol Chem* **288**: 8419-8432.

D'Elia, M.A., M.P. Pereira, Y.S. Chung, W. Zhao, A. Chau, T.J. Kenney, M.C. Sulavik, T.A. Black & E.D. Brown, (2006) Lesions in teichoic acid biosynthesis in *Staphylococcus aureus* lead to a lethal gain of function in the otherwise dispensable pathway. *J Bacteriol* **188**: 4183-4189.

D'Ulisse, V., M. Fagioli, P. Ghelardini & L. Paolozzi, (2007) Three functional subdomains of the *Escherichia coli* FtsQ protein are involved in its interaction with the other division proteins. *Microbiology* **153**: 124-138.

Dai, K. & J. Lutkenhaus, (1992) The proper ratio of FtsZ to FtsA is required for cell division to occur in *Escherichia coli. J Bacteriol **174***: 6145-6151.

Dalbey, R.E., P. Wang & A. Kuhn, (2011) Assembly of bacterial inner membrane proteins. *Annu Rev Biochem* **80**: 161-187.

Dalebroux, Z.D., S. Matamouros, D. Whittington, R.E. Bishop & S.I. Miller, (2014) PhoPQ regulates acidic glycerophospholipid content of the *Salmonella Typhimurium* outer membrane. *Proc Natl Acad Sci USA* **111**: 1963-1968.

Daniel, R.A. & J. Errington, (2000) Intrinsic instability of the essential cell division protein FtsL of *Bacillus subtilis* and a role for DivIB protein in FtsL turnover. *Mol Microbiol* **36**: 278-289.

Daniel, R.A. & J. Errington, (2003) Control of cell morphogenesis in bacteria: two distinct ways to make a rod-shaped cell. *Cell* **113**: 767-776.

Datsenko, K.A. & B.L. Wanner, (2000) One-step inactivation of chromosomal genes in *Escherichia* coli K-12 using PCR products. *Proc Natl Acad Sci USA* **97**: 6640-6645.

Datta, P., A. Dasgupta, S. Bhakta & J. Basu, (2002) Interaction between FtsZ and FtsW of *Mycobacterium tuberculosis*. *J Biol Chem* **277**: 24983-24987.

Datta, P., A. Dasgupta, A.K. Singh, P. Mukherjee, M. Kundu & J. Basu, (2006) Interaction between FtsW and penicillin-binding protein 3 (PBP3) directs PBP3 to mid-cell, controls cell

septation and mediates the formation of a trimeric complex involving FtsZ, FtsW and PBP3 in mycobacteria. *Mol Microbiol* **62**: 1655-1673.

de Andrade Rosa, I., M. Einicker-Lamas, R. Roney Bernardo, L.M. Previatto, R. Mohana-Borges, J.A. Morgado-Diaz & M. Benchimol, (2006) Cardiolipin in hydrogenosomes: evidence of symbiotic origin. *Eukaryot cell* **5**: 784-787.

de Boer, P.A., R.E. Crossley, A.R. Hand & L.I. Rothfield, (1991) The MinD protein is a membrane ATPase required for the correct placement of the *Escherichia coli* division site. *EMBO J* **10**: 4371-4380.

de Boer, P.A., R.E. Crossley & L.I. Rothfield, (1989) A division inhibitor and a topological specificity factor coded for by the minicell locus determine proper placement of the division septum in *E. coli*. *Cell* **56**: 641-649.

de Diesbach, P., T. Medts, S. Carpentier, L. D'Auria, P. Van Der Smissen, A. Platek, M. Mettlen, A. Caplanusi, M.F. van den Hove, D. Tyteca & P.J. Courtoy, (2008) Differential subcellular membrane recruitment of Src may specify its downstream signalling. *Exp Cell Res* **314**: 1465-1479.

de Jong, W., E. Vijgenboom, L. Dijkhuizen, H.A. Wosten & D. Claessen, (2012) SapB and the rodlins are required for development of *Streptomyces coelicolor* in high osmolarity media. *FEMS Microbiol Lett* **329**: 154-159.

de Jong, W., H.A. Wosten, L. Dijkhuizen & D. Claessen, (2009) Attachment of *Streptomyces coelicolor* is mediated by amyloidal fimbriae that are anchored to the cell surface via cellulose. *Mol Microbiol* **73**: 1128-1140.

De Keersmaeker, S., L. Van Mellaert, E. Lammertyn, K. Vrancken, J. Anne & N. Geukens, (2005a) Functional analysis of TatA and TatB in *Streptomyces lividans*. *Biochem Biophys Res Comms* **335**: 973-982.

De Keersmaeker, S., L. Van Mellaert, K. Schaerlaekens, W. Van Dessel, K. Vrancken, E. Lammertyn, J. Anne & N. Geukens, (2005b) Structural organization of the twin-arginine translocation system in *Streptomyces lividans*. *FEBS Lett* **579**: 797-802.

De Keersmaeker, S., K. Vrancken, L. Van Mellaert, J. Anne & N. Geukens, (2007) The Tat pathway in *Streptomyces lividans*: interaction of Tat subunits and their role in translocation. *Microbiology* **153**: 1087-1094.

de Pedro, M.A., K.D. Young, J.V. Holtje & H. Schwarz, (2003) Branching of *Escherichia coli* cells arises from multiple sites of inert peptidoglycan. *J Bacteriol* **185**: 1147-1152.

De Siervo, A.J. & M.R. Salton, (1971) Biosynthesis of cardiolipin in the membranes of *Micrococcus lysodeikticus*. *Biochem Biophys Acta* **239**: 280-292.

Dehus, O., M. Pfitzenmaier, G. Stuebs, N. Fischer, W. Schwaeble, S. Morath, T. Hartung, A. Geyer & C. Hermann, (2011) Growth temperature-dependent expression of structural variants of *Listeria monocytogenes* lipoteichoic acid. *Immunobiology* **216**: 24-31.

Deiorio-Haggar, K., J. Anthony & M.M. Meyer, (2013) RNA structures regulating ribosomal protein biosynthesis in bacilli. *RNA Biol* **10**: 1180-1184.

Del Sol, R., J.G. Mullins, N. Grantcharova, K. Flardh & P. Dyson, (2006) Influence of CrgA on assembly of the cell division protein FtsZ during development of *Streptomyces coelicolor*. *J Bacteriol* **188**: 1540-1550.

Del Sol, R., A. Pitman, P. Herron & P. Dyson, (2003) The product of a developmental gene, crgA, that coordinates reproductive growth in *Streptomyces* belongs to a novel family of small actinomycete-specific proteins. *J Bacteriol* **185**: 6678-6685.

Delaunay, J., G. Stewart & A. Iolascon, (1999) Hereditary dehydrated and overhydrated stomatocytosis: recent advances. *Curr Opin Hematol* **6**: 110-114.

DeLisa, M.P., P. Lee, T. Palmer & G. Georgiou, (2004) Phage shock protein PspA of *Escherichia coli* relieves saturation of protein export via the Tat pathway. *J Bacteriol* **186**: 366-373.

Dempwolff, F., H.M. Moller & P.L. Graumann, (2012) Synthetic motility and cell shape defects associated with deletions of flotillin/reggie paralogs in *Bacillus subtilis* and interplay of these proteins with NfeD proteins. *J Bacteriol* **194**: 4652-4661.

den Blaauwen, T., J.M. Andreu & O. Monasterio, (2014) Bacterial cell division proteins as antibiotic targets. *Bioorg Chem* **55**: 27-38.

den Hengst, C.D., N.T. Tran, M.J. Bibb, G. Chandra, B.K. Leskiw & M.J. Buttner, (2010) Genes essential for morphological development and antibiotic production in *Streptomyces coelicolor* are targets of BldD during vegetative growth. *Mol Microbiol* **78**: 361-379.

Deuerling, E., A. Schulze-Specking, T. Tomoyasu, A. Mogk & B. Bukau, (1999) Trigger factor and DnaK cooperate in folding of newly synthesized proteins. *Nature* **400**: 693-696.

Dewar, S.J., K.J. Begg & W.D. Donachie, (1992) Inhibition of cell division initiation by an imbalance in the ratio of FtsA to FtsZ. *J Bacteriol* **174**: 6314-6316.

Di Berardo, C., D.S. Capstick, M.J. Bibb, K.C. Findlay, M.J. Buttner & M.A. Elliot, (2008) Function and redundancy of the chaplin cell surface proteins in aerial hypha formation, rodlet assembly, and viability in *Streptomyces coelicolor*. *J Bacteriol* **190**: 5879-5889.

Di Lallo, G., M. Fagioli, D. Barionovi, P. Ghelardini & L. Paolozzi, (2003) Use of a two-hybrid assay to study the assembly of a complex multicomponent protein machinery: bacterial septosome differentiation. *Microbiology* **149**: 3353-3359.

Diaz, J.F., A. Kralicek, J. Mingorance, J.M. Palacios, M. Vicente & J.M. Andreu, (2001) Activation of cell division protein FtsZ. Control of switch loop T3 conformation by the nucleotide gamma-phosphate. *J Biol Chem* **276**: 17307-17315.

Diez, V., G.E. Schujman, F.J. Gueiros-Filho & D. de Mendoza, (2012) Vectorial signalling mechanism required for cell-cell communication during sporulation in *Bacillus subtilis*. *Mol Microbiol* **83**: 261-274.

Ditkowski, B., N. Holmes, J. Rydzak, M. Donczew, M. Bezulska, K. Ginda, P. Kedzierski, J. Zakrzewska-Czerwinska, G.H. Kelemen & D. Jakimowicz, (2013) Dynamic interplay of ParA with the polarity protein, Scy, coordinates the growth with chromosome segregation in *Streptomyces coelicolor*. *Open Biol* **3**: 130006.

Doan, T., J. Coleman, K.A. Marquis, A.J. Meeske, B.M. Burton, E. Karatekin & D.Z. Rudner, (2013) FisB mediates membrane fission during sporulation in *Bacillus subtilis*. *Genes Dev* **27**: 322-334.

Doan, T., K.A. Marquis & D.Z. Rudner, (2005) Subcellular localization of a sporulation membrane protein is achieved through a network of interactions along and across the septum. *Mol Microbiol* **55**: 1767-1781.

Doan, T., C. Morlot, J. Meisner, M. Serrano, A.O. Henriques, C.P. Moran, Jr. & D.Z. Rudner, (2009) Novel secretion apparatus maintains spore integrity and developmental gene expression in *Bacillus subtilis*. *PLoS Genet* **5**: e1000566.

Donovan, C. & M. Bramkamp, (2009) Characterization and subcellular localization of a bacterial flotillin homologue. *Microbiology* **155**: 1786-1799.

Doran, K.S., E.J. Engelson, A. Khosravi, H.C. Maisey, I. Fedtke, O. Equils, K.S. Michelsen, M. Arditi, A. Peschel & V. Nizet, (2005) Blood-brain barrier invasion by group B Streptococcus depends upon proper cell-surface anchoring of lipoteichoic acid. *J Clin Invest* **115**: 2499-2507.

Doull, J.L. & L.C. Vining, (1989) Culture conditions promoting dispersed growth and biphasic production of actinorhodin in shaken cultures of *Streptomyces coelicolor* A3(2). *FEMS Microbiol Lett* **53**: 265-268.

Douville, K., A. Price, J. Eichler, A. Economou & W. Wickner, (1995) SecYEG and SecA are the stoichiometric components of preprotein translocase. *J Biol Chem* **270**: 20106-20111.

Draper, G.C., N. McLennan, K. Begg, M. Masters & W.D. Donachie, (1998) Only the N-terminal domain of FtsK functions in cell division. *J Bacteriol* **180**: 4621-4627.

Driessen, A.J., (2001) SecB, a molecular chaperone with two faces. *Trends Microbiol* **9**: 193-196.

Dubarry, N., C. Possoz & F.X. Barre, (2010) Multiple regions along the *Escherichia coli* FtsK protein are implicated in cell division. *Mol Microbiol* **78**: 1088-1100.

Duncan, L., S. Alper, F. Arigoni, R. Losick & P. Stragier, (1995) Activation of cell-specific transcription by a serine phosphatase at the site of asymmetric division. *Science* **270**: 641-644.

Dworkin, J. & R. Losick, (2001) Differential gene expression governed by chromosomal spatial asymmetry. *Cell* **107**: 339-346.

Ebersbach, G. & K. Gerdes, (2005) Plasmid segregation mechanisms. *Annu Rev Genet* **39**: 453-479.

Ebmeier, S.E., I.S. Tan, K.R. Clapham & K.S. Ramamurthi, (2012) Small proteins link coat and cortex assembly during sporulation in *Bacillus subtilis*. *Mol Microbiol* **84**: 682-696.

el Hassan, A.M., A.H. Fahal, A.O. Ahmed, A. Ismail & B. Veress, (2001) The immunopathology of actinomycetoma lesions caused by *Streptomyces somaliensis*. *Trans R Soc Trop Med Hyg* **95**: 89-92.

Erickson, H.P., (2001) The FtsZ protofilament and attachment of ZipA--structural constraints on the FtsZ power stroke. *Curr Opin Cell Biol* **13**: 55-60.

Ernst, R.K., E.C. Yi, L. Guo, K.B. Lim, J.L. Burns, M. Hackett & S.I. Miller, (1999) Specific lipopolysaccharide found in cystic fibrosis airway *Pseudomonas aeruginosa*. *Science* **286**: 1561-1565.

Errington, J., R.A. Daniel & D.J. Scheffers, (2003) Cytokinesis in bacteria. *Microbiol Mol Biol Rev* **67**: 52-65, table of contents.

Fabelo, N., V. Martin, G. Santpere, R. Marin, L. Torrent, I. Ferrer & M. Diaz, (2011) Severe alterations in lipid composition of frontal cortex lipid rafts from Parkinson's disease and incidental Parkinson's disease. *Mol Med* **17**: 1107-1118.

Falcioni, T., A. Manti, P. Boi, B. Canonico, M. Balsamo & S. Papa, (2006) Comparison of disruption procedures for enumeration of activated sludge floc bacteria by flow cytometry. *Cytometry B Clin Cytom* **70**: 149-153.

Fallon, L., F. Moreau, B.G. Croft, N. Labib, W.J. Gu & E.A. Fon, (2002) Parkin and CASK/LIN-2 associate via a PDZ-mediated interaction and are co-localized in lipid rafts and postsynaptic densities in brain. *J Biol Chem* **277**: 486-491.

Farsad, K., N. Ringstad, K. Takei, S.R. Floyd, K. Rose & P. De Camilli, (2001) Generation of high curvature membranes mediated by direct endophilin bilayer interactions. *J Cell Biol* **155**: 193-200.

Fay, A. & J. Dworkin, (2009) *Bacillus* subtilis homologs of MviN (MurJ), the putative *Escherichia coli* lipid II flippase, are not essential for growth. *J Bacteriol* 191: 6020-6028.

Feinstein, M.B., S.M. Fernandez & R.I. Sha'afi, (1975) Fluidity of natural membranes and phosphatidylserine and ganglioside dispersions. Effect of local anesthetics, cholesterol and protein. *Biochem Biophys Acta* **413**: 354-370.

Fernandez-Martinez, L.T., R. Del Sol, M.C. Evans, S. Fielding, P.R. Herron, G. Chandra & P.J. Dyson, (2011) A transposon insertion single-gene knockout library and new ordered cosmid library for the model organism *Streptomyces coelicolor* A3(2). *Antonie Van Leeuwenhoek* **99**: 515-522.

Fields, P.I., E.A. Groisman & F. Heffron, (1989) A Salmonella locus that controls resistance to microbicidal proteins from phagocytic cells. *Science* **243**: 1059-1062.

Findlay, J.B.C., Evans, W. H. , (1987) Biological Membranes. A Practical Approach. IRL Press, Oxford.

Fischer, W., (1987) 'Lipoteichoic acid' of *Bifidobacterium bifidum* subspecies pennsylvanicum DSM 20239. A lipoglycan with monoglycerophosphate side chains. *Eur J Biochem* **165**: 639-646.

Fischer, W., (1988) Physiology of lipoteichoic acids in bacteria. *Adv Microb Physiol* **29**: 233-302.

Fischer, W., (1991) One-step purification of bacterial lipid macroamphiphiles by hydrophobic interaction chromatography. *Anal Biochem* **194**: 353-358.

Fischer, W., (1994) Lipoteichoic acid and lipids in the membrane of *Staphylococcus aureus*. *Med Microbiol Immunol* **183**: 61-76.

Fischer, W., (1997) Pneumococcal lipoteichoic and teichoic acid. *Microb Drug Resist* **3**: 309-325.

Fitzpatrick, D.A., C.J. Creevey & J.O. McInerney, (2006) Genome phylogenies indicate a meaningful alpha-proteobacterial phylogeny and support a grouping of the mitochondria with the Rickettsiales. *Mol Biol Evol* **23**: 74-85.

Flardh, K., (2003a) Essential role of DivIVA in polar growth and morphogenesis in *Streptomyces coelicolor* A3(2). *Mol Microbiol* **49**: 1523-1536.

Flardh, K., (2003b) Growth polarity and cell division in *Streptomyces*. *Curr Opin Microbiol* **6**: 564-571.

Flardh, K., (2010) Cell polarity and the control of apical growth in *Streptomyces*. *Curr Opin Microbiol* **13**: 758-765.

Flardh, K. & M.J. Buttner, (2009) *Streptomyces* morphogenetics: dissecting differentiation in a filamentous bacterium. *Nat Rev Microbiol* **7**: 36-49.

Flardh, K., D.M. Richards, A.M. Hempel, M. Howard & M.J. Buttner, (2012) Regulation of apical growth and hyphal branching in *Streptomyces*. *Curr Opin Microbiol* **15**: 737-743.

Frandsen, N., I. Barak, C. Karmazyn-Campelli & P. Stragier, (1999) Transient gene asymmetry during sporulation and establishment of cell specificity in *Bacillus subtilis*. *Genes Dev* **13**: 394-399.

Frickey, T. & E. Kannenberg, (2009) Phylogenetic analysis of the triterpene cyclase protein family in prokaryotes and eukaryotes suggests bidirectional lateral gene transfer. *Environ Microbiol* **11**: 1224-1241.

Fu, X., Y.L. Shih, Y. Zhang & L.I. Rothfield, (2001) The MinE ring required for proper placement of the division site is a mobile structure that changes its cellular location during the *Escherichia coli* division cycle. *Proc Natl Acad Sci USA* **98**: 980-985.

Fujita, M. & R. Losick, (2002) An investigation into the compartmentalization of the sporulation transcription factor sigmaE in *Bacillus subtilis*. *Mol Microbiol* **43**: 27-38.

Fujita, M. & R. Losick, (2005) Evidence that entry into sporulation in *Bacillus subtilis* is governed by a gradual increase in the level and activity of the master regulator Spo0A. *Genes Dev* **19**: 2236-2244.

Fukamizo, T. & R. Brzezinski, (1997) Chitosanase from *Streptomyces* sp. strain N174: a comparative review of its structure and function. *Biochem Cell Biol* **75**: 687-696.

Furt, F., S. Konig, J.J. Bessoule, F. Sargueil, R. Zallot, T. Stanislas, E. Noirot, J. Lherminier, F. Simon-Plas, I. Heilmann & S. Mongrand, (2010) Polyphosphoinositides are enriched in plant membrane rafts and form microdomains in the plasma membrane. *Plant Physiol* 152: 2173-2187.

Furt, F., B. Lefebvre, J. Cullimore, J.J. Bessoule & S. Mongrand, (2007) Plant lipid rafts: fluctuat nec mergitur. *Plant Signal Behav* **2**: 508-511.

Galbiati, F., D. Volonte, J.S. Goltz, Z. Steele, J. Sen, J. Jurcsak, D. Stein, L. Stevens & M.P. Lisanti, (1998) Identification, sequence and developmental expression of invertebrate flotillins from *Drosophila melanogaster*. *Gene* **210**: 229-237.

Gallop, J.L., C.C. Jao, H.M. Kent, P.J. Butler, P.R. Evans, R. Langen & H.T. McMahon, (2006) Mechanism of endophilin N-BAR domain-mediated membrane curvature. *EMBO J* **25**: 2898-2910.

Gamez, G. & S. Hammerschmidt, (2012) Combat pneumococcal infections: adhesins as candidates for protein-based vaccine development. *Curr Drug Targets* **13**: 323-337.

Garcia-Rodriguez, F.M. & N. Toro, (2000) *Sinorhizobium meliloti nfe* (nodulation formation efficiency) genes exhibit temporal and spatial expression patterns similar to those of genes involved in symbiotic nitrogen fixation. *Mol Plant Microbe Interact* **13**: 583-591.

Garcia Fernandez, M.I., D. Ceccarelli & U. Muscatello, (2004) Use of the fluorescent dye 10-N-nonyl acridine orange in quantitative and location assays of cardiolipin: a study on different experimental models. *Anal Biochem* **328**: 174-180.

Garcia Vescovi, E., F.C. Soncini & E.A. Groisman, (1996) Mg2+ as an extracellular signal: environmental regulation of Salmonella virulence. *Cell* **84**: 165-174.

Gazzerro, E., F. Sotgia, C. Bruno, M.P. Lisanti & C. Minetti, (2010) Caveolinopathies: from the biology of caveolin-3 to human diseases. *Eur J Hum Genet* **18**: 137-145.

Geiger, O., N. Gonzalez-Silva, I.M. Lopez-Lara & C. Sohlenkamp, (2010) Amino acid-containing membrane lipids in bacteria. *Prog Lipid Res* **49**: 46-60.

Geissler, B. & W. Margolin, (2005) Evidence for functional overlap among multiple bacterial cell division proteins: compensating for the loss of FtsK. *Mol Microbiol* **58**: 596-612.

Gerard, F. & K. Cline, (2006) Efficient twin arginine translocation (Tat) pathway transport of a precursor protein covalently anchored to its initial cpTatC binding site. *J Biol Chem* **281**: 6130-6135.

Gerding, M.A., Y. Ogata, N.D. Pecora, H. Niki & P.A. de Boer, (2007) The trans-envelope Tol-Pal complex is part of the cell division machinery and required for proper outer-membrane invagination during cell constriction in *E. coli. Mol Microbiol* **63**: 1008-1025.

Ghinet, M.G., S. Roy, D. Poulin-Laprade, M.E. Lacombe-Harvey, R. Morosoli & R. Brzezinski, (2010) Chitosanase from *Streptomyces coelicolor* A3(2): biochemical properties and role in protection against antibacterial effect of chitosan. *Biochem Cell Biol* **88**: 907-916.

Gierasch, L.M., (1989) Signal sequences. *Biochemistry* **28**: 923-930.

Gilmore, M.E., D. Bandyopadhyay, A.M. Dean, S.D. Linnstaedt & D.L. Popham, (2004) Production of muramic delta-lactam in *Bacillus subtilis* spore peptidoglycan. *J Bacteriol* **186**: 80-89.

Girardot, N., B. Allinquant, D. Langui, A. Laquerriere, B. Dubois, J.J. Hauw & C. Duyckaerts, (2003) Accumulation of flotillin-1 in tangle-bearing neurones of Alzheimer's disease. *Neuropathol Appl Neurobiol* **29**: 451-461.

Glaser, P., D. Ladant, O. Sezer, F. Pichot, A. Ullmann & A. Danchin, (1988a) The calmodulin-sensitive adenylate cyclase of *Bordetella pertussis*: cloning and expression in *Escherichia coli*. *Mol Microbiol* **2**: 19-30.

Glaser, P., H. Sakamoto, J. Bellalou, A. Ullmann & A. Danchin, (1988b) Secretion of cyclolysin, the calmodulin-sensitive adenylate cyclase-haemolysin bifunctional protein of *Bordetella pertussis. Embo J* **7**: 3997-4004.

Goffin, C. & J.M. Ghuysen, (1998) Multimodular penicillin-binding proteins: an enigmatic family of orthologs and paralogs. *Microbiol Mol Biol Rev* **62**: 1079-1093.

Gonzalez, M.D., E.A. Akbay, D. Boyd & J. Beckwith, (2010) Multiple interaction domains in FtsL, a protein component of the widely conserved bacterial FtsLBQ cell division complex. *J Bacteriol* **192**: 2757-2768.

Goriely, A. & M. Tabor, (2003) Biomechanical models of hyphal growth in actinomycetes. *J Theor Biol* **222**: 211-218.

Gould, G.W. & G.J. Dring, (1975) Heat resistance of bacterial endospores and concept of an expanded osmoregulatory cortex. *Nature* **258**: 402-405.

Goyard, S., P. Sebo, O. D'Andria, D. Ladant & A. Ullmann, (1993) *Bordetella pertussis* adenylate cyclase: a toxin with multiple talents. *Int. J. Med. Microbiol* **278**: 326-333.

Gramajo, H.C., E. Takano & M.J. Bibb, (1993) Stationary-phase production of the antibiotic actinorhodin in *Streptomyces coelicolor* A3(2) is transcriptionally regulated. *Mol Microbiol* **7**: 837-845.

Grant, W.D., (1979) Cell wall teichoic acid as a reserve phosphate source in *Bacillus subtilis*. *J Bacteriol* **137**: 35-43.

Grantcharova, N., U. Lustig & K. Flardh, (2005) Dynamics of FtsZ assembly during sporulation in *Streptomyces coelicolor* A3(2). *J Bacteriol* **187**: 3227-3237.

Green, J.B., B. Fricke, M.C. Chetty, M. von During, G.F. Preston & G.W. Stewart, (2004) Eukaryotic and prokaryotic stomatins: the proteolytic link. *Blood Cells Mol Dis* **32**: 411-422.

Green, J.B., R.P. Lower & J.P. Young, (2009) The NfeD protein family and its conserved gene neighbours throughout prokaryotes: functional implications for stomatin-like proteins. *J Mol Evol* **69**: 657-667.

Green, J.B. & J.P. Young, (2008) Slipins: ancient origin, duplication and diversification of the stomatin protein family. *BMC Evol Biol* **8**: 44.

Gregory, M.A., R. Till & M.C. Smith, (2003) Integration site for *Streptomyces* phage phiBT1 and development of site-specific integrating vectors. *J Bacteriol* **185**: 5320-5323.

Grenga, L., G. Guglielmi, S. Melino, P. Ghelardini & L. Paolozzi, (2010) FtsQ interaction mutants: a way to identify new antibacterial targets. *New Biotechnol* **27**: 870-881.

Groth, A.C. & M.P. Calos, (2004) Phage integrases: biology and applications. *J Mol Biol* **335**: 667-678.

Grundling, A. & O. Schneewind, (2007) Genes required for glycolipid synthesis and lipoteichoic acid anchoring in *Staphylococcus aureus*. *J Bacteriol* **189**: 2521-2530.

Guberman, J.M., A. Fay, J. Dworkin, N.S. Wingreen & Z. Gitai, (2008) PSICIC: noise and asymmetry in bacterial division revealed by computational image analysis at sub-pixel resolution. *PLOS Comput Biol* **4**: e1000233.

Gueiros-Filho, F.J. & R. Losick, (2002) A widely conserved bacterial cell division protein that promotes assembly of the tubulin-like protein FtsZ. *Genes Dev* **16**: 2544-2556.

Guillaume, E., F. Comunale, N. Do Khoa, D. Planchon, S. Bodin & C. Gauthier-Rouviere, (2013) Flotillin microdomains stabilize cadherins at cell-cell junctions. *J Cell Sci* **126**: 5293-5304.

Guo, D.A., M. Venkatramesh & W.D. Nes, (1995) Developmental regulation of sterol biosynthesis in *Zea mays*. *Lipids* **30**: 203-219.

Guo, L., K.B. Lim, C.M. Poduje, M. Daniel, J.S. Gunn, M. Hackett & S.I. Miller, (1998) Lipid A acylation and bacterial resistance against vertebrate antimicrobial peptides. *Cell* **95**: 189-198.

Guschina, I.A., K.M. Harris, B. Maskrey, B. Goldberg, D. Lloyd & J.L. Harwood, (2009) The microaerophilic flagellate, *Trichomonas vaginalis*, contains unusual acyl lipids but no detectable cardiolipin. *J Eukaryot Microbiol* **56**: 52-57.

Gust, B., G.L. Challis, K. Fowler, T. Kieser & K.F. Chater, (2003) PCR-targeted *Streptomyces* gene replacement identifies a protein domain needed for biosynthesis of the sesquiterpene soil odor geosmin. *Proc Natl Acad Sci USA* **100**: 1541-1546.

Haeusser, D.P., R.L. Schwartz, A.M. Smith, M.E. Oates & P.A. Levin, (2004) EzrA prevents aberrant cell division by modulating assembly of the cytoskeletal protein FtsZ. *Mol Microbiol* **52**: 801-814.

Haines, T.H. & N.A. Dencher, (2002) Cardiolipin: a proton trap for oxidative phosphorylation. *FEBS Lett* **528**: 35-39.

Hakomori, S., (2003) Structure, organization, and function of glycosphingolipids in membrane. *Curr Opin Hematol* **10**: 16-24.

Hakomori, S.I., (2008) Structure and function of glycosphingolipids and sphingolipids: recollections and future trends. *Biochem Biophys Acta* **1780**: 325-346.

Hale, C.A. & P.A. de Boer, (1997) Direct binding of FtsZ to ZipA, an essential component of the septal ring structure that mediates cell division in *E. coli*. *Cell* **88**: 175-185.

Hale, C.A., H. Meinhardt & P.A. de Boer, (2001) Dynamic localization cycle of the cell division regulator MinE in *Escherichia coli*. *EMBO J* **20**: 1563-1572.

Hale, C.A., D. Shiomi, B. Liu, T.G. Bernhardt, W. Margolin, H. Niki & P.A. de Boer, (2011) Identification of *Escherichia coli* ZapC (YcbW) as a component of the division apparatus that binds and bundles FtsZ polymers. *J Bacteriol* **193**: 1393-1404.

Hamid, M.E., (2011) Variable antibiotic susceptibility patterns among *Streptomyces* species causing actinomycetoma in man and animals. *Ann Clin Microbiol Antimicrob* **10**: 24.

Hamoen, L.W., J.C. Meile, W. de Jong, P. Noirot & J. Errington, (2006) SepF, a novel FtsZ-interacting protein required for a late step in cell division. *Mol Microbiol* **59**: 989-999.

Hamon, M.A. & B.A. Lazazzera, (2001) The sporulation transcription factor Spo0A is required for biofilm development in *Bacillus subtilis*. *Mol Microbiol* **42**: 1199-1209.

Han, W.D., S. Kawamoto, Y. Hosoya, M. Fujita, Y. Sadaie, K. Suzuki, Y. Ohashi, F. Kawamura & K. Ochi, (1998) A novel sporulation-control gene (spo0M) of *Bacillus subtilis* with a sigmaH-regulated promoter. *Gene* **217**: 31-40.

Han, X., J. Yang, K. Yang, Z. Zhao, D.R. Abendschein & R.W. Gross, (2007) Alterations in myocardial cardiolipin content and composition occur at the very earliest stages of diabetes: a shotgun lipidomics study. *Biochemistry* **46**: 6417-6428.

Hanada, M., K.I. Nishiyama, S. Mizushima & H. Tokuda, (1994) Reconstitution of an efficient protein translocation machinery comprising SecA and the three membrane proteins, SecY, SecE, and SecG (p12). *J Biol Chem* **269**: 23625-23631.

Hanahan, D., (1983) Studies on transformation of *Escherichia coli* with plasmids. *J Mol Biol* **166**: 557-580.

Hannich, J.T., K. Umebayashi & H. Riezman, (2011) Distribution and functions of sterols and sphingolipids. *Cold Spring Harb Perspect Biol* **3**.

Hartl, F.U., S. Lecker, E. Schiebel, J.P. Hendrick & W. Wickner, (1990) The binding cascade of SecB to SecA to SecY/E mediates preprotein targeting to the *E. coli* plasma membrane. *Cell* **63**: 269-279.

Hartner, T., K.L. Straub & E. Kannenberg, (2005) Occurrence of hopanoid lipids in anaerobic Geobacter species. *FEMS Microbiol Lett* **243**: 59-64.

Heaton, M.P., R.B. Johnston & T.L. Thompson, (1988) Controlled lysis of bacterial cells utilizing mutants with defective synthesis of D-alanine. *Can J Microbiol* **34**: 256-261.

Heichlinger, A., M. Ammelburg, E.M. Kleinschnitz, A. Latus, I. Maldener, K. Flardh, W. Wohlleben & G. Muth, (2011a) The MreB-like protein Mbl of S. *coelicolor* A3(2) depends on MreB for proper localization and contributes to spore wall synthesis. *J Bacteriol*.

Heichlinger, A., M. Ammelburg, E.M. Kleinschnitz, A. Latus, I. Maldener, K. Flardh, W. Wohlleben & G. Muth, (2011b) The MreB-like protein Mbl of *Streptomyces coelicolor* A3(2) depends on MreB for proper localization and contributes to spore wall synthesis. *J Bacteriol* **193**: 1533-1542.

Hempel, A.M., S.B. Wang, M. Letek, J.A. Gil & K. Flardh, (2008) Assemblies of DivIVA mark sites for hyphal branching and can establish new zones of cell wall growth in *Streptomyces coelicolor*. *J Bacteriol* **190**: 7579-7583.

Henriques, A.O., H. de Lencastre & P.J. Piggot, (1992) A *Bacillus subtilis* morphogene cluster that includes *spoVE* is homologous to the *mra* region of *Escherichia coli*. *Biochimie* **74**: 735-748.

Henriques, A.O., P. Glaser, P.J. Piggot & C.P. Moran, Jr., (1998) Control of cell shape and elongation by the rodA gene in *Bacillus subtilis*. *Mol Microbiol* **28**: 235-247.

Henriques, A.O. & C.P. Moran, Jr., (2007) Structure, assembly, and function of the spore surface layers. *Annu Rev Microbiol* **61**: 555-588.

Herron, P.R., G. Hughes, G. Chandra, S. Fielding & P.J. Dyson, (2004) Transposon Express, a software application to report the identity of insertions obtained by comprehensive transposon mutagenesis of sequenced genomes: analysis of the preference for *in vitro* Tn5 transposition into GC-rich DNA. *Nucleic Acids Res* **32**: e113.

Hiebl-Dirschmied, C.M., G.R. Adolf & R. Prohaska, (1991) Isolation and partial characterization of the human erythrocyte band 7 integral membrane protein. *Biochem Biophys Acta* **1065**: 195-202.

Hinderhofer, M., C.A. Walker, A. Friemel, C.A. Stuermer, H.M. Moller & A. Reuter, (2009) Evolution of prokaryotic SPFH proteins. *BMC Evol Biol* 9**:** 10.

Hirschberg, C.B. & E.P. Kennedy, (1972) Mechanism of the enzymatic synthesis of cardiolipin in *Escherichia coli*. *Proc Natl Acad Sci USA* **69**: 648-651.

Hizukuri, Y., S. Kojima & M. Homma, (2010) Disulphide cross-linking between the stator and the bearing components in the bacterial flagellar motor. *J Biochem* **148**: 309-318.

Hoehne, M., H.G. de Couet, C.A. Stuermer & K.F. Fischbach, (2005) Loss- and gain-of-function analysis of the lipid raft proteins Reggie/Flotillin in Drosophila: they are posttranslationally regulated, and misexpression interferes with wing and eye development. *Mol Cell Neurosci* **30**: 326-338.

Hoischen, C., K. Gura, C. Luge & J. Gumpert, (1997) Lipid and fatty acid composition of cytoplasmic membranes from *Streptomyces hygroscopicus* and its stable protoplast-type L form. *J Bacteriol* **179**: 3430-3436.

Holmes, N.A., J. Walshaw, R.M. Leggett, A. Thibessard, K.A. Dalton, M.D. Gillespie, A.M. Hemmings, B. Gust & G.H. Kelemen, (2013) Coiled-coil protein Scy is a key component of a multiprotein assembly controlling polarized growth in *Streptomyces*. *Proc Natl Acad Sci USA* **110**: E397-406.

Hooper, N.M., (2011) Glypican-1 facilitates prion conversion in lipid rafts. *J Neurochem* **116**: 721-725.

Hopkins, A., G. Buchanan & T. Palmer, (2014) Role of the twin arginine protein transport pathway in the assembly of the *Streptomyces coelicolor* cytochrome bc1 complex. *J Bacteriol* **196**: 50-59.

Hopwood, D.A., (1967) Genetic analysis and genome structure in *Streptomyces coelicolor*. *Bacteriol Rev* **31**: 373-403.

Horwitz, J.P., J. Chua, R.J. Curby, A.J. Tomson, M.A. Darooge, B.E. Fisher, J. Mauricio & I. Klundt, (1964) Substrates for Cytochemical Demonstration of Enzyme Activity. I. Some Substituted 3-Indolyl-Beta-D-Glycopyranosides. *J Med Chem* **7**: 574-575.

Hu, Z., E.P. Gogol & J. Lutkenhaus, (2002) Dynamic assembly of MinD on phospholipid vesicles regulated by ATP and MinE. *Proc Natl Acad Sci USA* **99**: 6761-6766.

Hu, Z. & J. Lutkenhaus, (1999) Topological regulation of cell division in *Escherichia coli* involves rapid pole to pole oscillation of the division inhibitor MinC under the control of MinD and MinE. *Mol Microbiol* **34**: 82-90.

Hu, Z. & J. Lutkenhaus, (2000) Analysis of MinC reveals two independent domains involved in interaction with MinD and FtsZ. *J Bacteriol* **182**: 3965-3971.

Huang, K.C., R. Mukhopadhyay & N.S. Wingreen, (2006) A curvature-mediated mechanism for localization of lipids to bacterial poles. *PLoS Comput Biol* **2**: e151.

Huang, X., K.L. Fredrick & J.D. Helmann, (1998) Promoter recognition by *Bacillus subtilis* sigmaW: autoregulation and partial overlap with the *sigmaX* regulon. *J Bacteriol* **180**: 3765-3770.

Huang, X., A. Gaballa, M. Cao & J.D. Helmann, (1999) Identification of target promoters for the *Bacillus subtilis* extracytoplasmic function sigma factor, sigma W. *Mol Microbiol* **31**: 361-371.

Huber, T.B., B. Schermer, R.U. Muller, M. Hohne, M. Bartram, A. Calixto, H. Hagmann, C. Reinhardt, F. Koos, K. Kunzelmann, E. Shirokova, D. Krautwurst, C. Harteneck, M. Simons, H. Pavenstadt, D. Kerjaschki, C. Thiele, G. Walz, M. Chalfie & T. Benzing, (2006) Podocin and MEC-2 bind cholesterol to regulate the activity of associated ion channels. *Proc Natl Acad Sci USA* **103**: 17079-17086.

Hunte, C., (2005) Specific protein-lipid interactions in membrane proteins. *Biochem Soc Trans* **33**: 938-942.

Hunter, S., P. Jones, A. Mitchell, R. Apweiler, T.K. Attwood, A. Bateman, T. Bernard, D. Binns, P. Bork, S. Burge, E. de Castro, P. Coggill, M. Corbett, U. Das, L. Daugherty, L. Duquenne, R.D. Finn, M. Fraser, J. Gough, D. Haft, N. Hulo, D. Kahn, E. Kelly, I. Letunic, D. Lonsdale, R. Lopez, M. Madera, J. Maslen, C. McAnulla, J. McDowall, C. McMenamin, H. Mi, P. Mutowo-Muellenet, N. Mulder, D. Natale, C. Orengo, S. Pesseat, M. Punta, A.F. Quinn, C. Rivoire, A. Sangrador-Vegas, J.D. Selengut, C.J. Sigrist, M. Scheremetjew, J. Tate, M. Thimmajanarthanan, P.D. Thomas, C.H. Wu, C. Yeats & S.Y. Yong, (2012) InterPro in 2011: new developments in the family and domain prediction database. *Nucleic Acids Res* **40**: D306-312.

Hurst, L.D., (2002) The Ka/Ks ratio: diagnosing the form of sequence evolution. *Trends Genet* **18**: 486.

Hutchings, M.I., T. Palmer, D.J. Harrington & I.C. Sutcliffe, (2009) Lipoprotein biogenesis in Gram-positive bacteria: knowing when to hold 'em, knowing when to fold 'em. *Trends Microbiol* **17**: 13-21.

Ikeda, M., T. Sato, M. Wachi, H.K. Jung, F. Ishino, Y. Kobayashi & M. Matsuhashi, (1989) Structural similarity among *Escherichia coli* FtsW and RodA proteins and *Bacillus subtilis* SpoVE protein, which function in cell division, cell elongation, and spore formation, respectively. *J Bacteriol* **171**: 6375-6378.

Imamura, D., R. Zhou, M. Feig & L. Kroos, (2008) Evidence that the *Bacillus subtilis* SpoIIGA protein is a novel type of signal-transducing aspartic protease. *J Biol Chem* **283**: 15287-15299.

Ipsen, J.H., G. Karlstrom, O.G. Mouritsen, H. Wennerstrom & M.J. Zuckermann, (1987) Phase equilibria in the phosphatidylcholine-cholesterol system. *Biochem Biophys Acta* **905**: 162-172.

Ishikawa, S., K. Yamane & J. Sekiguchi, (1998) Regulation and characterization of a newly deduced cell wall hydrolase gene (*cwlJ*) which affects germination of *Bacillus subtilis* spores. *J Bacteriol* **180**: 1375-1380.

Ishino, F., H.K. Jung, M. Ikeda, M. Doi, M. Wachi & M. Matsuhashi, (1989) New mutations *fts-36*, *lts-33*, and *ftsW* clustered in the mra region of the *Escherichia coli* chromosome induce thermosensitive cell growth and division. *J Bacteriol* **171**: 5523-5530.

Jacobowitz, D.M. & A.T. Kallarakal, (2004) Flotillin-1 in the substantia nigra of the Parkinson brain and a predominant localization in catecholaminergic nerves in the rat brain. *Neurotox Res* **6**: 245-257.

Jakimowicz, D., P. Zydek, A. Kois, J. Zakrzewska-Czerwinska & K.F. Chater, (2007) Alignment of multiple chromosomes along helical ParA scaffolding in sporulating *Streptomyces* hyphae. *Mol Microbiol* **65**: 625-641.

Jeong, J. & A.P. McMahon, (2002) Cholesterol modification of Hedgehog family proteins. *J Clin Invest* **110**: 591-596.

Jones, L.J., R. Carballido-Lopez & J. Errington, (2001) Control of cell shape in bacteria: helical, actin-like filaments in *Bacillus subtilis*. *Cell* **104**: 913-922.

Jones, S. & J.M. Thornton, (1996) Principles of protein-protein interactions. *Proc Natl Acad Sci USA* **93**: 13-20.

Jorasch, P., F.P. Wolter, U. Zahringer & E. Heinz, (1998) A UDP glucosyltransferase from *Bacillus subtilis* successively transfers up to four glucose residues to 1,2-diacylglycerol: expression of *ypfP* in *Escherichia coli* and structural analysis of its reaction products. *Mol Microbiol* **29**: 419-430.

Junier I., O. Rivoire, (2016) Conserved Units of Co-Expression in Bacterial Genomes: An Evolutionary Insight into Transcriptional Regulation. *PLoS One* **11**(5): e0155740.

Jyothikumar, V., K. Klanbut, J. Tiong, J.S. Roxburgh, I.S. Hunter, T.K. Smith & P.R. Herron, (2012) Cardiolipin synthase is required for *Streptomyces coelicolor* morphogenesis. *Mol Microbiol* **84**: 181-197.

Jyothikumar, V., E.J. Tilley, R. Wali & P.R. Herron, (2008) Time-lapse microscopy of *Streptomyces* coelicolor growth and sporulation. *Appl Environ Microbiol* 74**:** 6774-6781.

Kaiser, S.E., B.E. Riley, T.A. Shaler, R.S. Trevino, C.H. Becker, H. Schulman & R.R. Kopito, (2011) Protein standard absolute quantification (PSAQ) method for the measurement of cellular ubiquitin pools. *Nat Methods* **8**: 691-696.

Kang, C.M., S. Nyayapathy, J.Y. Lee, J.W. Suh & R.N. Husson, (2008) Wag31, a homologue of the cell division protein DivIVA, regulates growth, morphology and polar cell wall synthesis in mycobacteria. *Microbiology* **154**: 725-735.

Karasinska, J.M. & M.R. Hayden, (2011) Cholesterol metabolism in Huntington disease. *Nat Rev Neurol* **7**: 561-572.

Karimova, G., J. Pidoux, A. Ullmann & D. Ladant, (1998) A bacterial two-hybrid system based on a reconstituted signal transduction pathway. *Proc Natl Acad Sci USA* **95**: 5752-5756.

Karimova, G., A. Ullmann & D. Ladant, (2000) Bordetella pertussis adenylate cyclase toxin as a tool to analyze molecular interactions in a bacterial two-hybrid system. *Int J Med Microbiol* **290**: 441-445.

Karnovsky, M.J., A.M. Kleinfeld, R.L. Hoover & R.D. Klausner, (1982) The concept of lipid domains in membranes. *J Cell Biol* **94**: 1-6.

Karoui, M.E. & J. Errington, (2001) Isolation and characterization of topological specificity mutants of minD in *Bacillus subtilis*. *Mol Microbiol* **42**: 1211-1221.

Kato, Y., (2015) Tunable translational control using site-specific unnatural amino acid incorporation in *Escherichia coli*. *PeerJ* **3**: e904.

Katz, B. & R. Miledi, (1973) The characteristics of 'end-plate noise' produced by different depolarizing drugs. *J Physiol* **230**: 707-717.

Kawai, F., M. Shoda, R. Harashima, Y. Sadaie, H. Hara & K. Matsumoto, (2004) Cardiolipin domains in *Bacillus subtilis* marburg membranes. *J Bacteriol* **186**: 1475-1483.

Kawai, Y., R.A. Daniel & J. Errington, (2009) Regulation of cell wall morphogenesis in *Bacillus subtilis* by recruitment of PBP1 to the MreB helix. *Mol Microbiol* **71**: 1131-1144.

Kawai, Y. & N. Ogasawara, (2006) *Bacillus subtilis* EzrA and FtsL synergistically regulate FtsZ ring dynamics during cell division. *Microbiology* **152**: 1129-1141.

Keijser, B.J., E.E. Noens, B. Kraal, H.K. Koerten & G.P. van Wezel, (2003) The *Streptomyces coelicolor ssgB* gene is required for early stages of sporulation. *FEMS Microbiol Lett* **225**: 59-67.

Keijser, B.J., G.P. van Wezel, G.W. Canters & E. Vijgenboom, (2002) Developmental regulation of the *Streptomyces lividans ram* genes: involvement of RamR in regulation of the *ramCSAB* operon. *J Bacteriol* **184**: 4420-4429.

Kelemen, G.H., P.H. Viollier, J. Tenor, L. Marri, M.J. Buttner & C.J. Thompson, (2001) A connection between stress and development in the multicellular prokaryote *Streptomyces coelicolor* A3(2). *Mol Microbiol* **40**: 804-814.

Kerner, M.J., D.J. Naylor, Y. Ishihama, T. Maier, H.C. Chang, A.P. Stines, C. Georgopoulos, D. Frishman, M. Hayer-Hartl, M. Mann & F.U. Hartl, (2005) Proteome-wide analysis of chaperonin-dependent protein folding in *Escherichia coli*. *Cell* **122**: 209-220.

Kers, J.A., K.D. Cameron, M.V. Joshi, R.A. Bukhalid, J.E. Morello, M.J. Wach, D.M. Gibson & R. Loria, (2005) A large, mobile pathogenicity island confers plant pathogenicity on *Streptomyces* species. *Mol Microbiol* **55**: 1025-1033.

Kiebish, M.A., X. Han, H. Cheng, J.H. Chuang & T.N. Seyfried, (2008) Cardiolipin and electron transport chain abnormalities in mouse brain tumor mitochondria: lipidomic evidence supporting the Warburg theory of cancer. *J Lipid Res* **49**: 2545-2556.

Kiernan, J.A., (2007) Indigogenic substrates for detection and localization of enzymes. *Biotech Histochem* **82**: 73-103.

Kierszniowska, S., B. Seiwert & W.X. Schulze, (2009) Definition of Arabidopsis sterol-rich membrane microdomains by differential treatment with methyl-beta-cyclodextrin and quantitative proteomics. *Mol Cell Proteomics* **8**: 612-623.

Kieser, T., M.J. Bibb, K.F. Chater, D.A. Hopwood & M.J. Buttner, (2000) Practical *Streptomyces* Genetics. John Innes Foundation.

Kikuchi, S., I. Shibuya & K. Matsumoto, (2000) Viability of an *Escherichia coli* pgsA null mutant lacking detectable phosphatidylglycerol and cardiolipin. *J Bacteriol* **182**: 371-376.

Kim, K.S., J.S. Kim, J.Y. Park, Y.H. Suh, I. Jou, E.H. Joe & S.M. Park, (2013) DJ-1 associates with lipid rafts by palmitoylation and regulates lipid rafts-dependent endocytosis in astrocytes. *Human Mol Genet* **22**: 4805-4817.

Kim, S.H., B.R. Lee, J.N. Kim & B.G. Kim, (2012) NdgR, a common transcriptional activator for methionine and leucine biosynthesis in *Streptomyces coelicolor*. *J Bacteriol* **194**: 6837-6846.

Kimura, A., C.A. Baumann, S.H. Chiang & A.R. Saltiel, (2001) The sorbin homology domain: a motif for the targeting of proteins to lipid rafts. *Proc Natl Acad Sci USA* **98**: 9098-9103.

King, G.F., S.L. Rowland, B. Pan, J.P. Mackay, G.P. Mullen & L.I. Rothfield, (1999) The dimerization and topological specificity functions of MinE reside in a structurally autonomous C-terminal domain. *Mol Microbiol* **31**: 1161-1169.

Kioka, N., K. Ueda & T. Amachi, (2002) Vinexin, CAP/ponsin, ArgBP2: a novel adaptor protein family regulating cytoskeletal organization and signal transduction. *Cell Struct Funct* **27**: 1-7.

Kiriukhin, M.Y., D.V. Debabov, D.L. Shinabarger & F.C. Neuhaus, (2001) Biosynthesis of the glycolipid anchor in lipoteichoic acid of *Staphylococcus aureus* RN4220: role of YpfP, the diglucosyldiacylglycerol synthase. *J Bacteriol* **183**: 3506-3514.

Kleinschnitz, E.M., A. Heichlinger, K. Schirner, J. Winkler, A. Latus, I. Maldener, W. Wohlleben & G. Muth, (2011a) Proteins encoded by the mre gene cluster in *Streptomyces coelicolor* A3(2) cooperate in spore wall synthesis. *Mol Microbiol* **79**: 1367-1379.

Kleinschnitz, E.M., A. Latus, S. Sigle, I. Maldener, W. Wohlleben & G. Muth, (2011b) Genetic analysis of SCO2997, encoding a TagF homologue, indicates a role for wall teichoic acids in sporulation of *Streptomyces coelicolor* A3(2). *J Bacteriol* **193**: 6080-6085.

Klose, C., C.S. Ejsing, A.J. Garcia-Saez, H.J. Kaiser, J.L. Sampaio, M.A. Surma, A. Shevchenko, P. Schwille & K. Simons, (2010) Yeast lipids can phase-separate into micrometer-scale membrane domains. *J Biol Chem* **285**: 30224-30232.

Koch, A.L., (2000) The exoskeleton of bacterial cells (the sacculus): still a highly attractive target for antibacterial agents that will last for a long time. *Crit Rev Microbiol* **26**: 1-35.

Kodani, S., M.E. Hudson, M.C. Durrant, M.J. Buttner, J.R. Nodwell & J.M. Willey, (2004) The SapB morphogen is a lantibiotic-like peptide derived from the product of the developmental gene *ramS* in *Streptomyces coelicolor*. *Proc Natl Acad Sci USA* **101**: 11448-11453.

Kokubo, H., J.B. Helms, Y. Ohno-Iwashita, Y. Shimada, Y. Horikoshi & H. Yamaguchi, (2003) Ultrastructural localization of flotillin-1 to cholesterol-rich membrane microdomains, rafts, in rat brain tissue. *Brain Res* **965**: 83-90.

Kokubo, H., C.A. Lemere & H. Yamaguchi, (2000) Localization of flotillins in human brain and their accumulation with the progression of Alzheimer's disease pathology. *Neurosci Lett* **290**: 93-96.

Korade, Z. & A.K. Kenworthy, (2008) Lipid rafts, cholesterol, and the brain. *Neuropharmacology* **55**: 1265-1273.

Kormanec, J. & B. Sevcikova, (2002a) The stress-response sigma factor sigma(H) controls the expression of *ssgB*, a homologue of the sporulation-specific cell division gene ssgA, in *Streptomyces coelicolor* A3(2). *Mol Genet Genomics* **267**: 536-543.

Kormanec, J. & B. Sevcikova, (2002b) Stress-response sigma factor sigma(H) directs expression of the gltB gene encoding glutamate synthase in *Streptomyces coelicolor* A3(2). *Biochim Biophys Acta* **1577**: 149-154.

Kormanec, J., B. Sevcikova, N. Halgasova, R. Knirschova & B. Rezuchova, (2000) Identification and transcriptional characterization of the gene encoding the stress-response sigma factor sigma(H) in *Streptomyces coelicolor* A3(2). *FEMS Microbiol Lett* **189**: 31-38.

Kovacs, M., A. Halfmann, I. Fedtke, M. Heintz, A. Peschel, W. Vollmer, R. Hakenbeck & R. Bruckner, (2006) A functional dlt operon, encoding proteins required for incorporation of d-alanine in teichoic acids in gram-positive bacteria, confers resistance to cationic antimicrobial peptides in *Streptococcus pneumoniae*. *J Bacteriol* **188**: 5797-5805.

Kreutzenbeck, P., C. Kroger, F. Lausberg, N. Blaudeck, G.A. Sprenger & R. Freudl, (2007) *Escherichia coli* twin arginine (Tat) mutant translocases possessing relaxed signal peptide recognition specificities. *J Biol Chem* **282**: 7903-7911.

Kruse, T. & K. Gerdes, (2005) Bacterial DNA segregation by the actin-like MreB protein. *Trends Cell Biol* **15**: 343-345.

Kurokawa, K., H. Lee, K.B. Roh, M. Asanuma, Y.S. Kim, H. Nakayama, A. Shiratsuchi, Y. Choi, O. Takeuchi, H.J. Kang, N. Dohmae, Y. Nakanishi, S. Akira, K. Sekimizu & B.L. Lee, (2009) The Triacylated ATP Binding Cluster Transporter Substrate-binding Lipoprotein of *Staphylococcus aureus* Functions as a Native Ligand for Toll-like Receptor 2. *J Biol Chem* **284**: 8406-8411.

Kuwahara, Y., A. Ohno, T. Morii, H. Yokoyama, I. Matsui, H. Tochio, M. Shirakawa & H. Hiroaki, (2008) The solution structure of the C-terminal domain of NfeD reveals a novel membrane-anchored OB-fold. *Protein Sci* **17**: 1915-1924.

Kuwahara, Y., S. Unzai, T. Nagata, Y. Hiroaki, H. Yokoyama, I. Matsui, T. Ikegami, Y. Fujiyoshi & H. Hiroaki, (2009) Unusual thermal disassembly of the SPFH domain oligomer from *Pyrococcus horikoshii*. *Biophys J* **97**: 2034-2043.

Ladant, D., P. Glaser & A. Ullmann, (1992) Insertional mutagenesis of *Bordetella pertussis* adenylate cyclase. *J Biol Chem* **267**: 2244-2250.

Ladant, D., S. Michelson, R. Sarfati, A.M. Gilles, R. Predeleanu & O. Barzu, (1989) Characterization of the calmodulin-binding and of the catalytic domains of *Bordetella pertussis* adenylate cyclase. *J Biol Chem* **264**: 4015-4020.

Ladwig, N., M. Franz-Wachtel, F. Hezel, B. Soufi, B. Macek, W. Wohlleben & G. Muth, (2015) Control of Morphological Differentiation of *Streptomyces coelicolor* A3(2) by Phosphorylation of MreC and PBP2. *PLoS One* **10**: e0125425.

Laloi, M., A.M. Perret, L. Chatre, S. Melser, C. Cantrel, M.N. Vaultier, A. Zachowski, K. Bathany, J.M. Schmitter, M. Vallet, R. Lessire, M.A. Hartmann & P. Moreau, (2007) Insights

into the role of specific lipids in the formation and delivery of lipid microdomains to the plasma membrane of plant cells. *Plant Physiol* **143**: 461-472.

Lambert, P.A., (2002) Cellular impermeability and uptake of biocides and antibiotics in Gram-positive bacteria and mycobacteria. Symposium series: 46S-54S.

Lang, D.M., S. Lommel, M. Jung, R. Ankerhold, B. Petrausch, U. Laessing, M.F. Wiechers, H. Plattner & C.A. Stuermer, (1998) Identification of reggie-1 and reggie-2 as plasmamembrane-associated proteins which cocluster with activated GPI-anchored cell adhesion molecules in non-caveolar micropatches in neurons. *J Neurobiol* **37**: 502-523.

Langhorst, M.F., A. Reuter & C.A. Stuermer, (2005) Scaffolding microdomains and beyond: the function of reggie/flotillin proteins. *Cell Mol Life Sci* **62**: 2228-2240.

Langhorst, M.F., G.P. Solis, S. Hannbeck, H. Plattner & C.A. Stuermer, (2007) Linking membrane microdomains to the cytoskeleton: regulation of the lateral mobility of reggie-1/flotillin-2 by interaction with actin. *FEBS Lett* **581**: 4697-4703.

Larkin, M.A., G. Blackshields, N.P. Brown, R. Chenna, P.A. McGettigan, H. McWilliam, F. Valentin, I.M. Wallace, A. Wilm, R. Lopez, J.D. Thompson, T.J. Gibson & D.G. Higgins, (2007) Clustal W and Clustal X version 2.0. *Bioinformatics* **23**: 2947-2948.

Le, A.T. & W. Schumann, (2009) The Spo0E phosphatase of *Bacillus subtilis* is a substrate of the FtsH metalloprotease. *Microbiology* **155**: 1122-1132.

LeDeaux, J.R. & A.D. Grossman, (1995) Isolation and characterization of *kinC*, a gene that encodes a sensor kinase homologous to the sporulation sensor kinases KinA and KinB in *Bacillus subtilis*. *J Bacteriol* **177**: 166-175.

Lee, E.J., N. Karoonuthaisiri, H.S. Kim, J.H. Park, C.J. Cha, C.M. Kao & J.H. Roe, (2005) A master regulator sigmaB governs osmotic and oxidative response as well as differentiation via a network of sigma factors in *Streptomyces coelicolor*. *Mol Microbiol* **57**: 1252-1264.

Lee, T.H., W. McKleroy, A. Khalifeh-Soltani, S. Sakuma, S. Lazarev, K. Riento, S.L. Nishimura, B.J. Nichols & K. Atabai, (2014) Functional genomic screen identifies novel mediators of collagen uptake. *Mol Biol Cell*.

Lefebvre, B., F. Furt, M.A. Hartmann, L.V. Michaelson, J.P. Carde, F. Sargueil-Boiron, M. Rossignol, J.A. Napier, J. Cullimore, J.J. Bessoule & S. Mongrand, (2007) Characterization of lipid rafts from *Medicago truncatula* root plasma membranes: a proteomic study reveals the presence of a raft-associated redox system. *Plant Physiol* **144**: 402-418.

Lenarcic, R., S. Halbedel, L. Visser, M. Shaw, L.J. Wu, J. Errington, D. Marenduzzo & L.W. Hamoen, (2009) Localisation of DivIVA by targeting to negatively curved membranes. *EMBO J* **28**: 2272-2282.

Leopold, K. & W. Fischer, (1992) Hydrophobic interaction chromatography fractionates lipoteichoic acid according to the size of the hydrophilic chain: a comparative study with

anion-exchange and affinity chromatography for suitability in species analysis. *Anal Biochem 201*: 350-355.

Leskiw, B.K., E.J. Lawlor, J.M. Fernandez-Abalos & K.F. Chater, (1991) TTA codons in some genes prevent their expression in a class of developmental, antibiotic-negative, *Streptomyces* mutants. *Proc Natl Acad Sci USA* **88**: 2461-2465.

Letek, M., E. Ordonez, J. Vaquera, W. Margolin, K. Flardh, L.M. Mateos & J.A. Gil, (2008) DivIVA is required for polar growth in the MreB-lacking rod-shaped actinomycete *Corynebacterium glutamicum*. *J Bacteriol* **190**: 3283-3292.

Levental, I., M. Grzybek & K. Simons, (2010) Greasing their way: lipid modifications determine protein association with membrane rafts. *Biochemistry* **49**: 6305-6316.

Levin, P.A., N. Fan, E. Ricca, A. Driks, R. Losick & S. Cutting, (1993) An unusually small gene required for sporulation by *Bacillus subtilis*. *Mol Microbiol* **9**: 761-771.

Levin, P.A., I.G. Kurtser & A.D. Grossman, (1999) Identification and characterization of a negative regulator of FtsZ ring formation in *Bacillus subtilis*. *Proc Natl Acad Sci USA* **96**: 9642-9647.

Levin, P.A. & R. Losick, (1996) Transcription factor Spo0A switches the localization of the cell division protein FtsZ from a medial to a bipolar pattern in *Bacillus subtilis*. *Genes Dev* 10: 478-488.

Levin, P.A., P.S. Margolis, P. Setlow, R. Losick & D. Sun, (1992) Identification of *Bacillus subtilis* genes for septum placement and shape determination. *J Bacteriol* **174**: 6717-6728.

Lewis, J.C., N.S. Snell & H.K. Burr, (1960) Water Permeability of Bacterial Spores and the Concept of a Contractile Cortex. *Science* **132**: 544-545.

Liu, B., L. Persons, L. Lee & P.A. de Boer, (2015) Roles for both FtsA and the FtsBLQ subcomplex in FtsN-stimulated cell constriction in *Escherichia coli*. *Mol Microbiol* **95**: 945-970.

Liu, J., S.M. Deyoung, M. Zhang, L.H. Dold & A.R. Saltiel, (2005) The stomatin/prohibitin/flotillin/HflK/C domain of flotillin-1 contains distinct sequences that direct plasma membrane localization and protein interactions in 3T3-L1 adipocytes. *J Biol Chem* **280**: 16125-16134.

Lodish, H.F., (1988) Multi-spanning membrane proteins: how accurate are the models? *Trends Biochem Sci* **13**: 332-334.

Lonetto, M.A., K.L. Brown, K.E. Rudd & M.J. Buttner, (1994) Analysis of the *Streptomyces coelicolor sigE* gene reveals the existence of a subfamily of eubacterial RNA polymerase sigma factors involved in the regulation of extracytoplasmic functions. *Proc Natl Acad Sci USA* **91**: 7573-7577.

Lopez, D., M.A. Fischbach, F. Chu, R. Losick & R. Kolter, (2009) Structurally diverse natural products that cause potassium leakage trigger multicellularity in *Bacillus subtilis*. *Proc Natl Acad Sci USA* **106**: 280-285.

Lopez, D. & R. Kolter, (2010) Functional microdomains in bacterial membranes. *Genes Dev* **24**: 1893-1902.

Lorenz, M.G. & W. Wackernagel, (1994) Bacterial gene transfer by natural genetic transformation in the environment. *Microbiol Rev* **58**: 563-602.

Loria, R., D.R. Bignell, S. Moll, J.C. Huguet-Tapia, M.V. Joshi, E.G. Johnson, R.F. Seipke & D.M. Gibson, (2008) Thaxtomin biosynthesis: the path to plant pathogenicity in the genus *Streptomyces*. *Antonie van Leeuwenhoek* **94**: 3-10.

Lowe, J. & L.A. Amos, (1998) Crystal structure of the bacterial cell-division protein FtsZ. *Nature* **391**: 203-206.

Lowe, J., A. Ellonen, M.D. Allen, C. Atkinson, D.J. Sherratt & I. Grainge, (2008) Molecular mechanism of sequence-directed DNA loading and translocation by FtsK. *Mol Cell* **31**: 498-509.

Lu, S., S. Cutting & L. Kroos, (1995) Sporulation protein SpoIVFB from *Bacillus subtilis* enhances processing of the sigma factor precursor Pro-sigma K in the absence of other sporulation gene products. *J Bacteriol* **177**: 1082-1085.

Luevano-Martinez, L.A., (2015) The chimeric origin of the cardiolipin biosynthetic pathway in the Eukarya domain. *Biochem Biophys Acta* **1847**: 599-606.

Luger, K., (2003) Structure and dynamic behavior of nucleosomes. *Curr Opin Genet Dev* **13**: 127-135.

Luirink, J. & I. Sinning, (2004) SRP-mediated protein targeting: structure and function revisited. *Biochem Biophys Acta* **1694**: 17-35.

Ma, H. & K. Kendall, (1994) Cloning and analysis of a gene cluster from *Streptomyces coelicolor* that causes accelerated aerial mycelium formation in *Streptomyces lividans*. *J Bacteriol* **176**: 3800-3811.

MacNeil, D.J., K.M. Gewain, C.L. Ruby, G. Dezeny, P.H. Gibbons & T. MacNeil, (1992) Analysis of *Streptomyces avermitilis* genes required for avermectin biosynthesis utilizing a novel integration vector. *Gene* **111**: 61-68.

Madigan, M.T., J.M. Martinko, D.A. Stahl & D.P. Clark, (2012) Brock Biology of Microorganisms. Benjamin Cummins.

Mahato, S.B., A.K. Nandy & G. Roy, (1992) Triterpenoids. *Phytochemistry* **31**: 2199-2149.

Mahato, S.B. & S. Sen, (1997) Advances in triterpenoid research, 1990-1994. *Phytochemistry* **44**: 1185-1236.

Malaga-Trillo, E., U. Laessing, D.M. Lang, A. Meyer & C.A. Stuermer, (2002) Evolution of duplicated reggie genes in zebrafish and goldfish. *J Mol Evol* **54**: 235-245.

Maloney, E., S.C. Madiraju, M. Rajagopalan & M. Madiraju, (2011) Localization of acidic phospholipid cardiolipin and DnaA in mycobacteria. *Tuberculosis* **91** Suppl 1: S150-155.

Malott, R.J., B.R. Steen-Kinnaird, T.D. Lee & D.P. Speert, (2012) Identification of hopanoid biosynthesis genes involved in polymyxin resistance in *Burkholderia multivorans*. *Antimicrob Agents Chemother* **56**: 464-471.

Mancini, F. & A. Ciervo, (2015) Enzymatic characterization of *Chlamydophila pneumoniae* phospholipase D. *New Microbiol* **38**: 59-66.

Marston, A.L., H.B. Thomaides, D.H. Edwards, M.E. Sharpe & J. Errington, (1998) Polar localization of the MinD protein of *Bacillus subtilis* and its role in selection of the mid-cell division site. *Genes Dev* **12**: 3419-3430.

Martinez, Z., M. Zhu, S. Han & A.L. Fink, (2007) GM1 specifically interacts with alpha-synuclein and inhibits fibrillation. *Biochemistry* **46**: 1868-1877.

Massey, T.H., C.P. Mercogliano, J. Yates, D.J. Sherratt & J. Lowe, (2006) Double-stranded DNA translocation: structure and mechanism of hexameric FtsK. *Mol cell* **23**: 457-469.

Masson, S., T. Kern, A. Le Gouellec, C. Giustini, J.P. Simorre, P. Callow, T. Vernet, F. Gabel & A. Zapun, (2009) Central domain of DivIB caps the C-terminal regions of the FtsL/DivIC coiled-coil rod. *J Biol Chem* **284**: 27687-27700.

Matmati, N. & Y.A. Hannun, (2008) Thematic review series: sphingolipids. ISC1 (inositol phosphosphingolipid-phospholipase C), the yeast homologue of neutral sphingomyelinases. *J Lipid Res* **49**: 922-928.

McArthur, M. & M.J. Bibb, (2008) Manipulating and understanding antibiotic production in *Streptomyces coelicolor* A3(2) with decoy oligonucleotides. *Proc Natl Acad Sci USA* **105**: 1020-1025.

McCormick, J.R. & K. Flardh, (2012) Signals and regulators that govern *Streptomyces* development. *FEMS Microbol Rev* **36**: 206-231.

McGuinn, K.P. & M.G. Mahoney, (2014) Lipid rafts and detergent-resistant membranes in epithelial keratinocytes. *Methods Mol Biol* **1195**: 133-144.

McKenney, P.T., A. Driks & P. Eichenberger, (2013) The *Bacillus subtilis* endospore: assembly and functions of the multilayered coat. *Nat Rev Microbiol* **11**: 33-44.

McKenney, P.T., A. Driks, H.A. Eskandarian, P. Grabowski, J. Guberman, K.H. Wang, Z. Gitai & P. Eichenberger, (2010) A distance-weighted interaction map reveals a previously uncharacterized layer of the *Bacillus subtilis* spore coat. *Curr Biol* **20**: 934-938.

McKenney, P.T. & P. Eichenberger, (2012) Dynamics of spore coat morphogenesis in *Bacillus subtilis*. *Mol Microbiol* **83**: 245-260.

Meyer, P., J. Gutierrez, K. Pogliano & J. Dworkin, (2010) Cell wall synthesis is necessary for membrane dynamics during sporulation of *Bacillus subtilis*. *Mol Microbiol* **76**: 956-970.

Mielich-Suss, B., J. Schneider & D. Lopez, (2013) Overproduction of flotillin influences cell differentiation and shape in *Bacillus subtilis*. *mBio* **4**: e00719-00713.

Mielich-Suss, B., R.M. Wagner, N. Mietrach, T. Hertlein, G. Marincola, K. Ohlsen, S. Geibel & D. Lopez, (2017) Flotillin scaffold activity contributes to type VII secretion system assembly in *Staphylococcus aureus*. *PLoS Pathog* **13**: e1006728.

Miguelez, E.M., C. Martin, M.B. Manzanal & C. Hardisson, (1992) Growth and morphogenesis in *Streptomyces*. *FEMS Microbiol Lett* **79**: 351-359.

Mileykovskaya, E., (2007) Subcellular localization of *Escherichia coli* osmosensory transporter ProP: focus on cardiolipin membrane domains. *Mol Microbiol* **64**: 1419-1422.

Mileykovskaya, E. & W. Dowhan, (2000) Visualization of phospholipid domains in *Escherichia coli* by using the cardiolipin-specific fluorescent dye 10-N-nonyl acridine orange. *J Bacteriol* **182**: 1172-1175.

Mileykovskaya, E. & W. Dowhan, (2005) Role of membrane lipids in bacterial division-site selection. *Curr Opin Microbiol* **8**: 135-142.

Mileykovskaya, E., M. Zhang & W. Dowhan, (2005) Cardiolipin in energy transducing membranes. *Biochemistry* **70**: 154-158.

Miller, S.I., A.M. Kukral & J.J. Mekalanos, (1989) A two-component regulatory system (phoP phoQ) controls *Salmonella typhimurium* virulence. *Proc Natl Acad Sci USA* **86**: 5054-5058.

Mills, J.S. & A.E.A. Werner, (1955) The chemistry of dammar resin. *J Chem Soc* 3132-3140.

Mitchell, A.P., (1998) Dimorphism and virulence in *Candida albicans*. *Curr Opin Microbiol* **1**: 687-692.

Mohammadi, T., A. Karczmarek, M. Crouvoisier, A. Bouhss, D. Mengin-Lecreulx & T. den Blaauwen, (2007) The essential peptidoglycan glycosyltransferase MurG forms a complex with proteins involved in lateral envelope growth as well as with proteins involved in cell division in *Escherichia coli*. *Mol Microbiol* **65**: 1106-1121.

Mohammadi, T., V. van Dam, R. Sijbrandi, T. Vernet, A. Zapun, A. Bouhss, M. Diepeveen-de Bruin, M. Nguyen-Disteche, B. de Kruijff & E. Breukink, (2011) Identification of FtsW as a transporter of lipid-linked cell wall precursors across the membrane. *EMBO J* **30**: 1425-1432.

Molle, V., M. Fujita, S.T. Jensen, P. Eichenberger, J.E. Gonzalez-Pastor, J.S. Liu & R. Losick, (2003) The Spo0A regulon of *Bacillus subtilis*. *Mol Microbiol* **50**: 1683-1701.

Mongrand, S., J. Morel, J. Laroche, S. Claverol, J.P. Carde, M.A. Hartmann, M. Bonneu, F. Simon-Plas, R. Lessire & J.J. Bessoule, (2004) Lipid rafts in higher plant cells: purification and characterization of Triton X-100-insoluble microdomains from tobacco plasma membrane. *J Biol Chem* **279**: 36277-36286.

Morel, J., S. Claverol, S. Mongrand, F. Furt, J. Fromentin, J.J. Bessoule, J.P. Blein & F. Simon-Plas, (2006) Proteomics of plant detergent-resistant membranes. *Mol Cell Proteomics* **5**: 1396-1411.

Morrow, I.C. & R.G. Parton, (2005) Flotillins and the PHB domain protein family: rafts, worms and anaesthetics. Traffic 6: 725-740.

Morrow, I.C., S. Rea, S. Martin, I.A. Prior, R. Prohaska, J.F. Hancock, D.E. James & R.G. Parton, (2002) Flotillin-1/reggie-2 traffics to surface raft domains via a novel golgi-independent pathway. Identification of a novel membrane targeting domain and a role for palmitoylation. *J Biol Chem* **277**: 48834-48841.

Mueller, J.P. & A.L. Sonenshein, (1992) Role of the *Bacillus subtilis gsiA* gene in regulation of early sporulation gene expression. *J Bacteriol* **174**: 4374-4383.

Mukhopadhyay, R., K.C. Huang & N.S. Wingreen, (2008) Lipid localization in bacterial cells through curvature-mediated microphase separation. *Biophys J* **95**: 1034-1049.

Muller, P., C. Ewers, U. Bertsche, M. Anstett, T. Kallis, E. Breukink, C. Fraipont, M. Terrak, M. Nguyen-Disteche & W. Vollmer, (2007) The essential cell division protein FtsN interacts with the murein (peptidoglycan) synthase PBP1B in *Escherichia coli*. *J Biol Chem* **282**: 36394-36402.

Munita, J.M. & C.A. Arias, (2016) Mechanisms of Antibiotic Resistance. *Microbiol Spectr* **4**.

Murphy, K.C., (1998) Use of bacteriophage lambda recombination functions to promote gene replacement in *Escherichia coli*. *J Bacteriol* **180**: 2063-2071.

Nakae, K., Y. Yoshimoto, T. Sawa, Y. Homma, M. Hamada, T. Takeuchi & M. Imoto, (2000) Migrastatin, a new inhibitor of tumor cell migration from *Streptomyces* sp. MK929-43F1. Taxonomy, fermentation, isolation and biological activities. *J Antibiotic* **53**: 1130-1136.

Narita, S., S. Matsuyama & H. Tokuda, (2004) Lipoprotein trafficking in *Escherichia coli*. *Arch Microbiol* **182**: 1-6.

Natale, P., T. Bruser & A.J. Driessen, (2008) Sec- and Tat-mediated protein secretion across the bacterial cytoplasmic membrane--distinct translocases and mechanisms. *Biochem Biophys Acta* **1778**: 1735-1756.

Natale, P., M. Pazos & M. Vicente, (2013) The *Escherichia coli* divisome: born to divide. *Environ Microbiol* **15**: 3169-3182.

Nebl, T., K.N. Pestonjamasp, J.D. Leszyk, J.L. Crowley, S.W. Oh & E.J. Luna, (2002) Proteomic analysis of a detergent-resistant membrane skeleton from neutrophil plasma membranes. *J Biol Chem* **277**: 43399-43409.

Neubauer, C., N.F. Dalleska, E.S. Cowley, N.J. Shikuma, C.H. Wu, A.L. Sessions & D.K. Newman, (2015) Lipid remodeling in *Rhodopseudomonas palustris* TIE-1 upon loss of hopanoids and hopanoid methylation. *Geobiology* **13**: 443-453.

Neuhaus, F.C. & J. Baddiley, (2003) A continuum of anionic charge: structures and functions of D-alanyl-teichoic acids in gram-positive bacteria. *Microbiol Mol Biol Rev* **67**: 686-723.

Neumann-Giesen, C., B. Falkenbach, P. Beicht, S. Claasen, G. Luers, C.A. Stuermer, V. Herzog & R. Tikkanen, (2004) Membrane and raft association of reggie-1/flotillin-2: role of myristoylation, palmitoylation and oligomerization and induction of filopodia by overexpression. *Biochem J* **378**: 509-518.

Nijtmans, L.G., S.M. Artal, L.A. Grivell & P.J. Coates, (2002) The mitochondrial PHB complex: roles in mitochondrial respiratory complex assembly, ageing and degenerative disease. *Cell Mol Life Sci* **59**: 143-155.

Nimrichter, L., M.D. Cerqueira, E.A. Leitao, K. Miranda, E.S. Nakayasu, S.R. Almeida, I.C. Almeida, C.S. Alviano, E. Barreto-Bergter & M.L. Rodrigues, (2005) Structure, cellular distribution, antigenicity, and biological functions of *Fonsecaea pedrosoi* ceramide monohexosides. *Infect Immun* **73**: 7860-7868.

Nimrichter, L. & M.L. Rodrigues, (2011) Fungal glucosylceramides: from structural components to biologically active targets of new antimicrobials. *Front Microbiol* **2**: 212.

Nodwell, J.R., K. McGovern & R. Losick, (1996) An oligopeptide permease responsible for the import of an extracellular signal governing aerial mycelium formation in *Streptomyces coelicolor*. *Mol Microbiol* **22**: 881-893.

Noens, E.E., V. Mersinias, J. Willemse, B.A. Traag, E. Laing, K.F. Chater, C.P. Smith, H.K. Koerten & G.P. van Wezel, (2007) Loss of the controlled localization of growth stage-specific cell-wall synthesis pleiotropically affects developmental gene expression in an *ssgA* mutant of *Streptomyces coelicolor*. *Mol Microbiol* **64**: 1244-1259.

Nogales, E., S.G. Wolf & K.H. Downing, (1998) Structure of the alpha beta tubulin dimer by electron crystallography. *Nature* **391**: 199-203.

O'Connor, T.J., P. Kanellis & J.R. Nodwell, (2002) The *ramC* gene is required for morphogenesis in *Streptomyces coelicolor* and expressed in a cell type-specific manner under the direct control of RamR. *Mol Microbiol* **45**: 45-57.

O'Daniel, P.I., J. Zajicek, W. Zhang, Q. Shi, J.F. Fisher & S. Mobashery, (2010) Elucidation of the structure of the membrane anchor of penicillin-binding protein 5 of *Escherichia coli*. *J Am Chem Soc* **132**: 4110-4118.

Ogura, M., J. Yamaki, M.K. Homma & Y. Homma, (2014) Phosphorylation of flotillin-1 by mitochondrial c-Src is required to prevent the production of reactive oxygen species. *FEBS Lett* **588**: 2837-2843.

Ohlsen, K.L., J.K. Grimsley & J.A. Hoch, (1994) Deactivation of the sporulation transcription factor Spo0A by the Spo0E protein phosphatase. *Proc Natl Acad Sci USA* **91**: 1756-1760.

Okanishi, M., K. Suzuki & H. Umezawa, (1974) Formation and reversion of Streptomycete protoplasts: cultural condition and morphological study. *J Gen Microbiol* **80**: 389-400.

Oliva, M.A., S. Halbedel, S.M. Freund, P. Dutow, T.A. Leonard, D.B. Veprintsev, L.W. Hamoen & J. Lowe, (2010) Features critical for membrane binding revealed by DivIVA crystal structure. *EMBO J* **29**: 1988-2001.

Olukoshi, E.R. & N.M. Packter, (1994) Importance of stored triacylglycerols in *Streptomyces*: possible carbon source for antibiotics. *Microbiology* **140** (Pt 4): 931-943.

Ostermeyer, A.G., B.T. Beckrich, K.A. Ivarson, K.E. Grove & D.A. Brown, (1999) Glycosphingolipids are not essential for formation of detergent-resistant membrane rafts in melanoma cells. methyl-beta-cyclodextrin does not affect cell surface transport of a GPI-anchored protein. *J Biol Chem* **274**: 34459-34466.

Ou, L.T. & R.E. Marquis, (1970) Electromechanical interactions in cell walls of Gram-positive cocci. *J Bacteriol* **101**: 92-101.

Paetzel, M., A. Karla, N.C. Strynadka & R.E. Dalbey, (2002) Signal peptidases. *Chem Rev* **102**: 4549-4580.

Paget, M.S., L. Chamberlin, A. Atrih, S.J. Foster & M.J. Buttner, (1999) Evidence that the extracytoplasmic function sigma factor sigmaE is required for normal cell wall structure in *Streptomyces coelicolor* A3(2). *J Bacteriol* 181: 204-211.

Palmer, T. & B.C. Berks, (2012) The twin-arginine translocation (Tat) protein export pathway. *Nat Rev Microbiol* **10**: 483-496.

Pangborn, M.C., (1942) Isolation and purification of a serologically active phospholipid from beef heart. *J Biochem Chem* **143**: 247-256.

Parashar, A., K.R. Colvin, D.R. Bignell & B.K. Leskiw, (2009) BldG and SCO3548 interact antagonistically to control key developmental processes in *Streptomyces coelicolor*. *J Bacteriol* **191**: 2541-2550.

Pata, M.O., Y.A. Hannun & C.K. Ng, (2010) Plant sphingolipids: decoding the enigma of the Sphinx. *New Phytol* **185**: 611-630.

Pedrido, M.E., P. de Ona, W. Ramirez, C. Lenini, A. Goni & R. Grau, (2013) Spo0A links de novo fatty acid synthesis to sporulation and biofilm development in *Bacillus subtilis*. *Mol Microbiol* **87**: 348-367.

Perego, M., (1998) Kinase-phosphatase competition regulates *Bacillus subtilis* development. *Trends Microbiol* **6**: 366-370.

Persson, J., K.F. Chater & K. Flardh, (2013) Molecular and cytological analysis of the expression of *Streptomyces* sporulation regulatory gene *whiH*. *FEMS Microbiol Lett* **341**: 96-105.

Peschel, A., M. Otto, R.W. Jack, H. Kalbacher, G. Jung & F. Gotz, (1999) Inactivation of the dlt operon in *Staphylococcus aureus* confers sensitivity to defensins, protegrins, and other antimicrobial peptides. *J Biol Chem* **274**: 8405-8410.

Peter, B.J., H.M. Kent, I.G. Mills, Y. Vallis, P.J. Butler, P.R. Evans & H.T. McMahon, (2004) BAR domains as sensors of membrane curvature: the amphiphysin BAR structure. *Science* **303**: 495-499.

Phillips, G.J., (2001) Green fluorescent protein--a bright idea for the study of bacterial protein localization. *FEMS Microbiol Lett* **204**: 9-18.

Pichoff, S. & J. Lutkenhaus, (2002) Unique and overlapping roles for ZipA and FtsA in septal ring assembly in *Escherichia coli*. *EMBO J* **21**: 685-693.

Pichoff, S. & J. Lutkenhaus, (2005) Tethering the Z ring to the membrane through a conserved membrane targeting sequence in FtsA. *Mol Microbiol* **55**: 1722-1734.

Pichoff, S., B. Shen, B. Sullivan & J. Lutkenhaus, (2012) FtsA mutants impaired for self-interaction bypass ZipA suggesting a model in which FtsA's self-interaction competes with its ability to recruit downstream division proteins. *Mol Microbiol* **83**: 151-167.

Piette, A., A. Derouaux, P. Gerkens, E.E. Noens, G. Mazzucchelli, S. Vion, H.K. Koerten, F. Titgemeyer, E. De Pauw, P. Leprince, G.P. van Wezel, M. Galleni & S. Rigali, (2005) From dormant to germinating spores of *Streptomyces coelicolor* A3(2): new perspectives from the crp null mutant. *J Proteome Res* **4**: 1699-1708.

Pike, L.J., (2006) Rafts defined: a report on the Keystone Symposium on Lipid Rafts and Cell Function. *J Lipid Res* **47**: 1597-1598.

Pike, L.J., (2009) The challenge of lipid rafts. *J Lipid Res* **50** Suppl: S323-328.

Pogliano, K., E. Harry & R. Losick, (1995) Visualization of the subcellular location of sporulation proteins in *Bacillus subtilis* using immunofluorescence microscopy. *Mol Microbiol* **18**: 459-470.

Pollack, J.H., A.S. Ntamere & F.C. Neuhaus, (1992) D-alanyl-lipoteichoic acid in *LactoBacillus casei*: secretion of vesicles in response to benzylpenicillin. *J Gen Microbiol* **138**: 849-859.

Popham, D.L., M.E. Gilmore & P. Setlow, (1999) Roles of low-molecular-weight penicillin-binding proteins in *Bacillus subtilis* spore peptidoglycan synthesis and spore properties. *J Bacteriol* **181**: 126-132.

Popham, D.L., J. Helin, C.E. Costello & P. Setlow, (1996) Muramic lactam in peptidoglycan of *Bacillus subtilis* spores is required for spore outgrowth but not for spore dehydration or heat resistance. *Proc Natl Acad Sci USA* **93**: 15405-15410.

Popham, D.L. & P. Setlow, (1993) The cortical peptidoglycan from spores of *Bacillus megaterium* and *Bacillus subtilis* is not highly cross-linked. *J Bacteriol* **175**: 2767-2769.

Poralla, K., G. Muth & T. Hartner, (2000) Hopanoids are formed during transition from substrate to aerial hyphae in *Streptomyces coelicolor* A3(2). *FEMS Microbiol Lett* **189**: 93-95.

Posse De Chaves, E.I., D.E. Vance, R.B. Campenot, R.S. Kiss & J.E. Vance, (2000) Uptake of lipoproteins for axonal growth of sympathetic neurons. *J Biol Chem* **275**: 19883-19890.

Potekhina, N.V., E.M. Tul'skaya, I.B. Naumova, A.S. Shashkov & L.I. Evtushenko, (1993) Erythritolteichoic acid in the cell wall of *Glycomyces tenuis* VKM Ac-1250. *European J Biochem / FEBS* **218**: 371-375.

Pralle, A., P. Keller, E.L. Florin, K. Simons & J.K. Horber, (2000) Sphingolipid-cholesterol rafts diffuse as small entities in the plasma membrane of mammalian cells. *J Cell Biol* **148**: 997-1008.

Proszynski, T.J., R. Klemm, M. Bagnat, K. Gaus & K. Simons, (2006) Plasma membrane polarization during mating in yeast cells. *J Cell Biol* **173**: 861-866.

Quintana, E.T., K. Wierzbicka, P. Mackiewicz, A. Osman, A.H. Fahal, M.E. Hamid, J. Zakrzewska-Czerwinska, L.A. Maldonado & M. Goodfellow, (2008) *Streptomyces sudanensis* sp. nov., a new pathogen isolated from patients with actinomycetoma. *Antonie van Leeuwenhoek* **93**: 305-313.

Raetz, C.R. & W. Dowhan, (1990) Biosynthesis and function of phospholipids in *Escherichia coli*. *J Biol Chem* **265**: 1235-1238.

Raetz, C.R. & C. Whitfield, (2002) Lipopolysaccharide endotoxins. *Annu Rev Biochem* 71: 635-700.

Rahman, O., S.P. Cummings & I.C. Sutcliffe, (2009a) Phenotypic variation in *Streptomyces* sp. DSM 40537, a lipoteichoic acid producing actinomycete. *Lett Appl Microbiol* **48**: 226-229.

Rahman, O., L.G. Dover & I.C. Sutcliffe, (2009b) Lipoteichoic acid biosynthesis: two steps forwards, one step sideways? *Trends Microbiol* **17**: 219-225.

Rahman, O., M. Pfitzenmaier, O. Pester, S. Morath, S.P. Cummings, T. Hartung & I.C. Sutcliffe, (2009c) Macroamphiphilic components of thermophilic actinomycetes: identification of lipoteichoic acid in *Thermobifida fusca*. *J Bacteriol* **191**: 152-160.

Rahn-Lee, L., H. Merrikh, A.D. Grossman & R. Losick, (2011) The sporulation protein SirA inhibits the binding of DnaA to the origin of replication by contacting a patch of clustered amino acids. *J Bacteriol* **193**: 1302-1307.

Rajagopalan, S., V. Wachtler & M. Balasubramanian, (2003) Cytokinesis in fission yeast: a story of rings, rafts and walls. *Trends Genet* **19**: 403-408.

Rajendran, L., J. Beckmann, A. Magenau, E.M. Boneberg, K. Gaus, A. Viola, B. Giebel & H. Illges, (2009) Flotillins are involved in the polarization of primitive and mature hematopoietic cells. *PLoS One* **4**: e8290.

Rajendran, L., M. Masilamani, S. Solomon, R. Tikkanen, C.A. Stuermer, H. Plattner & H. Illges, (2003) Asymmetric localization of flotillins/reggies in preassembled platforms confers inherent polarity to hematopoietic cells. *Proc Natl Acad Sci USA* **100**: 8241-8246.

Ramamurthi, K.S., K.R. Clapham & R. Losick, (2006) Peptide anchoring spore coat assembly to the outer forespore membrane in *Bacillus subtilis*. *Mol Microbiol* **62**: 1547-1557.

Ramamurthi, K.S., S. Lecuyer, H.A. Stone & R. Losick, (2009) Geometric cue for protein localization in a bacterium. *Science* **323**: 1354-1357.

Ramamurthi, K.S. & R. Losick, (2008) ATP-driven self-assembly of a morphogenetic protein in *Bacillus subtilis*. *Mol Cell* **31**: 406-414.

Ramamurthi, K.S. & R. Losick, (2009) Negative membrane curvature as a cue for subcellular localization of a bacterial protein. *Proc Natl Acad Sci USA* **106**: 13541-13545.

Rand, R.P. & S. Sengupta, (1972) Cardiolipin forms hexagonal structures with divalent cations. *Biochim Biophys Acta* **255**: 484-492.

Randall, L.L. & S.J. Hardy, (1995) High selectivity with low specificity: how SecB has solved the paradox of chaperone binding. *Trends Biochem Sci* **20**: 65-69.

Rao, C.V., G.D. Glekas & G.W. Ordal, (2008) The three adaptation systems of *Bacillus subtilis* chemotaxis. *Trends Microbiol* **16**: 480-487.

Raskin, D.M. & P.A. de Boer, (1999a) MinDE-dependent pole-to-pole oscillation of division inhibitor MinC in *Escherichia coli. J Bacteriol* **181**: 6419-6424.

Raskin, D.M. & P.A. de Boer, (1999b) Rapid pole-to-pole oscillation of a protein required for directing division to the middle of *Escherichia coli*. *Proc Natl Acad Sci USA* **96**: 4971-4976.

Reardon-Robinson, M.E. & H. Ton-That, (2015) Disulfide-Bond-Forming Pathways in Gram-Positive Bacteria. *J Bacteriol* **198**: 746-754.

Rebeck, G.W., M. Kindy & M.J. LaDu, (2002) Apolipoprotein E and Alzheimer's disease: the protective effects of ApoE2 and E3. *J Alzheimers Dis* **4**: 145-154.

Redenbach, M., H.M. Kieser, D. Denapaite, A. Eichner, J. Cullum, H. Kinashi & D.A. Hopwood, (1996) A set of ordered cosmids and a detailed genetic and physical map for the 8 Mb *Streptomyces coelicolor* A3(2) chromosome. *Mol Microbiol* **21**: 77-96.

Regamey, A., E.J. Harry & R.G. Wake, (2000) Mid-cell Z ring assembly in the absence of entry into the elongation phase of the round of replication in bacteria: co-ordinating chromosome replication with cell division. *Mol Microbiol* **38**: 423-434.

Regan, G., M. Itaya & P.J. Piggot, (2012) Coupling of sigmaG activation to completion of engulfment during sporulation of *Bacillus subtilis* survives large perturbations to DNA translocation and replication. *J Bacteriol* **194**: 6264-6271.

Resh, M.D., (2013) Covalent lipid modifications of proteins. *Curr Biol* **23**: R431-435.

Resnekov, O. & R. Losick, (1998) Negative regulation of the proteolytic activation of a developmental transcription factor in *Bacillus subtilis*. *Proc Natl Acad Sci USA* **95**: 3162-3167.

Reumerman, R., (2014) Unpublished data. In., pp.

Reusch, V.M., Jr., (1984) Lipopolymers, isoprenoids, and the assembly of the gram-positive cell wall. *Crit Rev Microbiol* **11**: 129-155.

Rexroth, S., C.W. Mullineaux, D. Ellinger, E. Sendtko, M. Rogner & F. Koenig, (2011) The plasma membrane of the cyanobacterium *Gloeobacter violaceus* contains segregated bioenergetic domains. *Plant Cell* **23**: 2379-2390.

Rezwan, M., T. Grau, A. Tschumi & P. Sander, (2007) Lipoprotein synthesis in mycobacteria. *Microbiology* **153**: 652-658.

Rivera-Milla, E., C.A. Stuermer & E. Malaga-Trillo, (2006) Ancient origin of reggie (flotillin), reggie-like, and other lipid-raft proteins: convergent evolution of the SPFH domain. *Cell Mol Life Sci* **63**: 343-357.

Rodrigues, M.L., E.S. Nakayasu, D.L. Oliveira, L. Nimrichter, J.D. Nosanchuk, I.C. Almeida & A. Casadevall, (2008) Extracellular vesicles produced by *Cryptococcus neoformans* contain protein components associated with virulence. *Eukaryot Cell* **7**: 58-67.

Rodrigues, M.L., L. Nimrichter, D.L. Oliveira, S. Frases, K. Miranda, O. Zaragoza, M. Alvarez, A. Nakouzi, M. Feldmesser & A. Casadevall, (2007) Vesicular polysaccharide export in *Cryptococcus neoformans* is a eukaryotic solution to the problem of fungal trans-cell wall transport. *Eukaryot Cell* **6**: 48-59.

Rodrigues, M.L., L.R. Travassos, K.R. Miranda, A.J. Franzen, S. Rozental, W. de Souza, C.S. Alviano & E. Barreto-Bergter, (2000) Human antibodies against a purified glucosylceramide from *Cryptococcus neoformans* inhibit cell budding and fungal growth. *Infect Immun* **68**: 7049-7060.

Roels, S., A. Driks & R. Losick, (1992) Characterization of *spoIVA*, a sporulation gene involved in coat morphogenesis in *Bacillus subtilis*. *J Bacteriol* **174**: 575-585.

Rosa Ide, A., M. Einicker-Lamas, R.R. Bernardo & M. Benchimol, (2008) Cardiolipin, a lipid found in mitochondria, hydrogenosomes and bacteria was not detected in *Giardia lamblia*. *Exp Parasitol* **120**: 215-220.

Rozen, S. & H. Skaletsky, (2000) Primer3 on the WWW for general users and for biologist programmers. *Methods Mol Biol* **132**: 365-386.

Rudner, D.Z. & R. Losick, (2010) Protein subcellular localization in bacteria. *Cold Spring Harb Perspect Biol* **2**: a000307.

Ruiz, N., (2008) Bioinformatics identification of MurJ (MviN) as the peptidoglycan lipid II flippase in *Escherichia coli*. *Proc Natl Acad Sci USA* **105**: 15553-15557.

Ryter, A., P. Schaeffer & H. Ionesco, (1966) [Cytologic classification, by their blockage stage, of sporulation mutants of *Bacillus subtilis* Marburg]. *Ann Inst Pasteur Microbiol* **110**: 305-315.

Saenz, J.P., D. Grosser, A.S. Bradley, T.J. Lagny, O. Lavrynenko, M. Broda & K. Simons, (2015) Hopanoids as functional analogues of cholesterol in bacterial membranes. *Proc Natl Acad Sci USA* **112**: 11971-11976.

Saenz, J.P., E. Sezgin, P. Schwille & K. Simons, (2012) Functional convergence of hopanoids and sterols in membrane ordering. *Proc Natl Acad Sci USA* **109**: 14236-14240.

Sahm, H., M. Rohmer, S. Bringer-Meyer, G.A. Sprenger & R. Welle, (1993) Biochemistry and physiology of hopanoids in bacteria. *Adv Microb Physiol* **35**: 247-273.

Saito, H. & N. Suzuki, (2007) Distributions and sources of hopanes, hopanoic acids and hopanols in Miocene to recent sediments from ODP Leg 190, Nankai Trough. *Org Geochem* **38**: 1715–1728.

Salerno, P., J. Larsson, G. Bucca, E. Laing, C.P. Smith & K. Flardh, (2009) One of the two genes encoding nucleoid-associated HU proteins in *Streptomyces coelicolor* is developmentally regulated and specifically involved in spore maturation. *J Bacteriol* **191**: 6489-6500.

Sambrook, J., E.F. Fritsch & T. Maniatis, (1989) Molecular cloning a laboratory manual. Cold Spring Harbour Laboratory Press.

Sanderson, A.R., J.L. Strominger & S.G. Nathenson, (1962) Chemical structure of teichoic acid from *Staphylococcus aureus*, strain Copenhagen. *J Biol Chem* **237**: 3603-3613.

Sandoval-Calderon, M., O. Geiger, Z. Guan, F. Barona-Gomez & C. Sohlenkamp, (2009) A eukaryote-like cardiolipin synthase is present in *Streptomyces coelicolor* and in most actinobacteria. *J Biol Chem* **284**: 17383-17390.

Santos-Beneit, F., L.T. Fernandez-Martinez, A. Rodriguez-Garcia, S. Martin-Martin, M. Ordonez-Robles, P. Yague, A. Manteca & J.F. Martin, (2014) Transcriptional response to vancomycin in a highly vancomycin-resistant *Streptomyces coelicolor* mutant. *Future Microbiol* **9**: 603-622.

Schaller, H., (2004) New aspects of sterol biosynthesis in growth and development of higher plants. *Plant Physiol Biochem* **42**: 465-476.

Scheele, S., D. Oertel, J. Bongaerts, S. Evers, H. Hellmuth, K.H. Maurer, M. Bott & R. Freudl, (2013) Secretory production of an FAD cofactor-containing cytosolic enzyme (sorbitol-xylitol oxidase from *Streptomyces coelicolor*) using the twin-arginine translocation (Tat) pathway of *Corynebacterium glutamicum*. *Microb biotechnol* **6**: 202-206.

Scheffers, D.J., J.G. de Wit, T. den Blaauwen & A.J. Driessen, (2002) GTP hydrolysis of cell division protein FtsZ: evidence that the active site is formed by the association of monomers. *Biochemistry* **41**: 521-529.

Schengrund, C.L., (2010) Lipid rafts: keys to neurodegeneration. *Brain Res* **82**: 7-17.

Schertzer, J.W. & E.D. Brown, (2003) Purified, recombinant TagF protein from *Bacillus subtilis* 168 catalyzes the polymerization of glycerol phosphate onto a membrane acceptor in vitro. *J Biol Chem* **278**: 18002-18007.

Schiebel, E., A.J. Driessen, F.U. Hartl & W. Wickner, (1991) Delta mu H+ and ATP function at different steps of the catalytic cycle of preprotein translocase. *Cell* **64**: 927-939.

Schlame, M., (2008) Cardiolipin synthesis for the assembly of bacterial and mitochondrial membranes. *J Lipid Res* **49**: 1607-1620.

Schlame, M., J.A. Towbin, P.M. Heerdt, R. Jehle, S. DiMauro & T.J. Blanck, (2002) Deficiency of tetralinoleoyl-cardiolipin in Barth syndrome. *Ann Neurol* **51**: 634-637.

Schneewind, O. & D. Missiakas, (2014) Lipoteichoic acids, phosphate-containing polymers in the envelope of Gram-positive bacteria. *J Bacteriol* **196**: 1133-1142.

Schneider, J., B. Mielich-Suss, R. Bohme & D. Lopez, (2015) *In vivo* characterization of the scaffold activity of flotillin on the membrane kinase KinC of *Bacillus subtilis*. *Microbiology* **161**: 1871-1887.

Schneiter, R., B. Brugger, C.M. Amann, G.D. Prestwich, R.F. Epand, G. Zellnig, F.T. Wieland & R.M. Epand, (2004) Identification and biophysical characterization of a very-

long-chain-fatty-acid-substituted phosphatidylinositol in yeast subcellular membranes. *Biochem J* **381**: 941-949.

Schneiter, R., B. Brugger, R. Sandhoff, G. Zellnig, A. Leber, M. Lampl, K. Athenstaedt, C. Hrastnik, S. Eder, G. Daum, F. Paltauf, F.T. Wieland & S.D. Kohlwein, (1999) Electrospray ionization tandem mass spectrometry (ESI-MS/MS) analysis of the lipid molecular species composition of yeast subcellular membranes reveals acyl chain-based sorting/remodeling of distinct molecular species en route to the plasma membrane. *J Cell Biol* **146**: 741-754.

Schroeder, W.T., S. Stewart-Galetka, S. Mandavilli, D.A. Parry, L. Goldsmith & M. Duvic, (1994) Cloning and characterization of a novel epidermal cell surface antigen (ESA). *J Biol Chem* **269**: 19983-19991.

Schug, Z.T. & E. Gottlieb, (2009) Cardiolipin acts as a mitochondrial signalling platform to launch apoptosis. *Biochem Biophys Acta* **1788**: 2022-2031.

Schulte, T., K.A. Paschke, U. Laessing, F. Lottspeich & C.A. Stuermer, (1997) Reggie-1 and reggie-2, two cell surface proteins expressed by retinal ganglion cells during axon regeneration. *Development* **124**: 577-587.

Schultz, S.C., G.C. Shields & T.A. Steitz, (1991) Crystal structure of a CAP-DNA complex: the DNA is bent by 90 degrees. *Science* **253**: 1001-1007.

Schulz, G.E., (2002) The structure of bacterial outer membrane proteins. *Biochim Biophys Acta* **1565**: 308-317.

Schwedock, J., J.R. McCormick, E.R. Angert, J.R. Nodwell & R. Losick, (1997) Assembly of the cell division protein FtsZ into ladder-like structures in the aerial hyphae of *Streptomyces coelicolor*. *Mol Microbiol* **25**: 847-858.

Seipke, R.F. & R. Loria, (2009) Hopanoids are not essential for growth of *Streptomyces* scabies 87-22. *J Bacteriol* **191**: 5216-5223.

Sekimizu, K. & A. Kornberg, (1988) Cardiolipin activation of dnaA protein, the initiation protein of replication in *Escherichia coli*. *J Biol Chem* **263**: 7131-7135.

Serricchio, M. & P. Butikofer, (2012) An essential bacterial-type cardiolipin synthase mediates cardiolipin formation in a eukaryote. *Proc Natl Acad Sci USA* **109**: E954-961.

Sevcikova, B., O. Benada, O. Kofronova & J. Kormanec, (2001) Stress-response sigma factor sigma(H) is essential for morphological differentiation of *Streptomyces coelicolor* A3(2). *Arch Microbiol* **177**: 98-106.

Sevcikova, B. & J. Kormanec, (2002) Activity of the *Streptomyces coelicolor* stress-response sigma factor sigmaH is regulated by an anti-sigma factor. *FEMS Microbiol Lett* **209**: 229-235.

Sezgin, E., I. Levental, S. Mayor & C. Eggeling, (2017) The mystery of membrane organization: composition, regulation and roles of lipid rafts. *Nat Rev Mol Cell Biol* **18**: 361-374.

Shaner, N.C., R.E. Campbell, P.A. Steinbach, B.N. Giepmans, A.E. Palmer & R.Y. Tsien, (2004) Improved monomeric red, orange and yellow fluorescent proteins derived from *Discosoma* sp. red fluorescent protein. *Nature Biotechnol* **22**: 1567-1572.

Shashkov, A.S., G.M. Streshinskaya, V.A. Gnilozub, L.I. Evtushenko & I.B. Naumova, (1995) Poly(arabitol phosphate) teichoic acid in the cell wall of *Agromyces cerinus* subsp. cerinus VKM Ac-1340T. *FEBS Lett* **371**: 163-166.

Sherratt, D.J., L.K. Arciszewska, E. Crozat, J.E. Graham & I. Grainge, (2010) The *Escherichia* coli DNA translocase FtsK. *Biochem Soc Trans* **38**: 395-398.

Shimada, A., H. Niwa, K. Tsujita, S. Suetsugu, K. Nitta, K. Hanawa-Suetsugu, R. Akasaka, Y. Nishino, M. Toyama, L. Chen, Z.J. Liu, B.C. Wang, M. Yamamoto, T. Terada, A. Miyazawa, A. Tanaka, S. Sugano, M. Shirouzu, K. Nagayama, T. Takenawa & S. Yokoyama, (2007) Curved EFC/F-BAR-domain dimers are joined end to end into a filament for membrane invagination in endocytosis. *Cell* **129**: 761-772.

Short, S.A. & D.C. White, (1971) Metabolism of phosphatidylglycerol, lysylphosphatidylglycerol, and cardiolipin of *Staphylococcus aureus*. *J Bacteriol* **108**: 219-226.

Siafakas, A.R., L.C. Wright, T.C. Sorrell & J.T. Djordjevic, (2006) Lipid rafts in *Cryptococcus neoformans* concentrate the virulence determinants phospholipase B1 and Cu/Zn superoxide dismutase. *Eukaryot Cell* **5**: 488-498.

Siedenburg, G. & D. Jendrossek, (2011) Squalene-hopene cyclases. *Appl Environ Microbiol* **77**: 3905-3915.

Sievers, J. & J. Errington, (2000) Analysis of the essential cell division gene *ftsL* of *Bacillus subtilis* by mutagenesis and heterologous complementation. *J Bacteriol* **182**: 5572-5579.

Silvestri, L., V. Caputo, E. Bellacchio, L. Atorino, B. Dallapiccola, E.M. Valente & G. Casari, (2005) Mitochondrial import and enzymatic activity of PINK1 mutants associated to recessive parkinsonism. *Human Mol Genet* **14**: 3477-3492.

Simons, K. & E. Ikonen, (1997) Functional rafts in cell membranes. *Nature* **387**: 569-572.

Simons, K. & D. Toomre, (2000) Lipid rafts and signal transduction. *Nat Rev Mol Cell Biol* **1**: 31-39.

Simons, M. & D.A. Lyons, (2013) Axonal selection and myelin sheath generation in the central nervous system. *Curr Cell Opin Biol* **25**: 512-519.

Singer, S.J. & G.L. Nicolson, (1972) The fluid mosaic model of the structure of cell membranes. *Science* **175**: 720-731.

Skalweit, M.J., (2015) Profile of ceftolozane/tazobactam and its potential in the treatment of complicated intra-abdominal infections. *Drug Des Devel Ther* **9**: 2919-2925.

Smith, G.R., (1988) Homologous recombination in procaryotes. *Microbiol Rev* **52**: 1-28.

Sola-Landa, A., R.S. Moura & J.F. Martin, (2003) The two-component PhoR-PhoP system controls both primary metabolism and secondary metabolite biosynthesis in *Streptomyces lividans*. *Proc Natl Acad Sci USA* **100**: 6133-6138.

Solis, G.P., M. Hoegg, C. Munderloh, Y. Schrock, E. Malaga-Trillo, E. Rivera-Milla & C.A. Stuermer, (2007) Reggie/flotillin proteins are organized into stable tetramers in membrane microdomains. *Biochem J* **403**: 313-322.

Sone, M., S. Kishigami, T. Yoshihisa & K. Ito, (1997) Roles of disulfide bonds in bacterial alkaline phosphatase. *J Biol Chem* **272**: 6174-6178.

Song, C., A. Kumar & M. Saleh, (2009) Bioinformatic comparison of bacterial secretomes. *Genomics Proteomics Bioinformatics* **7**: 37-46.

Soto, M.J., A. Zorzano, F.M. Garcia-Rodriguez, J. Mercado-Blanco, I.M. Lopez-Lara, J. Olivares & N. Toro, (1994) Identification of a novel *Rhizobium meliloti* nodulation efficiency *nfe* gene homolog of *Agrobacterium ornithine* cyclodeaminase. *Mol Plant Microbe Interact* **7**: 703-707.

Spratt, B.G., P.J. Hedge, S. te Heesen, A. Edelman & J.K. Broome-Smith, (1986) Kanamycin-resistant vectors that are analogues of plasmids pUC8, pUC9, pEMBL8 and pEMBL9. *Gene* **41**: 337-342.

Stanislas, T., D. Bouyssie, M. Rossignol, S. Vesa, J. Fromentin, J. Morel, C. Pichereaux, B. Monsarrat & F. Simon-Plas, (2009) Quantitative proteomics reveals a dynamic association of proteins to detergent-resistant membranes upon elicitor signaling in tobacco. *Mol Cell Proteomics* **8**: 2186-2198.

Stover, C.K., X.Q. Pham, A.L. Erwin, S.D. Mizoguchi, P. Warrener, M.J. Hickey, F.S. Brinkman, W.O. Hufnagle, D.J. Kowalik, M. Lagrou, R.L. Garber, L. Goltry, E. Tolentino, S. Westbrock-Wadman, Y. Yuan, L.L. Brody, S.N. Coulter, K.R. Folger, A. Kas, K. Larbig, R. Lim, K. Smith, D. Spencer, G.K. Wong, Z. Wu, I.T. Paulsen, J. Reizer, M.H. Saier, R.E. Hancock, S. Lory & M.V. Olson, (2000) Complete genome sequence of *Pseudomonas aeruginosa* PAO1, an opportunistic pathogen. *Nature* **406**: 959-964.

Strain, S.M., I.M. Armitage, L. Anderson, K. Takayama, N. Qureshi & C.R. Raetz, (1985) Location of polar substituents and fatty acyl chains on lipid A precursors from a 3-deoxy-D-manno-octulosonic acid-deficient mutant of *Salmonella typhimurium*. Studies by 1H, 13C, and 31P nuclear magnetic resonance. *J Biol Chem* **260**: 16089-16098.

Streshinskaya, G.M., A.S. Shashkov, S.N. Senchenkova, O.V. Bueva, O.S. Stupar & L.I. Evtushenko, (2007) A novel teichoic acid from the cell wall of *Streptomyces* sp. VKM Ac-2275. *Carbohydr Res* **342**: 659-664.

Stuermer, C.A., D.M. Lang, F. Kirsch, M. Wiechers, S.O. Deininger & H. Plattner, (2001) Glycosylphosphatidyl inositol-anchored proteins and fyn kinase assemble in noncaveolar plasma membrane microdomains defined by reggie-1 and -2. *Mol Biol Cell* **12**: 3031-3045.

Stuermer, C.A., M.F. Langhorst, M.F. Wiechers, D.F. Legler, S.H. Von Hanwehr, A.H. Guse & H. Plattner, (2004) PrPc capping in T cells promotes its association with the lipid raft proteins reggie-1 and reggie-2 and leads to signal transduction. *FASEB J* **18**: 1731-1733.

Sun, J., G.H. Kelemen, J.M. Fernandez-Abalos & M.J. Bibb, (1999) Green fluorescent protein as a reporter for spatial and temporal gene expression in *Streptomyces coelicolor* A3(2). *Microbiology* **145** (Pt 9): 2221-2227.

Sutcliffe, I.C., D.J. Harrington & M.I. Hutchings, (2012) A phylum level analysis reveals lipoprotein biosynthesis to be a fundamental property of bacteria. *Protein Cell* **3**: 163-170.

Sutcliffe, I.C. & N. Shaw, (1991) Atypical lipoteichoic acids of Gram-positive bacteria. *J Bacteriol* **173**: 7065-7069.

Suzuki, T., K. Fujikura, T. Higashiyama & K. Takata, (1997) DNA staining for fluorescence and laser confocal microscopy. *J Histochem Cytochem* **45**: 49-53.

Swanwick, C.C., M.E. Shapiro, Z. Yi, K. Chang & R.J. Wenthold, (2009) NMDA receptors interact with flotillin-1 and -2, lipid raft-associated proteins. *FEBS Lett* **583**: 1226-1230.

Szwedziak, P., Q. Wang, S.M. Freund & J. Lowe, (2012) FtsA forms actin-like protofilaments. *EMBO J* **31**: 2249-2260.

Tai, V., A.F. Poon, I.T. Paulsen & B. Palenik, (2011) Selection in coastal Synechococcus (cyanobacteria) populations evaluated from environmental metagenomes. *PloS One* **6**: e24249.

Takeshita, N., G. Diallinas & R. Fischer, (2012) The role of flotillin FloA and stomatin StoA in the maintenance of apical sterol-rich membrane domains and polarity in the filamentous fungus *Aspergillus nidulans*. *Mol Microbiol* **83**: 1136-1152.

Tamura, K., J. Dudley, M. Nei & S. Kumar, (2007) MEGA4: Molecular Evolutionary Genetics Analysis (MEGA) software version 4.0. *Mol Biol Evol* **24**: 1596-1599.

Tan, B.K., M. Bogdanov, J. Zhao, W. Dowhan, C.R. Raetz & Z. Guan, (2012) Discovery of a cardiolipin synthase utilizing phosphatidylethanolamine and phosphatidylglycerol as substrates. *Proc Natl Acad Sci USA* **109**: 16504-16509.

Tan, I.S. & K.S. Ramamurthi, (2014) Spore formation in *Bacillus subtilis*. *Environ Microbiol Rep* **6**: 212-225.

Tatsuta, T., K. Model & T. Langer, (2005) Formation of membrane-bound ring complexes by prohibitins in mitochondria. *Mol Biol Cell* **16**: 248-259.

Tavernarakis, N., M. Driscoll & N.C. Kyrpides, (1999) The SPFH domain: implicated in regulating targeted protein turnover in stomatins and other membrane-associated proteins. *Trends Biochem Sci* **24**: 425-427.

Taylor, R.G., D.C. Walker & R.R. McInnes, (1993) *E. coli* host strains significantly affect the quality of small scale plasmid DNA preparations used for sequencing. *Nucleic Acids Res* **21**: 1677-1678.

Tenconi, E., P. Guichard, P. Motte, A. Matagne & S. Rigali, (2013) Use of red autofluorescence for monitoring prodiginine biosynthesis. *J Microbiol Methods* **93**: 138-143.

Theobald, D.L., R.M. Mitton-Fry & D.S. Wuttke, (2003) Nucleic acid recognition by OB-fold proteins. *Annu Rev Biophys Biomol Struct* **32**: 115-133.

Thi Nguyen, H.B. & W. Schumann, (2012) The sporulation control gene *spo0M* of *Bacillus subtilis* is a target of the FtsH metalloprotease. *Res Microbiol* **163**: 114-118.

Thoma, L., H. Dobrowinski, C. Finger, J. Guezguez, D. Linke, E. Sepulveda & G. Muth, (2015) A Multiprotein DNA Translocation Complex Directs Intramycelial Plasmid Spreading during *Streptomyces* Conjugation. *mBio* **6**: e02559-02514.

Thoma, L., B. Vollmer & G. Muth, (2016) Fluorescence microscopy of *Streptomyces* conjugation suggests DNA-transfer at the lateral walls and reveals the spreading of the plasmid in the recipient mycelium. *Environ Microbiol* **18**: 598-608.

Thompson, B.J., D.A. Widdick, M.G. Hicks, G. Chandra, I.C. Sutcliffe, T. Palmer & M.I. Hutchings, (2010) Investigating lipoprotein biogenesis and function in the model Gram-positive bacterium *Streptomyces coelicolor*. *Mol Microbiol* 77**:** 943-957.

Tian, H.F., J.M. Feng & J.F. Wen, (2012) The evolution of cardiolipin biosynthesis and maturation pathways and its implications for the evolution of eukaryotes. *BMC Evol Biol* **12**: 32.

Tinker, D.O., L. Pinteric, J.C. Hsia & R.P. Rand, (1976) Perturbation of lecithin bilayer structure by globoside. *Canadian J Biochem* **54**: 209-218.

Tipper, D.J. & P.E. Linnett, (1976) Distribution of peptidoglycan synthetase activities between sporangia and forespores in sporulating cells of *Bacillus sphaericus*. *J Bacteriol* **126**: 213-221.

Tocheva, E.I., J. Lopez-Garrido, H.V. Hughes, J. Fredlund, E. Kuru, M.S. Vannieuwenhze, Y.V. Brun, K. Pogliano & G.J. Jensen, (2013) Peptidoglycan transformations during *Bacillus subtilis* sporulation. *Mol Microbiol* **88**: 673-686.

Todsen, W.L., (2014) ChemDoodle 6.0. *J. Chem. Inf. Model.* **54**: 2391-2393.

Tokuda, H., (2009) Biogenesis of outer membranes in Gram-negative bacteria. *Biosci Biotechnol Biochem* **73**: 465-473.

Torrents, D., M. Suyama, E. Zdobnov & P. Bork, (2003) A genome-wide survey of human pseudogenes. *Genome Res* **13**: 2559-2567.

Tran, T.T., D. Panesso, N.N. Mishra, E. Mileykovskaya, Z. Guan, J.M. Munita, J. Reyes, L. Diaz, G.M. Weinstock, B.E. Murray, Y. Shamoo, W. Dowhan, A.S. Bayer & C.A. Arias, (2013) Daptomycin-resistant *Enterococcus faecalis* diverts the antibiotic molecule from the division septum and remodels cell membrane phospholipids. *mBio* **4**.

Tsai, M., R.L. Ohniwa, Y. Kato, S.L. Takeshita, T. Ohta, S. Saito, H. Hayashi & K. Morikawa, (2011) *Staphylococcus aureus* requires cardiolipin for survival under conditions of high salinity. *BMC Microbiol* **11**: 13.

Tsang, M.J. & T.G. Bernhardt, (2015) A role for the FtsQLB complex in cytokinetic ring activation revealed by an *ftsL* allele that accelerates division. *Mol Microbiol* **95**: 925-944.

Tschowri, N., M.A. Schumacher, S. Schlimpert, N.B. Chinnam, K.C. Findlay, R.G. Brennan & M.J. Buttner, (2014) Tetrameric c-di-GMP mediates effective transcription factor dimerization to control *Streptomyces* development. *Cell* **158**: 1136-1147.

Tschumi, A., C. Nai, Y. Auchli, P. Hunziker, P. Gehrig, P. Keller, T. Grau & P. Sander, (2009) Identification of apolipoprotein N-acyltransferase (Lnt) in mycobacteria. *J Biol Chem* **284**: 27146-27156.

Tzanis, A., K.A. Dalton, A. Hesketh, C.D. den Hengst, M.J. Buttner, A. Thibessard & G.H. Kelemen, (2014) A sporulation-specific, sigF-dependent protein, SspA, affects septum positioning in *Streptomyces coelicolor*. *Mol Microbiol* **91**: 363-380.

Umlauf, E., M. Mairhofer & R. Prohaska, (2006) Characterization of the stomatin domain involved in homo-oligomerization and lipid raft association. *J Biol Chem* **281**: 23349-23356.

Valenza, M. & E. Cattaneo, (2011) Emerging roles for cholesterol in Huntington's disease. *Trends Neurosci* **34**: 474-486.

van Bloois, E., R.T. Winter, D.B. Janssen & M.W. Fraaije, (2009) Export of functional *Streptomyces coelicolor* alditol oxidase to the periplasm or cell surface of *Escherichia coli* and its application in whole-cell biocatalysis. *Appl Microbiol Biotechnol* **83**: 679-687.

van den Brink-van der Laan, E., J.W. Boots, R.E. Spelbrink, G.M. Kool, E. Breukink, J.A. Killian & B. de Kruijff, (2003) Membrane interaction of the glycosyltransferase MurG: a special role for cardiolipin. *J Bacteriol* **185**: 3773-3779.

van den Ent, F., C.M. Johnson, L. Persons, P. de Boer & J. Lowe, (2010) Bacterial actin MreB assembles in complex with cell shape protein RodZ. *EMBO J* **29**: 1081-1090.

van den Ent, F., T.M. Vinkenvleugel, A. Ind, P. West, D. Veprintsev, N. Nanninga, T. den Blaauwen & J. Lowe, (2008) Structural and mutational analysis of the cell division protein FtsQ. *Mol Microbio*l 68: **110**-123.

van Keulen, G., H.M. Jonkers, D. Claessen, L. Dijkhuizen & H.A. Wosten, (2003) Differentiation and anaerobiosis in standing liquid cultures of *Streptomyces coelicolor*. *J Bacteriol* **185**: 1455-1458.

van Wezel, G.P., J. White, P. Young, P.W. Postma & M.J. Bibb, (1997) Substrate induction and glucose repression of maltose utilization by *Streptomyces coelicolor* A3(2) is controlled by *malR*, a member of the *lacI-galR* family of regulatory genes. *Mol Microbiol* **23**: 537-549.

Vance, J.E., (2012) Dysregulation of cholesterol balance in the brain: contribution to neurodegenerative diseases. *Dis Models Mech* **5**: 746-755.

Vance, J.E., R.B. Campenot & D.E. Vance, (2000) The synthesis and transport of lipids for axonal growth and nerve regeneration. *Biochem Biophys Acta* 1486: 84-96.

Vasudevan, P., A. Weaver, E.D. Reichert, S.D. Linnstaedt & D.L. Popham, (2007) Spore cortex formation in *Bacillus subtilis* is regulated by accumulation of peptidoglycan precursors under the control of sigma K. *Mol Microbiol* **65**: 1582-1594.

Veatch, S.L. & S.L. Keller, (2005) Seeing spots: complex phase behavior in simple membranes. *Biochem Biophys Acta* **1746**: 172-185.

Veening, J.W., H. Murray & J. Errington, (2009) A mechanism for cell cycle regulation of sporulation initiation in *Bacillus subtilis*. *Genes Dev* **23**: 1959-1970.

Villanelo, F., A. Ordenes, J. Brunet, R. Lagos & O. Monasterio, (2011) A model for the *Escherichia coli* FtsB/FtsL/FtsQ cell division complex. *BMC Struct Biol* **11**: 28.

Vlamakis, H., Y. Chai, P. Beauregard, R. Losick & R. Kolter, (2013) Sticking together: building a biofilm the *Bacillus subtilis* way. *Nat Rev Microbiol* **11**: 157-168.

von Heijne, G., (1990) The signal peptide. *J Membr Biol* **15**: 195-201.

Wachtler, V. & M.K. Balasubramanian, (2006) Yeast lipid rafts?--an emerging view. *Trends Cell Biol* **16**: 1-4.

Walker, C.A., M. Hinderhofer, D.J. Witte, W. Boos & H.M. Moller, (2008) Solution structure of the soluble domain of the NfeD protein YuaF from *Bacillus subtilis*. *J Biomol NMR* **42**: 69-76.

Wang, X., C. Possoz & D.J. Sherratt, (2005) Dancing around the divisome: asymmetric chromosome segregation in *Escherichia coli*. *Genes Dev* 19: 2367-2377.

Warth, A.D. & J.L. Strominger, (1972) Structure of the peptidoglycan from spores of *Bacillus subtilis*. *Biochemistry* 11: 1389-1396.

Watt, N.T., H.H. Griffiths & N.M. Hooper, (2014) Lipid rafts: linking prion protein to zinc transport and amyloid-beta toxicity in Alzheimer's disease. *Front Cell Dev Biol* 2: 41.

Watts, A., (1993) Protein-lipid interactions. Elsevier.

Weigel, L.M., D.B. Clewell, S.R. Gill, N.C. Clark, L.K. McDougal, S.E. Flannagan, J.F. Kolonay, J. Shetty, G.E. Killgore & F.C. Tenover, (2003) Genetic analysis of a high-level vancomycin-resistant isolate of *Staphylococcus aureus*. *Science* 302: 1569-1571.

Weiss, A.A. & E.L. Hewlett, (1986) Virulence factors of *Bordetella pertussis*. *Annu Rev Microbiol* 40: 661-686.

Welander, P.V., R.C. Hunter, L. Zhang, A.L. Sessions, R.E. Summons & D.K. Newman, (2009) Hopanoids play a role in membrane integrity and pH homeostasis in *Rhodopseudomonas palustris* TIE-1. *J Bacteriol* 191: 6145-6156.

Westermarck, J., J. Ivaska & G.L. Corthals, (2013) Identification of protein interactions involved in cellular signaling. *Mol Cell Proteomic*s 12: 1752-1763.

Wetzel, C., J. Hu, D. Riethmacher, A. Benckendorff, L. Harder, A. Eilers, R. Moshourab, A. Kozlenkov, D. Labuz, O. Caspani, B. Erdmann, H. Machelska, P.A. Heppenstall & G.R. Lewin, (2007) A stomatin-domain protein essential for touch sensation in the mouse. *Nature* **445**: 206-209.

Whiteway, M. & C. Bachewich, (2007) Morphogenesis in *Candida albicans*. *Annu Rev Microbiol* **61**: 529-553.

Widdick, D.A., K. Dilks, G. Chandra, A. Bottrill, M. Naldrett, M. Pohlschroder & T. Palmer, (2006) The twin-arginine translocation pathway is a major route of protein export in *Streptomyces coelicolor*. *Proc Natl Acad Sci USA* **103**: 17927-17932.

Wiegert, T., G. Homuth, S. Versteeg & W. Schumann, (2001) Alkaline shock induces the *Bacillus subtilis* sigma(W) regulon. *Mol Microbiol* **41**: 59-71.

Willemse, J., J.W. Borst, E. de Waal, T. Bisseling & G.P. van Wezel, (2011) Positive control of cell division: FtsZ is recruited by SsgB during sporulation of *Streptomyces*. *Genes Dev* **25**: 89-99.

Willemse, J., B. Ruban-Osmialowska, D. Widdick, K. Celler, M.I. Hutchings, G.P. van Wezel & T. Palmer, (2012) Dynamic localization of Tat protein transport machinery components in *Streptomyces coelicolor*. *J Bacteriol* **194**: 6272-6281.

Willemse, J. & G.P. van Wezel, (2009) Imaging of *Streptomyces coelicolor* A3(2) with reduced autofluorescence reveals a novel stage of FtsZ localization. *PLoS One* **4**: e4242.

Willey, J., R. Santamaria, J. Guijarro, M. Geistlich & R. Losick, (1991) Extracellular complementation of a developmental mutation implicates a small sporulation protein in aerial mycelium formation by *S. coelicolor*. *Cell* **65**: 641-650.

Willey, J., J. Schwedock & R. Losick, (1993) Multiple extracellular signals govern the production of a morphogenetic protein involved in aerial mycelium formation by *Streptomyces coelicolor*. *Genes Dev* **7**: 895-903.

Wimley, W.C., (2003) The versatile beta-barrel membrane protein. *Curr Opin Struct Biol* **13**: 404-411.

Winans, S.C., S.J. Elledge, J.H. Krueger & G.C. Walker, (1985) Site-directed insertion and deletion mutagenesis with cloned fragments in *Escherichia coli*. *J Bacteriol* **161**: 1219-1221.

Wosten, H.A., (2001) Hydrophobins: multipurpose proteins. *Annu Rev Microbiol* **55**: 625-646.

Wu, C.H., M. Bialecka-Fornal & D.K. Newman, (2015) Methylation at the C-2 position of hopanoids increases rigidity in native bacterial membranes. *eLife* **4**.

Wu, L.J. & J. Errington, (1998) Use of asymmetric cell division and *spoIIIE* mutants to probe chromosome orientation and organization in *Bacillus subtilis*. *Mol Microbiol* **27**: 777-786.

Wu, L.J. & J. Errington, (2003) RacA and the Soj-Spo0J system combine to effect polar chromosome segregation in sporulating *Bacillus subtilis*. *Mol Microbiol* **49**: 1463-1475.

Wu, R., M. Gu, R. Wilton, G. Babnigg, Y. Kim, P.R. Pokkuluri, H. Szurmant, A. Joachimiak & M. Schiffer, (2013) Insight into the sporulation phosphorelay: crystal structure of the sensor domain of *Bacillus subtilis* histidine kinase, KinD. *Protein Sci* **22**: 564-576.

Xiong, X.F., N. de la Cruz & W.S. Reznikoff, (1991) Downstream deletion analysis of the lac promoter. *J Bacteriol* **173**: 4570-4577.

Xu, H., K.F. Chater, Z. Deng & M. Tao, (2008) A cellulose synthase-like protein involved in hyphal tip growth and morphological differentiation in *Streptomyces*. *J Bacteriol* **190**: 4971-4978.

Xu, Q., B.A. Traag, J. Willemse, D. McMullan, M.D. Miller, M.A. Elsliger, P. Abdubek, T. Astakhova, H.L. Axelrod, C. Bakolitsa, D. Carlton, C. Chen, H.J. Chiu, M. Chruszcz, T. Clayton, D. Das, M.C. Deller, L. Duan, K. Ellrott, D. Ernst, C.L. Farr, J. Feuerhelm, J.C. Grant, A. Grzechnik, S.K. Grzechnik, G.W. Han, L. Jaroszewski, K.K. Jin, H.E. Klock, M.W. Knuth, P. Kozbial, S.S. Krishna, A. Kumar, D. Marciano, W. Minor, A.M. Mommaas, A.T. Morse, E. Nigoghossian, A. Nopakun, L. Okach, S. Oommachen, J. Paulsen, C. Puckett, R. Reyes, C.L. Rife, N. Sefcovic, H.J. Tien, C.B. Trame, H. van den Bedem, S. Wang, D. Weekes, K.O. Hodgson, J. Wooley, A.M. Deacon, A. Godzik, S.A. Lesley, I.A. Wilson & G.P. van Wezel, (2009) Structural and functional characterizations of SsgB, a conserved activator of developmental cell division in morphologically complex actinomycetes. *J Biol Chem* **284**: 25268-25279.

Xu, X., R. Bittman, G. Duportail, D. Heissler, C. Vilcheze & E. London, (2001) Effect of the structure of natural sterols and sphingolipids on the formation of ordered sphingolipid/sterol

domains (rafts). Comparison of cholesterol to plant, fungal, and disease-associated sterols and comparison of sphingomyelin, cerebrosides, and ceramide. *J Biol Chem* **276**: 33540-33546.

Yahr, T.L. & W.T. Wickner, (2001) Functional reconstitution of bacterial Tat translocation in vitro. *EMBO J* **20**: 2472-2479.

Yang, C., P. Li, H. Li, H. Liu, G. Yang, J. Xie, S. Yi, J. Wang, X. Cui, Z. Wu, L. Wang, R. Hao, L. Jia, S. Qiu & H. Song, (2015) Polymorphism of CRISPR shows separated natural groupings of Shigella subtypes and evidence of horizontal transfer of CRISPR. *RNA Biol*: **0**.

Yang, C.C., C.H. Huang, C.Y. Li, Y.G. Tsay, S.C. Lee & C.W. Chen, (2002) The terminal proteins of linear *Streptomyces* chromosomes and plasmids: a novel class of replication priming proteins. *Mol Microbiol* **43**: 297-305.

Yang, Z., (2007) PAML 4: phylogenetic analysis by maximum likelihood. *Mol Biol Evol* **24**: 1586-1591.

Yang, Z. & J.P. Bielawski, (2000) Statistical methods for detecting molecular adaptation. *Trends Ecol Evol* **15**: 496-503.

Yang, Z. & R. Nielsen, (2000) Estimating synonymous and nonsynonymous substitution rates under realistic evolutionary models, *Mol Biol Evol* **17**(1):32-43.

Yanisch-Perron, C., J. Vieira & J. Messing, (1985) Improved M13 phage cloning vectors and host strains: nucleotide sequences of the M13mp18 and pUC19 vectors. *Gene* **33**: 103-119.

Yard, B.A., L.G. Carter, K.A. Johnson, I.M. Overton, M. Dorward, H. Liu, S.A. McMahon, M. Oke, D. Puech, G.J. Barton, J.H. Naismith & D.J. Campopiano, (2007) The structure of serine palmitoyltransferase; gateway to sphingolipid biosynthesis. *J Mol Bio*l **370**: 870-886.

Yepes, A., J. Schneider, B. Mielich, G. Koch, J.C. Garcia-Betancur, K.S. Ramamurthi, H. Vlamakis & D. Lopez, (2012) The biofilm formation defect of a *Bacillus subtilis* flotillin-defective mutant involves the protease FtsH. *Mol Microbiol* **86**: 457-471.

Yoder, R.A. & J.N. Johnston, (2005) A case study in biomimetic total synthesis: polyolefin carbocyclizations to terpenes and steroids. *Chem Rev* **105**: 4730-4756.

Yokoyama, H., S. Fujii & I. Matsui, (2008a) Crystal structure of a core domain of stomatin from *Pyrococcus horikoshii* illustrates a novel trimeric and coiled-coil fold. *J Mol Biol* **376**: 868-878.

Yokoyama, H., S. Hamamatsu, S. Fujii & I. Matsui, (2008b) Novel dimer structure of a membrane-bound protease with a catalytic Ser-Lys dyad and its linkage to stomatin. *J Synchrotron Radiat* **15**: 254-257.

Yokoyama, H., E. Matsui, T. Akiba, K. Harata & I. Matsui, (2006) Molecular structure of a novel membrane protease specific for a stomatin homolog from the hyperthermophilic archaeon *Pyrococcus horikoshii*. *J Mol Biol* **358**: 1152-1164.

Yokoyama, H. & I. Matsui, (2005) A novel thermostable membrane protease forming an operon with a stomatin homolog from the hyperthermophilic archaebacterium *Pyrococcus horikoshii*. *J Biol Chem* **280**: 6588-6594.

Yu, X.C., A.H. Tran, Q. Sun & W. Margolin, (1998) Localization of cell division protein FtsK to the *Escherichia coli* septum and identification of a potential N-terminal targeting domain. *J Bacteriol* **180**: 1296-1304.

Zhang, H.M., Z. Li, M. Tsudome, S. Ito, H. Takami & K. Horikoshi, (2005) An alkali-inducible flotillin-like protein from *Bacillus halodurans* C-125. *Protein J* **24**: 125-131.

Zhang, T., J.K. Muraih, N. Tishbi, J. Herskowitz, R.L. Victor, J. Silverman, S. Uwumarenogie, S.D. Taylor, M. Palmer & E. Mintzer, (2014) Cardiolipin prevents membrane translocation and permeabilization by daptomycin. *J Biol Chem* **289**: 11584-11591.

Zhang, Y., S. Rowland, G. King, E. Braswell & L. Rothfield, (1998) The relationship between hetero-oligomer formation and function of the topological specificity domain of the *Escherichia coli* MinE protein. *Mol Microbiol* **30**: 265-273.

Zhao, C.R., P.A. de Boer & L.I. Rothfield, (1995) Proper placement of the *Escherichia coli* division site requires two functions that are associated with different domains of the MinE protein. *Proc Natl Acad Sci USA* 92: 4313-4317.

Zhao, F., J. Zhang, Y.S. Liu, L. Li & Y.L. He, (2011) Research advances on flotillins. *Virol J* 8: 479.

Zhu, L.L., Y. Cui, Y.S. Chang & F.D. Fang, (2010) A second protein marker of caveolae: caveolin-2. *Chin Med Sci* J 25: 119-124.

Zlokovic, B.V., (2013) Cerebrovascular effects of apolipoprotein E: implications for Alzheimer disease. *JAMA Neurol* 70: 440-444.

Zweers, J.C., P. Nicolas, T. Wiegert, J.M. van Dijl & E.L. Denham, (2012) Definition of the sigma(W) regulon of *Bacillus subtilis* in the absence of stress. *PLoS One* 7: e48471.

Appendix

Table 9-1. P-values for strains lacking a fully-functional copy of *SCO3607*.

Tip to cross-wall			
Strains	24 hours	48 hours	72 hours
CFW3607A and M145	0.0000	0.0000	0.8931
CFW3607A and CFW3607AC	0.0765	0.0000	0.8560
CFW3607M and M145	0.0000	0.2228	0.0054
CFW3607M and CFW3607MC	0.0000	0.0000	0.2144
CFW3607δ and M145	0.0000	0.7744	0.0988
CFW3607δ and CFW3607δC	0.0000	0.8700	0.0002

Table 9-2. P-values for strains lacking a fully-functional copy of *SCO3607*.

Tip to branch			
Strains	24 hours	48 hours	72 hours
CFW3607A and M145	0.0077	0.4270	0.0928
CFW3607A and CFW3607AC	0.0006	0.4900	0.3290
CFW3607M and M145	0.0000	0.0000	0.4661
CFW3607M and CFW3607MC	0.0000	0.0002	0.0195
CFW3607δ and M145	0.0000	0.0000	0.0109
CFW3607δ and CFW3607δC	0.0222	0.0040	0.2987

Table 9-3. P-values for strains lacking a fully-functional copy of *SCO3607*.

Cross-wall to cross-wall			
Strains	24 hours	48 hours	72 hours
CFW3607A and M145	0.0263	0.7792	0.0302
CFW3607A and CFW3607AC	0.0000	0.0031	0.2481
CFW3607M and M145	0.0000	0.5631	0.0139
CFW3607M and CFW3607MC	0.0218	0.8270	0.1007
CFW3607δ and M145	0.2179	0.0001	0.0000
CFW3607δ and CFW3607δC	0.4314	0.0000	0.0000

Table 9-4. P-values for strains lacking a fully-functional copy of *SCO3607*.

Branch to branch			
Strains	24 hours	48 hours	72 hours
CFW3607A and M145	0.4790	0.0182	0.0300
CFW3607A and CFW3607AC	0.0002	0.6484	0.4934
CFW3607M and M145	0.0635	0.0000	0.0934
CFW3607M and CFW3607MC	0.0306	0.0000	0.0871
CFW3607δ and M145	0.0000	0.0000	0.0215
CFW3607δ and CFW3607δC	0.0000	0.6142	0.9368

Table 9-5. P-values for CFW3608δ and M145.

Measurement	24 hours	48 hours	72 hours
Tip to cross-wall	0.0077	0.0000	0.0073
Tip to branch	0.0000	0.0298	0.0237
Cross-wall to cross-wall	0.3139	0.1513	0.0000
Branch to branch	0.1678	0.0000	0.8266

Table 9-6. P-values for CFW3608δ and CFW3608δC.

Measurement	24 hours	48 hours	72 hours
Tip to cross-wall	0.0723	0.0000	0.6358
Tip to branch	0.0794	0.1806	0.0416
Cross-wall to cross-wall	0.1432	0.0022	0.0577
Branch to branch	0.0004	0.4182	0.8124

Table 9-7. P-values for CFW36078δ and M145.

Measurement	24 hours	48 hours	72 hours
Tip to cross-wall	0.0000	0.7881	0.0000
Tip to branch	0.0111	0.0000	0.2393
Cross-wall to cross-wall	0.0125	0.0636	0.0000
Branch to branch	0.5072	0.0089	0.9959

Table 9-8. P-values for CFW36078δ and CFW36078δC.

Measurement	24 hours	48 hours	72 hours
Tip to cross-wall	0.0000	0.0000	0.0029
Tip to branch	0.0000	0.0000	0.8085
Cross-wall to cross-wall	0.2127	0.0000	0.0004
Branch to branch	0.3367	0.0275	0.0000

Table 9-9. Average spore length.

Strain	Length (in µm)	Standard deviation (in µm)
M145	1.01984	0.2919
CFW3607A	0.9659	0.3453
CFW3607AC	1.1775	0.3530
CFW3607M	0.9952	0.3023
CFW3607MC	0.9634	0.2532
CFW3607δ	1.0767	0.430843553
CFW3607δC	1.0164	0.3086
CFW3608δ	1.0079	0.3154
CFW3608δC	1.0213	0.2629
CFW36078δ	1.1586	0.2789
CFW36078δC	1.0879	0.4015

Table 9-10. P-values for the disrupted strains.

Strains	M145	CFW3607A	CFW3607AC	CFW3607M	CFW3607MC
M145		0.0964	$7.66E^{-6}$	0.4446	0.0522
CFW3607A	0.0964		$3.33669E-^{9}$		
CFW3607AC	$7.66E^{-6}$	$3.33669E^{-9}$			
CFW3607M	0.4446				0.2887
CFW3607MC	0.0522			0.2887	

Table 9-11. P-values for single-knock out strains.

Strains	M145	CFW3607δ	CFW3607δC	CFW3608δ	CFW3608δC
M145		0.1449	0.9144	0.7274	0.9620
CFW3607δ	0.1449		0.1245		
CFW3607δC	0.9144	0.1245			
CFW3608δ	0.7274				0.6977
CFW3608δC	0.9620			0.6977	

Table 9-12. P-value for CFW36078δ and its complemented strain.

Strains	M145	CFW36078δ	CFW36078δC
M145		$1.50251E^{-5}$	0.1433
CFW36078δ	$1.50251E^{-5}$		0.1306
CFW36078δC	0.1433	0.1306	